THE UNIVERSITY
of EDINBURGH

Matrix signalling and hippocampal neurogenesis

Alasdair G. Rooney

PhD (Neuroscience)

The University of Edinburgh

2018

Declaration

This thesis has been composed by me and is my own work, under the supervision of Prof. Charles ffrench-Constant and with guidance from Dr. Sally Lowell and Prof. Steven Pollard (all MRC Centre for Regenerative Medicine, University of Edinburgh).

RNA sequencing was conducted by Aros Applied Biotechnology (Denmark). Bioinformatic analysis was conducted by Dr. Jonathan Manning (MRC Centre for Regenerative Medicine, University of Edinburgh).

The contents have not been submitted for any other degree or professional qualification.

Signed..... Date.....

CONTENTS

List of Figures *Page*

High-resolution Figure versions can be found online via the following link:
https://datasync.ed.ac.uk/index.php/s/E5ghSrFFGpFo0Wk
(Password: Thesis2018)

List of Tables

List of main abbreviations

aNSC	Activated neural stem cell
AraC	Cytosine-B-D-arabinofuranoside
BMP	Bone morphogenetic protein
cKO	Conditional knockout
CNS	Central nervous system
DG	Dentate gyrus
E[χ]	Embryonic day of gestation, e.g. E12.5
ECM	Extracellular matrix
ECS	Electroconvulsive shock
GCL	Granule cell layer
icv	Intra-cerebro-ventricular
iKO	Inducible knockout

IP	Intermediate progenitor cell
ML	Molecular layer
NB	Neuroblast
NSC	Neural stem cell
NSPC	Neural stem and precursor cell – a broader term than NSC or RGL
P[χ]	Postnatal age in days, e.g. P7
RGC	Radial glial cell, developmental / embryonic neural stem cells
RGL	Radial glia-like cell; held to be hippocampal neural stem cells
RMS	Rostral migratory stream
SEZ	Subependymal zone (adult)
SGZ	Subgranular zone
VZ	Ventricular zone (embryonic)

Acknowledgements

To colleagues, teachers, and collaborators

Especially, the BRF staff

Carol, John, and Hollie

Caroline and Nacho

Ron, Debbie, Valeria, and Mike

Mark, Robbie, Betty, Donna, Vaila, Caroline, and Kelly

Anahi, Guillaume, Matt, Tyson, Julia, Antoniana, Jenny, Jennie, MA, Sofia, and Alex

Hannah, Donna, Gabby, Tina, Michelle, and Hayley

Tamar, Myriam, Sister Agatha, Eli, and his lab

Anne and Joanna

Bertrand and Jon

Ilias Kazanis and Caroline Stewart

Steve Lawrie, Robin Grant, and Anthony Chalmers

Malcolm Macleod

Steve Pollard, Sally Lowell, and Anna Williams

Jack Price, Jonathan Cavanagh, and David Porteous

The ffrench-Constant and Williams labs 2013-2017

Charles ffrench-Constant

Funding: MRF/MRC Psychiatric Scottish Training in Academic Research (PsySTAR) programme (Prof. Steven Lawrie, Division of Psychiatry, University of Edinburgh) (salary, consumables)
The Britain Israel Research and Academic Exchange (BIRAX) programme (additional consumables)

For Tom

1 INTRODUCTION

1.1 Background

Working as a junior doctor in neurology, I once met a man who was frozen in time. Many years before we met, this gentleman had suffered a type of brain inflammation called limbic encephalitis. His original presenting symptom had been severe impairment of memory, but no-one at that time had spotted the encephalitis. Instead he had been diagnosed incorrectly with dementia and was sent away to live in a nursing home. The doctors eventually had second thoughts about the diagnosis when staff noticed that he was beating all the other nursing home residents at dominoes.

Subsequently it was established that limbic encephalitis had destroyed some of the gentleman's cerebral functions while leaving others intact. Specifically the disease had affected a critical part of his brain: the hippocampus. He remained able to wash, dress, talk, and count (which explained his status as resident domino champion), but was completely unable to form new memories. This was an extremely disabling state of affairs. He thought he was much younger than he really was because he perceived his age to be that of the day he developed the encephalitis. He had to be reminded daily about anything important that had happened since. Doctors who had known him for years introduced themselves at every appointment. And as I sat talking to him I knew that when I left the room, he would forget - and that as you read this he has forgotten - that we ever met.

This true story is told to illustrate a critical function of the hippocampus in supporting learning and memory.[1] This function has been known for more than half a century [Scoville and Milner 1957] but only within the last two decades has it been widely accepted that mammalian hippocampi also possess the capacity to generate new neurons throughout adult life. This remarkable process is called adult hippocampal neurogenesis.[2]

I use the word 'remarkable' in a historical context. The possibility of postnatal neurogenesis was discounted or regarded sceptically throughout much of the 20th century. In part this

[1] It also recalls the more celebrated case of "H.M." reported by Scoville & Milner: an American patient who developed a similar dense anterograde amnesia after bilateral hippocampal resection for intractable epilepsy.
[2] I will use the terms "adult hippocampal neurogenesis", "adult neurogenesis", and "neurogenesis" synonymously unless otherwise specified.

attitude reflected the weight accorded the views of the venerable Nobel Laureate and acclaimed ‘father of neuroscience’ Santiago Ramon Y Cajal, who 100 years ago declared with respect to the brain:

> “Once development was ended, the fonts of growth and regeneration of the axons and dendrites dried up irrevocably. In adult centers, the nerve paths are something fixed and immutable: everything may die, nothing may be regenerated.” *Cajal 1913, as cited by Colucci-D’Amato et al. 2006*

In succeeding decades this influential dogma was perhaps reinforced in the minds of doctors and researchers. Routinely they observed patients failing to recover functionally after stroke or traumatic brain injury, or deteriorating inexorably from neurodegenerative processes such as dementia. [Colucci-D’Amato et al. 2006] These prevailing forces were such that I can remember sitting in a medical school lecture as recently as 1997 and learning that the number of neurons in my brain had been fixed at birth.

The truth, however, is that the adult mammalian brain harbours at least two germinal - or neurogenic - niches in which new neurons are born throughout life. These neurogenic niches comprise the subependymal zone which lines the ventricular system, and the subgranular zone in the hippocampal dentate gyrus. Post-natal hippocampal neurogenesis was in fact first identified experimentally in the 1960s. [Altman and Das 1965] However perhaps due partly to aforementioned institutionalised belief and partly to a lack of accessible experimental tools [Colluci-D’Amato et al. 2006], the phenomenon of hippocampal neurogenesis was widely recognised by the scientific community only shortly before the millennium. [Eriksson 1998]

Consequent study has established that adult hippocampal neurogenesis has been conserved through millions of years of evolution in nearly every mammalian species studied to date. [Amrein 2015] Importantly, post-mortem studies and radioisotope carbon dating techniques suggest that it also occurs in humans. [Eriksson et al. 1998; Spalding et al. 2013] A great deal of this research has focused on understanding the inner workings of the cells that undergo the transformation to become new adult-born neurons. By contrast, relatively little is known about the potential regulatory role of the surrounding extracellular microenvironment. This might be useful to know in light of much evidence that the extracellular matrix is a key regulator of developmental neurogenesis. [Ahmed and ffrench-Constant 2016] This thesis describes my study of whether extracellular matrix regulates hippocampal neurogenesis.

1.2 Adult hippocampal neurogenesis

1.2.1 Neuroanatomy and development of the dentate gyrus and subgranular zone

1.2.1.1 *Neuroanatomy*

Within the adult mouse brain, the hippocampus is positioned in such a way that one end lies dorsal, medial, and rostral while the other lies ventral, lateral, and caudal. By convention the resulting longitudinal axis of the hippocampus is called the septotemporal axis. Afferent input is via the entorhinal cortex. The hippocampus consists of four functionally, cellularly, and molecularly distinct subfields: CA1, CA2, CA3, and the dentate gyrus (DG). The DG itself has a characteristic layered architecture comprising an outer molecular layer (ML), a dense granule cell layer (GCL), and a deeper polymorphic layer known as the hilus. This laminated organisation reflects back upon itself along the septotemporal axis, creating a ventral half that is roughly the mirror image of the dorsal **(Figure 1)**.

The subgranular zone (SGZ) neurogenic niche lies at the base of the granule cell layer. Because it runs the length of the warped and auto-reflected DG, the SGZ is a topographically complex structure. No parenchymal or extracellular markers are known to specifically demarcate the SGZ on brain sections. Its location is signalled by the presence of a 2-3 cell layer-thick band of newly generating neurons (see **Figure 1A**). The SGZ can therefore be defined anatomically by its location in relation to the GCL, and/or functionally by its permissiveness for neurogenesis.

1.2.1.2 *Development*

In mice, morphological differences between hippocampal subfields - including the distinctive lamination of the dentate gyrus - become evident only after birth. However molecular markers can be used to determine when hippocampal cells first show features of CA1, CA3 or DG identity, thereby establishing earlier limits in terms of when subfield identity is specified. Using this approach researchers have established that the primordial hippocampus is fate-patterned within the medial telencephalon as early as embryonic day (E)12.5. The dentate gyrus subfield arises ultimately from cells first expressing key molecular markers at E15.5. [Grove et al. 1999]

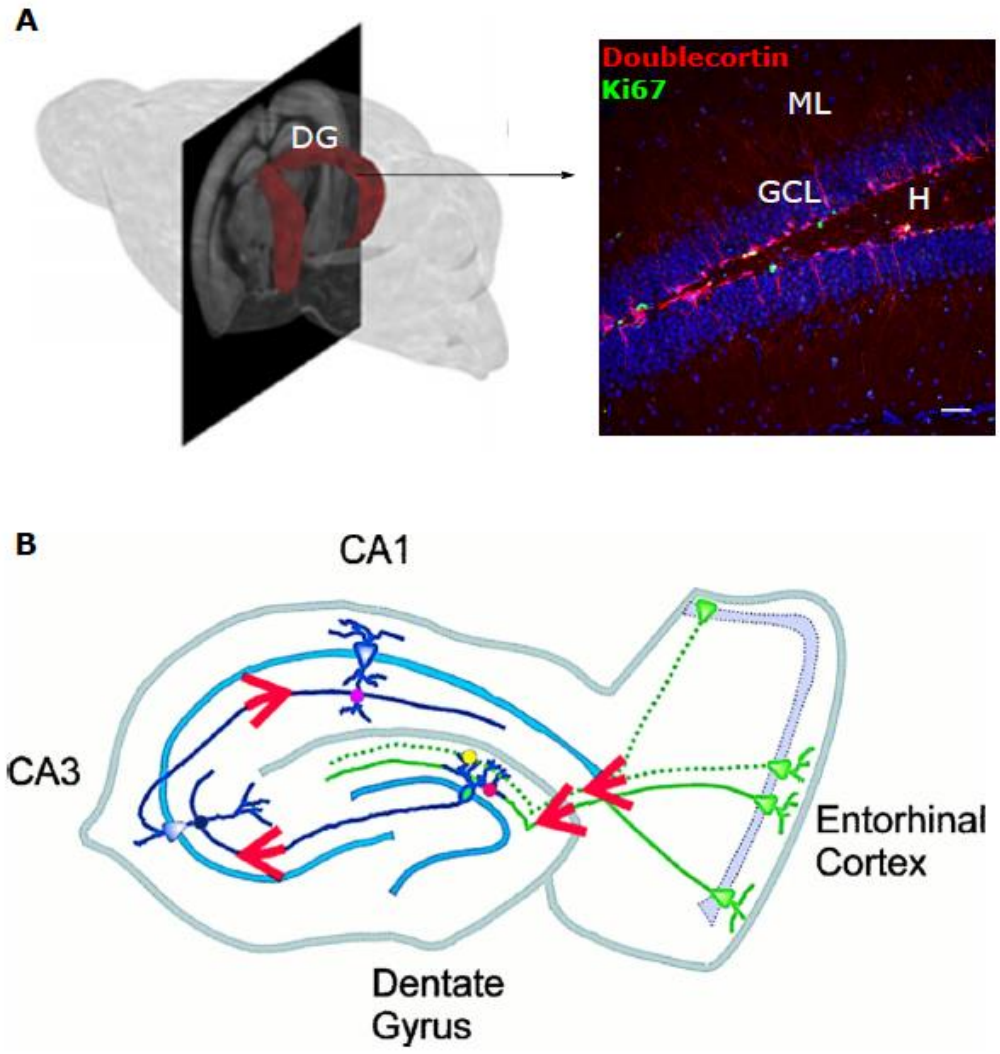

Figure 1. Gross anatomy of the dentate gyrus and its context within the hippocampus.
A: Left panel: 3D visualisation of the dentate gyrus (DG, red shaded area) within the adult mouse brain. *Image reprinted from* [Egger et al. 2016]. *Copyright 2016, with permission from Elsevier.* Right panel: In coronal section the laminar organization of the DG comprises the molecular layer (ML), granule cell layer (GCL) and hilus (H). New-born neurons are here stained in red (Doublecortin), proliferating cells in green (Ki67). Scale bar= 20 microns. **B:** Afferent inputs from the Entorhinal Cortex performant paths (green and dotted green lines) synapse with DG GCL neuronal dendrites in the Molecular Layer (pink and yellow dots). Granule cell axons project via the mossy fibre tract to synapse on neurons in area CA3 (navy dot), which in turn project to synapse in area CA1 (purple dot). *Image reprinted from* [Dobrunz et al. 1998]. *Copyright 1998, with permission from The National Academy of Sciences.*

One reason the laminated ultrastructure only develops after birth is that most granule cell neurons - the nuclei of which form the characteristic band of the GCL - are themselves born postnatally, from proliferating DG precursor cells arising from the hilar primordium. During the first postnatal week there is no marked restriction of proliferation to a specific locus; much of the primordium is highly proliferative and the SGZ cannot be demarcated. Starting from around postnatal day (P)7 the GCL and SGZ gradually condense into their respective laminae. By P14 the GCL is a crisp band of nuclei with the neurogenic SGZ clearly identifiable along the inferior boundary. [Nicola et al. 2015] Although the macroscopic organisation of the DG is largely complete by P14, neural stem and precursor cells may undergo further functional and transcriptional maturation until at least P28 [Gilley et al. 2011], if not longer.

1.2.2 The cellular basis of adult hippocampal neurogenesis

1.2.2.1 *Radial glia-like cells*

The adult SGZ harbours a population of neural stem cells (NSCs) capable of self-renewal and multilineage differentiation, which comprise the fundamental cellular reservoir from which adult neurogenesis proceeds. [Nicola et al. 2015, Sierra et al. 2015, Bonaguidi et al. 2011] These NSCs have a characteristic morphology with a cell body located in the SGZ and a single process extending radially through the GCL to the ML. There, it branches into a dendritic tree which makes physical contact with the local microvasculature, neuronal synapses and astrocytes. [Moss et al. 2016] Because this cyto-architecture is somewhat reminiscent of radial glial cells (RGCs) of embryonic cortical development, hippocampal NSCs are generally termed radial glia-like cells (RGLs, or Type 1 cells) **(Figure 2)**.[3]

Clonal analyses suggest that RGLs are multipotent with the ability to generate both astrocytes and neurons. They also self-renew, dividing asymmetrically to generate a daughter RGL and an IP or astrocyte, or else dividing symmetrically to generate two new RGLs. Uncertainty exists over both the long-term multilineage [Bonaguidi et al. 2011, Encinas et al. 2011] and self-renewal [Sierra et al. 2015] potential of at least some RGL subpopulations.

[3] In this thesis I will use the term RGL synonymously with NSC.

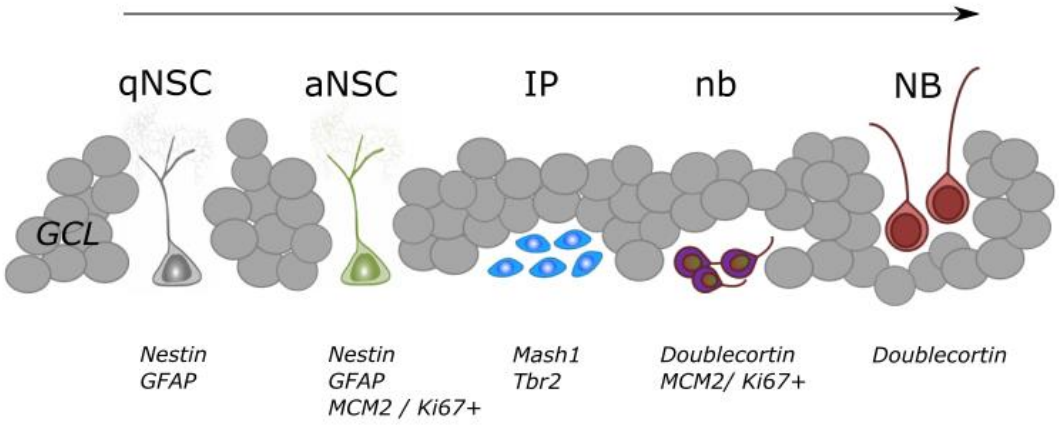

Figure 2. The cellular process of adult hippocampal neurogenesis.

Quiescent neural stem cells (radial glia-like cells, qNSC) activate in response to extracellular stimuli (aNSC), and divide asymmetrically to generate a new RGL and a daughter intermediate progenitor cell (IP). The IPs proliferate, differentiating into early neuroblasts that retain cell cycle markers (nb), before maturing into post-mitotic neuroblasts (NBs). Over a period of 2-3 weeks the neuroblasts further mature and functionally integrate into the GCL as new-born neurons (not shown). These lineage subpopulations of neural stem and progenitor cells can be identified by cellular markers. Key markers used in this thesis are listed underneath the schematic. GFAP= Glial fibrillary acidic protein; MCM2= Minichromosome maintenance complex component 2; Mash1= Mammalian achaete-scute homolog 1; Tbr2= T-box brain gene 2.

The extent to which RGLs are biologically homogenous is also far from clear. For example while they characteristically express markers including Glial fibrillary acidic protein (Gfap), Brain lipid binding protein (Blbp), Nestin, and Sox2 [e.g. Goncalves et al. 2016, Kriegstein and Alvarez-Buylla 2009, Suh et al. 2007], these markers do not necessarily occur together in all cells, suggesting that RGLs may form heterogeneous subsets with different functional characteristics. Reports that RGLs may also vary in density along the septotemporal DG axis [Jinno et al. 2011] and with age [Gebara et al. 2016, Gilley et al. 2011] further complicate the picture. In addition, a population of SGZ NSCs lies horizontally with non-radial morphology and processes extending along the border between the SGZ and the hilus. Non-radial NSCs are proposed to respond to different stimuli than classical RGLs. [Lugert et al. 2010] While RGLs are canonically regarded as SGZ stem cells therefore, the extent and biological significance of RGL heterogeneity remain active questions in the field.

Under physiological conditions the vast majority (c.95%) of RGLs in the SGZ are out of cell cycle at any given time and therefore are functionally quiescent. [Suh et al. 2007] The process of adult hippocampal neurogenesis begins with the activation of quiescent RGLs. In the SGZ, recently suggested markers of quiescence include the Notch target gene Hes5 [Lugert et al. 2010] and the phosphorylated form of the canonical BMP signal pathway component SMAD1. [Mira et al. 2010] The extent to which each of these markers sensitively and specifically defines the entire population of quiescent RGLs remains unclear. Many authors therefore continue to identify and study quiescent and activated RGLs by using a marker of stem cells (such as **GFAP** or **Nestin**) coupled with the absence or presence of a marker of cellular proliferation (such as **Ki67** or **MCM2**). [e.g. Beckervordesandforth et al. 2017, Andersen et al. 2014, Weber et al. 2013] By comparing the fraction of proliferating RGLs in the total population of each experimental group, effects upon the balance of RGL quiescence and activation can be inferred.

1.2.2.2 *Intermediate progenitors*

Activated RGLs divide to generate a rapidly proliferative pool of intermediate progenitor cells (IPs), also referred to as Type 2 cells. In indication of their neuronal lineage commitment IPs express the nuclear transcription factors mammalian achaete-scute homolog 1 (Mash1, also known as **Ascl1**) [Uda et al. 2007, Andersen et al. 2014] and T-box brain gene 2 (**Tbr2**, also known as Eomes) [Hodge et al. 2008] among others.

Ascl1 is a proneural basic helix-loop-helix (bHLH) transcription factor which is widely expressed by dividing progenitors in the developing nervous system and which specifies neurons and oligodendrocytes postnatally. [Parras et al. 2004] The dynamic intracellular balance of Ascl1 is under inhibitory notch control [Andersen et al. 2014] and thought to mediate the prevailing cellular status of proliferation versus differentiation. That is, oscillating concentrations of Ascl1 are thought to promote neural progenitor proliferation whereas its stable expression promotes differentiation. [Imayoshi et al. 2013]

The most thorough examination of Ascl1 in SGZ neurogenesis was undertaken by Andersen et al. [Andersen et al. 2014] These authors reported that in the adult DG Ascl1 expression was restricted to the SGZ where it is expressed by at least three populations of cells: GFAP+ RGLs (roughly 2% of the whole population of RGLs), non-radial GFAP+ cells (thought also

to be stem cells [Lugert 2010 et al.]), and IPs. Most Ascl1-expressing cells were in cell cycle indicating that it is expressed specifically by activated stem cells in the hippocampus. In response to a pro-neurogenic stimulus (intra-hippocampal kainic acid injection) Ascl1 was expressed in RGLs temporally antecedent to MCM2, indicating that activating signals induce Ascl1 expression in RGLs before exit from quiescence. The requirement for Ascl1 for RGLs to exit from quiescence was nearly if not entirely absolute: Cre-lox inducible knockout (iKO) of the Ascl1 gene from GLAST+ cells in adult mice reduced the number of recombined proliferating cells in the SGZ by over 99%. The Ascl1 iKO cells remained permanently unresponsive to neurogenic stimuli. Using ChIP-Seq the authors established that Ascl1 controls the proliferation of hippocampal RGLs by directly activating the expression of cell-cycle genes including Cyclin D2 (Ccnd2).

Tbr2 is a T-domain transcription factor which acts as part of a cascade regulating the development of glutamatergic neurons in the embryonic brain. [Englund et al. 2005, Arnold et al. 2008] In a series of papers published over the last decade [Hodge et al. 2008, 2012, and 2013] it has been established that Tbr2 is expressed by IPs in the SGZ throughout development. At the earliest stages of recognisable SGZ development postnatally (P7), immunofluorescent expression of the endogenous Tbr2 protein appears to be restricted largely to the SGZ, while the vast majority of GCL neurons are Tbr2-GFP+. This pattern suggests that the postnatal glutamatergic GCL is populated almost entirely by neurons derived from the Tbr2+ lineage. Consistent with this, Nestin-Cre;Tbr2cKO mice display markedly reduced granule cell neurogenesis and loss of IPs at birth, while eliminating Tbr2 from adult NSCs causes a marked reduction in adult neurogenesis.

In adult Nes-CreER;Tbr2 iKO mice the reduction in neurogenesis is accompanied by a marked increase in the number of proliferating RGLs, and in non-radial Sox2+ and Ascl1+ cells. Although Hodge et al. considered this to mean a simple increase in NSCs in the Tbr2-deficient SGZ, I think an alternative explanation could be that loss of regulatory negative feedback from neuroblasts triggers increased NSC proliferation, with subsequent accumulation of Sox2+ / Ascl1+ IPs that failed to progress through neurogenesis, leading to a bottleneck phenomenon. Consistent with this alternative explanation the authors noted that both in monolayer NSC cultures and in vivo, Tbr2 over-expression suppresses the expression of Sox2.

Together these experiments established Tbr2 as a critical regulator of IP fate, indispensable for neurogenesis during development and in the adult brain. Tbr2 has the capacity to directly bind and negatively regulate Sox2 and potentially thereby to influence the progression from uncommitted precursor to fate-specified IPs.

1.2.2.3 *Neuroblasts*

IPs expand the progenitor pool and gradually mature, first into neuronally-committed but immature neuroblasts (NBs) expressing the microtubule-associated protein doublecortin (Dcx). Dcx is developmentally essential for the proper lamination of the hippocampus. Mice lacking the Dcx gene show disrupted lamination, particularly in the CA3 region, and deficits in hippocampal-dependent conditioned behaviour. [Corbo et al. 2002]

Neuroblasts characteristically migrate to a site distal from where they were born: in the SEZ along the rostral migratory stream to the olfactory bulbs, and in the SGZ a short distance along blood vessels to a nearby location in the granule cell layer. [Sun et al. 2015] In the adult CNS, Dcx is necessary for the maintenance of bipolar morphology and nuclear translocation in migrating NBs. [Koizumi et al. 2006] In the SGZ the NBs further mature into new granule cell layer neurons which functionally integrate into the GCL**.** [Toni et al. 2008] Together, RGLs, IPs, and NBs may collectively be termed "neural stem and precursor cells" (NSPCs).

1.2.3 Biological relevance

The precise biological function of hippocampal neurogenesis remains unclear, but there is consensus that in general it serves to promote learning and memory. Several hypotheses have been advanced as to how this might be achieved. One hypothesis is that neurogenesis functions to underpin *cognitive flexibility*. This term describes the process whereby learned cognitive-behavioural strategies are modified to adapt to changes in the environment. The consequence of such modification is that the animal can more easily switch response strategies in the face of novel situations. In support, studies consistently find that neurogenesis is required to learn the reversal of a given behavioural rule, but not to learn the initial rule itself. [as cited by Anacker and Hen 2017] Neurogenesis may also promote the forgetting of old memories. [Akers et al. 2014] Indeed some authors propose that these two characteristics are linked: that suppressing 'old' memories may itself improve the ability to

encode similar ‘new’ ones, by means of reducing interference from the old during encoding of the new. [Epp et al. 2016, Anacker and Hen et al. 2017] A function of promoting cognitive flexibility would have clear implications for psychiatric treatments, which often seek to instill adaptive new behaviours at the expense of old, maladaptive ones.

A second hypothesis is that adult neurogenesis supports the correct encoding and recall of memories that are closely related in time or space. In this view, neurogenesis allows the animal to discretely encode highly similar new memories. The computational process of accurately encoding temporally or spatially similar pieces of information separately is known as *pattern separation*. This process is proposed as a major function of the dentate gyrus [Becker 2005] and – at least for spatial information – is thought to be adult neurogenesis-dependent. [Clelland et al. 2009] Consistent with this, increasing the number of adult- born neurons improves spatial pattern separation abilities in mice. [Sahay et al. 2011] If the pattern separation hypothesis is correct, then neurogenesis is a critical means by which we successfully find our cars when they are parked in different locations of the same street every morning.

A third possibility is that adult neurogenesis has evolved as an efficient method of encoding new information without disrupting previously stored but temporally distant memories. [Aimone et al. 2009] By this interpretation neurogenesis could form part of the biological basis on which we sequentially encode serial life events without wiping older memories - in other words, it may be a platform for our ‘life story’, which would make it a critical component of the neural circuitry that gives rise to our personal identity.

Each of these hypotheses is supported by experimental evidence and they may not be mutually exclusive. Each addresses subtly different cognitive functions, and each is founded upon the same characteristic of newly-born dentate granule cells. That characteristic is their relative excitability and plasticity, in the early weeks of their development, compared to older granule cell neurons. This early period is termed the ‘critical period’ and because neurogenesis continues throughout life, a moment’s reflection crystallises a mental image of constantly succeeding cohorts of highly plastic cells passing through the critical period, each at only one point in the entire life-span of the organism. This pattern suggests - as do computational studies [Aimone et al. 2006] - that young neurons in their critical period might also encode temporal information. One can speculate that neurogenesis could be a

biological substrate of our sense of time.[4]

There is therefore a considerable body of opinion, supported by experimental evidence, which holds that adult neurogenesis functions to underpin learning and memory, whether via cognitive flexibility, pattern separation, or the sequential temporal encoding of new memories. I wish to briefly recognise a few objections to this theory, and to acknowledge alternative theories as to its function in mammals. One objection arises from the observation that hippocampal neurogenesis varies widely between different strains of laboratory mice. [Kempermann et al. 1997] If neurogenesis was indeed a critical determinant of learning ability, one might expect to see a comparably wide range of cognitive abilities between strains. However this is not the case; the inter-strain range of variation in rates of adult neurogenesis instead outweighs any known differences in cognitive ability. A second, related problem is that between mammals, rates of neurogenesis appear to be lowest in primates, the most intelligent mammals with the greatest capacity to learn. Additionally neurogenesis is not known to occur in certain species of bats, and since they exhibit a high use of spatial awareness strategies in searching for food [Thiel et al. 2005] this might argue against a primary role for neurogenesis in spatial learning.

Alternative theories as to the function of adult neurogenesis have therefore been proposed, such as in the regulation of female mouse mating preferences. [Mak et al. 2007] Another theory was introduced indirectly by one of the original proponents of hippocampal neurogenesis, Joseph Altman. In the 1970s he and colleagues published a review of the behavioural effects of hippocampectomy in adult animals. Experimental animals tended to display what the authors described as "exuberant, reckless and inattentive" behaviours in learning paradigms, whereas control adult animals tended towards "placid, cautious, and observant" traits. This prompted the hypothesis that the hippocampus:

"…plays a major role in 'behavioural maturation' by contributing to the transformation of unrestrained juveniles into more restrained adults [via] its facilitation of response-braking mechanisms." *Altman et al. 1973*

[4] In passing and taking account of these various hypotheses, I have wondered whether the dynamics of postnatal neurogenesis might explain why Christmas takes so long to come round every year when we are children, whereas birthdays seem to come round so much faster when we are adults. More time-stamped new memories in childhood might make time seem to have dragged, and fewer in adulthood to make it fly.

The review methodology and conclusions of Altman et al. were rebutted by contemporaries. [Nadel et al. 1975] However, the idea persisted that the hippocampus might mediate changes in behavioural traits which associate with the transition from juvenile to adult. More recently, hippocampal neurogenesis has been somewhat shoe-horned into the original theory with the suggestion that the age-related decline in neurogenesis might somehow underlie the increased predictability of activities that is characteristic of adult behaviour. [Amrein and Lipp 2009] However, some of the "exuberant" behaviours as originally described by Altman et al. seem to me better explained by a failure of reverse-learning in reward paradigms - which would be to say, a failure of cognitive flexibility - than by attributing anthropomorphic qualities such as recklessness to rats.

1.2.4 Physiological regulatory mechanisms

1.2.4.1 *Intrinsic*

Adult hippocampal neurogenesis is regulated intrinsically by many transcription and secretory / synaptic factors. These modes of regulation are well-studied and well-reviewed. [Goncalves et al. 2016, Mahmoud et al. 2016, Bond et al. 2015, Beckervordesandforth et al. 2015, Christian et al. 2014, Aimone et al. 2014] For completeness **Figure 3** synthesises these selected reviews to summarise the main transcriptional and secretory signalling regulation of the different stages of neurogenesis.

1.2.4.2 *Extrinsic*

Similarly to intrinsic regulation, extrinsic regulatory factors acting on adult neurogenesis are well-studied and reviewed. [Holmes 2016, Clemenson et al. 2015, Seib and Martin-Villalba 2015, Farioli-Vecchioli and Tirone 2015, Egeland et al. 2015] Extrinsic forcings (factors influencing adult neurogenesis) reported in these reviews are summarised schematically in **Figure 4.**

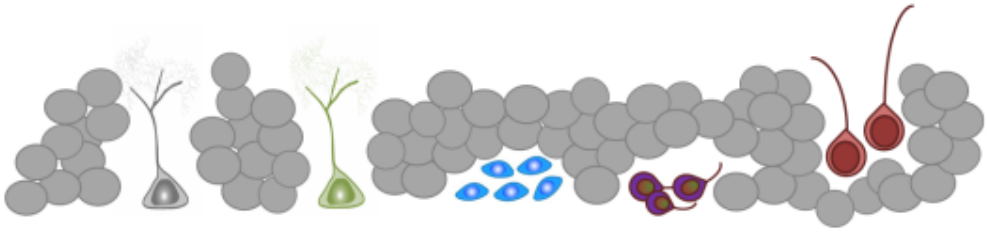

	NSC	aNSC	IP	nb	NB
A.k.a.	Type 1	Type 1/2a	Type 2b	Type 3	Immature neuron
State	Quiescence	Activation	Proliferation Differentiation		Postmitotic differentiation
Timeline (D)	0	1	3		7
TFs	Hes5	Ascl1	Tbr2	NeuroD	CREB
	Id1	Sox21	Sox4	Prox1	
	FoxO	Tis21	Sox11	CREB	
	Sox2	Sox2	NeuroD		
	TLX	TLX	Prox1		
	REST	REST			
	NFIX				
Niche signals	BMP	Wnt	IGF	Wnt	BDNF	Glutamate
	Notch	Shh	EGF	NT3	Reelin	
	GABA	FGF2	VEGF	EphB2	GABA	
		5-HT	Notch			

Figure 3: Intrinsic regulation of adult neurogenesis.

The schematic of hippocampal neurogenesis introduced in **Figure 2** is mapped against a commonly-used alternative nomenclature, the predominant cellular state at each point, and a timeline in days (D). Transcription factors (TFs) and secretory niche signalling molecules with known regulatory roles at each stage are listed. For references see text.

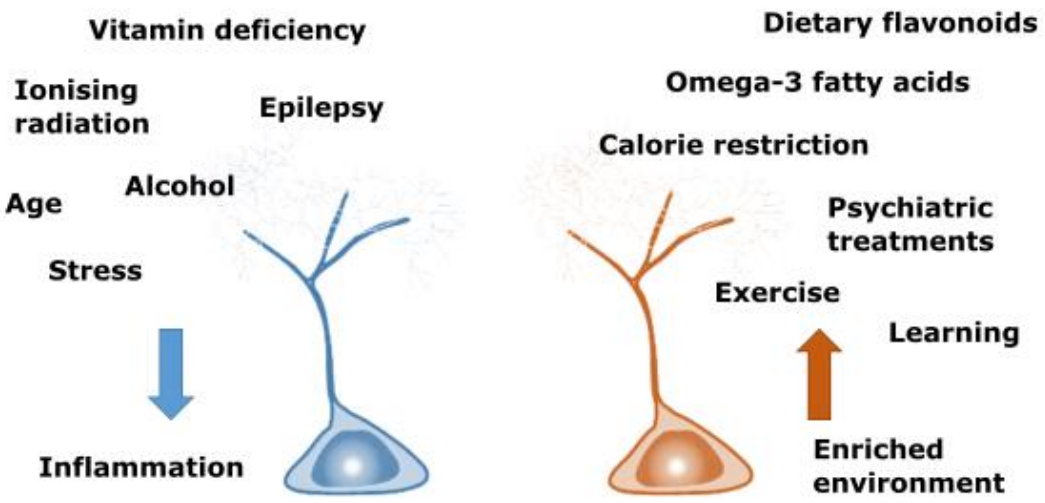

Figure 4. Extrinsic modulators of adult neurogenesis.

The best-studied extrinsic factors which can reduce (blue NSC) or increase (orange NSC) hippocampal neurogenesis are listed. For references see text.

1.2.5 Techniques for experimental manipulation

As Figure 4 illustrates, adult neurogenesis can be experimentally manipulated by altering aspects of the environmental context. In particular I think that such paradigms are valuable for understanding how social factors may influence neurogenesis. However some, for instance environmental enrichment or dietary manipulation, may vary considerably between studies in terms of how they are technically delivered [Clemenson et al. 2015], raising questions of reproducibility of results. This suggests a need too for simple models with a predictable response. To this end many groups adopt a strategy of using simple interventions to perturb neurogenesis and examine its recovery. As proof of principle some examples of chemical experimental strategies recovered from a brief literature search of Pubmed are listed in **Box 1.**

Kainic acid	Fluorouracil	Ibotenic acid	Vinblastine
Colchicine	Paclitaxel	Azacytidine	Cyclophosphamide
Trimethylin	Doxorubicin	ThioTEPA	Cytochalasin D
MAM	Procarbazol	Nocodazol	Temozolomide

Box 1: Examples of chemical strategies to manipulate adult neurogenesis.
MAM= methyazoxymethanol acetate.

Two methods of manipulating adult neurogenesis are of particular interest and will be discussed in detail. These methods are cytosine-B-D-arabinofuranoside (AraC) infusion, and electroconvulsive shock (ECS).

1.2.5.1 *AraC infusion*

AraC is a synthetic puridine analogue which is incorporated into the DNA of actively dividing cells. The drug is sufficiently similar to cytosine deoxyribose to be incorporated into DNA, but different enough to subsequently kill the cell via apoptosis. [Dietrich et al. 2006] Accordingly AraC functions primarily as an antimitotic drug. This property has led many investigators to use AraC to ablate mitotically active NSPCs in the adult mammalian brain. **Table 1** summarises my search for studies that used AraC to interrogate aspects of hippocampal functioning. Studies using AraC to examine other intracerebral processes (for example neurogenesis in the SEZ, or post-stroke recovery) were excluded.

Ref.	Animal	Question	n	AraC %	Location	Infusion	Rand	Blind	Result
Fagan et al. 1994	Rats	Does glial cell proliferation mediate cholinergic sprouting in the ML after perforate pathway lesion?	4-9	0.1	i.c.v.	4-14d	n.s.	n.s.	Cholinergic sprouting post-PP lesioning was independent of cellular proliferation.
Seri et al. 2001	Mice	What SGZ cell types incorporate BrdU, and what are the temporal dynamics, after AraC + Procarbazol treatment?	5	1.5	Brain surface	7d	n.s.	n.s.	Type B' cells form the majority (>90%) of Brdu+ cells in SGZ on Day0 and Day2 following AraC/Procarbazol. By Day4, 'Type D' cells (likely very early TAPs) have reappeared. Equilibrium with controls is reached after 15 days
Jung et al. 2004	Rats	Does neurogenesis mediate the development of new seizures following experimentally induced epilepsy?	6-9	2	i.c.v.	14d	n.s.	n.s.	AraC infusion was associated with reduced likelihood of recurrent seizures
Becq et al. 2005	Mice	Does prior anti-mitotic treatment ablate the seizure-induced increase in proliferation seen following administration of Kainic acid?	3-9	15mg/kg	i.p.	n.a.	n.s.	n.s.	AraC weakly attenuated seizure-induced neurogenesis when administered four days prior to Kainic acid, but had no effect when administered 30 days prior.
Dietrich et al. 2006	Mice	Do i.p. injections of AraC have a cytotoxic effect on the DG, how soon after administration, and upon what cell types?	3	250mg/kg	i.p.	n.a.	n.s.	n.s.	AraC injections cause an increase in TUNEL+ cells in the DG on day 1 post-injection regime, but not thereafter. Conversely, reduction in BrdU uptake is not seen until late follow-up (here day 56). Only BrdU is co-stained in vivo; DCX was reduced at day 56.
Colon-Cesario et al. 2006	Mice	Is memory consolidation sensitive to the DNA-disrupting	12-15	1g/kg; 1mM	i.p. CA3	n.a. 1h	n.s.	n.s.	Systemic and localised AraC, administered shortly before learning, impaired early and late consolidation of

		effects of systemic and localised (intrahippocampal) AraC?							fear memory. Memory reconsolidation following intact initial learning was unaffected.
Mak et al. 2007	Mice	Does neurogenesis mediate mating behaviour?	6	2	i.c.v.	7d	n.s.	Yes	AraC abolished the preference of females for dominant male pheromones
Li et al. 2008	Rats	Is recent and remote spatial memory affected by AraC, with respect to possible cytotoxic effects in post mitotic regions (CA1 and the anterior cingulate cortex)?	20	400mg/kg	i.p.	n.a.	Yes	Yes	AraC impaired remote, but not recent memory in a spatial memory task. No morphological changes could be seen in area CA1 neurons, but neurons in the ACC showed reduced dendritic length, spine density, and branch points.
Hodge et al. 2008	Mice	What are the temporal dynamics of recovery of Tbr2+ IPs after AraC?	3-4	1.5	i.c.v.	7d	n.s.	n.s.	Following AraC, Tbr2+ cells were initially ablated at D0, recovered to control levels by D5, showed a significant rebound increase by D15 post-infusion, and returned again to control levels by D30.
Lau et al. 2009	Rats	Does neurogenesis mediate hippocampal pre-pulse inhibition (PPI)?	7-10	2	i.c.v.	3-16d	n.s.	n.s.	Ablation of neurogenesis by AraC disrupted PPI.
Gobeske et al. 2009	Mice	Does cellular proliferation mediate the cognitive gains seen in mice with transgenic reduction of BMP signalling?	10	2	i.c.v.	15d	n.s.	Yes	AraC was associated with poorer performance than controls on the MWM, in BMP-inhibited mice, suggesting a role for cellular proliferation in the enhanced cognitive phenotype of that strain.
Li et al. 2010	Mice	Does neurogenesis mediate brain repair mechanisms following ischaemia?	10	2	i.c.v.	7d	Yes	Yes	AraC infusion was associated with increased CA1-3 neuronal loss, and worsened neurological function

Sultan et al. 2010	Mice	Is neurogenesis essential for long-term retention of olfactory learning?	10	4	i.c.v.	21d	Unclear	Yes	The retention of olfactory learning was abolished by AraC infusion before and during the learning period, but acquisition was not affected.
Yau et al. 2011	Rats	Does neurogenesis mediate the beneficial effects of running?	8-10	2	i.c.v.	28d	n.s.	Yes	AraC infusion diminished the effect of running on spatial learning and depression-like behaviour in 40 mg/kg CORT-treated animals
Zhang et al. 2012	Rats	Does neurogenesis mediate the antidepressant effect of wolfberry?	6	4	i.c.v.	28d	n.s.	Yes	Ara-C infusion did not prevent the antidepressant effects of Wolfberry
Lau et al. 2012	Rats	Does neurogenesis mediate the pro-sexual effects of wolfberry following corticosterone administration?	n.s.	n.s.	i.c.v.	7d	Yes	Yes	Ara-C infusion abolished the pro-sexual effects of Wolfberry
Zhang et al. 2012	Rats	Does neurogenesis mediate spatial learning following TBI?	6-7	2	i.c.v.	14d	n.s.	n.s.	AraC abolished EPO-promoted increases in all three of DG proliferating cells, new neurons and spatial learning following TBI
Walton et al. 2012	Mice	Does neurogenesis mediate oxidative stress in the SGZ?	3	2	i.c.v.	3d	n.s.	n.s.	Markers of oxidative stress (oxidised DNA and lipids) were reduced in Ara-C treated SGZ
Wu et al. 2012	Rats	What is the extent of regenerative neurogenesis after AraC ablation, in ageing rats which have received icariin?	3	2	i.c.v.	7d	n.s.	n.s.	Treatment with icariin was associated with increased density of GFAP+Brdu+, PSA-NCAM+, and Olig2+BrdU+ cells seven days after ablation by AraC.
DeCarolis et al. 2013	Mice	Do RGLs in Glast-cre-YFP mice and Nestin-cre-YFP mice	3-8	2	i.c.v.	7d	n.s.	Yes	RGCs in GLAST-Cre/YFP mice contributed to regeneration post-AraC, but RGCs labelled in Nestin-Cre/YFP mice did not.

		contribute similarly to neurogenesis?							
Monteiro et al. 2014	Mice	Does neurogenesis mediate social memory, in isolation and an enriched environment?	n.s.	2	i.c.v.	7d	n.s.	n.s.	AraC infusion was associated with blunting of social memory 'rescue' seen in socially isolated mice that were also exposed to an enriched environment
Gomez-Nicola et al. 2014	Mice	Does neurogenesis mediate the selective initial sparing of the DG observed during the course of chronic neurodegeneration?	4	2	i.c.v.	28d	n.s.	n.s.	Depletion of neurogenesis abolishes the selective preservation of the DG during the course of prion disease, suggesting that neurogenesis is integral to maintaining DG structure and synaptic connectivity during these illnesses.
Sun et al. 2015	Rats	Does neurogenesis mediate spatial learning and memory following TBI?	21-25	2	i.c.v.	7d	n.s.	Yes	Inhibition of TBI-induced proliferation in the week after injury impairs spatial learning after 35 and 60 days. AraC alone (without TBI) also adversely affected cognitive performance, transiently
Mohammed et al. 2016	Mice	Does neurogenesis mediate the anxiolytic effects of JNK-1 inhibition?	6-7	2	i.c.v.	42d	n.s.	n.s.	The anxiolytic effects of JNK1 inhibition were blocked by AraC, suggesting a role for neurogenesis in mediating this effect.
Apkarian et al. 2016	Mice	Does neurogenesis mediate sensitivity to experimentally-induced chronic pain?	2-10	2	i.c.v.	14d	n.s.	Yes	A reduction in tactile allodynia was seen during AraC infusion. This effect disappeared six days after pump removal, suggesting that neurogenesis mediates elements of chronic pain.
Pereira-Caixeta et al. 2017	Mice	Does neurogenesis mediate the pro-cognitive effects of an enriched environment?	6	2	i.c.v.	7d	n.s.	n.s.	The enhancement of social recognition by an enriched environment was ablated by AraC, suggesting a role for neurogenesis in mediating the cognitive effects of EE.

Table 1. Studies examining the effect of AraC on the adult rodent hippocampus.

What I concluded from this search was that AraC has generally been used with the aim of determining whether hippocampal neurogenesis is an essential mediator of a given outcome in a given experimental condition. These studies generally start with some kind of external manipulation (an illness or treatment model such as ischaemia, epilepsy, trauma, stress, running, antidepressants, herbal remedies, and experimentally-induced pain, among others), and ask whether the response of a homeostatic process (such as oxidative stress, social memory, spatial memory, sexual behaviour, and anxiety) to the manipulation depends on neurogenesis. So for example Pereira-Caixeta and colleagues used intra-cerebro-ventricular (icv) AraC infusion to propose that enriched environment, which improves social recognition memory in adult mice, depends on hippocampal neurogenesis for its effect. [Pereira-Caixeta et al. 2017]

In general my difficulty with interpreting studies of this nature is that they cannot exclude an antimitotic effect in other brain areas as an explanatory mechanism. For instance it is impossible to uncouple ablation of NSPCs in the SGZ from those in the SEZ using icv administration of AraC, because the drug is active everywhere in the brain. A second related objection is that AraC is likely to affect not only neurogenesis but any proliferating cellular population in the CNS including endothelial cells, oligodendrocyte precursor cells, microglia, and pericytes. It is therefore a rather blunt tool which confounds attempts to attribute an observed effect specifically to hippocampal neurogenesis.

There is a small literature that side-steps these problems by using AraC in a different way. In this second group of studies the hippocampal regenerative response to AraC is itself the question under study in terms of NSPC subpopulations, temporal dynamics of proliferation, and consequences of different routes of administration. These studies tell us simply what AraC does to hippocampal neurogenesis, and consequently are easier to interpret. In summary they suggest that AraC markedly ablates SGZ NSPC proliferation [DeCarolis et al. 2013, Hodge et al. 2008, Seri et al. 2001], and that this is probably followed by rebound proliferation in the period 4-15 days post-infusion. [Seri et al. 2001, Hodge et al. 2008, but note DeCarolis 2013] These few studies provide limited evidence to suggest that AraC could perhaps be used to study the sequential regeneration of NSPCs in a temporally predictable manner.

1.2.5.2 *Electroconvulsive shock*

Electroconvulsive shock (ECS) is generally considered to be the rodent analogue of electroconvulsive therapy (ECT) in humans. As such it is an experimental model of potential clinical relevance, as well as being relatively accessible in terms of the technical skill and equipment required. That ECS induces neuroplastic changes in the rodent hippocampus has been recognised for well over 20 years. Initially researchers - seeking perhaps to model the human analogue of ECT - generally delivered ECS in a series of multiple shocks, in studies which often used physiological read-outs of synaptic plasticity and long-term potentiation.

In recent decades abundant evidence has accrued however that the molecular and cellular impact of multiple shocks on the rodent DG differs from that of a single shock. [Ryan et al. 2017, Weber et al. 2013, Guo et al. 2011, Ma et al. 2009, Zetterstrom et al. 1998, Nibuya et al. 1995] These data support the notion that although related, the two model conditions are not merely interchangeable at fundamental levels. Reasoning that a single shock is simpler and may be less stressful for animals than multiple shocks, I sought evidence that a single shock is sufficient either to induce adult hippocampal neurogenesis or otherwise to alter the DG biological system in vivo **(Table 2)**.

Author	Species	Strain	Age	Timepoint(s)	Key findings	Suggesting that (authors' interpretation)	My additional thoughts
Nibuya et al. 1995	R	Sprague-Dawley	Not stated	2h, 18h	A single shock differentially upregulated BDNF and TrkB after in the DG GCL at 2h, but not at 18h. This contrasted with chronic ECS, where BDNF levels were up-regulated to a slightly lesser extent, but the effect was still significant at 18h.	Compared to a single ECS, repeated ECS induces adaptive molecular changes in the DG.	As authors. Single and repeated ECS have distinct transcriptional profiles at a given time-point in the hippocampus.
Zetterstrom et al. 1998	R	Sprague-Dawley	Not stated	6h, 1d, 2d, 21d	A single shock differentially up-regulated BDNF in the DG GCL at 6h, but levels had returned to baseline by 24h. This contrasted with chronic ECS where BDNF levels were up-regulated to a slightly lesser extent, but the effect persisted for longer.	Compared to a single ECS, repeated ECS induces adaptive molecular changes in the DG.	As authors. Single and repeated ECS have distinct transcriptional profiles at a given time-point in the hippocampus.
Madsen et al. 2000	R	Wistar	'Adult'	1d, 3d, 5d, 7d, 21d, 1 month, 3 months	Maximal cell proliferation occurred 3-5 days post a single shock. A single shock induced significant neurogenesis which persisted for at least 3 months. There was a dose response with repeated ECS leading to more neurogenesis.	Cerebral seizure activity induces neurogenesis.	As authors - a simple study with a convincing conclusion.

Valentinea et al. 2000	R	Sprague-Dawley	Not stated	2h, 6h	Fmrp mRNA was upregulated in the DG 6h after a single shock.	ECS may unmask relevant activity-dependent regulatory mechanisms that modulate *fmr1* gene transcription in vivo.	Relevance to neurogenesis is not studied.
Hellsten et al. 2002	R	Wistar	'Adult'	d7	Following two weeks of corticosterone injection, a single shock normalised BrdU-assayed GCL proliferation (in the window of d2-7 post-shock), to the basal level of proliferation and neuronal phenotype seen in vehicle-injected, sham-treated rats.	A single ECS normalises CORT-induced deficiencies in SGZ proliferation.	Whether the data are specific to the SGZ, and indeed how the SGZ might have been defined in this study, is unclear.
Newton et al. 2003	R	Sprague-Dawley	Not stated	2h, 6h	Following a single shock, a custom-built growth factor microarray found differential expression of an unspecified number of genes in the hippocampus, or which 9 were validated at the mRNA level and 5 at the protein level by the authors. Significance included genes for growth factor signalling, angiogenesis, neurotransmitter signalling, transcription factors, and kinases.	The therapeutic effects of ECS could be mediated by several signaling cascades, including neurotrophic–growth factors and angiogenic systems.	Although the authors' conclusions seem valid, use of a custom chip means the study is at high risk of bias. RNA was also extracted from whole hippocampi rather than the SGZ, so the signal from genes important for neurogenesis may have been missed in the noise, although ISH validation did provide some DG-specific data for a select group of genes.

Wennstrom et al. 2003	R	Wistar	'Adult'	d2, d4, d6, d7, d8, d21	A single shock induced proliferation of NG2+ glia in the GCL, but to a much greater extent in the Hilus and ML. In all DG subregions, proliferation was greatest at D2 post-shock. After three weeks, many cells which had been proliferating at D2-4 retained NG2+ expression, although this effect was again far stronger in the ML and Hilus than in the GCL, where nearly all BrdU label-retaining cells expressed NeuN.	A single ECS induces glial cell proliferation in the DG (primarily in the ML and Hilus) alongside neurogenesis.	The cellular identify and function of these NG2+ glia remains to be determined.
Hellsten et al. 2004	R	Wistar	Adult'	2d, 4d, 6d, 8d	A single shock induced RECA+ cell proliferation in the ML, GCL, SGZ, and hilus, which was most pronounced at D2 post shock. There was again a fairly linear dose response. The peak of RECA+ proliferation occurred slightly before the peak of SGZ clusters (D4), and showed a greater dynamic range (x14) than NSPCs (x3). No evidence was found for loss of EBA staining post ECS.	ECs induces proliferation of hippocampal microvascular endothelial cells, with no evidence found for sustained blood-brain-barrier breakdown.	As authors. Whether EBA staining is sufficient to demonstrate BBB integrity is not clear.

Altar et al. 2004	R	Sprague-Dawley	4-6 months	4h	Following a single shock, Affymetrix U34A microarray found differential expression of 79 genes in the hippocampus, of which 23 were validated by the authors.	A paper 'of record' which lists gene changes rather than exploring a specific biological pathway.	False Discovery Rate p values seemingly not reported. Note also data from whole hippocampus rather than SGZ, meaning that the signal to noise ratio of genes implicated in neurogenesis could have been very low.
Banerjee et al. 2005	R	Sprague-Dawley	Not stated	2h, 4h, 6h, 1d	A single shock increased the expression levels of Ptc mRNA, and down-regulated Smo mRNA in the DG, with no impact on Shh mRNA or protein at 2h. The upregulation was transient: Ptc returned to baseline by 4h, Smo by 24h. Neither change was observed in the SEZ. Interestingly Cyclopamine infusion prevented ECS-induced SGZ proliferation.	Shh signalling mediates ECS-induced neurogenesis.	A novel method of countering the proliferative response to ECS (Cyclopamine), although presumably not at all specific to NSPCs in its biological effects. One might be better with an iKO of signaling pathways in NSCs.
Ma et al. 2009	M	C57Bl/6	6-8 weeks	1h, 4h, 3d	A single shock induced demethylation within the regulatory region IX of Bdnf and the brain-specific promoter B of Fgf-1. CHiP analysis showed specific binding of Gadd45b to the *Bdnf* IX and *Fgf-1B* regulatory regions. Demethylation at 4h, mRNA/protein expression of Bdnf and Fgf-1 at 4h, and the proliferative response to s-ECS at D3 post-shock, were	After a single shock *Gadd45b* is essential for gene-specific local demethylation and later-onset expression of Bdnf and Fgf-1 in the adult dentate gyrus. *Gadd45b* has an essential role in activity-induced, but not basal dynamics.	As authors. Note the time-course of demethylation (rapid within 4h, gradually recovering but not quite to baseline by 24h; a second shock at 24h therefore inducing demethylation to a slightly greater extent). This provides a possible model for explaining why repeated shocks induce longer-lasting protein changes. (see also Guo et al. 2011 for a broader corroboration of this)

					found to be dependent upon Gadd-45b.		
Ohtomo et al. 2011	R	Wistar	Not stated	1h, 3h, 6h, 12h, 1d, 2d, 3d	YARP mRNA was unchanged after a single shock, but differentially regulated after chronic ECS.	YARP mRNA is significantly decreased after repeated ECS, not single ECS	Single and repeated ECS have distinct transcriptional profiles at a given time-point in the hippocampus (repeatedly shown elsewhere too).
Guo et al. 2011	M	C57Bl/6	8-10 weeks	4h, 1d	Following a single shock, c.1.4% of CpGs in the DG showed rapid demethylation or *de novo* methylation. Genes were associated with brain-specific genes related to calcium signalling, neuronal plasticity, Notch signalling, and LTP. A significant number of CpGs showed sustained changes at 24h post-shock. Pretreatment with an NMDAr blocker largely abolished methylation changes in selected genes. A single shock did not cause significant inflammation of Iba1+ microglia.	A large number of CpGs are rapidly modified by a single shock. The DNA modifications are due (at least in selected cases) to NMDAr-dependent neuronal activity, and relatively long-lasting. Epigenetic DNA methylation in the adult brain is inducibly reversible by neuronal activation and behavioural stimulation.	As authors. Role of DG GCL neuronal methylation changes in neurogenesis (in depressed mice) would be an interesting 'upstream' study.
Yanpallewar et al. 2012	M	C57Bl/6	Not stated	<1d; 3d	A single shock increased mRNA expression of the scaffold protein Tamalin 1-12h post-shock, peaking at 3h. This effect was specific to the	That Tamalin - which is not required for neurodevelopment - may still be a critical factor in many pathways which	This study highlights the interesting concept of a protein that is only expressed and functionally activated following ECS. But it is

					hippocampus. Tamalin was essential for the 72h BrdU/PCNA proliferative, DCX+ NB, and BrdU-birthdated 28 day NeuN+ neurogenesis response to a single ECS.	mediate ECS effects. That ECS-induced Tamalin upregulation causes the assembly of signaling complexes that are required to promote proliferation, neurogenesis, and neuronal sprouting after ECS.	difficult to be sure that the Tamalin KO is pure - could there be compensatory upregulation of other proteins, or secondary knock-on LOF which confound the interpretation?
Nakamura et al. 2013	R	Sprague-Dawley	'Adult'	3d, 14d	A single shock robustly increased the number of BrdU+ proliferating cells in the SGZ four days post-shock, but significantly suppressed acute SGZ proliferation at the timepoint of 14 days post-shock.	ECS induces a biphasic response. Postulate a reduction in proliferation affecting IPs/NBs rather than NSCs.	A possible explanatory mechanism would be that the reduction in proliferation (which, in passing, has not been reported before) could be secondary to increased negative feedback signalling from the already expanded NB population.
Weber et al. 2013	M	Transgenic (see text)	P60	d3, d6	A single shock significantly increased the number of Ki67+Type 1 aNSC at D3 and D6 post-shock. It also caused a significant increase of the total population of previously GFAP-GFP fate-labelled NSCs.	A single shock activates adult hippocampal neural stem cells.	Best current evidence that a single shock activates RGLs. However whether a single shock led to increased neurogenesis in daughter cells of GFAP-GFP+ NSCs was not reported.
Ryan et al. 2013	R	Sprague-Dawley	Not stated	4h	A single shock differentially up-regulated the BDNF-associated miRNA miR212 in the DG, but not the hippocampus entire.	Upregulation of miR-212 in the dentate gyrus may contribute to the behavioural response to ECS but this requires further investigation.	As authors. Relevance to neurogenesis is not studied.

Otabe et al. 2014	R	Sprague-Dawley	42	4h	Two shocks (single shock was not studied) induced autophagy signalling molecular pathways. There was a fairly linear dose response with further shocks inducing a stronger response.	Enhanced autophagy signalling may contribute to post-ECS neuroplasticity.	Relevance to neurogenesis is not studied.
Glaviano et al. 2014	R	Sprague-Dawley	Not stated	4h	A single shock differentially regulated 150 acute phase plasma (blood) proteins, of which 12 were identified by mass spectrometry, although none could be validated independently. Two acute phase proteins were validated following repeated ECS.	Haptoglobin and apolipoprotein A-IV are potential candidate peripheral markers of response to ECS administration.	The rats were not 'depressed' so the significance of the findings as 'markers of response' is unclear. Single and repeated ECS have distinct proteomic profiles at a given timepoint in peripheral blood.
O'Donovan et al. 2014	R	Sprague-Dawley	Not stated	4h	A single shock differentially regulated 67 hippocampal proteins in a proteomic analysis, of which 5 were identified by MS, and none validated.	ECS induces widespread changes in the hippocampal proteome, in mainly cytoskeletal and metabolism related proteins.	Relevance to neurogenesis is not studied. Further studies required on the SGZ proteome following ECS.

Husain et al. 2015	M	C57Bl/6	Not stated	1d	A single shock tripled the proportion of NesGFP+ cells that co-express GFAP in the SGZ.	Acute ECS increases the number of quiescent NSCs.	Quiescence is not demonstrated and where the huge increase in 'NSC' numbers would come from within a day is never addressed. Increased expression of GFAP is a consistent finding after s-ECS but its meaning remains unclear.
Jun et al. 2015	M	C57Bl/6	8-10w	3d	Gadd45b critically mediates the MCM2+ proliferative response to a single shock.	Gadd45b activity-dependent demethylation of BDNF and FGF may underlie RGL activation following ECS.	Convincing result at the time-point studied, though whether the KO is behaviourally relevant (e.g. in recovery from the depressed state), and the effects of chronic ECS, were not reported.
Ryan et al. 2017	R	Sprague-Dawley	Not stated	4h	Hippocampal PEDF mRNA levels were unchanged after a single shock, but differentially regulated after chronic ECS.	Chronic, but not acute, ECS induces alterations in PEDF levels.	Single and repeated ECS have distinct transcriptional profiles in the hippocampus (repeatedly shown elsewhere too).
Su et al. 2017	M	C57Bl/6		1h, 4h, 1d	Following a single shock, genome-wide changes in DG chromatin accessibility were seen 1 h after activation, with enrichment of accessibility at active enhancer regions and at binding sites for AP1-complex components, including c-Fos.	A single shock causes chromatin accessibility changes, enriched at active enhancer regions, which in turn govern DG gene expression.	As authors. Role of DG GCL neuronal chromatin changes in neurogenesis (in depressed mice) would be an interesting 'upstream' study.

Table 2: Studies examining a single electroconvulsive shock in the rodent hippocampus.

Summarising this search, the first demonstration that a single shock induces proliferation in SGZ NSPCs was obtained in rats using a BrdU fate labelling strategy. [Madsen et al. 2000] In mice meanwhile, the most persuasive evidence has come from transgenic reporter technology, with the authors convincingly demonstrating that a single shock triggers activation of SGZ GFAP+ RGLs, the lineage descendants of which are newborn neurons. [Weber et al. 2013] The key finding of both these sentinel studies - that a single shock is sufficient to stimulate hippocampal neurogenesis in otherwise healthy rodents - has been independently replicated many times. [Jun et al. 2015, Nakamura et al. 2013, Yanpallewar et al. 2012, Ma et al. 2009, Banerjee et al. 2005, Hellsten et al. 2002] Interestingly, new neurons born as a result of a single shock may still be detected in the GCL three months after the stimulus [Madsen et al. 2000], suggesting that a single shock may have functional relevance in the adult brain.

As well as promoting neurogenesis, a number of groups have deployed a single shock strategy to explore molecular mechanisms that may underlie the proliferative response of NSPCs to the stimulus. A detailed review of these mechanisms is out-of-scope here (see Ch. 6 for further discussion), but in summary it is apparent that a single shock induces profound alterations in the DG at epigenetic [Su et al. 2017, Jun et al. 2015, Guo et al. 2011, Ma et al. 2009], transcriptional [Ryan et al. 2013, Yanpallewar et al. 2012, Banerjee et al. 2005, Altar et al. 2004, Newton et al. 2003, Valentinea et al. 2003], and protein levels [Yanpallewar et al. 2012, Ma et al. 2009, Banerjee et al. 2005, Newton et al. 2003], as well as responses in granule cell neuronal [Su et al. 2017, Guo et al. 2011, Ma et al. 2009], glial [Wennstrom et al. 2003] and endothelial cellular compartments [Hellsten 2004] alongside the response of NSPCs. Many of the molecular changes occur rapidly after the stimulus, as early as 1h post-shock [Su et al. 2017], with effects persisting for a variable duration. [Guo et al. 2011, Ma et al. 2009]

Therefore as a result of these searches, I anticipated that both AraC and a single ECS could be used as experimental models to manipulate hippocampal neurogenesis in vivo.

1.3 The neurogenic niche and extracellular matrix

1.3.1 Hippocampal neurogenesis occurs in a neurogenic niche

The mechanisms by which the SGZ offers a permissive milieu to neurogenesis remain to be fully clarified. One likely factor is that as well as harbouring a specialised population of NSPCs, local microenvironmental characteristics in the SGZ may preferentially support neurogenesis. This permissive local milieu can be considered a "neurogenic niche" to which diverse cellular and molecular components are likely to contribute.

For instance the SGZ is located adjacent to a rich network of blood vessels. [Palmer et al. 2000] A microvascular plexus runs its length and breadth, and these capillaries closely associate with NSPCs in the SGZ. [Sun et al. 2015] The radial processes of RGLs also extend through the GCL and make direct contact with blood vessels in the ML. [Moss et al. 2016] Although the precise functional roles of the microvasculature remain to be fully clarified, endothelial cells are well recognised to secrete neurotrophic growth factors, perhaps the best example in this context being BDNF. [Ehret et al. 2015, Ma et al. 2009, Zetterstrom et al. 1998] An instructive role for blood vessels in neurogenesis is further suggested by the findings that microvascular expansion is associated not only with increased hippocampal neurogenesis [Licht et al. 2011] but also attenuation of its usual age-associated decline. [Licht et al. 2016]

Other components of the niche have been implicated in the regulation of hippocampal neurogenesis. These components include astrocytes [Ashton et al. 2012, Cao et al. 2013], microglia [Sierra et al. 2010, Vukovic et al. 2012], pericytes [Ehret et al. 2015], interneurons [Song et al. 2013], locally secreted factors (see **Figure 3**), soluble factors derived from systemic blood [Villeda et al. 2011], and a differential oxygen tension. [Zhang et al. 2015] Detailed review of these components of the neurogenic niche is beyond the scope of this introduction. However, a further key component of the neurogenic niche, to which I will now turn, is the extracellular matrix.

1.3.2 The role of extracellular matrix in neurogenesis

Extracellular matrix is essential for multicellular life. It is in very basic terms an interlocking mesh of modular glycoproteins, collagens, and proteoglycans whose primary function is to provide structural support to cells. However the whole is considerably more complicated. The 'matrisome' is a consensus list first proposed by Hynes and colleagues to represent the entire repertoire of ECM proteins in mammals. This list contains 1098 genes divided into a "core matrisome" of 274 glycoproteins, collagens, and proteoglycans, and a further group of 824 matrisome-associated proteins, regulators and secreted factors. [Naba et al. 2012] The list entire excludes many proteases, growth factors and cytokines, although these molecules may also interact with ECM.

The role of ECM signalling in the regulation of adult hippocampal neurogenesis is considerably less well understood than is the case for neurodevelopment and, to some extent, the adult subependymal zone. I wanted to better understand the extent and depth of current knowledge about the role of ECM signalling in neural stem cell regulation. I conducted a systematic search for studies describing any relationship with NSCs for each of the genes in the core matrisome (see **Box 2**). The results give an instructive (if introductory) overview of the general landscape of knowledge **(Figure 5)**.

I began by listing the 274 core matrisome genes as described by Naba et al., 2012. Each gene was then processed through several distinct searches which collectively captured high-quality peer-reviewed studies and agnostic datasets.

Each matrisome gene was input separately to Pubmed using the Boolean search string: *"Gene"* AND (neural or NSC or SGZ or subgranular or SEZ or subependymal or dentate or stem). I reviewed all titles and abstracts captured by this search to determine eligibility. Included as eligible were all studies of mammalian NSPCs in developmental, post-natal, and adult models; both in vitro and in vivo. Excluded were studies of NSPCs in non-mammalian systems (e.g. chick, zebrafish), or studies of NSPCs in conditions of injury or disease. I obtained the full text of all eligible studies and summarised the results in a narrative review.

Additionally, each was separately examined using the "Pubmed Gene" curated publication list for the model *Mus musculus*. The same review and selection procedures were followed as outlined above.

In recognition that Pubmed and Pubmed Gene are selected and/or curated samples of available knowledge, I added an agnostic element to the search. For this, each gene was individually examined using the Allen Mouse Brain Atlas for in situ hybridisation (ISH) signal in the adult Dentate Gyrus. Signal was qualitatively judged as strong (+++), medium (++), weak (+), or absent. The spatial location of the signal within the DG (SGZ, GCL, Hilus) was also recorded with the aim of identifying matrisome genes expressed directly within the neurogenic SGZ versus within the neighbouring areas.

Box 2: Systematic search strategy: matrix genes and neurogenesis.

When conducting the search, the laminins, collagens, and fibronectin posed particular difficulties owing to their ubiquitous use in culture systems. Thousands of studies have used these proteins as a technical substrate for in vitro experiments with neural stem cells, making it difficult if not impossible to demarcate their effects from those of whichever (unrelated) experimental system was deployed in parallel. Additionally with respect to laminin and collagen, many in vitro studies simply report their generic use without specifying which laminin(s) or collagen(s) were used (see Joo et al. 2015, Arulmoli et al. 2015, and Moeton et al. 2014 for but three recent examples of this). A third difficulty was that laminins are heterotrimeric molecules comprised of an α, β, and γ chain. Even a seemingly 'specific' laminin such as the widely-used Laminin 1 is therefore the product of three separate genes (in the case of Laminin 1: Lama1, Lamb1, and Lamc1), making attribution of a given effect to a single gene impossible unless this is the question under direct study. To get round these rather murky problems I restricted my review of the various laminin, collagen and fibronectin genes to studies with an a priori focus on the same and which specified precisely which gene product was being studied.

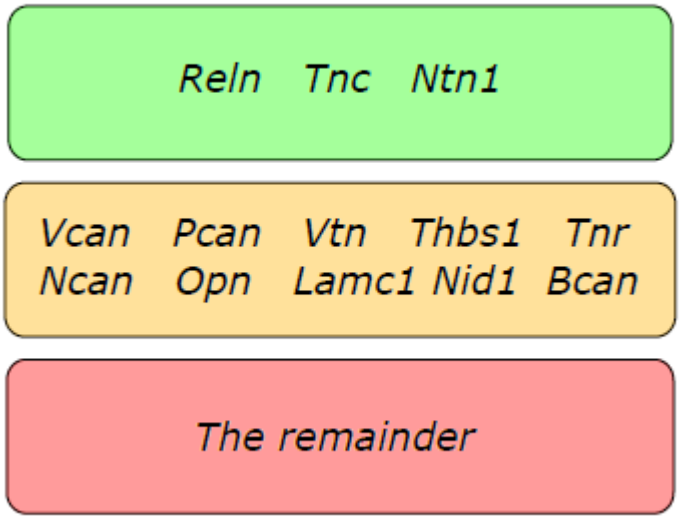

Figure 5. Summary of knowledge of matrisome in relation to neural stem cell biology. Three genes have been well-studied (>10 publications) with knockout mice*: Reelin, Tenascin C,* and *Netrin-1*. Another ten genes are relatively well-understood (>3 publications) from a variety of methodologies including simple expression studies: *Versican, Perlecan, Vitronectin, Thrombospondin 1, Tenascin R, Neurocan, Osteopontin, Laminin γ1, Nidogen1,* and *Brevican*. Knowledge of the role of the remaining core matrisome in neurogenesis is sparse or absent.

I was surprised to find that of 274 genes in the core matrisome, only 57 had been studied in relation to neural stem cell regulation. Of these, only 32 were the subject of more than one publication. One way of looking at this result is that the global scientific community knows almost nothing about how almost 90% of ECM glycoproteins, collagens and proteoglycans contribute to neural stem cell biology. If the existence of four studies is taken as a permissive indication of "good understanding" of a given gene, then one may argue that life scientists have a good understanding of less than 5% of the potential contribution of core ECM genes. For adult neurogenesis specifically the figure is even lower. This knowledge deficit provides a clear rationale to study the functional role of ECM in adult hippocampal neurogenesis.

1.3.2.1 Special cases: laminin, collagen and fibronectin

The laminin family provides a major culture substrate for NSCs. It is widely recognised that "laminin" in a general sense is relatively permissive for NSC proliferation, differentiation,

survival, and migration. However as alluded to above, the most widely-used culture systems have used either human placental laminin or else specific laminin isoforms (such as laminin 1 or laminin 10), none of which are monogenic. Indeed as regards neurogenesis, and considering how familiar laminin is to neural stem cell biologists, specific laminin gene products have been surprisingly sparsely studied. I will however discuss them here as a group.

Laminin α2 (Lama2), **laminin α 4** (Lama4) and **laminin β 2** (Lamb2), but not **laminin α 1** (Lama1) proteins are expressed during cortical development in the mouse, with higher levels of Lama4 and Lamb2 near the neurogenic ventricular surface in particular. [Lathia et al. 2007] Although one might suppose that each gene is functionally critical, there appears to be a degree of biological redundancy within the laminin family. Mice with mutations in either the Lama2 or Lama4 subunit genes do not show any obvious defect in cortical size and morphology. In α2/α4 double mutants however, cortical size is significantly smaller. These double mutants show detachment of RGC processes from the meningeal basement membrane (BM) and increased apoptosis throughout the embryonic ventricular neuroepithelium. [Radakovits et al. 2009] Interestingly, similar α subunit redundancy is shown in the adult brain, where Lama2, and Lama4 mRNA and/or protein is highly expressed by cells in the SEZ and RMS, with ablation of both genes being required to show RMS disruption. [Belvindrah et al. 2007] Similarly too, **laminin b2** (Lamb2) / **laminin c3** (Lamc3) double mutants display a disrupted pial BM, with abnormal development of radial glial cells and disruption of RGC pial attachment. The developmental consequences of these defects include prominent disruption of the orderly boundary between layers 1 and 2 in the cerebral cortex with malpositioned cortical neurons. [Radner et al. 2012]

A few laminin family genes, however, appear to have critical functions in neurodevelopment that cannot be compensated. **Laminin B1** (LAMB1) is also expressed in the pial basement membrane and its monogenic deficiency causes cobblestone lissencephaly. [Radmanesh et al. 2013] **Laminin c1** (Lamc1) meanwhile is expressed (together with Lamb1) by fractones in the adult mouse SEZ [Kerever et al. 2007] and may interact with Netrin-4 to trigger α6-β1 integrin-mediated signalling [Staquicini et al. 2009]; its deficiency causes aberrant migration and neuronal differentiation during late stages of embryonic neurodevelopment in mice. [Haubst et al. 2006]

Because many laminin isoforms are major ligands for the integrin family of cell-surface receptors, some authors have used integrin-blocking antibodies (e.g. those to α6 or β1 integrins) to interrogate a possible in vivo role for "laminin" in regulating NSCs. [Kazanis et al. 2010, Loulier et al. 2009, Shen et al. 2008, Ma et al. 2008, Flanagan et al. 2006]. Positive results in these studies are not inconsistent with 'laminin family' regulation of NSCs, but cannot by themselves specify the critical laminin gene products involved. The last decade has however seen the facility to culture cells on precisely molecularly-defined recombinant laminins. Such studies propose, for instance, a necessary role of **laminin α 5** (Lama5) rather than other laminin α subunits in maintaining embryonic stem cell self-renewal [e.g., Domogatskaya et al. 2008]. In a similar fashion, Lama5 and Lama1 are thought to differentially promote neurite outgrowth from adult mouse peripheral neurons. [Plantman et al. 2008] Intriguingly, intersecting the results of these precise dissections with other in vivo studies could reveal clues about the composition of the adult neurogenic niches. For instance, Plantman et al. also reported that integrin α6-β1 preferentially binds laminin 8 (laminin α 4, β 1, γ 1) and laminin 10 (α 5, β 1, γ 1), thereby isolating the Lama4 and/or Lama5 genes as the potential critical mediators of NSPC-blood vessel adhesion in the adult SEZ. [Shen et al. 2008] These studies raise the future prospect of dissecting the contributory role of each laminin gene product to NSC biology.

Collagen is analogous to laminin in the technical sense that perhaps the most widely-used collagen substrates in vitro are the product of more than one gene. Collagen Type 1 is composed of **Collagen type 1 α 1** (Col1a1) and **Collagen type 1 α 2** (Col1a2). Collagen Type 4, meanwhile, is the product of six genes: **Collagen type 4 α 1-6**. With these caveats Collagen Type 1 has been shown in vitro to differentially promote the formation of neural rosettes from human embryonic stem cells, as compared to Poly-D-Lysine substrates, although not as strongly as a cryptic mixture of laminins. [Ma et al. 2008] Interestingly the stiffness of collagen matrix may influence migration of the progeny of NSPCs. GFAP+ astrocytes differentiated from embryonic cortex-derived NSPCs were reported to migrate faster on stiff than on soft Type 1 collagen artificial matrices. [Mori et al. 2013] Meanwhile Collagen Type 4 is reported to differentially restrict proliferation and promote differentiation of cultured neural stem cells derived from both the embryonic rat cortex [Ali et al. 1998], and - in a separate study - adult rat dentate gyrus, in the latter case when admixed with Nidogen 1 and an undefined mixture of laminins, and compared to culture on laminin 1 alone. [Ariza et al. 2010] Whether the observed differential effect was dependent on the addition of collagen or of Nidogen 1 in the later study was unclear. In vivo, the ventricular

zones in the embryonic VZ, the perinatal RMS [Eagleson et al. 1996], and fractones in the adult SEZ [Kerever et al. 2007] are reported to express Collagen Type 4 while Col4a1 and Col4a2 expression is specifically reported on the adult cerebral microvasculature. [Urabe et al. 2002] Interestingly, **Collagen type 19 α 1** (Col19a1), **Collagen type 19 α 3** (Col19a3), and **Collagen type 25 α1** (Col25a1) mRNAs are expressed by cells located in the adult SGZ. [Miller et al. 2013] In all the above embryonic and adult niches, the cell types expressing these genes, and their function in vivo, are not known.

Fibronectin (Fn) is a large, multidomain extracellular glycoprotein that is thought to bind between nine and 12 different integrin heterodimers. [To and Midwood 2011, Plow et al. 2000] Like the laminins and collagens it is a common component of in vitro cell culture systems, making it difficult to sift the literature to identify its biological effects. Nevertheless in vitro, Fn is expressed by postnatally-derived neurospheres [Milner et al. 2007], and promotes the neural differentiation and migration of ESC-derived neurospheres, as compared to gelatine substrates, via both Itgb1-dependent and -independent mechanisms. [Andressen et al. 2005] Similar effects have been reported in a priori comparisons to other substrates, of Fn promoting the migration of neurospheres derived from the postnatal cerebellum [Kearns et al. 2003], and of NSPCs derived from the embryonic ganglionic eminence. [Tate et al. 2004] Using high-throughput microwell arrays the Fn 9-10 domain has been shown to promote renewal, migration, and survival of postnatal SEZ-derived NSPCs, again possibly via integrin-dependent mechanisms. [Roccio et al. 2012] In vivo, Fn protein is expressed in the pial basement membrane of the embryonic mouse brain. [Lathia et al. 2007] The role of Fn in regulating neural stem cell biology in adult systems remains unclear.

1.3.2.2 Well-studied core matrisome genes

Reelin (Reln) is a large extracellular protein expressed in the CNS by parvalbumin–containing interneurons. [Alcantara et al. 1998] The central role of Reln in embryonic neurodevelopment is well-studied and reviewed. [Hirota and Nakajima 2017, Rice and Curran 2001, Alcantara et al. 1998, D'Arcangelo et al. 1995] It is perhaps best known as a critical mediator of proper embryonic neuronal migration, but is thought in addition to regulate both radial glial cell development [Keilani et al. 2008] and the pace of neuronal differentiation. [Lakoma et al. 2011] Accordingly, Reln is also essential for the correct architectural development of the postnatal dentate gyrus. [Brunne et al. 2013, Sibbe et al. 2009, Frotscher et al. 2003, Forster et al. 2002] With regard to a specific role in the

regulation of adult hippocampal NSCs, Reln has been found to regulate RGL radial fibre orientation [Zhao et al. 2004] and to upregulate notch signalling [Keilani et al. 2012, Lakoma et al. 2011, Sibbe et al. 2009], promoting SGZ NSPC proliferation [Sibbe et al. 2015, Pujadas 2010] and differentiation. [Teixera et al. 2012, Pujadas et al. 2010, Zhao et al. 2007, Won et al. 2006] Reln further regulates the complexity, gross morphology, spine morphology, synaptic complexity, and astroglial synaptic ensheathement of the dendrites of adult-born neurons, together with their correct migration into the GCL. [Bosch et al. 2016, Teixera et al. 2012, Pujadas et al. 2010, Zhao et al. 2004] Interestingly Reln has also been found to promote proper migration of adult SEZ-derived neuroblasts both along the RMS [Kim et al. 2002, Hack et al. 2002], and out of it [Pujadas et al. 2010] towards sites of injury or disease [Courtes et al. 2011, Massalini et al. 2009], in some cases mediating recovery. [Won et al. 2006]

Tenascin-C (Tnc) is expressed in vitro by NSCs [Abaskharoun et al. 2010b] and in vivo by outer radial glial cells – thought to be neural stem cells – in the human embryo [Pollen et al. 2015], neuroglial precursors in the developing murine spinal cord [Karus et al. 2011], and by cells in the postnatal [Yuasa et al. 2001, Gates et al. 1995] and adult murine [Miller et al. 2013, Kazanis et al. 2007, Thomas et al. 1996] and human [Kukekov et al. 1999] neurogenic niches. It has been found to regulate the proliferation and differentiation of perinatal forebrain [Garcion et al. 2004, Garcion et al. 2001], striatum [Yagi et al. 2010], and spinal cord NSPCs. [Karus et al. 2011] It is highly alternatively spliced, a process which is developmentally regulated [Joester et al. 1999] in response to key NSC transcription factors. [von Holst et al. 2007] Tnc has a reciprocal instructive role in NSC gene expression [Moritz 2008], indicating a dynamic, bidirectional interaction between ECM and neurogenesis. Indeed, in the perinatal mouse brain Tnc interacts directly with NSCs expressing the cell surface markers CD15+ [Hennen et al. 2013] and HNK-1 [Yagi et al. 2010], and mediates both NSC density and responsiveness to growth factors. [Garcion et al. 2004] Meanwhile in the injured adult CNS, it is dispensable for regeneration of SEZ NSPCs following AraC [Kazanis et al. 2007], but astrocyte-derived Tnc [Nishio et al. 2005] may mediate the response to traumatic brain [Laywell et al. 1992] and spinal cord injury. [Pan et al. 2014]

The role of the axon-guidance factor **Netrin 1** (Ntn1) in neurogenesis has also been relatively well-studied. The availability of knockout mice has prompted many neurodevelopmental studies, implicating it variously in the directed migration of embryonic cortical [Stanco et al. 2009] and cerebellar interneurons [Guijarro et al. 2009], and pontine

[Yee et al. 1999], olivary [Bloch-Gallego et al. 1999], cerebellar [Alcantara et al. 2000] and striatal neurons [Hamasaki et al. 2001]; the projection of commissural [Shoja-Taheri 2015, Serafini 1996], thalamic [Braisted et al. 2000], and hippocampal axons [Barrallobre et al. 2000]; and neuronal survival. [Llambi et al. 2001, Bloch-Gallego et al. 1999] Ntn1 is also expressed by neural and glial progenitors in the embryonic Ventricular Zone and Rostral Migratory Stream, where it is required for their efficient migration to the olfactory bulb. [Murase and Horwitz 2002] In the healthy adult SEZ its homeostatic mRNA expression is restricted however to ependymal cells [Hakanen et al. 2011], where interestingly, infusion of recombinant Ntn1 promotes SEZ angiogenesis. [Cayre et al. 2013] Ntn1 is further implicated in the CNS response to injury. It is upregulated by adult SEZ NSPCs in response to experimental demyelination, where it may mediate reactive vascular expansion and subsequent NSPC migration out of the lesion. [Cayre et al. 2013] In the ischaemic brain, adenoviral overexpression of Ntn1 increases the density of SEZ Nestin+ processes compared to saline-transfected controls. [Lu et al. 2016] Together these studies implicate Ntn1 in multiple aspects of neurogenesis, from developmental to adult and injury responses, although its role in hippocampal neurogenesis remains unknown.

1.3.2.3 Moderately studied core matrisome genes

Versican (Vcan) is a major extracellular proteoglycan in the developing and mature brain. [Popp et al. 2003] It is expressed in vitro by astrocytic, neuronal, and oligodendrocytic lineages derived from NSCs [Abaskharoun 2010a, et al. Gu et al. 2007] and implicated in the early differentiation of embryonic NSCs towards an astrocytic fate. [Han et al. 2015] Different splice variant isoforms of Vcan are expressed in vivo. The V1 isoform is most highly expressed during late embryonic and early postnatal brain development whereas the V2 isoform is present predominantly in adult brain, suggesting that the two isoforms may have different biological functions. [Milev et al. 1998] The V1 isoform promotes neurite outgrowth and neuronal differentiation of rat NSCs [Wu et al. 2004], and the maturation of chick retinal axons [Yamagata et al. 2005], whereas the V2 isoform has an inhibitory effect on axonal outgrowth from chick retina. [Schmalfeldt et al. 2000] Interestingly, neurospheres derived from rat embryonic spinal cord up-regulate expression of the V2 isoform after proinflammatory stimuli, suggesting a role for chondroitin sulfate proteoglycan-mediated inhibition of axonal regeneration after central nervous system injury. [Gu et al. 2007]

Perlecan (Hspg2) is a multidomain proteoglycan that binds to and cross-links many ECM components and cell-surface molecules. It is known to be expressed in the basal laminae of the neuroepithelium and of blood vessels, during embryonic neurodevelopment. [Lathia et al. 2007, Soulintzi and Zagris 2007] In neurospheres derived from embryonic cortex, putative NSCs also express Hspg2 and can sequester soluble FGF2. In vivo, Hspg2 potentiates cell cycle progression and neuronal differentiation in the cerebral hemispheres and ventral forebrain, in part likely mediating the effects of sonic hedgehog signalling. [Giros et al. 2007] It is also a constituent of fractones, which are structures within the neurogenic niche known to sequester FGF2 and thereby regulate adult neurogenesis. [Kerever et al. 2007] In the adult SEZ, Hspg2 regulates NSC maintenance and neurogenesis, including neuroblast migration along the RMS to the OB. Together these data suggest that it can sequester extracellular signalling factors in the niche, thereby regulating NSC proliferation. [Kerever et al. 2014] The close relationship between Hspg2 and extracellular signalling is conserved in drosophila [Park et al. 2003] and is bidirectional: infusion of FGF2 into the cisterna magna of mouse pups increases neural cell proliferation and Hspg2 expression in the cerebral cortex. [Asclayekhi et al. 2011]

Vitronectin (Vtn) is an ECM glycoprotein with binding sites for multiple ECM- and ECM-associated proteins including integrins, collagens, complement proteins, and plasminogen. [Pons and Marti 2000, Schnapp et al. 1995] Vtn is induced during the early stages of chick neural tube development where it promotes motor neuron differentiation [Martinez-Morales et al. 1997] by synergistically interacting with the amino-terminal peptide of Sonic hedgehog protein. [Pons and Marti 2000] Likewise Vtn is expressed by neural crest cells in the developing quail, where it mediates their adhesive and migratory behaviour in an RGD-dependent manner. [Delannet et al. 1994] In adult systems, Vtn is a possible extracellular substrate for αV integrin-mediated migration of neural stem cells to areas of ischaemic CNS injury [Prestoz et al. 2001] and together with laminin and collagen, a component of the neurovascular unit basement membrane that has been observed to form in co-cultures of human endothelial and human neural stem cells. [Chou et al. 2014]

The thrombospondins are a family of secreted extracellular matrix glycoproteins that mediate cell-cell and cell-matrix interactions by binding with various ECM proteins, membrane receptors and cytokines, and have a critical role in synaptogenesis. [Christopherson et al. 2005] The best-studied is **Thrombospondin 1** (Thbs1), which is expressed by both proliferating and differentiating NSPCs and positively regulates these

states in the adult neurogenic niches in vivo. In vitro, Thbs1-null adult NSCs display impaired proliferation and stemness whereas those derived from early postnatal mice do not, suggesting a role for Thbs1 specifically in adult neurogenesis. Thbs1 indeed was critical for astrocyte-induced neuronal differentiation of adult SEZ NSCs. Overall these data suggest that Thbs1 is a key astrocyte-derived molecule responsible for astrocyte-mediated neuronal differentiation in an adult neurogenic niche. [Lu et al. 2010] It is however also expressed by NSCs and mediates the trophic effect of co-cultured human embryonic cortex-derived NSCs on rat embryonic cortical neurons. [Andres et al. 2011] As well as plasticity of neurons, Thbs1 further regulates the plasticity of neuroblast chains and their migration both in vitro and in the postnatal brain. Postnatal Thbs1-null mice display an altered morphology of the RMS and a decrease of postnatal neurons in the OB. [Blake et al. 2008] Expression of Thbs1 mRNA is increased following treatment of NSCs with BDNF [Rosenblum et al. 2015], βFGF [Miyasaka et al. 2000], and LIF. [Wright et al. 2003] The functional role of Thbs1 in these expression studies was not explored.

Tenascin-R (Tnr) is a large and multifunctional ECM glycoprotein implicated in cell adhesion and neuritogenesis. Genetic knockout and synthetic biology experiments suggest additional roles in NSC biology, however. Tnr protein inhibits migration [Huang et al. 2009] and proliferation [Liao et al. 2008a] of NSCs derived from embryonic rat cortex, possibly in association with microglia. [Liao et al. 2008b] Tnr similarly regulates the migration of SEZ-derived neuroblasts in the adult forebrain. [Saghatelyan et al. 2004] Its expression in the adult DG is evident in the ML and Hilus [Bruckner et al. 2003] where Tnr regulates the proliferation and neuronal differentiation of NSCs. Adult Tnr-null mice display hypertrophic abnormalities in the GCL suggesting a role for Tnr in negatively regulating the generation of GABAergic inhibitory interneurons. [Xu et al. 2014]

Neurocan (Ncan) is another member of the lectican family of chondroitin sulfate proteoglycans that includes aggrecan, brevican, and versican. Like those other family members Ncan is expressed in vitro by ESC-derived neurons and astrocytes. [Abaskharoun et al. 2010a] In vivo, peak concentrations are attained in the early postnatal period, with gradually declining levels in the brain thereafter. [Milev et al. 1998] Its potential for interaction with adhesion molecules in the ECM is exemplified by the observation that expression of Ncan overlaps spatially and temporally with that of adhesion-related proteins (e.g., NCAM and NgCAM) in embryonic rat brain. [Friedlander et al. 1994] Indeed in the developing chick retina, the N-terminal fragment of Ncan inhibits N-cadherin- and Itgb1-

mediated adhesion and neurite extension of neural retinal cells. [Li et al. 2000] In the adult mouse dentate gyrus, immunoreactivity for the N-terminal portion gradually increases as one progresses dorsally from the GCL into the outer molecular layer, suggesting that Ncan may have a functional role relating to the distal dendritic trees of newly-born granule cells. [Bruckner et al. 2003]

Secreted phosphoprotein 1 (Spp1, also known as **Osteopontin**) has a functional role in tissue homeostasis, wound healing, immune regulation, and the stress response, which is expressed by macrophages in the CNS. [Rabenstein et al. 2015] It is a potent chemoattractant: both in vitro and in vivo experiments suggest that NSCs migrate towards sources of Spp1, mediated by signalling via both integrin β1 [Yan 2009a, Yan 2009b] and CXCR4. [Rabenstein et al. 2015] The roles of Spp1 in mediating other parameters of NSC biology remain unclear. For instance it may promote NSC proliferation in vitro [Kalluri et al. 2012] and infusion of recombinant Spp1 has been reported to increase proliferation in the adult rat SEZ. [Rabenstein et al. 2015] However other groups report no effect of Spp1 infusion [Sailor et al. 2003], and genetic knockout experiments find it to be dispensable [Yan et al. 2009a, Yan et al. 2009b], for proliferation in vivo. Its role in mediating NSC differentiation is also opaque: Spp1 may promote neurogenesis in embryonic NSCs in vitro, but not in adult NSCs in vivo. [Rabenstein et al. 2015] Therefore despite a small clutch of papers examining the role of Spp1 in the context of NSC biology, little is settled beyond its role as a chemoattractant for NSCs following injury.

Nidogen 1 (Nid1) is a major component of basement membranes and of fractones [Kerever et al. 2007] with a key role in the adhesion of NSCs to laminin. In vitro, Nid1 is expressed by embryonic NSCs but not by mature neurons; laminin in the ECM may itself stimulate this process, and anti-nidogen antibodies inhibit NSC adhesion to laminin by about 50%. [Li et al. 2008] In vivo deletion of the nidogen-binding site of the laminin γ1 chain results in disintegration and rupture of the BM in various organs including the developing brain. [Halfter et al. 2002] Loss of nidogen-mediated NSC connection to the pial BM subsequently impairs neuronal migration, leading to defects in the overall architecture of the late-embryonic cortex. [Haubst et al. 2006] Its function in the adult brain remains to be explored.

Brevican (Bcan) is a chondroitin sulfate proteoglycan with expression that appears to be specific to nervous tissue. In vitro, Bcan has been implicated transcriptionally in the early differentiation of embryonic NSCs towards an astrocytic fate. [Radice et al. 2015] In vivo

however, only traces of Bcan can be detected in embryonic brain. Its expression increases steadily after birth, reaching by P140 a level approximately 14-fold higher than that present in neonatal brain. [Milev et al. 1998] Indeed, Bcan is expressed widely by cells in the adult hippocampus including in the SGZ. [Miller et al. 2013] Bcan immunoreactivity in the adult mouse DG is most prominent in the polymorphic layer and the middle third of the molecular layer. [Bruckner et al. 2003] Whether this expression pattern points to a role in adult neural stem cell biology remains unclear.

1.3.2.4 Scarcely-studied core matrisome genes

Slit1 and **Slit2** are the principal ECM ligands for the Robo receptors, to which they bind in association with proteoglycans. In Drosophila, Slit signalling modulates neurogenesis by promoting asymmetric terminal divisions in neural precursor cells. [Mehta et al. 2001] In mice, Slit1 and Slit2 are expressed in the E12.5-E14.5 telencephalon and regulate the proliferation of basal progenitors. [Yeh et al. 2014, Borrell et al. 2012] Although these independently-run studies established the principle that Slit/Robo signalling modulates developmental mammalian neurogenesis, its precise functional effect remains unclear. Despite similar experimental designs, reports directly conflicted over whether Slit1/2 mutant mice display increased [Borrell et al. 2012] or decreased [Yeh et al. 2014] levels of VZ/SVZ proliferation. As noted by Yeh et al. it is possible that the contrasting results were due to differences in the genetic strains and backgrounds of the animals used.

SCO-spondin (Sspo) is secreted by the subcommissural organ from the roof plate into the CSF and extracellular matrix of the developing brain, suggesting a role for Sspo in developmental neurogenesis. Indeed Sspo protein is critical for proper development of the chick diencephalon and mesencephalon, negatively regulating apoptosis and proliferation, and promoting neural differentiation. [Vera et al. 2013] Integrin β1 (Itgb1) is co-expressed and colocalises with Sspo in the chick embryo suggesting that Itgb1 may mediate its actions, although this remains to be proven. [Caprile et al. 2009] Sspo is also expressed from the floorplate - a small group of neuroepithelial cells located at the ventral midline of the neural plate – leading to suggestions that it may also participate in patterning of the neural tube. [Guinazu et al. 2002]

Thrombospondin 4 (Thbs4) promotes the neuronal differentiation in vitro of NG2+ cells derived from the cerebral cortex of the embryonic rat. [Yang et al. 2016] However in NSC

cultures derived from the SEZ of postnatal mice, Thbs4 has the opposite effect of inhibiting neuronal differentiation, suggesting species-, culture-, cell-type, or developmental stage-specific effects. [Benner et al. 2013] Indeed the same authors showed that Thbs4 is expressed selectively in vivo by astrocytes in the SEZ but not those in cortex: its expression is up-regulated in association with gliogenesis following cortical injury. [Benner et al. 2013] These findings implicate Thbs4 in astrocyte-mediated regulation of adult neurogenesis and the response of the SEZ to injury. Thrombospondin family members also regulate the migration of postnatally-born neurons. Similar to its expression in SEZ, in the postnatal and adult RMS Thbs4 is expressed by astrocytes where it is thought to regulate neuroblast migration towards the olfactory bulb. [Girard et al. 2014]

Thrombospondin 2 (Thbs2), like Thbs1, mediates the trophic effect of co-cultured human embryonic cortex-derived NSCs on rat embryonic cortical neurons. [Andres et al. 2011] In neurosphere and in vivo assays of NSPCs derived from adult knockout mice, the Thbs2 gene has been reported to not compensate for the experimental ablation of Thbs1, suggesting that Thbs2 - which is expressed only at a low level in the healthy adult brain - may not have a major biological role in maintaining adult neurogenesis under homeostatic conditions. [Lu et al. 2010] However following exposure to BDNF, human embryo-derived NSCs upregulate Thbs2, which is associated with improved functional outcomes following their transplantation into ischaemic brain. [Rosenblum et al. 2015] A role for Thbs2 in mediating outcomes after brain injury therefore remains to be fully explored.

During neural stem cell differentiation from mouse embryonic stem cells in vitro, expression of the proteoglycan **Aggrecan** (Acan) increases in both the astrocytic and neuronal lineages. [Abaskharoun et al. 2010a] In vivo, Acan expression increases steadily during brain development, reaching a level by P90 that is approximately 18-fold that of the embryonic brain. [Milev et al. 1998] Interestingly in the adult mouse dentate gyrus, Acan protein is expressed detectably in the polymorphic and inner molecular layers which ‘sandwich’ the neurogenic SGZ/GCL [Bruckner et al. 2003], suggesting a possible role for Acan in adult hippocampal neurogenesis.

NEL-like 2 (NELL2) is a secreted ECM glycoprotein which is predominantly expressed in neural tissues. NELL2 expression gradually increases during embryonic development. Ha et al. transfected a NELL2 expression vector into an immortalised E16 rat hippocampal progenitor cell line. Using this system they visualised NELL2-containing vesicles being

transported to the plasma membrane, where it was secreted by the immortalised embryonic stem cells. [Ha et al. 2013] In vitro, recombinant NELL2 protein significantly enhances survival of neurons derived from embryonic rat hippocampus. [Aihara et al. 2003] Meanwhile in the adult rat dentate gyrus NELL2 protein is prominently expressed by cells in the polymorphic layer and by some cells in the SGZ. The identity of the adult NELL2-expressing cells is however unclear; it does not co-label with GFAP+, suggesting that it is not expressed by adult NSCs. [Jeong et al. 2008] What role NELL2 may play in adult neurogenesis, if any, therefore remains unclear.

In plated neurospheres derived from the adult rat SEZ, **Fibulin-2** (Fbln2) was highly upregulated following treatment with the pro-neurogenic cytokine TGF-β1. The in vitro increase was seen in both mRNA and protein, notably on GFAP+ astrocytic cells, and was required for the proneurogenic effects of TGF-β1. Intracerebroventricular infusion of TGF-β1 caused an increase in Fbln2 protein in astrocytes of the adult SEZ. [Radice et al. 2015] Together with the observation that embryonic mouse NSCs upregulate Fbln2 during astrocytic differentiation [Han et al. 2015], these data suggest that astrocyte-derived Fbln2 may act non-cell-autonomously to mediate TGF β1-induced neurogenesis.

In the developing chick mesencephalon, Itgb1-mediated signalling increases neuronal differentiation in neighbouring cells in vivo. The pro-neurogenesis effect acts via a non cell-autonomous mechanism involving the ECM proteoglycan **Decorin** (Dcn). Blocking Dcn with morpholino knockdown ex-vivo abrogates the effect of increased Itgb1 signalling, implicating Dcn as a positive regulator of neurogenesis and neuronal differentiation. [Long et al. 2016] However Dcn is also expressed by astrocytes cultured from adult rat spinal cord and significantly reduces the neuronal differentiation of adult rat hippocampal NSPCs in vitro. [Barkho et al. 2006] These conflicting results could be explained by species differences, differential actions of Dcn on NSCs at differing developmental stages, fundamental differences in the properties of mesencephalic versus hippocampal NSCs, or technical differences relating to culture conditions.

Overexpression of **Insulin-like growth factor binding protein 1** (Igfbp1) is thought to inhibit Insulin-like growth factor (IGF) signalling, and causes marked deficiency in postnatal brain growth. [D'Ercole et al. 1994] However, overexpression of Igfbp1 has no effect on NSPC proliferation and differentiation in the adult neurogenic niches, suggesting that it may act during a critical developmental period. [He et al. 2007]

Secreted protein acidic and rich in cysteine (SPARC) is expressed during development by glial cells in the neurogenic regions. In adult mice, SPARC is expressed by a subpopulation of cells in the SGZ [Miller et al. 2013] and positively regulates NSPC proliferation without altering the proportion of cells expressing DCX. [Campologno et al. 2012]

In vitro, **Adiponectin** (Adipoq) stimulates proliferation of adult hippocampal NSCs by acting on GSK-3β to promote nuclear accumulation of β-catenin. [Zhang et al. 2011]

During neural crest specification in zebrafish, the secreted **BMP binding endothelial regulator** (BMPER) enhances BMP activity and is required for neural crest cell fate. [Reichert et al. 2013] A role in mammalian neurogenesis remains unknown.

In vitro, the secreted protein **Connective-tissue growth factor** (Ctgf) induces mouse embryonic NSCs to express glial and stem cell markers via the p44/42 MAPK pathway, without increasing proliferation. [Mendes et al. 2015]

At an early neurodevelopmental stage in Xenopus laevis, **Cysteine-rich motor neuron protein 1** (Crim1) is necessary for the proper functioning of cadherin-dependent junctions and subsequently for normal neural development. [Ponferrada et al. 2012] A role in mammalian neurogenesis remains unknown.

In vitro, **Fibulin-1** (Fbln1) binds to amyloid precursor protein to block APP-mediated proliferation of primary cultured rat NSCs. [Ohsawa et al. 2001]

The vitamin K-dependent protein **Growth arrest specific 6** (Gas6) is expressed in the adult mouse SEZ and functions to promote stem cell proliferation and/or maintenance. [Gely-Pernot et al. 2012]

In vitro, primary P1 mouse SEZ-derived neurospheres express higher levels of **Insulin growth factor binding protein 3** (Igfbp3) than differentiated neurospheres derived from cortex. [Easterday et al. 2003]

In rats, expression of **Nephroblastoma-overexpressed** (NOV) increases during the postnatal period of cerebellar development, where it is secreted by Purkinje neurons and (in vitro)

reduces SHH-induced granule cell precursor proliferation in a B3 integrin-dependent manner. [Le Dreau et al. 2010]

In adult mice **Netrin-4** (Ntn4) is produced by astrocytes in the anterior part of the rostral migratory stream (RMS) and OB, where it interacts with Lamc1 and, in vitro, can be shown to promote NSC proliferation. [Staquicini et al. 2009]

Meanwhile in adult rats **Netrin-5** (Ntn5) is expressed by Ascl1+ IPCs and DCX-positive NBs in the SGZ, suggesting that Ntn5 may play a role in adult hippocampal neurogenesis. [Yamagishi et al. 2015] What that role might be remains to be studied.

In postnatal and adolescent mice, **Periostin** (Postn) positively regulates SGZ NSC proliferation, both in vivo and in vitro. [Ma et al. 2015]

R-spondin (Rspo1) is proposed to demarcate the boundary between the roof plate and neuroepithelium and may contribute to the development of dorsal neural tube under the regulation of Wnts. [Kamata et al. 2004]

During rat development **F-spondin** (Spon1) is expressed at high levels in the floor plate (a group of cells implicated in the control of neural cell patterning in the developing vertebrate nervous system). In vitro, Spon1 promotes neural cell adhesion. [Klar et al. 1992]

Finally **Secreted protein acidic and rich in cysteine-like 1** (SPARCL1) is expressed by RGCs passing through the cortical plate and may function to promote anti-adhesive signals to migrating neurons, signalling the end of migration in the developing cerebral cortex. [Gongidi et al. 2004]

Additionally to these studies Miller et al. used a combination of publicly available ISH data, RNA microarray analysis, or both, to identify genes enriched in the murine SGZ relative to the GCL. [Miller et al. 2013] Genes with differential expression in the SGZ are - one presumes - candidate genes for the regulation of hippocampal neurogenesis. By intersecting this list with the core matrisome it is possible to identify a number of ECM genes putatively enriched in the SGZ: Thrombospondin type I domain containing 4 (Thsd4); Milk fat globule-EGF factor 8 (Mfge8); Sparc/osteonectin, cwcv and kazal-like domains proteoglycan 1 (Spock1); SPARC; Neuron-derived neurotrophic factor; Brevican; Tenascin C; Reelin; and

various collagens (Col9a1, Col9a3, Col19a1, Col25a1). The functional relevance of many of the genes thus identified remains unclear.

1.3.2.5 Allen Brain Atlas results

A total of 130 (47.4%) of the 274 core matrisome genes were identifiably expressed at the transcriptional level in the adult mouse DG. Fifty were expressed at a qualitatively high level in SGZ, GCL, or Hilus, with nine enriched specifically in the SGZ. (**Table 3**)

I was interested to explore whether any matrisome genes were expressed solely within the neurogenic niche. Inspection of the Allen Brain Atlas showed that most matrisome genes expressed within the DG were also expressed in multiple non-neurogenic brain areas. Three genes - Mfge8, Thbs4, and Vwa3a - were intriguing exceptions, being restricted mainly to the adult SEZ and SGZ. Another n=37 matrisome genes were relatively enriched within the DG compared to the rest of the brain (see **Table 3**). Although it was not possible to study these genes in my thesis, they may benefit from study in future.

Gene ID	Gene symbol	Gene name	Expression	Main location	Other locations	Specific to HC?
11603	Agrn	agrin	+++	SGZ	GCL	No
77018	Col25a1	collagen, type XXV, alpha 1	+++	SGZ	GCL	No
14456	Gas6	growth arrest specific 6	+++	SGZ	GCL / Hilus	No
12823	Col19a1	collagen, type XIX, alpha 1	+++	SGZ	Hilus	No
16010	Igfbp4	insulin-like growth factor binding protein 4	+++	SGZ	Hilus	No
246316	Lgi2	leucine-rich repeat LGI family, member 2	+++	SGZ	Hilus	No
20745	Spock1	sparc/osteonectin, cwcv and kazal-like domains proteoglycan 1	+++	SGZ	Hilus	No
17304	Mfge8	milk fat globule-EGF factor 8 protein	+++	SGZ	Hilus	Neurogenic areas only
20692	Sparc	secreted acidic cysteine rich glycoprotein	+++	SGZ		No
12826	Col4a1	collagen, type IV, alpha 1	+++	Hilus	GCL	No
19699	Reln	reelin	+++	Hilus	SGZ	No
83691	Crispld1	cysteine-rich secretory protein LCCL domain containing 1	+++	Hilus	SGZ	Relatively
21826	Thbs2	thrombospondin 2	+++	Hilus		Relatively
75740	6130401L20Rik	RIKEN cDNA 6130401L20 gene	+++	GCL		Relatively
64074	Smoc2	SPARC related modular calcium binding 2	+++	GCL		Relatively
54003	Nell2	NEL-like 2 (chicken)	+++	GCL	Hilus	No
75426	Igfbpl1	insulin-like growth factor binding protein-like 1	+++	GCL	Hilus	No
140703	Emid1	EMI domain containing 1	+++	GCL	SGZ	No
18419	Otog	otogelin	+++	GCL	SGZ	No
373864	Col27a1	collagen, type XXVII, alpha 1	+++	GCL	SGZ	No
14264	Fmod	fibromodulin	+++	GCL	SGZ	No
94214	Spock2	sparc/osteonectin, cwcv and kazal-like domains proteoglycan 2	+++	GCL	SGZ	No
72902	Spock3	sparc/osteonectin, cwcv and kazal-like domains proteoglycan 3	+++	GCL	SGZ	No
12833	Col6a1	collagen, type VI, alpha 1	+++	GCL		No
11450	Adipoq	adiponectin, C1Q and collagen domain containing	+++	GCL		No
171508	Creld1	cysteine-rich with EGF-like domains 1	+++	GCL		No
14161	Fga	fibrinogen alpha chain	+++	GCL		No

80883	Ntng1	netrin G1	+++	GCL		No
13602	Sparcl1	SPARC-like 1	+++	GCL		No
233744	Spon1	spondin 1, (f-spondin) extracellular matrix protein	+++	GCL		No
21930	Tnfaip6	tumor necrosis factor alpha induced protein 6	+++	GCL		No
22786	Zp1	zona pellucida glycoprotein 1	+++	GCL		No
269120	Optc	opticin	+++	GCL		No
236790	Ddx26b	DEAD/H (Asp-Glu-Ala-Asp/His) box polypeptide 26B	+++	GCL		Relatively
16011	Igfbp5	insulin-like growth factor binding protein 5	+++	GCL		Relatively
56839	Lgi1	leucine-rich repeat LGI family, member 1	+++	GCL		Relatively
213469	Lgi3	leucine-rich repeat LGI family, member 3	+++	GCL		Relatively
67532	Mfap1a	microfibrillar-associated protein 1A	+++	GCL		Relatively
216760	Mfap3	microfibrillar-associated protein 3	+++	GCL		Relatively
171171	Ntng2	netrin G2	+++	GCL		Relatively
69675	Pxdn	peroxidasin homolog (Drosophila)	+++	GCL		Relatively
20562	Slit1	slit homolog 1 (Drosophila)	+++	GCL		Relatively
20564	Slit3	slit homolog 3 (Drosophila)	+++	GCL		Relatively
21827	Thbs3	thrombospondin 3	+++	GCL		Relatively
21960	Tnr	tenascin R	+++	GCL		Relatively
70853	Vwa3b	von Willebrand factor A domain containing 3B	+++	GCL		Relatively
12834	Col6a2	collagen, type VI, alpha 2	+++	GCL		Relatively
13004	Ncan	neurocan	+++	GCL		Relatively
22370	Vtn	vitronectin	+++	General		No
29817	Igfbp7	insulin-like growth factor binding protein 7	+++	General		No
14268	Fn1	fibronectin 1	++	SGZ	BV	No
81877	Tnxb	tenascin XB	++	SGZ	GCL	Relatively
16008	Igfbp2	insulin-like growth factor binding protein 2	++	SGZ		No
21825	Thbs1	thrombospondin 1	++	SGZ		No
21923	Tnc	tenascin C	++	SGZ		No
12841	Col9a3	collagen, type IX, alpha 3	++	SGZ		No
13717	Eln	elastin	++	SGZ		No
16777	Lamb1-1	laminin B1 subunit 1	++	SGZ		Relatively

21828	Thbs4	thrombospondin 4	++	SGZ		Neurogenic areas only
330790	Hapln4	hyaluronan and proteoglycan link protein 4	++	Hilus		No
12835	Col6a3	collagen, type VI, alpha 3	++	Hilus		Relatively
18295	Ogn	osteoglycin	++	GCL		Relatively
114249	Npnt	nephronectin	++	GCL		Relatively
233813	Vwa3a	von Willebrand factor A domain containing 3A	++	GCL		Neurogenic areas only
328643	Vwa5b2	von Willebrand factor A domain containing 5B2	++	GCL	Hilus	No
17181	Matn2	matrilin 2	++	GCL	SGZ	No
12824	Col2a1	collagen, type II, alpha 1	++	GCL	SGZ	No
68792	Srpx2	sushi-repeat-containing protein, X-linked 2	++	GCL	SGZ	Relatively
12813	Col10a1	collagen, type X, alpha 1	++	GCL	SGZ, Hilus	Relatively
14115	Fbln2	fibulin 2	++	GCL		No
320181	Fndc7	fibronectin type III domain containing 7	++	GCL		No
226519	Lamc1	laminin, gamma 1	++	GCL		No
108075	Ltbp4	latent transforming growth factor beta binding protein 4	++	GCL		No
18133	Nov	nephroblastoma overexpressed gene	++	GCL		No
76737	Creld2	cysteine-rich with EGF-like domains 2	++	GCL		Relatively
68655	Fndc1	fibronectin type III domain containing 1	++	GCL		Relatively
76293	Mfap4	microfibrillar-associated protein 4	++	GCL		Relatively
72780	Rspo3	R-spondin 3 homolog (Xenopus laevis)	++	GCL		Relatively
22371	Vwf	Von Willebrand factor homolog	++	General		No
12950	Hapln1	hyaluronan and proteoglycan link protein 1	++	General		No
12032	Bcan	brevican	++	General		No
12111	Bgn	biglycan	+	SGZ		No
71768	Vwce	von Willebrand factor C and EGF domains	+	SGZ	GCL	No
208777	Sned1	sushi, nidogen and EGF-like domains 1	+	SGZ	GCL	No
16774	Lama3	laminin, alpha 3	+	SGZ	General DG	No
243914	Lgi4	leucine-rich repeat LGI family, member 4	+	SGZ	General DG	No
12814	Col11a1	collagen, type XI, alpha 1	+	SGZ	Hilus	No
12816	Col12a1	collagen, type XII, alpha 1	+	SGZ	Hilus	No
71690	Esm1	endothelial cell-specific molecule 1	+	SGZ		No

16998	Ltbp3	latent transforming growth factor beta binding protein 3	+	SGZ		No
73230	Bmper	BMP-binding endothelial regulator	+	SGZ		No
14119	Fbn2	fibrillin 2	+	SGZ		No
53867	Col5a3	collagen, type V, alpha 3	+	SGZ		No
12839	Col9a1	collagen, type IX, alpha 1	+	SGZ		No
12840	Col9a2	collagen, type IX, alpha 2	+	SGZ		No
224224	Impg2	interphotoreceptor matrix proteoglycan 2	+	SGZ		No
116847	Prelp	proline arginine-rich end leucine-rich repeat	+	SGZ		No
18209	Ntn3	netrin 3	+	SGZ		Relatively
407800	Ecm2	extracellular matrix protein 2, female organ and adipocyte specific	+	SGZ		Relatively
14118	Fbn1	fibrillin 1	+	SGZ		Relatively
100689	Spon2	spondin 2, extracellular matrix protein	+	SGZ		Relatively
12818	Col14a1	collagen, type XIV, alpha 1	+	SGZ		Relatively
57764	Ntn4	netrin 4	+	SGZ		No
107581	Col16a1	collagen, type XVI, alpha 1	+	Hilus	GCL	No
12810	Coch	coagulation factor C homolog (Limulus polyphemus)	+	Hilus		No
239405	Rspo2	R-spondin 2 homolog (Xenopus laevis)	+	Hilus		No
12819	Col15a1	collagen, type XV, alpha 1	+	Hilus		No
68588	Cthrc1	collagen triple helix repeat containing 1	+	Hilus		Relatively
12827	Col4a2	collagen, type IV, alpha 2	+	Hilus		Relatively
12836	Col7a1	collagen, type VII, alpha 1	+	GCL	SGZ	No
74199	Vit	vitrin	+	GCL		No
240675	Vwa2	von Willebrand factor A domain containing 2	+	GCL		No
16775	Lama4	laminin, alpha 4	+	GCL		No
58859	Efemp2	epidermal growth factor-containing fibulin-like extracellular matrix protein 2	+	GCL		No
73368	Col20a1	collagen, type XX, alpha 1	+	GCL		No
11704	Amelx	amelogenin X chromosome	+	GCL		No
13601	Ecm1	extracellular matrix protein 1	+	GCL		No
100952	Emilin1	elastin microfibril interfacer 1	+	GCL		No
14114	Fbln1	fibulin 1	+	GCL		No

231470	Fras1	Fraser syndrome 1 homolog (human)	+	GCL		No
16780	Lamb3	laminin, beta 3	+	GCL		No
12815	Col11a2	collagen, type XI, alpha 2	+	GCL		No
12817	Col13a1	collagen, type XIII, alpha 1	+	GCL		No
12843	Col1a2	collagen, type I, alpha 2	+	GCL		No
236690	Nyx	nyctalopin	+	GCL		No
242608	Podn	podocan	+	GCL		No
53856	Prg3	proteoglycan 3	+	GCL		No
17313	Mgp	matrix Gla protein	+	General		No
17183	Matn4	matrilin 4	+	General		No
13003	Vcan	versican	+	General		No

Table 3. Core matrisome genes expressed transcriptionally in the adult dentate gyrus.

Data from Allen Brain Atlas, ranked by qualitative visual assessment of level of expression. Core matrisome genes not listed here show no detectable expression. SGZ= subgranular zone, GCL= granule cell layer; DG= dentate gyrus.

1.3.2.6 Summary of search

In summary, current knowledge of how core ECM genes regulate neurogenesis is highly skewed towards a few model genes (laminins, collagens, and fibronectin) which comprise routine substrates in laboratory research with the precise biology remaining rather poorly understood, and a few well-characterised genes (Reelin, Tenascin C and Netrin 1) for which productive transgenic animals exist. Together these six genes account for about 2% of the core matrisome. Roughly a further 10% of matrisome genes have been studied with varying degrees of methodological rigour and depth. My search reveals a small existing literature on a number of ECM genes implicated in hippocampal neurogenesis including: Postn, Ntn5, SPARC, Dcn, NELL2, Thbs1, Tnr, Tnc, and Reln. A further small subset of ECM genes – Thbs4, Mfge8, and Vwa3a – show relative spatial restriction to the adult SGZ, but are unstudied in this neurogenic zone. The relative scarcity of studies also belies the large number (n=130) of ECM genes that are transcriptionally expressed in the adult SGZ.

It is appropriate to acknowledge some limitations of this search and literature review. Publications using an alias of current standard gene names may not have been captured; and studies not listed in Pubmed will have largely been excluded. A small number of matrisome genes did not appear to be included in the Allen Brain Atlas, and for those that were, RNA expression may not correlate to protein expression. Additionally I did not attempt to review the potentially important roles of ECM genes in conditions of injury or disease.

Nevertheless, strengths of this systematic search included being a detailed survey of the state of the science with respect to ECM genes and mammalian neural stem cells. By accessing the agnostic Allen Brain Atlas I was able to report spatial information about the transcriptional expression of 130 ECM genes within the adult DG and in the neurogenic SGZ. In many cases this spatial information is more specific than that which would be achievable by more routine transcriptional analysis of hippocampal or DG lysates. Overall, these suggestive signals support the hypothesis that extracellular matrix might regulate adult hippocampal neurogenesis.

I now turn to the major cell-surface receptor family connecting the cell to the ECM, namely integrins and specifically Integrin β1.

1.3.3 Integrins

The integrin family of cell-membrane receptors are evolutionarily ancient: all metozoa have integrins [Hynes 2002], placing their emergence in pre-Cambrian times [Hynes and Zhao 2000]. Integrins are a group of heterodimeric glycoproteins that mediate bidirectional molecular signalling between the cell and its microenvironment. The heterodimer comprises one α and one non-covalently associated β subunit. Eighteen α and eight β subunits are currently known to exist which combine variously to create potentially 24 different integrin heterodimers [Hynes 2002].

Integrins have the functional capability to bind to molecules in the extracellular matrix (ECM), and thereby anchor the cell, via the intracellular cytoskeleton, to its surroundings [Brakebusch et al. 2005, Barczyk et al. 2010, Plow et al. 2000]. Cell adhesion to ECM is the 'quintessential' integrin function: the path that led directly to their first definitive identification [Tamkun et al. 1986] began thirteen years prior, with the discovery and identification of fibronectin adhering to the cell surface. [Hynes 1973, Hynes 2004] Fibronectin aside, the list of ECM ligands for integrins is long (see below) and includes most prominently collagens and laminins. [Barczyk et al. 2010, Plow et al. 2000]

Integrins have several other important functions at the cell surface besides their historically primary role in cell adhesion. Integrins can bind secreted signalling factors present in the ECM, and may also interact with other receptors on the cell surface **(Figure 6)**. [E.g. Takada et al. 2017, Yamada and Even-Ram 2002]

Integrins may exist in an active or inactive state. Integrin activation is thought to occur when extracellular ligand binding triggers a conformational change in the heterodimer (conceptualised as an 'outside-in' process). The conformational change can be synergistically enhanced by the additional binding of intracellular proteins (for example talin) to the β-subunit cytoplasmic tail. [Tadokoro et al. 2003] Such events trigger a cascade which activates intracellular signalling pathways. [Kim et al. 2011] Integrins may also be activated by signaling pathways originating within the cell (conceptualised as 'inside-out' signaling), which can increase affinity for and increase communication with ligands in the ECM. [Honda et al. 2009, Michael et al. 2009]

The capacity for dynamic regulation of integrin activation and inactivation, coupled with the potential for integrins to signal bi-directionally, allows cells to integrate spatial and soluble cues in the microenvironment, and also to modulate the microenvironment, according to need.

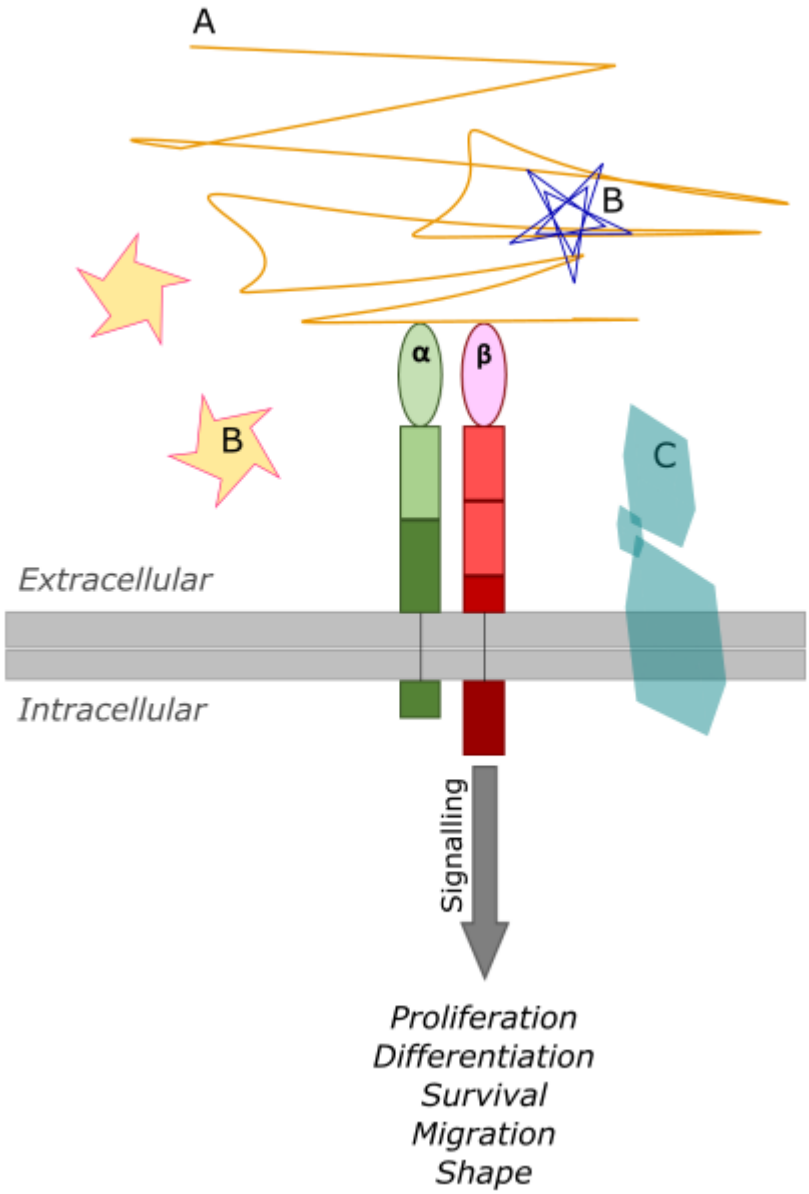

Figure 6. Integrins anchor cells to the ECM and transduce extracellular signals.
In the extracellular space integrins may interact directly with structural molecules in the ECM such as laminin, collagen, and fibronectin (A); with soluble factors dispersed within the ECM (B), and with other kinds of cell-surface receptor (C). Ligand binding triggers a complex series of intracellular signaling cascades that can alter multiple aspects of the cellular phenotype. Together this complex

system equips the cell to sense and respond to chemical and mechanical properties of its microenvironment.

1.3.4 Integrin β 1

Integrin β 1 (hereafter Itgb1) is the most common β subunit and a component of 12 of the possible 24 integrin configurations (potentially dimerising with α subunits I-XI, and α V). In the most general terms, the α subunit is thought to determine ligand specificity and the β subunit to modulate intracellular signalling pathways as a result of ligand binding. [Barczyk et al. 2010] For instance a5b1 functions as the receptor for fibronectin while a6b1 binds laminin. Different integrin heterodimers preferentially bind different ECM ligands, but there is considerable overlap. Even restricting to heterodimers containing the b1 subunit, specificity is the exception rather than the rule **(Table 4)**.

Integrin alpha subunit	Major ECM ligands*
α1	Collagen, Laminin
α2	Collagen, Laminin, Thrombospondin
α3	Laminin, Thrombospondin, Netrin
α4	Osteopontin, Fibronectin, VCAM-1, MAdCAM1, Thrombospondin
α5	Osteopontin, Fibronectin
α6	Laminin
α7	Laminin
α8	Vitronectin, Fibronectin, Tenascin
α9	Tenascin, VCAM-1
α10	Collagen, Laminin
α11	Collagen
αV	Osteopontin, Fibronectin, TGF-β

Table 4. Major ECM ligands of *αχ*β1 heterodimers.

*****Adapted from [Plow et al. 2000, Humphries et al. 2006].

In experiments designed to describe the phenotype of the Itgb1 knockout mouse, homozygous mutants comprised 0/438 offspring, indicating their early death during development. It was discovered that the Itgb1 gene is dispensable for embryonic development only up to the blastocyst stage (which in mice is E3.5). Embryos lacking Itgb1

can attach to the uterine epithelia and invade the stroma. They then die owing to failure of the developing blastocyst to express Laminin 111 and thereby to form a basement membrane. [Fassler and Meyer 1995, Stephens et al. 1995, Aumailley 2001] However Itgb1 does not seem to be critical for the survival of individual cells in an otherwise viable organism. Chimeric experiments have established that in embryos with <25% Itgb1-null cells, null cells contribute to most regions of the central nervous system, including olfactory bulb, cortex, striatum, septum, hippocampus, cerebellum, and spinal cord. [Fassler and Meyer 1995]

1.3.5 Integrin β 1 function in the murine CNS

Since the discovery of Itgb1 [Tamkun 1986, Takada 1987] and the subsequent generation of mice with null [Fassler 1995] and floxed Itgb1 alleles [Potocnik 2000, Raghavan 2000, Graus-Porta 2001], researchers have sought to interrogate Itgb1 function in the brain. In order to deepen my understanding of the roles of Itgb1 in vivo, I searched for studies reporting the effects of conditional (Cre-LoxP) Itgb1 knockout in the murine CNS. The results of that search are presented in **Table 5**. It is apparent that although the most commonly used Cre driver is Nestin, a wide range of drivers have been used, studying various cell types emerging at varying stages of embryonic development. Indeed embryonic and early post-natal developmental stages are the best characterised, while relatively few studies have examined the effects of conditional Itgb1 loss in the adult.

1.3.5.1 *Embryonic*

Nestin is expressed from approximately E10 by the neuroepithelial precursors of radial glial cells (RGCs) in the CNS. A nestin-Cre strategy therefore has the effect of inducing conditional knockout (cKO) of the target gene in RGCs and all their descendants. Because most neurons and glia in the brain are derived directly or indirectly from RGCs [Gotz and Huttner 2005], NesCre;Itgb1cKO represents a profound loss of Itgb1 in the CNS.

The loss of Itgb1 in RGCs causes severe defects in embryonic brain development. These defects include reactive gliosis [Belvindrah et al. 2007], reduced brain size, reduced fissures in the cerebellum and cerebral hemispheres, aberrant positioning of cortical neurons, defective ECM deposition onto meningeal basement membrane, and defective development

of glial endfeet [Graus-Porta et al. 2001] Itgb1 has a critical role in anchoring RGC processes to the basement membrane, which in turn is essential for their survival during the period of symmetrical division and RGC population expansion. Itgb1-deficient RGC processes detach from the meningeal basement membrane and die by apoptosis. This reduction in the pool of RGCs contributes to a consequent reduction in Pax6+ and Tbr2+ progenitors before E15, leading to a functional microcephaly. [Radakovits et al. 2009]

One of the difficulties in interpreting NesCre;Itgb1 cKO data arises from the fact that Nestin is expressed from E10 by cells destined to generate both neurons and glia. This confound makes it impossible to determine whether the *neural* effects of Itgb1 cKO are cell-autonomous (arising primarily from Itgb1 loss on neurons) or non-cell-autonomous (arising primarily from the effects of Itgb1 loss on glia). To unpick this confound Belvindrah et al. compared Nes-Cre with a neural-specific Cre driver (Nex, expressed by cortical pyramidal neurons arising from embryonic ventricular zone progenitors). A pronounced reactive gliosis was seen in NesCre cKO mice from as early as P10, but was not in the neural-specific Nex-Cre cKO. Crucially and unlike Nes-Cre cKO mice, cortical layers in Nex-Cre cKO mice appeared normal. [Belvindrah et al. 2007]

These experiments suggested that the cause of neural deficits seen in Nes-Cre;Itgb1cKO mice lay at least partially in the downstream glial lineage of Nestin-expressing cells; in other words that Itgb1 functions in a non-cell-autonomous way to modulate the development of neurons. This hypothesis is supported by experiments in the developing and adult cerebellum in which Itgb1 loss from Math1+ neuronal progenitors causes no discernible neural phenotype, but Itgb1 loss in hGFAP+ Bergmann glia causes marked neural abnormalities. [Frick et al. 2012] Also consistent is the observation that loss of Itgb1 in Emx1+ neuroepithelial precursors leads to RGC endfoot detachment, which precedes the consequent aberrant positioning of neuronal cells. [Kwon et al. 2011]

Ref	Cre/ CreER	Cre driver	Target cell	Developmental stages analysed	Itgb1 allele	Effect of Itgb1 KO	Suggesting that
Graus-Porta et al. 2001	Cre	Nes	All descendants of CNS radial glial cells (neurons and glia) from E10.5	E12-5 - P28	Ibid	Severe defects in brain development, ataxia, reduced brain size, reduced fissures in the cerebellum, incomplete fissuring of cerebral hemispheres. Aberrant positioning of cortical neurons; defective ECM deposition onto meningeal basement membrane; defective development of glial endfeet. However neuronal migration continued.	Itgb1-class integrins regulate the formation of cortical layers by affecting cells and signals in the cortical marginal zone that are essential for the assembly of neurons into defined layers.
Forster et al. 2002	Cre	Nes	All descendants of CNS radial glial cells from E10.5	P6	Graus-Porta 2001	Aberrant dentate gyrus development with malpositioned granule cells and disorientated dendritic arbors. No outgrowth of Itgb1 cKO cells on 'Reelin stripes'.	Itgb1 is necessary for proper development of the DG, and (possibly in an unrelated way) interacts with Reelin in the hippocampus.
Schwander et al. 2004	Cre	Nes	All descendants of CNS radial glial cells, but here specifically spinal motor neurons	E10.5 - E12.5	Graus-Porta 2001	Impaired neurite outgrowth of E10.5 ventral spinal cord motor neurons on laminin substrates. In vivo, Itgb1 cKO mice displayed normal peripheral axon outgrowth and synaptic differentiation during neuromuscular development.	Itgb1 in spinal motor neurons is required for efficient neurite outgrowth on LN1/2 substrates in vitro. This was not a consequence of a general inability of the cells to extend neurites, but a more restricted phenotype of defects in a LN/integrin-dependent pathway.
Blaess et al. 2004	Cre	Nes	All descendants of CNS radial glial cells, but here specifically	E12.5 - P14	Graus-Porta 2001	Reduced postnatal GCP proliferation without an increase in apoptosis; potentially due to premature differentiation although this was not	Itgb1-containing heterodimers, laminins, and Shh cooperate to regulate GCP

			cerebellar granule cell precursors			actually quantified. In vitro, Itgb1-null cells adhered to and could be cultured on plates coated with a mix of PLL and LN or VN. The synergistic effect of LN and Shh on GCP proliferation was lost in the mutant cells (suggesting that LN and Shh synergise via Itgb1).	proliferation in the developing cerebellum.
Huang et al. 2006	Cre	Emx1 CamKII	Emx1: progenitors from the dorsal telencephalon at E9.5, destined to become radial glia, Cajal-Retzius cells, glutamatergic neurons, astrocytes, and oligodendrocytes. Here targeting pyramidal cells of CA1 and CA3. CamkII: Forebrain glutamatergic neurons	E14.5-Adult (Emx1); P14-adult (CamkII)	Graus-Porta 2001	Emx1Cre: Aberrant cortical development with altered layering and neuronal displacement, but macroscopically normal hippocampus. Specifically, normal dendritic architecture and dendritic spines in CA1 and CA3, with normal presynaptic and post-synaptic staining patterns. Normal basal synaptic transmission but impaired LTP with deficits at both presynaptic and postsynaptic locations. CamkIICre: No morphological deficits of cortical or hippocampal development. Again impaired LTP but this time normal presynaptic function.	Itgb1 is necessary during the developmental period, for the maintenance of normal adult synaptic function. In particular adult presynaptic function may depend on Itgb1 expression during stages of development prior to P14. Itgb1 is, additionally, required during adult life for normal LTP.
Chan et al. 2006	Cre	CamKII	Forebrain glutamatergic neurons	P180	Raghavan et al. 2000	No alterations in CNS gross anatomy; no detectable structural hippocampal synaptic differences in size or density (in CA1 at P180). Reduction in basal synaptic transmission (excitatory post-synaptic potentials); and possibly related to this, a deficit in NMDAr-dependent LTP; However no difference in water maze performance (‘normal spatial memory’) or pavlovian fear conditioning. Worsened performance on a working memory task.	Itgb1 contributes to at least three aspects of adult hippocampal function: basal synaptic transmission, synaptic plasticity, and working memory.

Benninger et al. 2006	Cre	CNP	Oligodendrocyte precursors from approximately E13.	P60 (optic nerves/CC); P5/P90 (spinal cord); P5 (cerebellum)	Potocnik et al. 2000	No evidence of dysmyelination in optic nerves, corpus callosum, or spinal cord of Itgb1 mutants. No evidence of impaired demyelination after lysolecithin injection to SC. Increased apoptosis of cerebellar oligodendrocyte precursors, but again no apparent myelination defect.	Itgb1 signaling is involved in the control of oligodendrocyte survival in the cerebellum, but otherwise it may not be required in a cell-autonomous way for CNS myelination and remyelination.
Belvindrah et al. 2007	Cre	Nes Nex	All descendants of CNS radial glial cells from E10.5 (Nes); Cortical pyramidal neurons arising from embryonic VZ progenitors (Nex)	E11-1 year	Graus-Porta 2001	Unlike *Nes*Cre cKO mice, cortical layers in *Nex*Cre cKO mice appeared normal, including cortical thickness. A pronounced reactive gliosis was seen in *Nes*Cre cKO mice, evident as early as P10, but was not seen in the neural-specific *Nex*Cre cKO. Explant cultures showed normal development of *Nex* Cre cKO neurons on *Nex* Cre (unrecombined) glia. As whole these findings suggest that the cause for the deficit in lies predominantly in the glial cells.	Loss of Itgb1 from RGCs causes a pronounced reactive gliosis, for reasons that are not explored here. As a whole the findings suggest that the cause for the deficit in the *Nes*Cre cKO model lies predominantly in the glial cells, although for this to be certain the degree of neural overlap in the Nes and Nex models would need to be total, and this is not shown.
Belvindrah et al. 2007	Cre	Nes	All descendants of CNS radial glial cells from E10.5	P60	Graus-Porta 2001	Microarray and RT-qPCR of SEZ and RMS-derived neuroblasts showed detectable expression of Itgb1 (along with b5, a1, a3, a6, and a7). In adult Nes cKO mice, the RMS was present, but it appeared less compact and the cells were no longer assembled into chains. The OB was reduced in size.	Itgb1 plays an intrinsic role regulating migration of SEZ-derived NBs through the RMS to the OB.

						No deficits in proliferation/apoptosis were seen in the OB or SEZ. The primary deficit was impaired migration from the SEZ via the RMS to the OB: cells remained in the RMS or migrated from it ectopically, rather than making their way to the OB. EM and explant culture experiments suggested defects in the glial tubes of the RMS and the formation of cell chains as causes of the impaired migration.	
Radakovits et al. 2009	Cre	Nes	All descendants of CNS radial glial cells from E10.5	E11-P21	Graus-Porta 2001	Itgb1-deficient RGCs processes detach from the meningeal basement membrane and die by apoptosis; this reduction in the pool of RGLs is the primary deficit causing a consequent reduction in Pax6+ and Tbr2+ progenitors before E15, leading to a functional microcephaly. Attachment to the meningeal BM may be mediated via laminins a2/a4.	Itgb1 has a role in anchoring RGC processes to the BM, which in turn is essential for their survival during the period of symmetrical division and RGC population expansion.
Robel et al. 2009	Cre	hGFAP Nex	hGFAP: descendants of RGCs after E13. Nex: Cortical pyramidal neurons arising from embryonic VZ progenitors from E11.5	E13 - P180	Potocnik et al. 2000	hGFAP: Itgb1 protein levels took two weeks to fall to 37% of E13 baseline. Normal cell density, structural morphology and myelin immunoreactivity in the brain. Pronounced cortical upregulation of GFAP and associated upregulation of Vimentin, Tenascin C, and DSD-1. Secondary upregulation of microglia. Disruption of astrocyte endfeet and (astrocytic) laminin a1/a2 deposition. However no proliferative or apoptotic phenotype, and no disruption of BBB. NEX: No gliosis phenotype.	

Barros et al. 2009	Cre	Nes Ng2	Nes: All descendants of CNS radial glial cells, here targeting oligodendrocytes. Ng2: OPCs (and pericytes)	P0-P60	Graus-Porta 2001	Nes: Reduced myelin thickness on a subset of spinal cord and optic nerve axons (greater relative loss on bigger axons). Reduced MBP and PLP in SC lysates. Ng2: similar pattern of reduced myelin thickness, but to a lesser extent. Cre-mediated recombination may have been less effective in Ng2-Cre mice. There was reduced myelin sheet outgrowth (in sheet number and total area) in both cortex and SC. There was no apparent loss of oligodendrocytes.	In the CNS, Itgb1 regulates oligodendrocyte sheet number and area; whether this is primarily a cell-autonomous or non-cell autonomous effect is unclear.
Kwon et al. 2011	Cre	Emx1 Wnt3a	Emx1: progenitors from the dorsal telencephalon at E9.5, here targeting Cajal-Retzius cells. Wnt3a: cortical hem-derived C-R cells, used here as a more specific C-R cell Cre driver than Emx1	E14.5-15.5	Graus-Porta 2001	Deletion of Itgb1 using emx1-cre caused dramatic retraction of RGC endfeet at E14.5, without obvious defects in cortical BM. Associated with displacement of C-R cells. RGC endfoot retraction precedes C-R displacement. No effect on RGC density, nor proliferation either in VZ RGCs or in basal IPs. Itgb1 deletion by *wnt3a-cre* had no obvious effects on C-R cell localisation.	Itgb1 plays a critical role in C-R cell targeting during early stages of corticogenesis. It is required in the RG scaffold and not in C-R cells themselves.
Parkash et al. 2012	Cre	GnRH	GnRH-expressing neurons projecting to the ME of the hypothalamus	E14.5 - 5 months	Raghavan et al. 2000	Fewer GnRH+ neurons migrated successfully to the ventral forebrain by E14.5. The defect had normalised by P7 but adult animals again showed reduced number of GnRH+ cells, and reduced innervation to the hypothalamic ME. Female mutants (though not males) were less fertile, possibly secondary to reduced number of ovulations. Female mice also had delayed puberty and abnormal oestrus cycles.	Itgb1 contributes to development of the GnRH neuronal system, and in female mice to proper establishment and function of the hypothalamic–pituitary–gonadal axis and the initiation of puberty.

Lei et al. 2012	Cre	Emx1 (standard cross); Turbo-Cre (in utero electroporation)	Emx1: progenitors from the dorsal telencephalon at E9.5, destined to become radial glia, Cajal-Retzius cells, glutamatergic neurons, astrocytes, and oligodendrocytes.	E14.5 - P3	Raghavan et al. 2000	Reduced level of SAD kinases and phosphorylated (active) LKB1 in cKO cortex and hippocampus; Aberrant axonal development in major white matter tracts shown by DiI labelling and TAG1 immunostaining. Altered morphology of (P3) cortical plate neurons in (E15.5) electroporated brain: a marked lack of axonal processes.	Itgb1 is necessary for normal development of axonal projections in at least a subset of neurons arising from the dorsal telencephalon.
Mortillo et al. 2012	Cre	CamKII	Forebrain glutamatergic neurons, here targeting CA1	P100	Raghavan et al. 2000	Itgb1 is present in the synaptic cleft in CA1 neurons. cKO caused increased compensatory expression of N-Cad and neuroligin. Overall synapse structure remained intact.	
Warren et al. 2012	Cre	Nex	Excitatory neurons arising from embryonic VZ progenitors from E11.5, here targeting pyramidal neurons in CA1	P21, P42	Graus-Porta 2001	Itgb1 cKO caused reduced length and complexity of apical dendritic arbor in CA1 pyramidal neurons at P42, with a corresponding decrease in synapses onto the Schaffer collateral pathway. Impairment in a hippocampal dependent memory task, also with greater sensitivity to the stimulant properties of cocaine.	Itgb1 in excitatory hippocampal neurons contributes to regulation of apical dendritic arbor size in the CA1 stratum radiatum, maintenance of synapses, and hippocampal-dependent behaviour.
Frick et al. 2012	Cre	Math1; hGFAP	Math1: Cerebellar neuronal granule cell precursors; hGFAP: cerebellar Bergmann glia	P7; ‘adult’	Raghavan et al. 2000	Itgb1 cKO from Math1+ cerebellar granule cell precursors caused no alterations in cerebellar structure at P7 or adulthood; nor altered proliferation or apoptosis at P7. However Itgb1 cKO from postnatal cerebellar Bergmann glia (in the hGFAP-Cre line) caused marked structural abnormalities, with islands of ectopic cells expressing neuronal markers.	Expression of Itgb1 in GCPs is not required for the proper formation of the murine cerebellum. Itgb1 in the Bergmann glial scaffold is required for proper positioning and development of glial processes. Without this,

							granule neurons are prohibited from physiological migration and undergo premature differentiation.
Riccomagno et al. 2014	Cre	Six3 (pan-retinal); Pax6a (neural retinal)	Developing Retinal Ganglion Cells	E14.5 - P14	Raghavan et al. 2000	Failure of retinal ganglion cells to develop a normal single-celled thickness retinal ganglion cell layer, with ectopic clusters of cells seen instead; associated with markedly reduced Cas phosphorylation in the inner neuroblastic layer. Preserved formation of basal lamina of the retinal inner limiting membrane.	Itgb1 is required for the formation of the single-cell GCL during retina development; Itgb1 mediates Cas phosphorylation in developing retinal ganglion cells which may impact on cellular migratory capabilities.
Robel et al. 2015	Cre	hGFAP; Nex	hGFAP: descendants of RGCs after E13. Nex: Cortical pyramidal neurons arising from embryonic VZ progenitors from E11.5	P14-P100	Potocnik et al. 2000	Widespread upregulation of GFAP by P28 with gradual increase in this 'reactive gliosis' until at least P100. Mild 'secondary micrgliosis' starting at P42. In vivo video EEG showed tonic-clonic seizures and interictal spiking in mutant mice. Neuron-specific Itgb1 deletion did not show the same phenotype.	Itgb1 functions to restrain astrogliosis in the postnatal and adult brain. Astrogliosis (or possibly separately, Itgb1 loss in astrocytes) causes increased excitability of neurons and an epileptiform phenotype.
Venkatesen et al. 2015	Cre	mGFAP	Astrocytes generated during the perinatal period, largely if not entirely before P2	P2-15	Raghavan et al. 2000	No differences in cortical lamination, neuronal or oligodendrocyte distribution, myelination, or distribution or morphology of GFAP+ astrocytes. However a decrease in AQP4 labelling on astrocytic perivascular endfeet, with decreased blood vessel branching. There was no physiological functional BBB leakage. After hypoxic-ischaemic injury Itgb1	Itgb1 contributes in the perinatal period to the physiological development of astrocytic endfeet / AQP4 expression, and either through this or another mechanism influences blood vessel architecture.

						mutants showed markedly worse cerebral architecture.	
North et al. 2015	CreER	FoxJ1 in vivo; adeno-Cre in vitro	Adult spinal cord ependymal cells	P56 in vivo; P1 in vitro	Raghavan et al. 2000	*In vivo:* Itgb1 was upregulated in the ependymal zone (EZ) after SCI. After injury a greater proportion of Itgb1-floxed recombined cells expressed GFAP, with increased pSMAD1/5/8 expression. *In vitro:* cre-mediated deletion of Itgb1 in cells grown from P1 spinal cord and P1 SEZ (not necessarily the same cells as adult in vivo) led to greater astrocytic differentiation. Co-IP showed interaction between Itgb1 and BMPR1a and 1b. Levels of BMPR1b in lipid raft fractions were increased after Itgb1 deletion.	Itgb1 prevents astrocytic differentiation after SCI, and functions to restrain BMP signalling after injury. Mechanistically, suggests that Itgb1 physically interacts with BMPR1b in the cell membrane, limiting its ability to move into lipid rafts and signal, thereby attenuating astrocytic differentiation.
Tan et al. 2016	Cre	Nkx2.1	Medial ganglionic eminence / Preoptic area Radial Glial Precursors	E12.5-E16.5	Raghavan et al. 2000	Impaired anchoring of RGP endfoot to blood vessels; Reduced proliferation index in the MGE; Reduced cortical interneuron density at P21-P30	Itgb1 is essential for the proper development of MGE-derived interneurons, possibly via their attachment to blood vessels to access proliferative signals.

Table 5: Studies examining the effect of conditional Itgb1 loss in the murine CNS.

These data suggest that Itgb1 functions to maintain the glial scaffold necessary to direct neuronal proliferation and migration during embryonic neurogenesis. Notably, if unsurprisingly, there seems to be a critical period for Itgb1 on glial cells to direct neurogenesis in this way. Experiments using mGFAP-Cre (which induces recombination perinatally, after the peak of developmental neurogenesis) report no effect on cortical lamination or neuronal distribution. [Venkatesen et al. 2015]

Other cellular phenotypes are latent, with effects critically dependent upon extracellular parameters. For example embryonic spinal motor neurons lacking Itgb1 display normal peripheral axon outgrowth and synaptic differentiation in vivo, with impaired neurite outgrowth only evident in vitro on laminin substrates. [Shwander et al. 2004]

1.3.5.2 *Post-natal*

Postnatally, Itgb1 is necessary for proper postnatal development of the dentate gyrus. Experiments targeting both Nes-Cre and Nex-Cre lineages indicate a role for Itgb1 in proper postnatal positioning of granule cells, the size and orientation of dendritic arbors in the CA1 stratum radiatum, maintenance of synapses, and hippocampal-dependent behaviour. [Forster et al. 2002, Warren et al. 2012]

Itgb1 also contributes to the development of medial ganglionic eminence (MGE)-derived interneurons, possibly via their attachment to blood vessels to access proliferative signals. Nkx2.1-Cre;Itgb1cKO mice displayed impaired anchoring of RGP endfoot to blood vessels, with a reduced proliferation index in the MGE and reduced cortical interneuron density at P21-P30. [Tan et al. 2016] Furthermore Itgb1 co-operates with laminins and Shh to regulate post-natal granule cell precursor proliferation in the developing cerebellum. [Blaess et al. 2004]

In addition to these effects on neurogenesis, Itgb1 also regulates aspects of glial cell biology. It regulates oligodendrocyte survival in the cerebellum [Benninger et al. 2006] together with oligodendrocyte sheet number and area, with evidence in cKO mice of reduced myelin thickness on a subset of spinal cord and optic nerve axons. [Barros et al. 2009]

1.3.5.3 *Adult*

In contrast to the rather dramatic effects of Itgb1 cKO in embryonic and post-natal development, its reported effects in adulthood (defined here as post-natal day 56 onwards) tend to be more subtle. Considering a functional role for Itgb1 in adult hippocampal function, a few groups have studied CamKII-Cre;Itgb1cKO mice. These animals lack Itgb1 in forebrain glutamatergic neurons, but display no alterations in CNS gross anatomy and no detectable structural hippocampal synaptic differences in size or density. There is, however, compensatory overexpression of N-Cadherin and neuroligin. [Mortillo et al. 2012] Physiologically, adult mice display a reduction in basal synaptic transmission with deficits in NMDAr-dependent long-term potentiation (LTP). They display worsened performance on a working memory task but normal spatial memory and fear conditioning. [Chan et al. 2006]

A similarly subtle deficit is seen in the hippocampus of adult Emx1-Cre;Itgb1cKO mice. Mutants display normal dendritic architecture and dendritic spines in CA1 and CA3, with normal presynaptic and post-synaptic staining patterns. Basal synaptic transmission is also normal, but LTP is impaired with deficits at both presynaptic and postsynaptic locations. [Huang et al. 2006] These results indicate that in adult animals Itgb1 contributes to at least three aspects of adult hippocampal function: basal synaptic transmission, synaptic plasticity, and working memory.

In terms of adult neurogenesis, conditional knockout studies suggest that Itgb1 plays an intrinsic role regulating migration of SEZ-derived neuroblasts through the rostral migratory stream (RMS) to the olfactory bulb (OB). In adult Nes-Cre;Itgb1cKO mice the RMS was less compact, the migrating cells were no longer assembled into chains, and the OB was reduced in size. No deficits in proliferation/apoptosis were seen: the primary deficit was impaired migration from the SEZ via the RMS to the OB. Cells either remained in the RMS or migrated from it ectopically rather than making their way to the OB. However electron microscopy and explant culture experiments suggested defects in the glial tubes of the RMS as one possible cause of the impaired migration, again suggesting the possibility of a non cell-autonomous (glial-mediated) effect of Itgb1 loss on neurogenesis.

A few groups have identified a possible functional role, spanning all developmental stages, for Itgb1 in moderating astrocytic differentiation and the presence of gliosis. Robel et al. reported that Itgb1 loss in hGFAP+ glia, but not neurons, causes a reactive gliosis in

embryonic, postnatal, and adult mice. [Robel et al. 2009, Robel et al. 2015] Whether the late effects in adulthood are of new and adult onset, or simply a persistence of developmental abnormalities, remains unclear. However an adult-onset function for Itgb1 in mediating gliotic phenotype is also evident in the only study to use an inducible Cre (CreER) strategy in the adult murine CNS to date. North et al. used FoxJ1CreER;Itgb1iKO mice to report an enhanced gliotic response to injury of the spinal cord after inducible deletion of Itgb1 from adult spinal cord ependymal zone stem cells (EZSCs) in vivo. [North et al. 2015] Following a series of in vitro experiments using P1 EZSCs the authors suggested that mechanistically, Itgb1 physically interacts with the cell surface BMP receptor 1b (BMPR1b), limiting its ability to move into lipid rafts and promote astrocytic differentiation. In the course of their study they also demonstrated that Itgb1 interacts with BMPR1a, shown elsewhere to be a key driver of NSC quiescence in adult hippocampal neurogenesis. [Mira et al. 2010]

Taken together the literature on conditional Itgb1 knockout in the murine CNS suggests several key functions. First, Itgb1 is necessary for the proper development of the CNS, with multiple abnormalities arising from knockouts targeting early lineage precursors. Second, Itgb1 is implicated in vivo most often in the proliferation, survival, adhesion, and migration of neurons. Third, it can be difficult to attribute the neural phenotypes to cell-autonomous or non cell-autonomous functions of Itgb1. Where direct comparisons can be made there is some evidence to suggest that the role of Itgb1 in maintaining neurogenesis is often mediated through non-neural cells. Fourth, deficits in adult animals are often more subtle than those seen in embryonic or postnatal stages. Lastly, Itgb1 may mediate a phenotype of reactive gliosis in the CNS across all developmental stages.

1.3.6 Integrin β1 in the regulation of neural stem cells

Multiple lines of evidence directly or indirectly implicate Itgb1 in neural stem cell (NSC) biology. The evidence includes observational and interventional studies of embryonic and early post-natal neurogenesis, disease models, and neurogenesis in the adult mammalian SEZ and SGZ niches. **Table 6** summarises my search for studies of Itgb1 manipulation in neural stem cells. In summary, most authors have examined Itgb1 function using a loss-of-function strategy during embryonic neurodevelopment. Fewer studies have examined disease modelling, gain-of-function, or NSCs in the postnatal or adult developmental stages.

Ref.	Species	Stage	Region	Itgb1-NSC manipulation	Function	Culture system	Results	Suggesting that
Murase et al. 2002	Mouse	Embryo, postnatal	Saggital section of RMS	Ex vivo slice culture with antibody blocking	LOF	NA	Itgb1 was expressed until P10 in tangentially migrating cells in the RMS. In P3 and P5-derived slices, Itgb1 blocking antibody markedly reduced migration speed.	Itgb1 (along with other integrins) is required for cellular migration in the postnatal RMS.
Yanagisawa et al. 2004	Mouse	Embryo	Telencephalon	Incubation with RGD peptide	LOF	Monolayer	Incubation of NSCs with RGD peptide inhibited their adhesion to fibronectin. Itgb1 also found to localise in the same fraction of NSC homogenate as Flotillin-1, a protein found in lipid rafts. Disrupting lipid raft architecture caused impaired adhesion.	NSCs adhere to fibronectin in an integrin-dependent manner. Itgb1 is present in lipid rafts and this is required for proper adhesive function.
Tate et al. 2004	Mouse	Embryo	Ganglionic eminence	In vitro antibody blocking	LOF	Neurosphere / coverslip adhesion and migration	Itgb1 coimmunoprecipitated with α1, α2, α3, α5, α6 and αV. Blocking Itgb1 and Itga6 reduced adhesion to laminin-1, while blocking Itgb1 and Itga5 reduced adhesion to fibronectin. NSCs migrated faster on laminin-1 than on other substrates (FN, Col1 and Col4); this was largely blocked, again, by antibodies to Itgb1 and Itga6. NSC migration on FN was blocked by antibodies to Itgb1 and Itga5. LN1 promoted differentiation to Tuj1+ neurons compared to other substrates.	NSCs adhere to and migrate on laminin-1 primarily via α6β1; and FN via α5β1.
Campos et al. 2004	Rat; Mouse	Postnatal	Forebrain	In vitro adeno-cre transfection of Itgb1 f/f NSCs; blocking antibody	LOF	Neurosphere	Itgb1 and Itga6 are both expressed in the ventricular region of the E12.5 mouse, and Itgb1 colocalises with nestin in the SEZ at P0-2. LNa2 is expressed during embryogenesis with reduced level postnatally. Cells from	β1 integrins are expressed at a high level on NSCs during embryogenesis and the early postnatal period, and in neurospheres;

							primary neurospheres, FACS-sorted for Itgb1-Hi, generated more secondary neurospheres. EGFR and Itgb1 co-label cells at the edge of neurospheres. Inhibition of MAPK P42,44 reduced the number of secondary spheres, but inhibition of PI3K or p38 MAPK did not. Itgb1 blocking antibodies reduced the level of p-MAPK. Itgb1 gene excision showed a transient decrease in p-MAPK, but p-MAPK levels returned to normal after several (<10) passages. A blocking antibody to EGFR abrogated this recovery suggesting that EGFR was 'taking the strain' of the Itgb1 iKO.	the laminin α2 chain is present in the stem cell-containing regions of the developing CNS; MAPK signalling is required for stem cell maintenance; EGFR signalling is likely to compensate for the deleterious effects of Itgb1 iKO on activation of the MAPK pathway.
Andressen et al. 2005	Mouse	NA	Unclear	Genetic KO (null)	LOF	Neurosphere adherent to coverslips for migration; monolayer for differentiation	No significant difference in neurosphere size, proliferation or apoptosis was seen in Itgb1 -/- spheres. For both groups, dendritic ramification and process extension was better on laminin than fibronectin or gelatine. Itgb1 null cells had reduced magnitude of migration and morphological development than control cells, but whether these outcomes were statistically significantly poorer was not stated.	Itgb1 may not be required for proliferation and survival of ESC-derived NSCs.
Leone et al. 2005	Mouse	Postnatal	Forebrain	In vitro adeno-cre transfection of Itgb1 f/f NSCs	LOF	Neurosphere / coverslip adhesion	Loss of Itgb1 impaired sphere adhesion to laminin and (to a lesser extent) fibronectin. However loss of Itgb1 did not impair neurosphere self-renewal, but did affect sphere size	Itgb1 signalling is not an absolute requirement for NSC renewal; however it regulates proliferation and

							with significantly smaller spheres in the iKO, associated with significantly smaller proportion of Nes+ cells and a significantly greater proportion GFAP+ and Tuj1+ cells. Itgb1 KO was associated with reduced total proliferation, and with increased death of Nes+ cells. Low concentrations of growth factors could almost entirely override the	survival of Nes+ progenitors in spheres, and interacts with growth factors (EGF/FGF/NGF) to mediate these effects.
Mueller et al. 2006	Human	Embryo	Ventricular zone	In vitro antibody blocking	LOF	Neurosphere ; monolayer culture	Using TNF-a treated endothelial cells as a model to simulate 'injured cerebrovascular endothelium', the authors showed that antibodies to Itgb1 (and α2 and α6) inhibited rolling of hNSCs. FACS analysis showed that hNSCs express β1, α2, α6, and αV integrin.	Itgb1 may mediate attachment of systemic ally-arising NSCs to the vascular endothelium. The relevance of this is unclear though; NSCs have not been shown to arise from the periphery!
Flanagan et al. 2006	Human; mouse	Embryo	Cortex (both)	In vitro antibody / chemical blocking	LOF	Neurosphere adherent to coverslips	Laminin or laminin-containing substrates promoted expansion, migration, differentiation (to neurons and astrocytes) and neurite extension of adherent NSCs. FACS analysis showed NSCs expressed b1, a3, a5, a6 and a7 integrins. Treatment with Echistatin (blocks a5b1) disrupted migration on fibronectin **but not on laminin.** Conversely an a6 antibody - possibly blocking a6b1 - had disruptive effects on laminin but not on Fn.	Human and mouse embryonic NSCs can express Itgb1 in vitro, and differential effects on read-out can be seen depending on the extent to which the culture system triggers expression of different heterodimers.
Campos et al. 2006	Mouse	Embryo, postnatal	Forebrain	Morpholino KD; Mn++	LOF;GOF	Neurosphere ; ES-cell derived	Notch1 and Itgb1 are co-expressed in the E14.5 VZ in vivo, and in vitro in neurospheres and ES-cell derived	Itgb1 and Notch interact on NSCs. Itgb1 and EGFR may cross-

						monolayer NSCs	NSCs. Activation of Itgb1 with Mn++, ECM, or EGF (but not FGF2) triggered Notch pathway activation in monolayers. Itgb1 and Notch1 coimmunoprecipitated. Itgb1 KD of primary neurospheres reduces the number of secondary spheres to a greater extent when spheres were grown in FGF2 than EGF. Itgb1 had been compensating for the lack of EGF in the FGF2-grown spheres. Conversely, that EGF was able partially to compensate for the lack of Itgb1 in EGF/KD spheres.	compensate for the lack of each other.
Cao et al. 2007	Chick	Embryo	Spinal cord	RNAi KD and overexpression (by in ovo electroporation)	LOF, GOF	NA	When miR-124 was ectopically expressed in neural progenitors, the syntheses of laminin γ1 and integrin β1 were decreased, leading to the disintegration of basal laminae. This effect could be partially recapitulated by transfection of Itgb1 KD, and partially rescued by co-transfection of miR124 with an Itgb1 overexpression construct.	The 3'UTR of the chick Itgb1 gene may be a target for repression by miR-124. But miR-124 overexpression and KD had no effect on neuronal differentiation.
Liao et al. 2008	Rat	Embryo	Coronal sections containing SEZ	In vitro antibody blocking	LOF	Neurosphere ; monolayer culture for differentiation	In vitro, Itgb1 co-immunoprecipitates with recombinant EGFL and FN6-8 domains of TNR. The FN6-8 domain reduces NSC proliferation and neurogenesis, and promotes gliogenesis while the EGFL domain promotes differentiation; in the combined presence of Itgb1 antibody these effects are all lost. However Itgb1 LOF only returns outcomes to control levels. Note Fig 7 showing	Itgb1 may restrain NSC proliferation and neurogenic differentiation by binding to the FN6-8 domain of TNR in the ECM. In vitro there is no evidence that LOF causes rebound phenomena on these outcomes but it is not

							that Itgb1 blocking antibody alone had **no effect** on proliferation of NSCs in monolayer culture.	clear what effect LOF would have on in vivo.
Hall et al. 2008	Human	Embryo	Cortex	In vitro antibody blocking	LOF	Neurosphere	Itgb1 blockade increased apoptosis of hNSCs in neurospheres, but **only in the presence of added soluble laminin.** Without laminin, Itgb1 blockade had no effect on apoptosis.	The effects of integrin knockout may be critically dependent on the composition of the ECM.
Ma et al. 2008	Human ESC	NA	Unclear	In vitro antibody blocking	LOF	EBs and neural rosettes	Nearly all hESC-derived NSCs (98%) detectably expressed Itgb1. Antibody blocking caused reduced migration on PDL/Laminin.	a6β1 integrin mediates hESC-derived neural progenitor responses to laminin.
Loulier et al. 2009	Mouse	Embryo	VZ	In utero ventricular injection of Itgb1 blocking antibody	LOF	NA	Itgb1 is expressed sub-apically on radial fibres contacting the VZ. Ventricular Injection of a blocking antibody transiently (<2h) disrupts Itgb1 signalling. Infusion of Itgb1 blocking antibody caused an increase in proliferation (PH3 and BrdU) in the abventricular compartment after 18h, with no change in the number of ventricular divisions. Itgb1 blockade reduced the number of horizontal mitoses (i.e. proportionally more vertical mitoses) but it is not clear what this means for cell fate; there was no effect on differentiation at the 18h timepoint. Itgb1 blockade also caused partial detachment of the ventricular endfeet of NSCs, and altered cortical cell layering at P4.	Note another paper showing increased proliferation after Itgb1 blocking.
Bruggeman et al. 2009	Mouse	Postnatal	SEZ	In vitro antibody blocking	LOF	Monolayer	NSCs lacking the epigenetic repressor gene Bmi1 display increased monolayer adhesion to various substrates, including	Loss of Bmi1 - an event implicated in the development of brain cancer - alters cell

							untreated plastic. This effect was blocked by adding an Itgb1-blocking antibody to culture. Co-culture experiments suggested that Bmi1-/- NSCs deposit ECM to plastic which causes increased adhesion of Bmi1WT/WT cells, when these are added after removal of the Bmi1-/- cells.	adhesive properties, which remain integrin-dependent (as they are in control cells).
Kazanis 2010	Mouse	Adult	SEZ	In vivo infusion of Itgb1 blocking antibody	LOF	Neurosphere	Itgb1 upregulated on activated neural stem cells following AraC infusion. Itgb1 blocking antibody infusion led to an increase in Soz2+ proliferating intermediate progenitor cells, with aberrantly placed DCX+ neuroblasts, interpreted as ectopic migration.	In the adult SEZ Itgb1 negatively regulates proliferation of Sox2+ intermediate progenitors, and regulates migration of neuroblasts.
Sakaguchi et al. 2010	Mouse	Adult	SEZ	In vivo infusion of Itgb1 blocking antibody	LOF	Neurosphere	Itgb1 colabels cells that also express Galectin in the SEZ. It's not clear from the data shown what the Itgb1+Galectin+ cells are. Infusion of Itgb1 blocking antibody concomitantly with BrdU led to a decrease in labelled SEZ BrdU+ cells ten days later. Two possible interpretations: reduced proliferation (and thereby reduced BrdU uptake) during infusion, or reduced quiescence (and thereby increased BrdU washout, and fewer LRCs at d10). The Itgb1-mediated effect dominated a weaker proliferative effect of Galectin.	Infusion of Itgb1 blocking antibody caused an ambiguous BrdU phenotype. Study needed an assay of fast-proliferating cells too (e.g. CldU). More evidence here of Itgb1 antibody preventing neurosphere formation in vitro though.
Suzuki et al. 2010	Mouse	Embryo	Telencephalon	siRNA KD; RGD peptide	LOF	Monolayer to generate	Itgb1 is upregulated on the cell surface of NECs after culture with bFGF or EGF, via the MAPK	Itgb1 mediates EGF- and FGF-induced

						NECs, rich in NSCs	pathway. SiRNA KD inhibited adhesion to fibronectin and attenuated - but did not abolish - proliferation of NECs. RGD peptide caused increased apoptosis.	proliferation and survival of NECs.
Fainstein et al. 2013	Mouse	Embryo	Forebrain	Transplantation of NSCs to lesioned adult mouse striatum, followed by in vivo infusion of Itgb1 blocking antibody	LOF	Neurosphere	Increased survival of transplanted NSCs was seen in the striatum after 6-OHDA lesion, compared to uninjured striatum. Itgb1 blocking antibody abrogated this effect. Whether these Itgb1-dependent effects are limited to the striatum (post-injury) was not shown.	Injury to the adult striatum triggers some kind of change in the local milieu that enhances the survival of transplanted NSCs. Itgb1 mediates that survival.
Arvanitis et al. 2014	Mouse	Embryo	Cortex	In vitro antibody blocking	LOF	Monolayer	Itgb1 blocking antibody prevented increased adhesion of WT NSCs to culture plates coated with laminin and Ephb2.	Itgb1 mediates adhesion of E14.5 NSCs to Ephb2 and laminin.
Bergstrom et al. 2014	Mouse	Embryo, postnatal, adult	E14.5 cortex; P6 and P60-90 SEZ	In vitro antibody blocking	LOF	Neurosphere ; then monolayer culture after 2nd neurosphere passage	NSPCs isolated from the SVZ of postnatal day 6 mice readily (<1h) adhere to collagen 1 and establish focal adhesions in an integrin-dependent manner. The corresponding cells isolated from the adult SVZ or embryonic cortex do not, although - like P6 - they do adhere readily to fibronectin. qPCR revealed higher expression of a2 and a11 mRNA specifically in P6 neurospheres. P6 NSC adhesion to collagen was blocked by Itgb1-blocking antibody in a dose-dependent fashion.	Collagen 1 adhesion of early postnatal NSPCs is mediated by a2b1 and a11b1 integrin heterodimers. These heterodimers are less expressed in adult NSCs.
Pan et al. 2014	Mouse	Postnatal	SEZ	In vitro adeno-cre transfection of Itgb1 f/f NSCs;	LOF; GOF	Neurosphere ; monolayer culture for	Both cre-mediated Itgb1 KO and dominant negative Itgb1 transfection caused an increase in GFAP protein	In P1 SEZ NSCs, Itgb1 functions to restrain glial lineage

				transfection of dominant negative Itgb1; IKVAV-PA co-culture		differentiation	and/or mRNA. IKVAV-PA both increased Itgb1 expression and abolished the gliotic effect of Itgb1 KO/KD, in a manner dependent on Itgb1 expression and via ILK. Integrin overexpression also maintained cells in an undifferentiated state with an increase in proliferative Sox2-expressing cells.	differentiation, and when overexpressed maintains NSCs in an undifferentiated, proliferative state.
Brooker et al. 2016	Mouse	Adult	Dentate gyrus/SGZ	In vivo lentiviral Cre transfection of Itgb1 f/f hippocampus	LOF	Neurosphere	Profound architectural disruption of the SGZ niche, associated with increased proliferation of non-recombined cells, increased astrocytic fate differentiation of recombined cells, and a reduction of neuroblast density in the DG.	Itgb1 maintains integrity of the adult neurogenic niche and may serve to restrict astrocytic differentiation of NSPCs.
Long et al. 2016	Chick	Embryo	Mesencephalon	In ovo electroporation of a constitutively active Itgb1 construct (CA*B1)	GOF	Explant	CA*B1 increased midbrain proliferation in a cell-autonomous manner. It increased differentiation (neurogenesis) in a non cell-autonomous manner. Microarray revealed upregulation of Wnt7a in CA*B1+ electroporated cells, and upregulation of Decorin in non-electroporated cells. Morpholino knockdown of Wnt7a and Decorin showed that both molecules were necessary for the CA*B1-mediated increase in neurogenesis.	Integrin signalling in neuroepithelial cells of the chick midbrain has cell autonomous effect on proliferation and differentiation of cells expressing the activated integrin. Meanwhile a non-cell autonomous effect in adjacent, non-integrin-expressing cells which is driven by Wnt7a and the consequent upregulation of Decorin.

Table 6: Studies examining the effect of Itgb1 manipulation in neural stem cells.

1.3.6.1 *Embryonic*

Itgb1 is highly expressed during normal embryonic CNS development. Fluorescent Activated Cell Sorting (FACS)-based studies corroborate the notion that during a critical period in the developing embryo, Itgb1 is expressed by proliferative, neural stem-like cells. For example in E14.5 mice Itgb1, together with Notch1 and Syndecan1, can be used to select for neurosphere-initiating cells with multidifferentiation potential. [Nagato et al. 2005] Meanwhile in E14.5 mouse telencephalon-derived NSCs, Itgb1 co-immunoprecipitates with the stem cell marker SSEA1/LeX. [Yanagisawa et al. 2005] During embryonic neurodevelopment Itgb1 is expressed along with Itga6 and Itga7, with higher expression of integrins towards the Ventricular Zone (VZ) where the stem cells reside. [Lathia et al. 2007] In vivo and cell culture experiments suggest that Itgb1+ cells co-express the stem cell marker Sox2. A population of Itgb1-negative cells meanwhile gradually expands and appear to be those committed to neuronal differentiation. [Lathia et al. 2007, Yoshida et al. 2003]

The close relationship between Itgb1 and embryonic neural stem/progenitor markers is conserved across species. In human embryonic stem cell (hESC)-derived neural cultures, Itgb1 can be used to select proliferative neural stem cell-like cells. Cultured hESCs expressing the stem cell markers Pax6 or Sox2 colabel with Itgb1, whereas DCX+ differentiating neuroblasts do not. [Pruszak et al. 2009] Similarly, human NSCs derived from 8-10wk post-conception fetal cortex express mRNA for Itgb1 together with Itga1-3, 5-10, and V, and Itgb5 and Itgb8. FACS sorting of Itgb1-hi cells from primary neurospheres selects multipotent cells with significantly greater potential to generate secondary neurospheres. Itga6 is also expressed on hNSCs and - interestingly - selects for neurosphere-generating cells in a similar way, with no additive effect of sorting for b1 and a6 heterodimers together. This finding suggests that a6 and b1 heterodimerise at high levels in neurosphere-generating cells from the embryonic human cortex. Not all Itgb1+ cells express a6 - indeed, only 20% of Itgb1+ cells did - but it is possible that other b1-a heterodimers are expressed on more differentiated cell types. This speculation is supported by the observation that 90% of CD133+ stem-like cells express Itgb1. [Hall et al. 2006]

A number of studies have built on these observations to interrogate the function of Itgb1 in NSCs during embryonic development. In sum, these studies indicate that Itgb1 interacts with molecules in the ECM to regulate NSC dynamics and adhesion to the embryonic ventricular surface. For instance in E12.5 mice, Itgb1 is expressed sub-apically on radial fibres

contacting the VZ. Ventricular injection of a blocking antibody transiently disrupts Itgb1 signalling, causing an increase in proliferation in the abventricular compartment after 18h. Itgb1 blockade also causes partial detachment of the ventricular endfeet of NSCs. [Loulier et al. 2009] Similarly in human embryonic cortical-derived neurospheres, Itgb1 mediates the survival of neural stem and progenitor cells [Hall et al. 2008]. Interestingly however, Itgb1 antibody blockade had no effect on cell survival in the absence of exogenous laminin.

The necessity for exogenous laminin is an important finding with analogues in other papers. [Flanagan et al. 2006, Liao et al. 2008a] It suggests that differential effects on read-out can be seen depending on the extent to which the culture system triggers the expression of different heterodimers. On laminin (or laminin-containing substrates) NSCs more favourably expand, migrate, differentiate to neurons and astrocytes, and extend neurites. [Flanagan et al. 2006, Tate et al. 2004] In addition to laminins Itgb1 is known to interact with the extracellular matrix molecules Tenascin R and fibronectin to mediate control over embryonic NSPC proliferation and differentiation [Liao et al. 2008a, Yanagisawa et al. 2004, Suzuki et al. 2010], and to mediate their adhesion to substrates containing Ephrin B2. [Arvanitis et al. 2014] Taken together these observations reinforce the general principle that interactions between Itgb1 and the extracellular matrix are key mediators of NSPC dynamics.

Mechanistically and in utero, Itgb1 can be up-regulated on NSCs in response to EGF or bFGF via the MAPK pathway. [Suzuki et al. 2010] MAPK signalling is also required for NSC maintenance in vitro. [Campos et al. 2004] Additionally, Itgb1 activation triggers upregulation of Notch pathway components. [Campos et al. 2006] Meanwhile Itgb1-mediated adhesion to fibronectin depends on intact lipid raft architecture, suggesting that Itgb1 clusters in lipid rafts to mediate NSC adhesion. [Yanagisawa et al. 2004]

1.3.6.2 *Post-natal*

A role for Itgb1 can also be demarcated in early post-natal life. In the SEZ of P0-2 mice, Itgb1 co-localises with the stem cell marker Nestin and - as in the embryo - can be used as a marker to immunoselect for neurosphere-initiating cells. [Campos et al. 2004] Consistent with this finding Itgb1 may function to restrain glial lineage differentiation In P1 SEZ NSCs cultured in vitro, and when overexpressed may maintain NSCs in an undifferentiated, proliferative state. [Pan et al. 2014]

Expression of Itgb1 tails off sharply after birth and is much reduced by P10; nonetheless it is required for cellular migration in the postnatal rostral migratory stream (RMS). [Murase et al. 2002] The decline in expression continues and in the adult mammalian CNS where Itgb1 expression is lower still than post-natal levels. [Bergstrom et al. 2014]

Postnatally and in vitro, Itgb1 regulates NSC proliferation, cell survival, and response to growth factors in neurospheres cultured from the SEZ. Itgb1 signalling is not an absolute requirement for NSC renewal, but interacts with growth factors to regulate the proliferation and survival of Nes+ progenitors in neurospheres. [Leone et al. 2005] This introduces an additional and indirect function of Itgb1, namely its potential for interaction with growth factors. Indeed such interactions may be essential for secondary neurosphere development when spheres are cultured in low levels of growth factor. [Campos et al. 2006] Combined with the observation that genetic deletion of Itgb1 can be compensated by increased EGFR signaling [Campos et al. 2004], some overlap in Itgb1 and growth factor receptor function becomes apparent.

Itgb1 on postnatal NSCs also interact with components of the ECM. NSPCs isolated from the SEZ of postnatal D6 mice adhere to collagen 1 and establish focal adhesions in an Itgb1-dependent manner, whereas those isolated from the adult SEZ do not. qPCR experiments suggested that the ready adhesion of early postnatal NSPCs to collagen 1 was mediated by a2b1 and a11b1 integrin heterodimers. [Bergstrom et al. 2014] These data raise the possibility that that Itgb1 heterodimer expression may be dynamically regulated at different developmental stages on postnatal NSCs, in response perhaps to dynamic changes in the microenvironment.

A small number of studies have examined the role of Itgb1 in NSCs under injury or disease conditions. For example embryonic NSPCs from the mouse forebrain transplanted into the adult mouse striatum were found to survive better after striatal lesioning with 6-hydroxydopamine. Using an antibody-blocking model this increased survival was dependent on Itgb1, suggesting that its reactive expression in response to injury modulates the microenvironment in a way that enhances neural stem cell survival. [Fainstein et al. 2013] Interestingly, Itgb1 has also been implicated in the biology of psychiatric illness: in adult schizophrenia patients, Itgb1 mediates the adherence and motility of cells cultured from

olfactory mucosa-derived neurospheres. Patient-derived cells were less adherent and more motile, with fewer and smaller focal adhesions. [Fan et al. 2013]

Together these studies - most of which have been conducted largely or entirely in vitro - implicate Itgb1 in the adhesion, proliferation, differentiation, migration, and survival of embryonic or postnatal NSCs at different developmental stages, as well as in models of injury or disease. Itgb1 function, both in vitro and in vivo, can be seen often to depend on interactions with molecules in the extracellular matrix.

1.3.6.3 *Adult*

Relative to what is known about developing and early postnatal NSCs, the functions of Itgb1 in adult NSCs are less well understood. A small number of studies have demonstrated the importance of Itgb1 in maintaining NSPC adhesion and architectural integrity in the adult subependymal zone [Kazanis et al. 2010, Shen et al. 2008] and SGZ niches. [Brooker et al. 2016]. A role for Itgb1 in regulating hippocampal neurogenesis has recently been theorised by two groups. [Brooker et al. 2016, Porcheri et al. 2014] I will discuss these studies in detail later (see **Ch. 4**), but they neither entirely agree on, nor definitively answer the question of the function of Itgb1 in adult hippocampal NSPCs.

1.4 Summary of Introduction and Research Question

In this Chapter I introduced the topic of adult hippocampal neurogenesis, briefly summarizing the current state of knowledge on the cellular process, its hypothesized function, the major known regulatory mechanisms, and models of its experimental manipulation. In particular I introduced AraC and a single ECS as promising ways to manipulate neurogenesis.

I then turned to discuss studies of the role of extracellular matrix in the regulation of neural stem cells. Most core matrisome genes remain unstudied with respect to NSCs, with the literature skewed towards a small number of genes which act as model systems or for which productive transgenic models exist. There is only a small literature on the ECM regulation of adult hippocampal neurogenesis.

Last, I discussed the archetypal matrix receptor Integrin β1. In vitro, Itgb1 is implicated in the positively regulation of adhesion, proliferation, differentiation, migration, and/or survival of NSCs at different developmental stages. In vivo, conditional genetic knockout studies suggest a critical role for Itgb1 in neurodevelopment, regulating the proliferation, survival, adhesion, and migration of developing neurons. However both in vitro and in vivo, relatively little is known about the role of Itgb1 in regulating adult neurogenesis.

Taken together I hypothesised a potentially instructive role for ECM in adult NSC biology. I therefore asked the question: does extracellular matrix regulate hippocampal neurogenesis?

2 METHODS

2.1 Animals

10-12 week-old male C57Bl/6 mice were used for establishing Itgb1 expression and for characterising the AraC procedure. NesCre^{ERT2} mice [Lagace et al. 2007] were purchased from Jackson laboratories (C57BL/6-Tg[Nes-cre/ERT2]KEisc/J, Jax stock #016261) and crossed with mice bearing floxed Itgb1 [Raghavan et al. 2000] and RFP [Madisen et al. 2010] alleles (kind gifts from Prof. S. Forbes, University of Edinburgh) to generate experimental groups. The genotype of iKO mice was NesCre^{ERT2};Itgb1$^{f/f}$;RFP$^{f/f}$ (or RFP$^{f/WT}$). Mice heterozygous for the Itgb1 floxed allele (Itgb1$^{f/WT}$) served as controls for gene effect. The NesCre^{ERT2} transgene was transmitted solely in the male line. Male and female mice were used for Itgb1 iKO experiments. To induce recombination, tamoxifen (180mg/kg, 30mg/ml, Sigma T5648) dissolved in sunflower seed oil (Sigma S5007) was administered when mice were 8-10 weeks old. Initial attempts at inducing genetic recombination by IP injection of Tamoxifen led to unacceptably high levels of mortality secondary to sterile peritonitis. We switched to administering Tamoxifen by oral gavage which reduced the mortality rate to zero. Because of the known in-vivo half-life of Itgb1 protein [Robel et al. 2009, Brooker et al. 2016] we allowed a ‘chase’ period of six weeks from recombination to sacrifice during which mice received no further intervention. All mice were housed in standard cages except where noted below, under a 12hr light/dark cycle, and had ad libitum access to food and water.

2.2 AraC procedure

Minipumps (Charles River, 1007D and BIK3) were prepared in line with Good Laboratory Practice. AraC pumps contained 2% AraC (Sigma C6645) made up in sterile filtered 0.9% NaCl. Control pumps contained NaCl only. For experiments designed to characterise the NSPC response to AraC, 11 week-old male C57Bl/6 mice were randomised preoperatively to AraC or control. Mice received inhalational anaesthesia with isoflurane (Merial), and post-induction analgesia with Carprofen (50mg/ml, Zoetis). Mice were kept warm with eye care throughout and standard sterile operating precautions were taken. Mice were positioned in the stereotaxic frame and a midline incision was made over the skull. Bregma was identified, then a 1mm burrhole was carefully drilled targeting the left lateral ventricle (AP -0.5, ML+1.5). The intracerebroventricular (ICV) catheter was gently placed at 2.5mm depth.

Tissue glue (3M 1469sb) was used to attach the cannula holder to the exterior of the skull. The wound was carefully closed with vicryl sutures and the mouse moved to a recovery chamber until fully recovered. Post-operatively, animals were housed singly in IVC cages to prevent cage-mates dislodging the brain cannula. Bedding was shredded to further prevent animals pulling the cannula off. Animals in which the cannula was dislodged despite these efforts were immediately culled and excluded from analyses. Pumps were left in situ for six days before being removed entirely, under general anaesthesia and using standard operating techniques as above. Pumps were aspirated to confirm successful discharge. Other than where stated, all analyses following the AraC procedure were conducted solely on the non-operated hemisphere to minimise confounding from local effects of surgery.

2.3 Electroconvulsive shock

To characterise the response to a single ECS (s-ECS), 8-9 week-old male NesCreER^{T2};RFP$^{f/f}$ mice received Tamoxifen by oral gavage. At 10-11 weeks of age animals were anaesthetised with an admixture of isoflurane and O2 running at 4L/min for 45 seconds. These parameters were sufficient to induce general anaesthesia lasting for the duration of the procedure. They were rapidly positioned in ear clips attached to a custom-built ECS unit (a kind gift from Dr. C.A. Stewart, University of Dundee). A single electrical stimulus was delivered (1 sec duration, 150V, 25mA). Mice were closely observed for seizure activity. All mice receiving s-ECS had motor seizures lasting >10 and <30 seconds. Mice were moved to a recovery chamber until awake and ambulant (c. 5 minutes). Control mice were handled and treated in exactly the same way including anaesthesia and positioning in ear clips, but minus delivery of the shock. For Itgb1 iKO experiments the same procedures were followed using mice harbouring the genotypes stated above.

2.4 Laser capture microdissection and RNA extraction

11 week-old male C57Bl/6 mice were implanted with minipumps containing AraC or saline as described. Groups were: Saline D1 (n=4 mice), AraC D1 (n=4), AraC D3 (n=4), and AraC D6 (n=4). After a 6-day infusion, pump removal, and the appropriate chase period, animals were killed by cervical dislocation. Brains were quickly removed and bisected longitudinally. The ipsilateral (operated) hemisphere was post-fixed for 24h in 4% PFA at 4°C and subsequently processed for immunofluorescence as below. The contralateral (non-operated) hemisphere was snap-frozen on liquid nitrogen and stored at -80°C until

sectioning. Coronal sections from the septal half of the hippocampus were cut on a Leica Cryostat (chamber -20C, head -16C), in a 1:8 series at 8µm with eight hemisections per slide. Sections were firmly mounted to RNAse-free PEN slides (Zeiss) by fingertip thawing, then immediately re-frozen.

Immediately prior to laser capture slides were immersed in 70% RNAse-free ethanol (Sigma E7023) with RNAse-free water (Invitrogen 10977-035) and 1% Cresyl Violet (Acros Organics 229630050) for ten seconds, then 90% ethanol for 60 seconds, and 100% ethanol for 60 seconds. Slides were allowed to air dry at room temperature for three minutes then processed using a PALM laser capture microdissection microscope (Zeiss) on x20 magnification. The subgranular zone was defined as three granule cell nuclei widths above and below the hilar border. From each mouse, a minimum of 24 hemisections were collected in 200µl Adhesivecaps (Zeiss 415190-9191-000, one cap per slide) which were kept on dry ice until RNA extraction.

In a preliminary experiment, I ran an exploratory comparison of four different RNA extraction methods (FFPE [Quiagen 73504], Microkit [Quiagen 74004], miRNeasy FFPE [Quiagen 217504], and Masterpure [MCR85102]). The best balance of quality and yield was obtained using the Quiagen FFPE kit (see **Fig. 20** for details of the comparison). RNA was extracted from microdissected tissue according to manufacturer instructions, omitting the deparaffinisation but including the Proteinase K and DNase steps. The RNeasy FFPE kit also typically recovers smaller RNA molecules (~80bp+) than most microdissection-compatible kits. The quality of extracted RNA was checked on an Agilent Tapestation 2200 using the High-sensitivity Screentape (Agilent 5067-5579). All samples which progressed to sequencing had RIN $\geq$ 7.2 (range 7.2-8.7, mean 8.2). Sample concentrations, eluted in 14 microlitres of RNAse-free water, ranged from 0.95ng/microliter to 2.8ng/microliter.

2.5 Tissue preparation

Mice were deeply anaesthetised with an IP injection of medetomidate (1mg/kg, Orion Pharma) and ketamine (75mg/kg, Zoetis). They were then transcardially perfused with ice-cold 0.9% NaCl followed by 4% PFA (Sigma P6148) made up in 0.9% NaCl. Brains were excised and stored in 4% PFA for 18 hours at 4C, cryoprotected in 15% and then 30% sucrose solution until sunk, and embedded in OCT (Cell Path, KMA-0100-00A). Brain blocks were stored at -80C until further use. For experiments using slide sections,

cryosections were cut from the septal/medial hippocampus in a 1:10 ratio and 16 micron thickness on a cryotome (Leica), mounted on Superfrost Plus slides (Thermo Scientific 10149870), and stored at -20C until staining. For later experiments using floating sections, cryosections were cut from throughout the length of the septotemporal axis of the hippocampus in a 1:6 ratio and 40 micron thickness and washed in 1xPBS for immediate use. For all experiments a minimum of three brain sections were analysed and averaged per replicate.

2.6 Immunofluorescence and confocal microscopy

Slides and floating sections were blocked for one hour with 10% NDS (Millipore S30) in 0.3% Triton X-100 (Fisher Scientific BP151-500) and 1xPBS (Gibco 7001-036, diluted to 1X in distilled water). Primary antibodies were incubated in blocking solution for 24h at 4C. **(Table 7)**. Sections were washed x3 in PBS for a total of 15 minutes (slides) or one hour (floating sections). Secondary antibodies were incubated in blocking buffer for 12h (slides) or 24h (floating sections) at 4C. Sections were washed, counterstained with Hoechst 33342 (Thermo Fisher Scientific 62249), and mounted with Fluoromount-G (SouthernBiotech 0100-01). Images were taken with a Leica SP8 confocal microscope at 40X magnification in 10 micron (slides) or 20 micron z-stacks (floating sections). Slice thickness was 2 microns for slides and 3 microns for floating sections. Sequential scanning of channels was performed to avoid spectral bleed-through. Images were processed using FIJI freeware (https://fiji.sc/).

2.7 RNA sequencing workflow

Following laser-capture microdissection and RNA extraction (see **Ch 2.4**) eluted RNA was stored at -80C until further processing. Sequencing was performed by Aros Applied Biotechnology (Denmark). RNA was processed using the SMARTer Ultra Low Input RNA kit (ClonTech) according to manufacturer protocol. Briefly, one nanogram of total RNA per animal was synthesized to cDNA which was amplified, sheared, and used to prepare the library. All samples passed all quality control checks at stages of total RNA, cDNA, library, and post-sequencing. Between five and six samples were run per flow cell lane of the Illumina HiSeq 2500 platform. Libraries were 100bp paired-end reads with final depths of 30-45M reads depending on sample.

Antibody	Company	Cat. No	Species	Dilution
Ki67	Abcam	ab16667	Rabbit	1:200
MCM2	Abcam	ab4461	Goat	1:200
MCM2	Santa Cruz	sc-9879	Rabbit	1:200
Mash1	BD Pharmingen	556604	Mouse	1:100
Tbr2	Abcam	ab23345	Rabbit	1:500
Doublecortin	Millipore	AB2253	Guinea pig	1:500
Integrin beta 1	Millipore	MAB1997	Rat	1:75
Integrin beta 3	Abcam	ab38460	Rabbit	1:100
CD31	BD Pharmingen	550274	Rat	1:100
Olig2	Millipore	AB9610	Rabbit	1:100
GFAP	Dako	Z0334	Rabbit	1:400
Anti- mCherry	Sicgen	ab0081-500	Goat	1:500
Alexafluor 488 Dk anti Rb	Invitrogen	A21206	Donkey	1:1000
Alexafluor 568 Dk anti Rb	Invitrogen	A10042	Donkey	1:1000
Alexafluor 647 Dk anti Rb	Invitrogen	A31573	Donkey	1:1000
Alexafluor 488 Dk anti Gt	Invitrogen	A11055	Donkey	1:1000
Alexafluor 568 Dk anti Gt	Invitrogen	A11057	Donkey	1:1000
Alexafluor 647 Dk anti Gt	Invitrogen	A21447	Donkey	1:1000
Alexafluor 568 Dk anti Mse	Invitrogen	A10037	Donkey	1:1000
Alexafluor 647 Dk anti Mse	Invitrogen	A31571	Donkey	1:1000
Alexafluor 488 Gt anti Gp	Invitrogen	A11075	Donkey	1:1000
Alexafluor 647 Dk anti Gp	Millipore	AP193SA6	Donkey	1:1000
Alexafluor 488 Dk anti Rat	Invitrogen	A21208	Donkey	1:1000

Table 7: Antibodies and dilutions.

2.8 Bioinformatic analysis

Bioinformatic analysis of sequenced RNA was conducted by Dr. Jonathan Manning (MRC Centre for Regenerative Medicine) as follows. An initial quality check revealed low-level adapter contamination from Illumina TruSeq and Clontech SMARTer adapters. Both were successfully removed prior to downstream analysis, requiring a minimum 36bp after

trimming. After trimming, 89-94% of reads were retained, corresponding to 28-42 million paired-end reads.

Transcript quantification was carried out with Kallisto (version 0.42.3) [Bray et al. 2015] applied against a reference mouse transcriptome from Ensembl (GRCm38) composed of cDNAs and non-coding RNAs. Between 69% and 82% of the reads which aligned to the genome were pseudo-aligned to the transcriptome. Estimated counts adjusted for library size and transcript length were derived from the Kallisto results and reported as estimated counts per million (eCPM). Matrices for both transcript and gene level were derived. Matrices were filtered to remove rows without a value of at least 2 in at least 25% of samples, and normalized. A lane-wise batch corrected version of each normalised matrix was derived.

Differential expression analysis was carried out on the normalised estimated counts matrices, generating p values and adjusted p values for specified contrasts while adjusting for the batch effect. Six gene set libraries were downloaded from version 5.0 of the molecular signatures database [Liberzon et al. 2011]: canonical pathways, hallmarks, KEGG, and the three parts of the gene ontology. Differences in gene set expression between experimental groups were examined as implemented in the limma package of Bioconductor (version 3.27.4). [Ritchie et al. 2015]

2.9 Fluorescent in situ hybridization

Mice were killed by cervical dislocation. Brains were rapidly dissected and snap frozen on liquid nitrogen. Frozen brains were coronally sectioned at 10 micron thickness on a cryotome, mounted on Superfrost Plus slides, and stored at -80°C until further use. In situ hybridization was conducted using RNAScope technology [Wang et al. 2012] as per manufacturer protocols (ACD) with some optimisation. Briefly, slides were transferred directly from dry ice to immersion in freshly made ice-cold 4% PFA for 20 minutes. Tissue was dehydrated in an ethanol gradient then baked in an oven at 37°C for 20 minutes before incubation with RNAScope Protease 3 for 20 minutes. Probes were warmed to 40°C before target probe and then amplifier probe hybridization rounds at 40°C in a humidified HybEZ oven (ACD). Two different RNAScope products were used: the RNAScope 2.5 HD assay – Red; and the RNAScope multiplex fluorescent assay. With the 2.5 HD assay, two final rounds of amplification were conducted at room temperature before signal detection using Fast Red and counterstaining with Hoechst 33342. With both assays, slides were imaged

within 24h as for confocal microscopy. Using Fiji software, fluorescent Mgp signal was isolated and a threshold applied to remove background before quantitative ROI analysis. The mean signal area per DG was calculated using 8 sections per animal (four ipsilateral and four contralateral to infusion).

2.10 Statistical analyses

Data were entered on Microsoft Excel spreadsheets and analysed using SPSS v.25. Experimental analyses were conducted blind to group. Cell density counts were normalised to the length of the inner border of the SGZ and presented as density/mm. Simple proportions were presented as % +/- 95% confidence intervals. I am grateful to Prof. Malcolm MacLeod for his guidance in selecting key statistical tests. In addition for each analysis I followed step-by-step guidance in test selection, execution, and reporting, via subscription to the online statistical textbook at www.laerd.com. Individual statistical test choice is described and justified at each point in the following three chapters.

Following the oral examination I was asked to add contextualizing summaries of the question, hypothesis, methods, and statistical analysis plan for each experiment as they arise throughout the Results Chapters. This information is given throughout the next three chapters in shaded boxes like this.

3 ADULT HIPPOCAMPAL NEUROGENESIS CAN BE MANIPULATED BY ARA-C AND BY A SINGLE ELECTROCONVULSIVE SHOCK.

3.1 Introduction

To study whether extracellular matrix regulates adult hippocampal neurogenesis, I first optimised techniques to experimentally manipulate neurogenesis. Homeostasis - no external manipulation - is an important basal condition, but disrupting the system and observing the response is a widely-used method of studying the instructive role of candidate cellular or molecular regulators of neurogenesis. This is clear from the introductory **Table 1** and **Table 2**, where studies used external manipulation to examine (for example) the functional contribution of NSC subpopulations and epigenetic DNA modification to adult neurogenesis. [Su et al. 2017, DeCarolis et al. 2013, Weber et al. 2013, Guo et al. 2011, Ma et al. 2009]

To manipulate neurogenesis I chose two techniques: 1) AraC infusion, and 2) a single electroconvulsive shock. The literature outlined earlier in **Table 1** suggested AraC as a potent method of ablating hippocampal neurogenesis, with an injury-like rebound of SGZ proliferation seen following removal of the infusion pump. AraC is a synthetic puridine analogue that is incorporated by cells during S phase, subsequently causing cell death. In mice following forced ablation of the progenitor pool, quiescent NSCs activate, proliferate, and re-populate the stem cell niche. The dynamics of this process have been reported for subependymal zone (SEZ) NSPCs [Doetsch et al. 1999, Kazanis et al. 2010] and to a degree in the SGZ. [DeCarolis et al. 2013, Hodge et al. 2008, Seri et al. 2001] However these latter studies did not seek to fully characterise the temporal response of progenitor subpopulations to AraC. I reasoned that if NSPC regeneration was temporally predictable, it could be used to study the role of ECM in the sequential regeneration of different NSPC subpopulations.

The effects of a single ECS in the SGZ are understood in slightly more detail - most persuasively following Weber et al., who established that a single ECS activates SGZ GFAP+ RGLs at Day 3 post-shock. [Weber et al. 2013] However that study left unanswered the important questions of whether other RGL subpopulations were activated (such as those in the Nestin lineage), and whether activation causes increased neurogenesis in their lineage descendants.

Here I report experiments designed to characterise the AraC procedure and a single ECS as

techniques to experimentally manipulate adult hippocampal neurogenesis. I found that AraC effectively ablates proliferating NSPCs, causing the sequential recovery of NSPC sub-populations after the infusion is stopped. A single ECS meanwhile triggers robust activation of Nestin+ RGLs, which generate a large increase in proliferating daughter neuroblasts seven days later. I conclude that these two techniques can be used to target points of expansion of individual NSPC subpopulations, maximising the power to detect the signal of molecular candidates in downstream experiments.

3.2 Results

3.2.1 AraC ablates proliferating NPSCs in the SGZ neurogenic niche

I first asked the question: "What is the baseline effect of a six-day AraC infusion on SGZ neurogenesis?". My hypothesis was that AraC infusion would effectively ablate all proliferative NSPC subpopulations (MCM2+ total proliferating cells, Nes+MCM2+ aNSCs, Ascl1+ IPs, and Dcx+ NBs). To test this hypothesis I infused adult male WT mice with saline (n=3) or AraC (n=3) for six days as described in **Ch 2.2.** The experimental design was a comparison of adult WT animals infused with AraC versus control animals infused with 0.9% saline, on the baseline day of pump removal (**Figure 7A**). I used immunofluorescence and confocal microscopy of the SGZ in the contralateral (non-operated) hemisphere to determine the cellular density of: MCM2 (proliferation); Nestin co-labelling with MCM2 (aNSC); Ascl1 (IPs); and Dcx (NBs).

In this cross-sectional analysis there were no outliers in the data as assessed by inspection of box plots. There was no evidence of abnormally distributed dependent variables in either treatment group (all Shapiro-Wilk's test $p>0.05$), with the exception of aNSC in saline-treated animals (Shapiro-Wilk's $p<0.001$). There was homogeneity of variances for all dependent variables in both treatment groups (all Levene's test $p>0.05$). The analyses of MCM2+, Ascl1+ IP, and Dcx+ NB density were therefore conducted using independent-samples t-tests, and aNSC density using the Mann-Whitney U test.

On the day of infusion pump removal AraC had reduced the magnitude of density of all SGZ NSPC populations (Saline [n=3]: MCM2=17.7/mm [SD=4.5], aNSC=2.6/mm [0.6], Ascl1+ IP=3.4/mm [1.6], Dcx+ NB=39.2/mm [9.0] versus AraC [n=3]: MCM2=2.5/mm [SD=2.2],

aNSC=1.2/mm [1.1], Ascl1+ IP=0.7/mm [0.8], Dcx+ NB=17.9/mm [5.9]). These differences reached statistical significance for MCM2 and Dcx (MCM2 t[4]=5.230, p=0.006; Dcx t[4]=3.445, p=0.026), but not aNSC and Ascl1+ IPs (aNSC Mann-Whitney U test p=0.100; Ascl1+ IP t[4]=2.682, p=0.055, **Figure 7B-C**). Therefore AraC effectively ablated proliferating SGZ NSPCs with significant effects detectable in more populous MCM2+ cells and Dcx+ NBs.

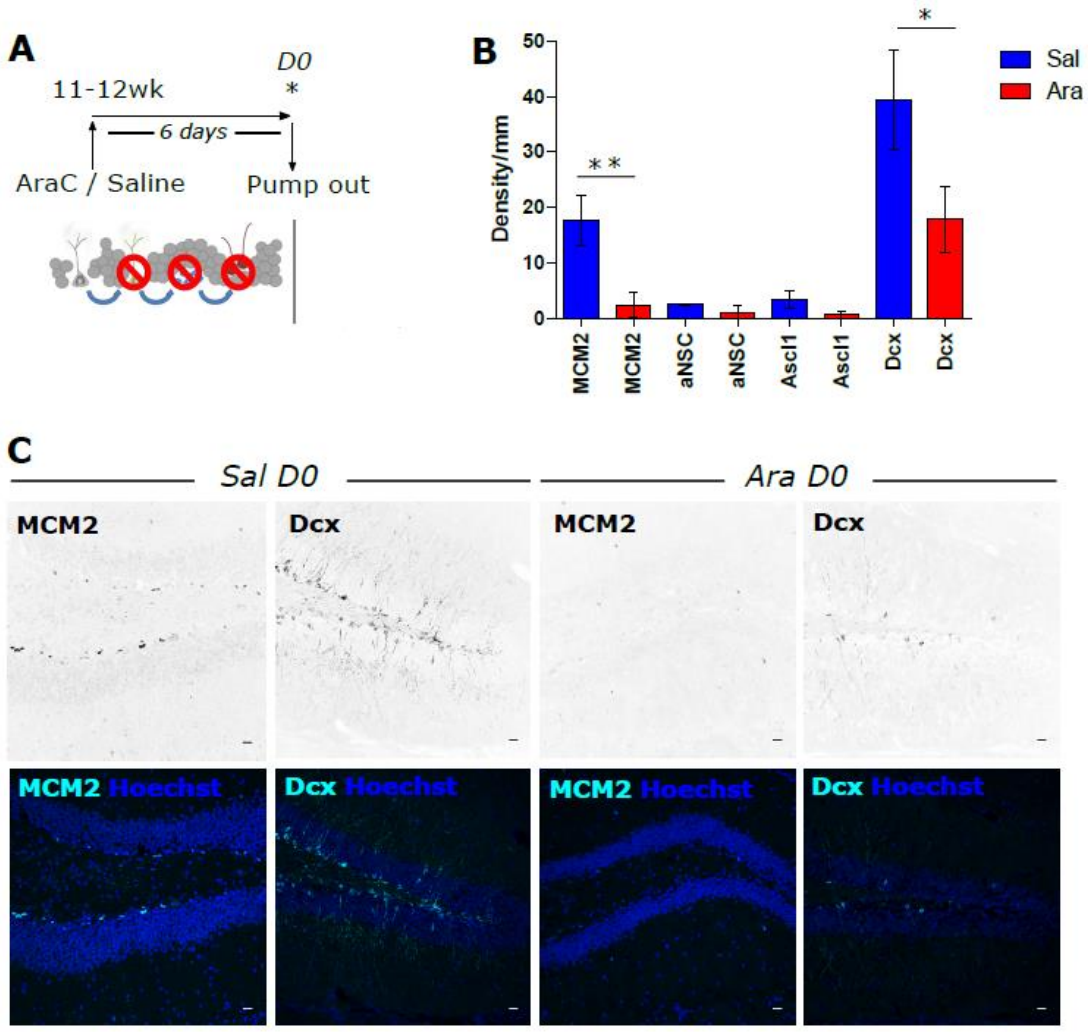

Figure 7. AraC ablates proliferating NSPCs in the SGZ neurogenic niche.

A: Experimental schematic. **B:** Density (n/mm) of SGZ NSPC subpopulations between Saline- and AraC-infused animals. C: Representative images of significant differences in (B). * $p<0.05$; ** $p<0.01$; n= 3 animals per group; scale bars= 20 microns.

3.2.2 After AraC, regenerative neurogenesis occurs in biological sequence.

Next I asked: "What are the temporal dynamics of regenerative neurogenesis after the end of AraC infusion?" My hypothesis was that AraC would cause a significant expansion in all recovering NSPC populations in biological sequence (aNSC, then IPs, then NBs). To test this hypothesis I conducted a time-series experiment examining the same NSPC subpopulations (MCM2+ proliferating cells, Nestin+MCM2+ aNSCs, Ascl1+ IPs, and Dcx+ NBs) at the time-points of Day 1 (D1), D2, D3, D4, D6, D8, and D10 following the removal of saline or AraC infusion pumps. For each NSPC subpopulation I used 2-way ANOVA to test the entire dataset for a multivariate interaction between treatment and time, and to examine simple effects of time within each treatment group. I ran Bonferroni-corrected comparisons between the treatment groups at each individual time-point to identify points of AraC-mediated reduction or expansion in NSPCs, and used Tukey's HSD test to examine the dynamic recovery of NSPC density within the entire dataset over time.

For the analysis of IPs I had planned also to examine the additional marker Tbr2. Unfortunately I encountered technical difficulties with the Tbr2 antibody due to lot-to-lot variability (ultimately, it was temporarily withdrawn from sale). Because of this I was unable to complete Tbr2 staining at the time of running the initial time-series. When the antibody became available again, I conducted a similar time-series experiment specifically to examine Tbr2, taking the opportunity to increase power by adding new animals to those in the original cohort. In this additional experiment I studied fewer time-points: D1, D3, D6, D8, and D10.

There was evidence of a multivariate interaction between treatment and time for all NSPC sub-populations except aNSC (MCM2+ proliferating cell density $F[6,46]=8.030$, $p<0.001$, partial $\eta^2 = .593$; Nestin+MCM2+ aNSC density $F[6,46]=1.582$, $p=0.184$, partial $\eta^2 = .223$; Ascl1+ IP density $F[6,46]=5.034$, $p=0.001$, partial $\eta^2 = .478$; Tbr2+ IP density $F[4,56]=7.321$, $p<0.001$, partial $\eta^2 = .384$; Dcx+ NB density $F[6,46]=2.427$, $p=0.047$, partial $\eta^2 = .306$) **(Figure 8)**.

There was a significant simple effect of time in AraC-treated animals for all NSPC subpopulations (MCM2+ proliferating cell $F[6,33]=15.826$, $p<0.001$, partial $\eta^2 = .742$; aNSC $F[6,33]=3.049$, $p=0.017$, partial $\eta^2 = .357$, Ascl1+ IP $F[6,33]=10.474$, $p<0.001$, partial $\eta^2 = .656$, Tbr2+ IP $F[4,47]=14.481$, $p<0.001$, partial $\eta^2 = .552$, Dcx+ NB $F[6,33]=2.545$,

p=0.039, partial η^2 = .316). Importantly there was no such effect of time in any saline-treated controls (MCM2+ F[6,33]=1.768, p=0.136, partial η^2 = .243, aNSC F[6,33]=1.145, p=0.359, partial η^2 = .172, Ascl1+ IP F[6,33]=1.825, p=0.125, partial η^2 = .249, Tbr2+ IP F[4,47]=0.130, p=0.971, partial η^2 = .011, Dcx+ NB F[6,33]=1.964, p=0.099, partial η^2 = .263).

Bonferroni-corrected pairwise comparisons of each time-point showed a significant AraC-mediated reduction in the density of: MCM2+ proliferating cells at D1 (F[1,33]=12.937, p=0.001, partial η^2 = .282) and D2 (F[1,33]=19.993, p<0.001, partial η^2 = .377); Ascl1+ IPs at D1 (F[1,33]=4.370, p=0.047, partial η^2 = .115) and D2 (F[1,33]=7.077, p=0.012, partial η^2 = .177); Tbr2+ IPs at D1 (F[1,47]=14.368, p<0.001, partial η^2 = .234); and Dcx+ NBs at D1 (F[1,33]=11.724, p=0.002, partial η^2 = .262), D2 (F[1,33]=31.327, p<0.001, partial η^2 = .487), D3 (F[1,33]=6.015, p=0.020, partial η^2 = .154), and D6 (F[1,33]=6.150, p=0.018, partial η^2 = .157). No significant reduction in aNSC density was observed relative to controls at any time-point.

Using the same approach of corrected pairwise comparisons there was significant AraC-mediated expansion in the density of: MCM2+ proliferating cells at D10 (F[1,33]=7.606, p=0.009, partial η^2 = .187); Ascl1+ IPs at D8 (F[1,33]=13.122, p=0.001, partial η^2 = .285); and Tbr2+ IPs at D6 (F[1,47]=8.198, p=0.006, partial η^2 = .149) and D8 (F[1,47]=4.804, p=0.033, partial η^2 = .093). No significant expansion of aNSC or NB density was observed at any time-point. In AraC-treated animals, a significant recovery (but not expansion) of aNSCs was suggested in pairwise comparisons between D1 (mean aNSC density=0.4/mm [95%CI 0-1.4/mm]) and D3 (mean aNSC density=3.0/mm [1.9-4.0/mm], p=0.027).

Tukey's HSD post-hoc test, which compared D1 baseline data in both groups to all later time-points, showed significant dynamic recovery of: MCM2+ proliferation by D3 (mean MCM2+ proliferating cell density increase over D1= 4.9/mm [95%CI=2.7-16.3], p=0.002), persisting at D6 (mean MCM2+ increase over D1= 14.1/mm [7.3-20.9], p<0.001), D8 (mean MCM2+ increase= 11.8/mm [5.0-18.6], p<0.001), and D10 (mean MCM2+ increase= 9.3/mm [2.2-16.4], p=0.004); Ascl1+ IPs by D6 (mean Ascl1+ density increase over D1= 4.2/mm [95%CI=1.7-6.6], p<0.001) and persisting at D8 (mean Ascl1+ increase= 3.4/mm [0.9-5.8], p=0.002); and Tbr2+ IPs at D6 (mean Tbr2+ density increase over D1= 7.2/mm [2.4-12.1], p=0.001) and similarly persisting at D8 (mean Tbr2+ increase= 9.2/mm [3.2-

15.2], p=0.001). Using this test there were no differences in overall aNSC or NB density between baseline and any other time-point overall **(Figure 8)**.

However I noticed that the morphology of NBs was qualitatively different between treatment groups. This difference was most evident at later time-points. In general, NBs of saline-treated animals were of the usual morphology with strong radial processes extending through the GCL. By contrast the NBs of AraC-treated animals generally lacked a radial process and instead displayed tangential processes running along the SGZ (**Figure 8F**). The most likely explanation for these morphological differences was that because Dcx+ NBs were effectively ablated by AraC treatment, a cohort of newly-born NBs was gradually expanding to replace them.

Together these experiments characterise the effect of AraC on SGZ NSPCs and the early period of a subsequent regenerative neurogenesis. A six-day AraC infusion effectively ablated proliferating SGZ NSPCs with effects seen most strongly in the MCM2+ population and Dcx+ NBs. Over ten days following mini-pump removal, significant dynamic regenerative effects occurred in every studied NSPC population, in contrast to the absence of similar temporal effects after saline infusion. These regenerative effects followed the biological sequence of neurogenesis. Following AraC, proliferation recovered to control levels by D3. Post-hoc tests suggested the possibility that these initial proliferating cells were aNSC. There was no subsequent evidence of rebound aNSC expansion. In IPs there *was* significant rebound expansion, which depending on the IP marker occurred either at or between the points of D6 and D8 post-infusion. There was no expansion of NBs during the time-points studied, but there was clear morphological evidence of a gradually recovering population of newly-born NBs, which was still increasing by D10. The IP and NB sub-populations probably each contributed to the increase in total MCM2+ proliferation observed at this final time-point.

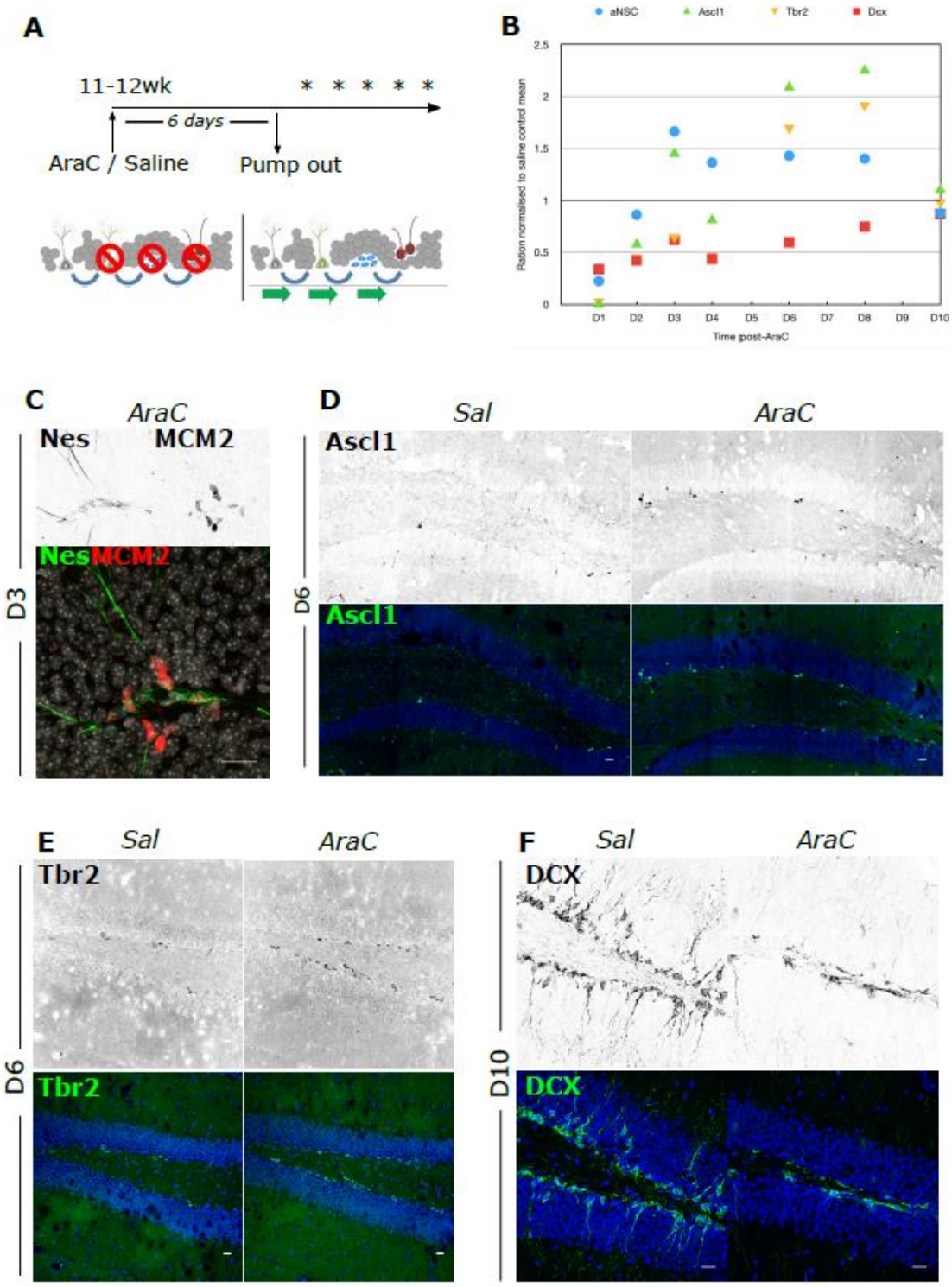
A
11-12wk
6 days
AraC / Saline
Pump out
B
aNSC
Ascl1
Tbr2
Dcx
Ration normalised to saline control mean
Time post-AraC
C
AraC
Nes
MCM2
NesMCM2
D3
D
Sal
AraC
Ascl1
D6
E
Sal
AraC
Tbr2
D6
F
Sal
AraC
DCX
D10

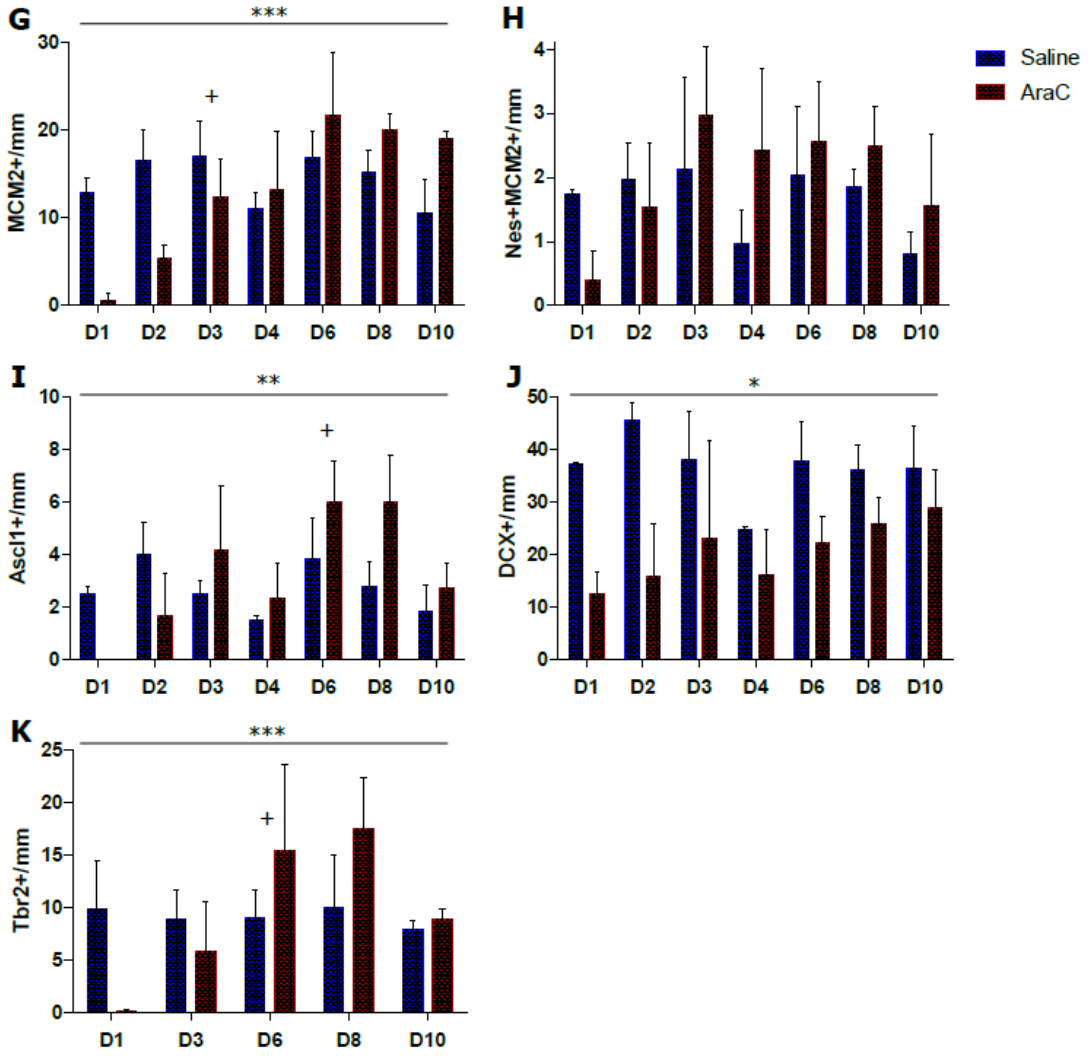

Figure 8. After AraC, regenerative neurogenesis occurs in biological sequence.

A: Experimental schematic. **B:** Summary of dynamic response of NSPCs, in which AraC density has been normalised to Saline control mean for each NSPC population and timepoint. Note that the recovery of aNSC precedes that of Tbr2+ IPs, with Dcx+ NBs still recovering at D10. **C:** Representative image of Nestin+MCM2+ proliferating NSCs at D3. **D:** Ascl1+ IPs in saline-treated controls (left panels) and AraC-treated animals (right panels) at D6. **E:** Tbr2+ IPs at D6. **F:** Dcx+ NBs at D10. Note the lack of radial processes in AraC-treated animals, indicating newly born neuroblasts in a regenerating niche. **G:** Quantifications of MCM2+ proliferating cell density. **H:** Quantifications of Nes+MCM2+ aNSC density. **I:** Quantification of Ascl1+ IP density. **J:** Quantification of DCX+ NB density. **K**: Quantification of Tbr2+ IP density. * $p<0.05$; ** $p<0.01$; *** $p<0.001$ (all for interaction between time and treatment on 2-way ANOVA); + = earliest point of recovery from D1 baseline (Tukey's HSD); note that only selected significant comparisons are shown (see text for full analysis); n=3-5 animals per group per timepoint except Sal D1 (n=2); all scale bars= 20 microns.

Next I wished to know whether the most obvious AraC-mediated change - the D6-8 expansion of IPs - occurred within the Nestin+ NSC lineage. This question was important because my planned upcoming experiments (reported in **Ch. 4**) would use Nestin-lineage tracing, and would require AraC to exert effects in this particular lineage. Yet a recently-published report had argued that AraC did not have any effect in Nestin-lineage NSPCs. [DeCarolis et al. 2013] My hypothesis was however that the expansion of Tbr2+ IPs did indeed occur in Nestin-lineage cells.

To test this I induced recombination in a new group of Nes-CreER^{T2};RFP$^{f/f}$ animals, infused them with saline or AraC as outlined in **Ch. 2.2**, and sacrificed the animals at a single time-point (D8) post-infusion. Although the time-series experiment had shown Tbr2+ IP expansion as early as at D6 I chose D8 for this specific experiment in order to mitigate against individual variation in the initial tempo of response to AraC. Using immunofluorescence and confocal microscopy I determined the proportion of recombined Nestin-lineage cells expressing Tbr2 between the treatment groups.

There were no outliers in the data as assessed by inspection of box plots. There was no evidence of abnormally distributed dependent variables (Shapiro-Wilk's test $p>0.05$ in both groups). The assumption of homogeneity of variances for the dependent variable was met (Levene's test $p>0.05$). I therefore used an independent-samples t-test to compare the Tbr2+RFP/RFP proportion between experimental groups.

Relative to saline-treated controls, AraC caused significant expansion in the Tbr2+ fraction of NesRFP+ IPs (Tbr2+RFP/RFP (Sal) = 14.0% [SD= 6.8%], (AraC) = 33.8% [4.8%], $t[5] =4.560$, $p=0.006$) **(Figure 9)**. This result confirmed that after AraC, Tbr2+ IP expansion occurred in the daughter cells of Nestin-lineage NSCs.

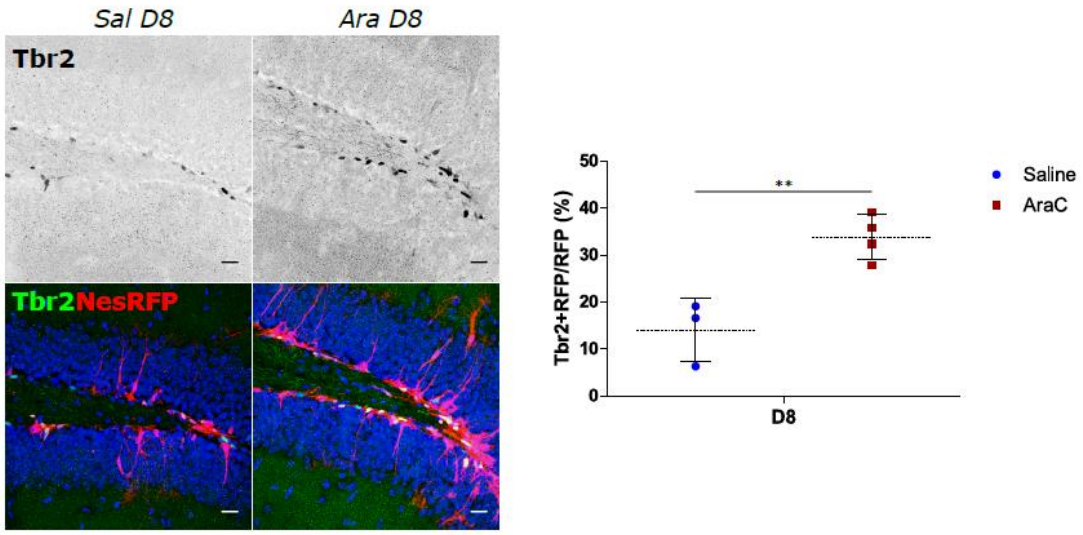

Figure 9. AraC causes neurogenesis in the Nestin+ stem cell lineage.

Representative images of colabelling of Tbr2+ IPs (green) with Nestin-RFP (red) indicating that IP expansion after AraC is seen in the Nestin+ stem cell lineage, with quantification of the fraction of Nestin-lineage expansion of Tbr2+ IPs. ** $p<0.01$; n= 4 animals per group; scale bars= 20 microns.

For subsequent experiments (reported in **Ch.4**) I used the results above to choose key time-points for further study of separate NSPC populations. To study aNSC I chose D3, because D3 was the time-point by which the MCM2+ proliferating population had significantly recovered following AraC. To study IPs I chose D6, because D6 was the earliest time-point both of recovery of Ascl1+ IP density from baseline and of Tbr2+ IP rebound expansion. To study NBs I chose D10. Although by this time-point there was as yet no significant expansion of NBs, their density had returned to control levels with strong morphological evidence of a population of newly-born NBs.

3.2.3 AraC causes increased food intake and weight gain.

Unexpectedly I observed that a proportion of mice receiving AraC became fat during follow-up after mini-pump removal. When these animals were sacrificed their stomachs could be full of food, and their abdominal and thoracic viscera surrounded by fat. This phenotype was not seen in any saline-treated animals. I hypothesised that AraC treatment caused increased food intake and weight gain relative to controls.

To test this hypothesis I measured the average daily food intake in 'paired' observations, where each individually-housed animal's food supply was weighed at the start of the six-day infusion, again when the mini-pump was removed, and once again after a six-day follow-up. I calculated average daily food intake during the infusion period ('weight of food in hopper at start of infusion' minus 'weight remaining at end of infusion', divided by six) and during follow-up ('weight of food remaining at end of infusion' minus 'weight remaining at end of follow-up', divided by six). For each treatment group I compared individual animals' food eaten during *infusion* versus during *follow-up* using tests as outlined below.

I first calculated the differential values (average daily food eaten during follow-up minus average food eaten during infusion) for each treatment group. I inspected these differential values for outliers and normality of distribution. One outlier was detected in each treatment group that was more than 1.5 box-lengths from the edge of the box in a boxplot. The values of these two outliers were not extreme and they were kept in the analysis. The differential food intake between infusion and follow-up was normally distributed in AraC-treated animals (Shapiro-Wilk's test $p>0.05$) but not in saline-treated animals (Shapiro-Wilk's test $p=0.001$). Data from saline-treated animals also failed the assumption of symmetrical distribution required for a non-parametric Wilcoxon Signed-Rank test. I therefore analysed paired data from saline-treated animals using the non-parametric Sign test, and those from AraC-treated animals using a paired-samples t-test.

Saline-treated animals (n=16) ate less food during the six-day period of follow-up after minipump removal than they had during the infusion (median decrease in food intake= -0.2g/day, Sign test $p=0.004$). By contrast AraC-treated animals (n=14) ate more food during follow-up than during infusion (mean increase in food intake= 0.8g/day [95%CI= 0.1g to 1.5g], $t[13]=2.593$, $p=0.022$).

I also weighed the same cohort of animals at five time-points extending up to D21 post-infusion. The correct statistical test to analyse weight changes over time within each treatment group would be 2-way repeated measures ANOVA. However, because some animals were sacrificed at each time-point, the total 'n' of animals in the whole experiment reduced over time. Running one ANOVA would effectively analyse only those animals that survived to the D21 endpoint. However the alternative of conducting independent t-tests between between treatment groups at each time-point would mean testing each individual animal up to five times. To analyse all data while testing each individual animal only once I divided the data into three cohorts. Cohort 1 consisted of animals weighed on the day of pump insertion (baseline) and again on the day of pump removal (D0), and which were then sacrificed (n=7 per treatment group). Cohort 2 was different animals weighed at baseline, again at D0, and at D6, then sacrificed (n=4 animals per treatment group). Cohort 3 consisted of different animals again, weighed throughout the full time-series (baseline, D0, D6, D10, and D21, n=4 animals per group).

For weight, there was no statistically significant two-way interaction between treatment and time from baseline to D0, (Cohort 1, $F[1,6]=0.986$, $p=0.359$, n=7 animals per treatment group), nor from baseline through D0 and D6 (Cohort 2, $F[2,6]=1.862$, $p=0.235$, n=4 animals per treatment group). However there was a significant interaction from baseline through D0, D6, D10 and D21 (Cohort 3, $F[4,12]=4.618$, $p=0.017$, n=4 animals per treatment group). Analysis of simple main effects in Cohort 3 revealed an effect of time in AraC-treated animals ($F4,12]=6.362$, $p=0.005$), but not in controls ($F4,12]=2.295$, $p=0.119$), which was first apparent at the D6 timepoint (AraC mean weight increase over saline at D6=2.8g [95%CI=0.9g-4.6g], $F[1,3]=22.080$, $p=0.018$) **(Figure 10)**. These results suggested that AraC caused increased food intake and weight gain over time.

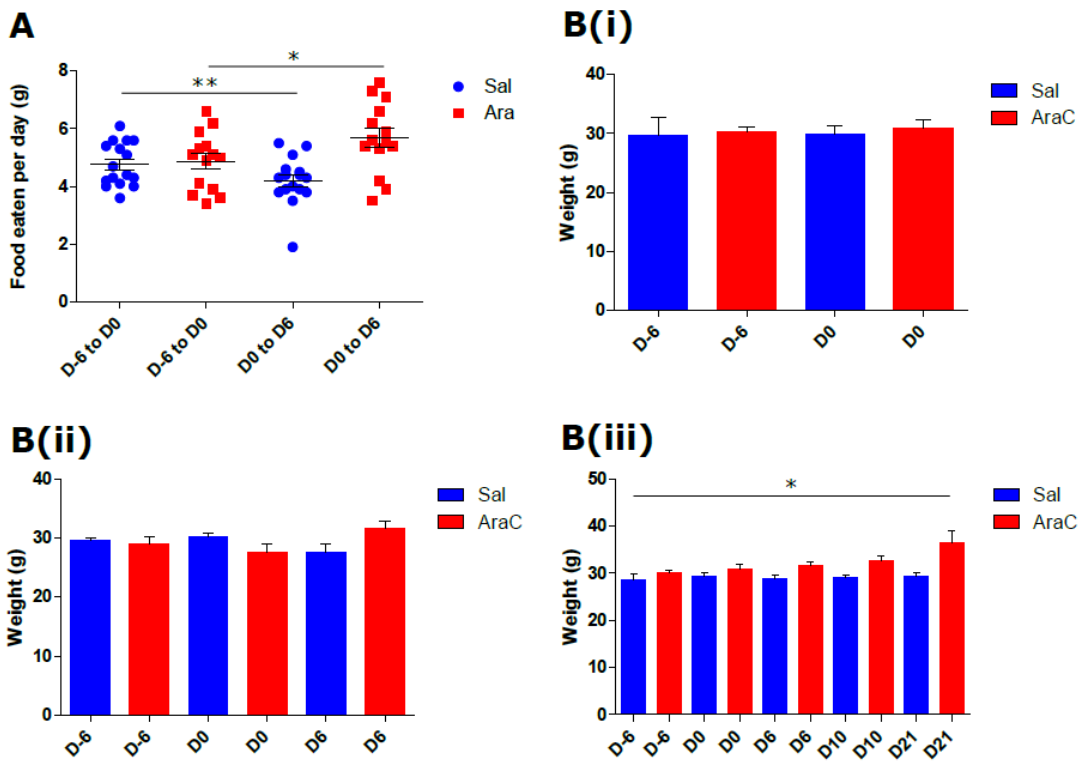

Figure 10. AraC causes weight gain and increased food intake.

A: Graph of longitudinal change in food intake within saline-treated (blue circles) and AraC-treated (red squares) mice. For each treatment group, mean food intake during the infusion period (D-6 to D0) is compared against the mean intake of the same animals during the first six days post-infusion. Note the post-infusion reduction of intake in saline-treated animals, but the increase in AraC-treated animals. **B(i-iii):** Analyses of longitudinal changes in weight within three discrete cohorts of animals: (i)= D-6 to D0; (ii)=D-6 to D6; (iii)=D-6 to D21. * $p<0.05$ **$p<0.01$; n= minimum of 4 animals per group per timepoint.

3.2.4 ECS activates Nestin+ stem cells and increases neurogenesis.

Although AraC infusion triggered a regenerative expansion of IPs at D6-D8 with a still-increasing population of newly-born NBs at D10, it did not cause detectable expansion of aNSC (see **Figure 8H**). In order to focus future experiments on these NSPC subpopulations, including aNSC, I sought an additional technique that would reliably expand the aNSC population. I turned to electroconvulsive stimulus (ECS). ECS is the animal analogue of electroconvulsive therapy (ECT) in humans [Ma et al. 2009] and a single ECS activates GFAP-lineage NSCs in mice. [Weber et al. 2013]

My hypothesis was that a single ECS would also reliably activate Nestin-lineage stem cells. A second hypothesis was that a single ECS would increase neuronal fate commitment in the descendants of these Nestin+ stem cells. To test these hypotheses I first induced recombination in 8-10 week-old Nes-CreER^{T2};RFP$^{f/f}$ animals, labelling Nestin-lineage stem cells. Two weeks later animals received a single ECS ("ECS") or Sham ECS ("Sham") treatment as detailed in **Ch 2.3**. They were sacrificed at the time-points of D1 and D7 post-shock (see **Figure 11A**). At each time-point data from ECS- and Sham-treated animals were compared using statistical tests as outlined below.

At the D1 time-point I analysed the proportion of RFP-labelled NSCs co-expressing the proliferative marker MCM2. NSCs were identified by their SGZ-located cell body and characteristic radial glial morphology. I maintained the confocal Z-stack as individual planes in order to accurately track the radial processes of NSCs through the depth of the section. There were no outliers as assessed by inspection of box plots. Data were normally distributed in each group (Shapiro-Wilk's test $p>0.05$). Equality of variances was met (Levene's test $p=0.105$). I therefore compared the D1 aNSC proportions using an independent-samples t-test.

Compared to controls, ECS caused a significant increase in the proportion of proliferating RFP-labelled RGLs at D1 (Sham: mean MCM2+RGL/RFP=5.4% [95%CI=4.4-6.3%]; ECS: mean=10.6% [95%CI= 7.5-13.8%]; $t[6]=5.181$, $p=0.002$, n=3 animals per group) (**Figure 11B** and **D**).

Next I studied the effect of a single ECS on IP and NB subpopulations at D7. For all analyses presented at this time-point and unless otherwise stated there were no outliers as assessed by inspection of box plots, data in each group were normally distributed as assessed by Shapiro-Wilk's test, and variances were equal as assessed by Levene's test.

Unpaired t-tests of Nestin-lineage RFP+ cells showed that a single ECS caused significantly increased proliferation (Sham: mean Ki67+RFP/RFP=13.1% [SD= 2.6]; ECS: mean=28.9% [SD=5.0]; $t[4]=4.815$, $p=0.009$, n=3 animals per group) and neuroblast fate specification at D7 (Sham: mean Dcx+RFP/RFP=55.8% [SD=3.3]; ECS: mean=72.1% [SD=2.4]; $t[4]=6.957$, $p=0.002$, n=3 animals per group**) (Figure 11C and E-F).** This effect was strong

enough to be readily detectable in the total density of proliferating neuroblasts (Sham: mean Ki67+Dcx+ = 12.6/mm [SD= 2.1]; ECS= 25.4/mm [SD= 2.3]; t[4]=7.132, p=0.002, n=3 animals per group) (**Figure 11G**). At D7 post-shock, there was no evidence of significant difference in Nestin-lineage IPs expressing either Ascl1 (Sham: mean Ascl1+RFP/RFP=4.2% [95%CI=2.3-6.1%]; ECS: mean=5.5% [95%CI=2.4-8.7%], t[6]=1.123, p=0.305, n=4 animals per group) or Tbr2 (Sham: mean Tbr2+RFP/RFP=12.9% [95%CI=5.2-20.5%]; ECS: mean=21.3% [95%CI=12.2-30.4%], t[6]=2.248, p=0.066, n=4 animals per group).

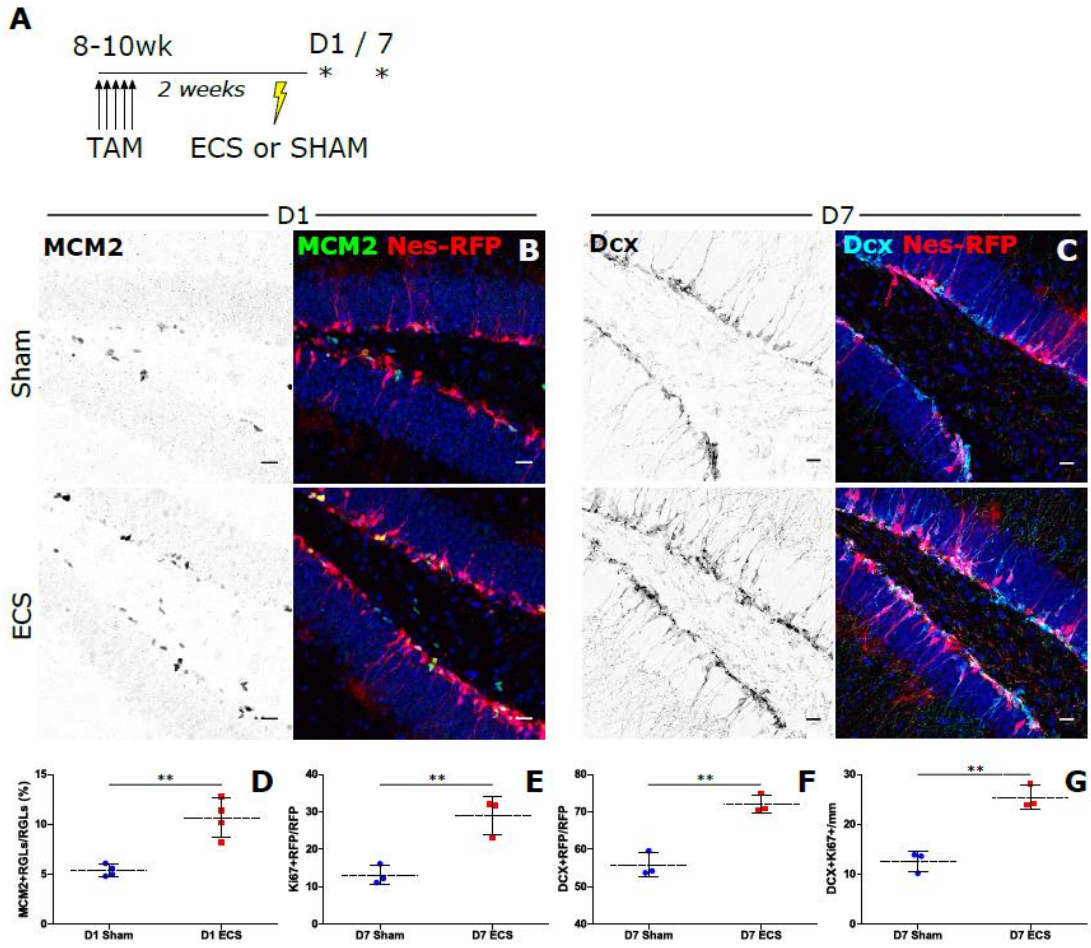

Figure 11. ECS activates Nestin+ stem cells and increases neurogenesis.

A: Experimental schematic for establishing the effects of a single ECS. Mice for this experiment were NesCre^{ERT2};RFP$^{f/f}$. **B:** Representative images of MCM2+ RGL density at D1 post-ECS. The image shown is a z-projection. To avoid missing short processes the analysis was done in a stereological manner on the original z-stacks. **C:** Image showing increased neuroblast density at D7 post-ECS. Note

both the increased density of cell bodies and thickness of radial processes/dendrites. **D:** Quantification of [B]. **E:** Quantification of Ki67+ proliferating cell density at D7 post-ECS. **F:** Quantification of [C]. **G:** Quantification of total proliferating neuroblast density at D7 post-ECS. ** $p<0.01$; n=3-5 animals per group; scale bars= 20 microns. ECS= Electroconvulsive shock group; SHAM= control (no shock) group.

I was interested in whether a single ECS might stimulate NSPCs in more than one stem cell lineage, and whether its effects might differ between lineages. I therefore analysed the same Sham- and ECS-treated animals at D7. This time I determined the density of the same NSPC markers in RFP-negative (non Nestin-lineage) cells. RFP-negative data for Ki67 and Dcx met all assumptions for unpaired t-tests. The data for Sham Tbr2 were not normally distributed (Shapiro-Wilk's test p=0.008) and those for Ascl1 displayed unequal between-group variances (Levene's test p=0.038). I therefore analysed Tbr2 data using the non-parametric Mann-Whitney U test, and Ascl1 using an independent-samples t-test with unequal variances assumed.

In the RFP-negative (non Nestin) lineage, a single ECS caused a significant increase in the density of proliferating NSPCs (Sham: mean RFP-ve Ki67=5.1/mm [95%CI=2.7-7.5/mm]; ECS: mean=15.0/mm [95%CI=9.7-20.3/mm]; t[4]=7.314, p=0.002, n=3 animals per group). There were however no significant differences in Ascl1+ IPs (Sham: mean RFP-ve Ascl1=2.8/mm [95%CI=0.7-5.0/mm]; ECS: mean=4.9/mm [95%CI=0.9-8.9/mm]; t[4.589]=1.436, p=0.216, n=4 animals per group) or Dcx+ NBs (Sham: mean RFP-ve Dcx=26.7/mm [95%CI=10.8-42.5/mm]; ECS: mean=37.2/mm [95%CI=13.5-60.9/mm]; t[4]=1.595, p=0.186, n=3 animals per group). As noted above, I used the Mann-Whitney U test to compare RFP-ve Tbr2+ IP density between Sham- and ECS-treated animals. Visual inspection of a population pyramid showed that distributions of the Tbr2+ IP density differed between Sham- and AraC-treated animals, so mean ranks were reported rather than medians. There was no difference in Tbr2+ IP density between groups (Sham: mean rank RFP-ve Tbr2=2.75; ECS: mean rank=6.25; U=1.000, z=2.021, p=0.057, n=4 animals per group) (**Figure 12**).

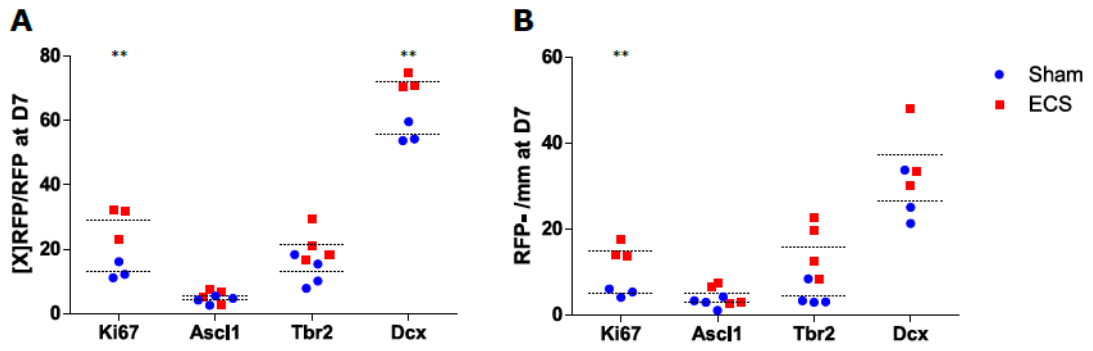

Figure 12. ECS has differential effects on Nestin-positive and Nestin-negative lineages. Quantification of response to ECS of NSPC subpopulations, both Nestin RFP+ **(A)** and RFP- **(B)**. In both lineages ECS caused a significant expansion of Ki67+ proliferating cells, but with differential effects observed on the Dcx subpopulation at the time-point and groups sizes studied. * $p<0.05$; ** $p<0.01$; n=3-4 animals per group.

Taken together these results showed that a single ECS robustly and efficiently activates Nes-RFP labelled RGLs at D1, causing increased proliferation and neurogenesis in the Nestin lineage at D7. Exploratory analyses suggested the possibility that NSPCs from different stem cell lineages may differ in their early response to ECS, with evidence of significant neurogenesis in Nestin-lineage cells but not in non Nestin-lineage cells. Qualitatively, I observed that AraC was feasible to deliver in an experimental setting (all-cause mortality < 10%), but ECS was far quicker, safer, and better tolerated (all-cause mortality 0%).

3.2.5 A single ECS does not alter DG NG2+ density at D7.

Because one previous group has reported an association between a single ECS and a transient reduction in myelination in the DG [Meier et al. 2004], I also examined the response of dentate gyrus oligodendroglial-lineage cells to a single ECS. At D7 post-shock, no difference was seen in the density of Olig2+ cells per 40X field (Olig2+/field Ctr=118.7 [SD=10.9], ECS=123.0 [SD=10.1], p=n.s.).

3.3 Discussion

In these initial experiments I found that hippocampal neurogenesis can be reliably manipulated by AraC infusion and by a single electroconvulsive shock. AraC effectively ablates dividing SGZ NSPCs with evidence of significant effect in the total proliferating and neuroblast populations and a suggestive trend ($p<0.06$) to ablation in IPs. This ablation essentially 're-boots' neurogenesis, which recovers in a biologically sequential and temporally significant manner. Results of a time-series experiment analysed with multivariate ANOVA suggest that activated neural stem cells (and proliferation in general) recover to baseline by D3 post-infusion. This is followed by a rebound expansion of Ascl1+ and Tbr2+ IP populations in the time periods D6-D8, with a still-emerging population of newly-born Dcx+ NBs by D10. Meanwhile a single electroconvulsive shock efficiently activates Nestin lineage NSCs as early as D1 post-shock, causing an expansion in NBs in the same lineage at D7. Interestingly my data leave open the possibility that different NSPC subpopulations may respond differently to the same intervention (see below).

3.3.1 Limitations

Before discussing these results in a wider context I would like to consider some limitations. The first is general and applies not only to this Chapter but to experiments throughout this thesis. It is the problem of small group sizes, and in particular the difficulty of choosing and interpreting statistical analyses in experimental designs involving fewer than 16-20 animals per group. Small group sizes make it difficult to interpret negative results because the power to exclude a Type II error is low. One might consider this simply to be a relevant concern after a negative result. But it is a problem which also affects the upstream choice of statistical test. Parametric statistical tests assume a normal distribution. Tests of normality distribution (e.g. the Shapiro-Wilks' test which I used here) may falsely exclude an abnormal distribution when power to exclude a Type II error is low. Consequently, the results of parametric statistical analyses may be given more weight than they should. For a wider discussion of this point see **Ch. 6;** its relevance in the current chapter is to suggest a cautious interpretation even of my positive results.

Second, AraC is a potent antimitotic drug. It is likely to have had effects throughout the entire CNS and not just the SGZ. My experiments were not designed to study whether and

how non-SGZ brain mechanisms may regulate hippocampal neurogenesis, so I cannot exclude that such distal mechanisms may regulate how AraC exerted its effects. This limitation is common to all studies using AraC in the CNS that I am aware of.

Third, in the AraC experiments aNSC were identified by co-labelling of Nestin and MCM2 immunofluorescence in the same RGL. Because Nestin is a protein of the radial process whereas MCM2 localises to the nucleus, identification of aNSC was technically difficult, even at high magnification. Identifying a co-labelled cell was usually a judgement rather than an obvious categorisation. This judgement was unlikely to be biased to one group or another, because I was blind to group and therefore approached both in the same way. However the accuracy of this approach is unclear and I therefore cannot exclude a subtle rebound expansion of aNSC after AraC. This experience was one of the reasons I used nestin reporter mice in the later ECS experiments.

Fourth, there was variability in the tempo and extent of NSPC subpopulation recovery in individual mice. It was most noticeable for Tbr2 where some animals showed scant recovery of IP populations by D6 and D8, whereas others showed a striking rebound. Reasons for variability in the tempo of response are unknown but may include technical (differences in rate of AraC delivery from the cannula, or permeation of AraC through the hippocampal interstitium) or biological causes (e.g., a different natural response of NSPCs to AraC between individual mice). The effect was perhaps to dilute the precision with which NSPC subpopulations could be targeted after AraC, albeit without entirely preventing it.

Fifth, I did not characterise other cell populations in the SGZ neurogenic niche that may also have been affected by AraC. Endothelial, microglial cells, and astrocytes are known to regulate neurogenesis [Ehret et al. 2015, Ashton et al. 2012, Cao et al. 2013, Sierra et al. 2010, Vukovic et al. 2012]; all are likely to have been perturbed by the procedure (for example by acquisition of an ‘activated’ state, or by apoptosis), and unmeasured differences in their response may have contributed to some of the variability seen in the extent of regenerative neurogenesis.

Sixth regarding ECS, although identification of aNSC was easier following CreER-mediated Nes-RFP induction, in these experiments I could not exclude a lingering effect of Tamoxifen administration two weeks previously on the NSPC response to a single shock. The use of constitutive reporter mice would have avoided this particular limitation.

Seventh, although I used Nes-RFP expression to identify RGLs post-shock, I did not confirm that the RGLs expressed Nestin at the time of sacrifice using immunofluorescence. The interpretation that my ECS data describe what happens to Nestin+ NSCs therefore involves a degree of assumption (see below).

Eighth, it is worth noting qualitative differences between the tolerability of the AraC and ECS procedures. The AraC paradigm requires two invasive neurosurgical operations under general anaesthesia with a week, separated by a toxic infusion. The infusion catheter had to be glued to the skull, and following its removal closure of the scalp wound was difficult owing to any glued skin having to be debrided first. Neurological morbidity (e.g., stroke) was low - approximately 1:30 animals - but failure of the infusion catheter glue was more common - perhaps 1:15 animals. In both situations the affected animals had to be culled to prevent suffering. Even without these outcomes, animals receiving AraC tended to show a reduced level of care for self, often with failure to create a neat "nest" of their cage bedding during the period of follow-up. Overall I felt the whole procedure was relatively toxic. By comparison, the ECS paradigm involved a single brief general anaesthetic, with animals back in their home cage and ambulant within five minutes. No animal that received ECS required to be culled for any complications. None appeared to be in discomfort or experiencing reduced care for self. I concluded that ECS was fast, safe, and more effective in triggering neurogenesis than AraC infusion. These differences reinforce that the AraC and ECS models should not be considered as directly comparable - unsurprisingly, since AraC is a model of injury, and ECS is not.

3.3.2 Results in context: AraC

The dynamic response of hippocampal NSPCs to AraC ablation has been rarely studied. One previous study suggested that following co-administration of AraC and Procarbazol there is an initial reduction of BrdU+ proliferating cells in the SGZ, followed by a rebound proliferation which recovers to baseline over approximately 10 days. [Seri et al. 2001] I report similar – if not quite identical - findings using AraC alone and extended it to describe the temporal dynamics of separate NSPC subpopulations. This has been partially characterised previously for Tbr2+ IPs. [Hodge et al. 2008] The current study encompassed aNSC, Ascl1+ IPs, Tbr2+ IPs, and Dcx+ NBs making it a more detailed characterisation of how the adult mouse SGZ responds after AraC. My data support the conclusion of Hodge et

al., in the sense that both our studies show evidence of a rebound expansion of Tbr2+ IPs, although they did not examine identical time-points.

My lineage-tracing data suggested that Nestin+ NSCs contribute to the regenerative response. DeCarolis et al. reported however that seven days after AraC, GLAST-YFP+ RGLs showed a rebound proliferative expansion whereas Nestin-YFP+ RGLs did not. The authors also reported a persisting reduction in the total number of NestinYFP+ cells at D7, compared to saline-infused controls. They concluded that "YFP+ RGCs in GLAST-Cre/YFP mice contribute to neurogenic recovery 7d after AraC-induced ablation, whereas RGCs labeled in Nestin- Cre/YFP mice do not." [DeCarolis et al. 2013]

My seemingly contrary finding that AraC induced a proliferative expansion of NSPCs in the Nestin lineage (see **Figure 9**) requires explanation. First, DeCarolis et al. and I agree that there was no observable difference in proliferating Nestin+ RGLs after AraC. My data suggest instead that in the Nestin lineage at least, proliferative expansion after AraC does not happen before the IP stage. Data on IPs were not reported by DeCarolis et al. Second, the expansion which I observed in the proportion of Nestin-lineage Tbr2+ cells at D6-D8 is hard to compare directly to the overall reduction in Nestin-lineage cells observed by DeCarolis et al at a similar time-point. One is a proportion of a specific subpopulation, the other a total number of all subpopulations.

Besides lineage status, subpopulation marker expression, and read-out, neither DeCarolis nor I exclude the possibility of differential sensitivity of different NSC lineage populations to cell death during AraC injury. The reduction in total Nestin-YFP+ cells at D7 observed by DeCarolis et al. could be explained by greater total initial Nestin-lineage cell death, meaning a lower baseline from which to regenerate. Examining their paper, the reported magnitude of ablation in Nestin-lineage cells at D0 was indeed proportionally greater than that for GLAST-lineage cells, suggesting potential differential sensitivity.

Last I would consider the tempo of regenerative response in each lineage. A differential rate of recovery between Nestin-lineage and GLAST-lineage NSPCs could explain the discrepant data obtained by DeCarolis et al.

Overall my results suggest that Nestin-lineage NSPCs contribute to regenerative neurogenesis after AraC. DeCarolis et al. reached a contrary conclusion. However the data

from our two studies remain potentially consistent if one hypothesises differential sensitivity to AraC and/or dynamics of regenerative response in NSPCs of different lineages.

My first interpretation of the surprising observation of AraC-induced weight gain was that neurogenesis might regulate food intake. I discovered however that Gouaze and colleagues had previously reported a similar phenotype during long-term AraC infusion (i.e., in a condition of ongoing inhibition of neurogenesis). [Gouaze et al. 2013] I did not explore mechanisms of AraC-induced weight gain further experimentally, but would note the recent study by Djogo et al. suggesting that oligodendrocyte precursor cells (OPCs) maintain hypothalamic sensitivity to the appetite-inhibiting hormone leptin. [Djogo et al. 2016] OPCs are a proliferative cell population in the adult brain and therefore likely to be sensitive to AraC. OPC apoptosis-mediated leptin sensitivity loss is a possible mechanism to explain why AraC-treated mice got so fat.

3.3.3 Results in context: ECS

Among the studies which examine the effect of a single shock on hippocampal neurogenesis, Weber and colleagues conducted what I think is the most sophisticated analysis to date. [Weber et al. 2013] The authors asked whether ECS triggers RGL activation. They showed that a single ECS stimulus significantly increased the number of Ki67+Type 1 GFAP-lineage aNSC at D3 and D6 post-shock, over both sham and virgin controls. The increase was significantly greater at D6 than at D3, suggesting that a single shock has sustained effects on NSC activation and proliferation.

Although I found their data convincing, the study by Weber et al. left some unanswered questions. They did not report whether a single shock led directly to increased neurogenesis in a fate-labelled lineage, choosing to focus instead on the effect of multiple shocks. Additionally the adult hippocampal stem cell population is molecularly heterogeneous: those expressing nestin only partially overlap with those expressing GFAP. [Filippov 2003] The effect of ECS on other NSC subpopulations remained unknown, and the effect of a single shock on IP and NB progeny of aNSC remained unclear.

I was able to address these points in my experiments. My data confirm RGL activation (at the earlier time-point of D1), and extend to report an effect in Nestin+ RGLs. It is tempting to assume that the labelled RGLs were positive for Nestin at the point of sacrifice. This is not

a given however: ECS may smartly up-regulate GFAP in SGZ NSCs as early as D1 post-shock [Husain et al. 2015]. It would have strengthened my data to stain for Nestin (and GFAP) at D1 to show whether the activated NSC population was truly Nestin-positive at the point of sacrifice.

My experiments also established that a single shock robustly increases Dcx+ neurogenesis in direct lineage descent from Nestin+ NSCs. A clearer understanding of the mechanistic effect of electrical stimulation on hippocampal neurogenesis, and the function of these new-born neurons, could have implications for the psychiatric treatment of depression.

Finally I found the analysis of the effect of a single shock on RFP+ and RFP- NSPC subpopulations (see **Figure 12**) interesting, because it suggested the possibility of differential dynamics between NSC lineages. At D7 in the Nestin lineage, proliferating progenitors were mostly Dcx+ NBs. However in the Nestin negative lineages at the same time-point, there was no evidence of increased neurogenesis. The data for Tbr2 were suggestive of an expansion of IPs, but using the rigorously conservative non-parametric test appropriate to this specific analysis, there was no evidence of significance. If the effect was real one explanation could be that NSCs in different lineages respond differently either to an electrical stimulus or its consequences. This preliminary finding may be a stimulus for future studies.

3.3.4 Chapter summary

In this Chapter I asked the questions of whether AraC infusion, or a single electrical shock, could be used to reliably manipulate hippocampal neurogenesis. The aim was to establish experimental models that would allow me to more precisely target NSPC subpopulations in future studies. I found that AraC and a single ECS induced proliferative expansion of different NSPCs at different time-points. Characterising the dynamics of the response prepared me to use these techniques appropriately in my study of ECM candidate regulators of adult neurogenesis.

In Chapter 4 I study a candidate ECM regulator of neurogenesis and the principal route by which cells communicate with the ECM: Integrin β1.

4 THE MATRIX RECEPTOR INTEGRIN β1 REGULATES HIPPOCAMPAL NEUROGENESIS

4.1 Introduction

Adult hippocampal neurogenesis is a biological process which continues throughout life in the mammalian dentate gyrus. [Goncalves 2016, Bond 2015, Spalding 2013 and **Ch. 1**] It is thought to support learning, memory, and cognitive flexibility [Epp et al. 2016, Akers et al. 2014, Sahay et al. 2011] making it a potential therapeutic target for a wide range of neuropsychiatric and neurodegenerative diseases. The transcriptional regulation of this process is increasingly understood [Shin et al. 2015, Beckervordersandforth et al. 2015], but little is yet known about the contributory role of signalling from the extracellular matrix (ECM).

Signalling from the ECM is primarily transduced to the intracellular environment via integrins. [Hynes 2002] The main integrin β subunit, Integrin β1 (also here referred to as its gene symbol **Itgb1**) thereby regulates multiple critical aspects of cell function. Data from in vitro studies (see **Ch. 1** and **Table 5**) suggest that Itgb1 signalling promotes the proliferation, neural differentiation, survival, and migration of NSCs. [Jacques et al. 1998, Leone et al. 2005, Flanagan et al. 2006]

In contrast to in vitro data, the role of Itgb1 on NSCs in the living adult brain remains far from clear. Others have reported the counterintuitive finding that Itgb1 *negatively* regulates (restricts) progenitor proliferation in the adult subependymal zone (SEZ). [Kazanis et al. 2010, Shen et al. 2008] The antibody blocking techniques used by these studies caused significant architectural disruption of the neurogenic niche however, creating a potential confound. Genetic knockout techniques were subsequently used by two groups to study putatively integrin-mediated signalling in adult hippocampal neurogenesis. [Porcheri et al. 2014, Brooker et al. 2016] They report conflicting findings regarding the role of Itgb1 in regulating neurogenesis, and neither studied the in vivo role of Itgb1 specifically in hippocampal NSPCs.

In light of this uncertainty I asked: what is the role of Itgb1 in adult hippocampal neurogenesis? From in vitro and the conflicting in vivo data available, I hypothesised a positive regulatory role.

4.2 Results

4.2.1 Itgb1 is expressed by proliferating precursors in the SGZ.

I first asked whether Itgb1 was expressed by subgranular zone NSPCs. My hypothesis was that NSPCs did express Itgb1. Adult WT animals were processed for immunofluorescence as described in **Ch. 2**. The frequency of Itgb1 co-labelling with NSPC markers was calculated +/- 95% CI (minimum n=3 animals per analysis). In preliminary experiments, widespread co-localisation of Itgb1 was observed with GFAP+ radial processes of SGZ NSCs. However n-1 controls **(Figure 13)** suggested that this apparent staining was a technical artefact. GFAP staining was omitted thereafter and NSCs identified solely by the combination of a Nestin+ radial process and cell body located in the SGZ.

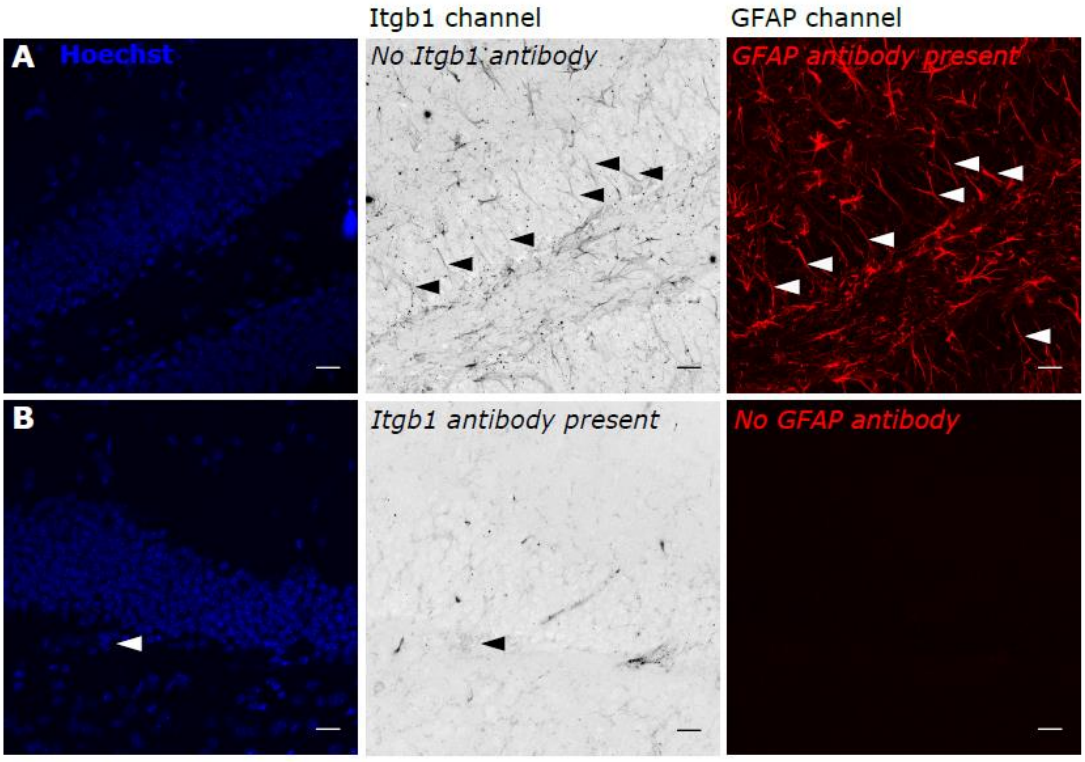

Figure 13. Itgb1 staining of GFAP+ processes was suspected technical artefact.

A: Representative Itgb1-GFAP immunofluorescence omitting Itgb1 primary antibody from the incubation solution. Signal in the Itgb1 channel persists and completely colocalises with GFAP+ processes (arrowheads). **B:** Representative images omitting GFAP primary antibody. Note absence of any clear staining of radial processes in the Itgb1 channel. There is a small Itgb1+ cell cluster in the

SGZ (arrowhead; best seen on high-resolution images available via the link on **Page vi**). Scale bars= 20 microns.

There was no evidence of Itgb1 staining on quiescent NSCs (identifiable by their singular Nestin+ radial process arising from the SGZ, n=0/26 cells screened, 0% [95%CI 0-12.9%]). However, weak Itgb1 staining was observed on the radial process and cell body of activated neural stem cells (aNSC, identified by co-labelling of Nestin and MCM2, n=14/26, 53.8% [35.5-71.2%]). Staining was detectably stronger on Ascl1+ intermediate progenitors (IPs, n= 98/146, 67.1% [59.1-74.2%]), Tbr2+ IPs (n=166/203, 81.8% [75.9-86.5%]), and Dcx+ immature neuroblasts (identifiable by their absence of a radial process, n=62/106, 60.8% [51.1-69.7%]). I noticed a similar pattern of Itgb1 expression on MCM2+ proliferating progenitors (n= 283/430, 65.8% [61.2-70.1%]), particularly within MCM2+ cell clusters. However more mature NBs with Dcx+ radial processes, which are largely post-mitotic, again showed a lack of Itgb1 staining (n=0/18, 0% [0-17.6%]) **(Figure 14)**. These results suggested that Itgb1 expression in adult hippocampal NSPCs is tightly linked to cell cycle.

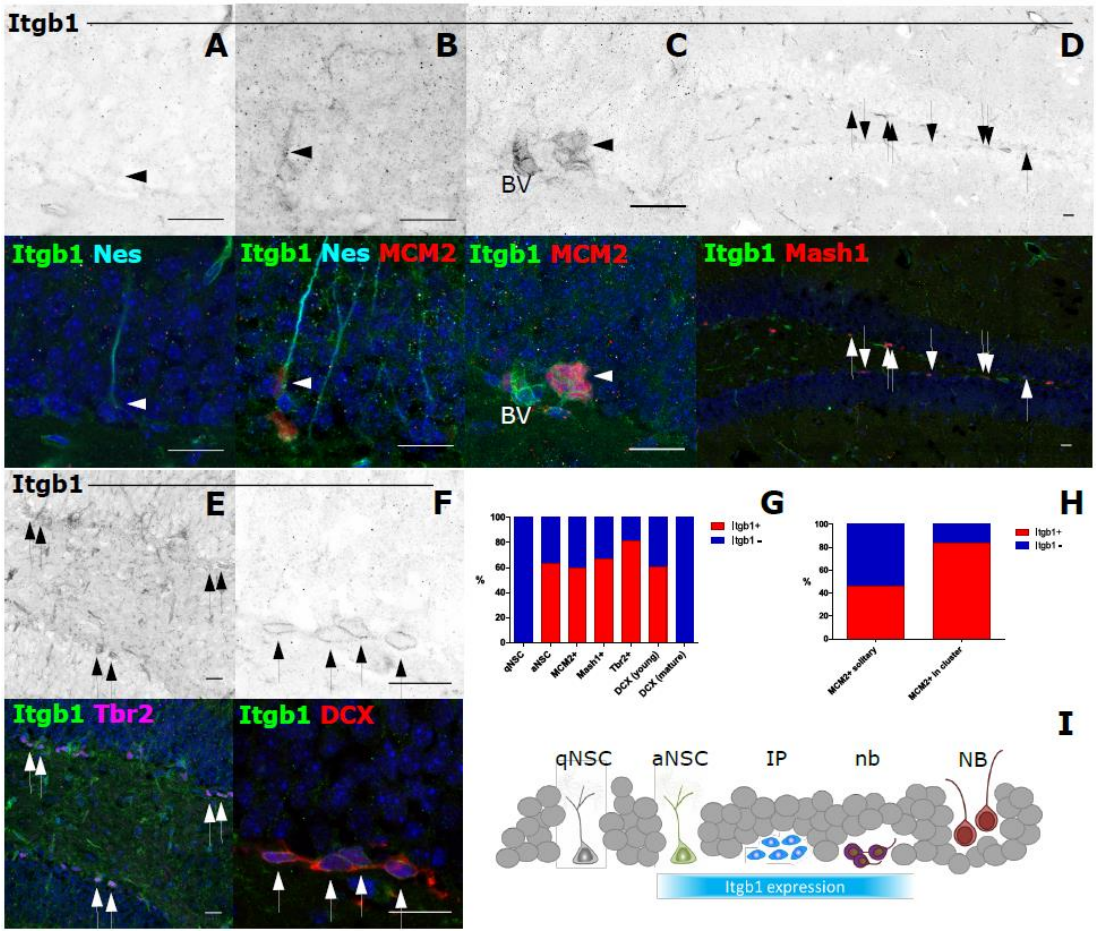

Figure 14. Itgb1 is expressed by proliferating precursors in the SGZ.

A-F: Representative images of Itgb1 co-labelling on individual subpopulations of NSPCs in the SGZ. Itgb1 channel is included as an inverted greyscale for clarity. Arrowheads indicate Itgb1+ cells of interest. Itgb1 staining is undetectable on qNSC (A), faint on aNSC (B), and stronger on MCM2+ proliferating cells (C), Ascl1+ IPs (D), Tbr2+ IPs (E), and new Dcx+ NBs that are yet to generate a radial process (F). **G:** Quantification of Itgb1 staining among the different NSPC subpopulations. **H:** MCM2+ cells in clusters, characteristic of SGZ IPs in neurogenesis, display more Itgb1 staining than solitary MCM2+ cells, some of which may represent primed quiescent cells. **I:** Visual summary. qNSC=quiescent neural stem cells; aNSC= activated neural stem cells; IP= intermediate progenitors; nb= new neuroblasts lacking a radial process; NB= older postmitotic neuroblasts with a radial process. All scale bars= 20 microns.

4.2.2 Itgb1 negatively regulates homeostatic neurogenesis.

Next I asked "what is the function of Itgb1 on adult hippocampal NSPCs?" My hypothesis was that Itgb1 would positively regulate (increase) neurogenesis. To study this question I used the CreER-LoxP system to inducibly delete the Itgb1 gene in adult Nestin-lineage NSCs. Experimental animals were $NesCre^{ERT2}$;$Itgb1^{f/f}$;$RFP^{f/f}$. Controls were $NesCre^{ERT2}$;$Itgb1^{f/WT}$;$RFP^{f/f}$. Eight-to-ten week-old animals were recombined using Tamoxifen as described in **Ch. 2.1**. To examine Itgb1 function under homeostatic conditions, animals were returned to their cages for six weeks with no further intervention. They were then sacrificed and processed for immunofluorescence as described in **Ch. 2.5 / 2.6** (and see **Figure 15A**). The genotypes of experimental and control animals were double-checked and found to be correct.

Data are mean and S.D. unless otherwise stated. For each analysis, inspection of box plots revealed no outliers in the data, dependent variables were normally distributed (Shapiro-Wilk's test $p>0.05$) and there was homogeneity of variances (Levene's test $p>0.05$). Each outcome was therefore analysed using an independent samples t-test (n=4 animals per group). The exception was one outcome (the density of total RFP+ cells) which was not normally distributed in control animals. I used the non-parametric Mann-Whitney U test to analyse total RFP+ density between the two groups.

Itgb1 protein was significantly reduced in recombined, proliferating iKO NSPCs (Itgb1+MCM2+RFP/MCM2+RFP Ctr= 39.1% [SD=10.1], iKO= 18.1% [SD=8.5], $t[6]= 3.088$, $p=0.021$, **Figure 15B-C**). No gross architectural disruption to the SGZ was observed, and there was no significant difference in total RFP+ density between groups (RFP Ctr Median= 54.1/mm, iKO median=42.2/mm, $U=6.000$, $z=0.577$, $p=0.686$), **Figure 15D**).

After Itgb1 iKO a higher proportion of recombined NSPCs were in cell cycle (Ki67+RFP/RFP Ctr=8.5% [SD=2.6], iKO=15.7% [SD=3.4], $t[6]=3.353$, $p=0.015$, **Figure 15E** and **G**). Itgb1 iKO increased neural fate specification of recombined cells (Dcx+RFP/RFP Ctr=33.2% [SD=3.6], iKO=51.7% [SD=6.5], $t[6]=4.985$, $p=0.002$, **Figure 15F** and **H**). There was no evidence of a between-group difference in S100β+ mature astrocytes, either in cell-autonomous (S100β+RFP/RFP Ctr=1.8% [SD=1.1], iKO=1.8%

[SD=0.9], t[6]=0.108, p=0.917) or non cell-autonomous analyses (S100β+ Ctr= 13.2/mm [SD=2.9], iKO=15.8/mm [SD=1.8], t[6]=1.527, p=0.178). There was no evidence of a difference in TUNEL+ apoptotic cell density in the SGZ (TUNEL+ Ctr= 0.4/mm [SD=0.2], iKO= 0.5/mm [SD=0.1], t[6]=0.758, p=0.477).

These results suggested that under homeostatic conditions, Itgb1 *negatively* regulates hippocampal NSPC proliferation and neurogenesis in a cell-autonomous manner.

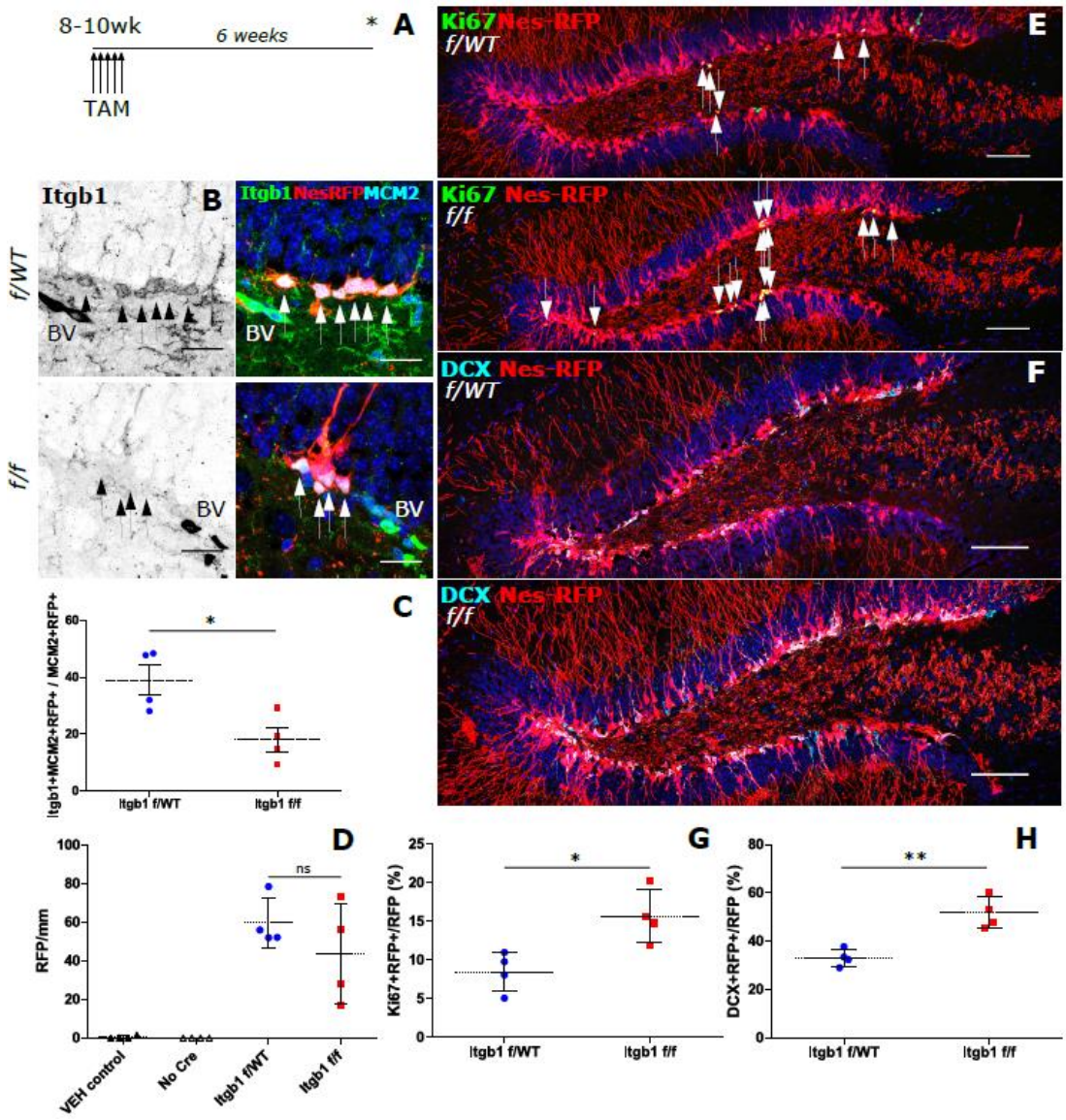

Fig 15. Itgb1 negatively regulates homeostatic neurogenesis.

A: Experimental schematic. **B:** Itgb1 protein was reduced specifically in NSPCs of iKO mice. The upper panels show characteristically strong Itgb1 expression in a cluster of RFP+MCM2+ cells (arrowheads). The lower panels show ablation of the protein on an equivalent cluster in iKO mice (arrowheads). The specificity of the knockout is shown by preservation of Itgb1 staining on an adjacent blood vessel. **C:** Quantification of Itgb1 iKO by immunofluorescence. **D:** RFP+ cell density across experimental groups. Note the absence of RFP expression in VEH-recombined mice. **E:** Upper panel – Ki67+ proliferating RFP+ NSPCs in control mice (arrowheads indicate double-labelled cells). Lower panel – iKO. **F:** Upper panel – Dcx+ RFP+ NBs in control mice. Lower panel – iKO. **G:** Quantification of proliferation. **H:** Quantification of differentiation. * $p<0.05$; ** $p<0.01$; ns= not significant; n=4 animals per group; TAM= tamoxifen; VEH= vehicle; BV= blood vessel. Scale bars in Panel B= 20 microns; bars in panels E and F= 100 microns.

4.2.3 Itgb1 negatively regulates neurogenesis after injury.

I next asked whether Itgb1 regulates neurogenesis after CNS injury, such as via i.c.v. infusion of AraC. Taking account of the results reported in **Ch. 4.2.2** my revised hypothesis was that Itgb1 would negatively regulate neurogenesis after AraC-mediated injury. To test this hypothesis, $Itgb1^{f/f}$ ('Itgb1 iKO') and $Itgb1^{f/WT}$ (control) animals were Tamoxifen-recombined as described in **Ch. 2.1.** The AraC procedure was conducted six weeks after recombination (see **Ch. 2.2.**). Because the primary question was of the 'gene effect' of Itgb1, all animals in the current experiment received a six day infusion of AraC; none received Saline. In view of the results of **Ch. 3**, following mini-pump removal animals were followed up for the key time-points of three, six, or ten days until sacrifice and processing for immunofluorescence on slides as described in **Ch. 2.5 / 2.6**.

NSPC subpopulations were identified by co-labelling of NesRFP with MCM2 (for proliferation), Tbr2 (for IPs), and Dcx (for NBs). At each time-point I conducted four main analyses: total RFP+ density, MCM2+RFP+ proliferating fraction, Tbr2+RFP+ IP fraction, and Dcx+RFP+ NB fraction. Each analysis used 2-way ANOVA to test for a multivariate interaction between gene group and time. Where indicated by evidence for a significant interaction, I further analysed simple main effects. Where there was no evidence of interaction I analysed main effects. Where appropriate I conducted Bonferroni-corrected pairwise comparisons to inform the interpretation.

There was no statistically significant interaction between Itgb1 gene status and time for total RFP+ cell density ($F[2,24]=0.291$, $p=0.750$, partial $\eta^2=0.024$). As expected there was a significant main effect of time, whereby RFP+ cell density increased over time in both groups (D3 unweighted marginal mean=24.8/mm [95%CI=15.4-34.1]; D6 mean=31.4/mm [95%CI=24.5-38.4]; D10 mean=48.8/mm [95%CI=40.9-56.7], $F[2,24]=9.585$, $p=0.001$, partial $\eta^2=0.444$), indicative of AraC-mediated regenerative neurogenesis (**Figure 16C**).

There was a significant interaction between gene and time in the MCM2+ fraction of RFP+ NSPCs ($F[2,24]=4.750$, $p=0.018$, partial $\eta^2=0.284$). A simple main effect of gene was observed between control and Itgb1 iKO animals at D6 ($F[1,24]=7.479$, $p=0.012$, partial $\eta^2=0.238$) and D10 ($F[1,24]=24.761$, $p<0.001$, partial $\eta^2=0.508$). At these time-points corrected pairwise comparisons of the MCM2+ fraction of RFP+ cells showed a significant

expansion, relative to control, in Itgb1 iKO animals (*control* D3 MCM2+RFP+/RFP mean=16.6% [95%CI=6.3-26.9%]; D6 mean=19.0% [95%CI=11.0-27.0%]; D10 mean=25.3% [95%CI=17.9-32.6%], all pairwise test p >0.05; *Itgb1 iKO* D3 MCM2+RFP+/RFP mean=18.1% [95%CI=9.1-27.0%]; D6 mean=32.5% [95%CI=26.2-38.9%], p=0.036 relative to D3; D10 mean=53.1% [95%CI= 44.2-62.0%], p=0.002 relative to D6]. These data indicated an acceleration in the MCM2+ fraction of RFP+ cells over time in Itgb1 iKO animals (**Figure 16D**). This effect on proliferation was large enough to be apparent in the total density of proliferating cells at D10 (**Figure 16E**).

To examine whether this increased proliferation was explained by an expansion of IPs, I analysed the Tbr2+RFP+ fraction of RFP+ cells. I found no evidence of a significant interaction between gene and time-point (F[2,24]=0.295, p=0.747, partial η^2=0.024). There was a significant main effect of time-point (F[10.823], p<0.001, partial η^2=0.474) suggesting a significant expansion of the Tbr2+ IP fraction in both gene groups, likely most pronounced at D6. There was no evidence of a main effect of gene status however (F[1,24]=1.999, p=0.170, partial η^2=0.077) (**Figure 16F**).

Next I examined whether the Dcx+RFP+ NB fraction contributed to Itgb1-mediated proliferative expansion. There was no evidence of significant interaction between gene status and time (F[2,24]=1.503, p=0.243, partial η^2=0.111). There was a significant main effect of time (F[2,24]=14.757, p<0.001, partial η^2=0.552) in keeping with AraC-mediated stimulation of neurogenesis in both groups. There was also a significant main effect of gene (F[21.193], p<0.001, partial η^2=0.469), with evidence of a relative expansion of Itgb1 iKO NBs (mean increase in Dcx+RFP+/RFP over control=15.8% [95%CI=8.7-22.8%], Bonferroni-corrected p<0.001) (**Figure 16G**), many of which were proliferating (**Figure 16H**).

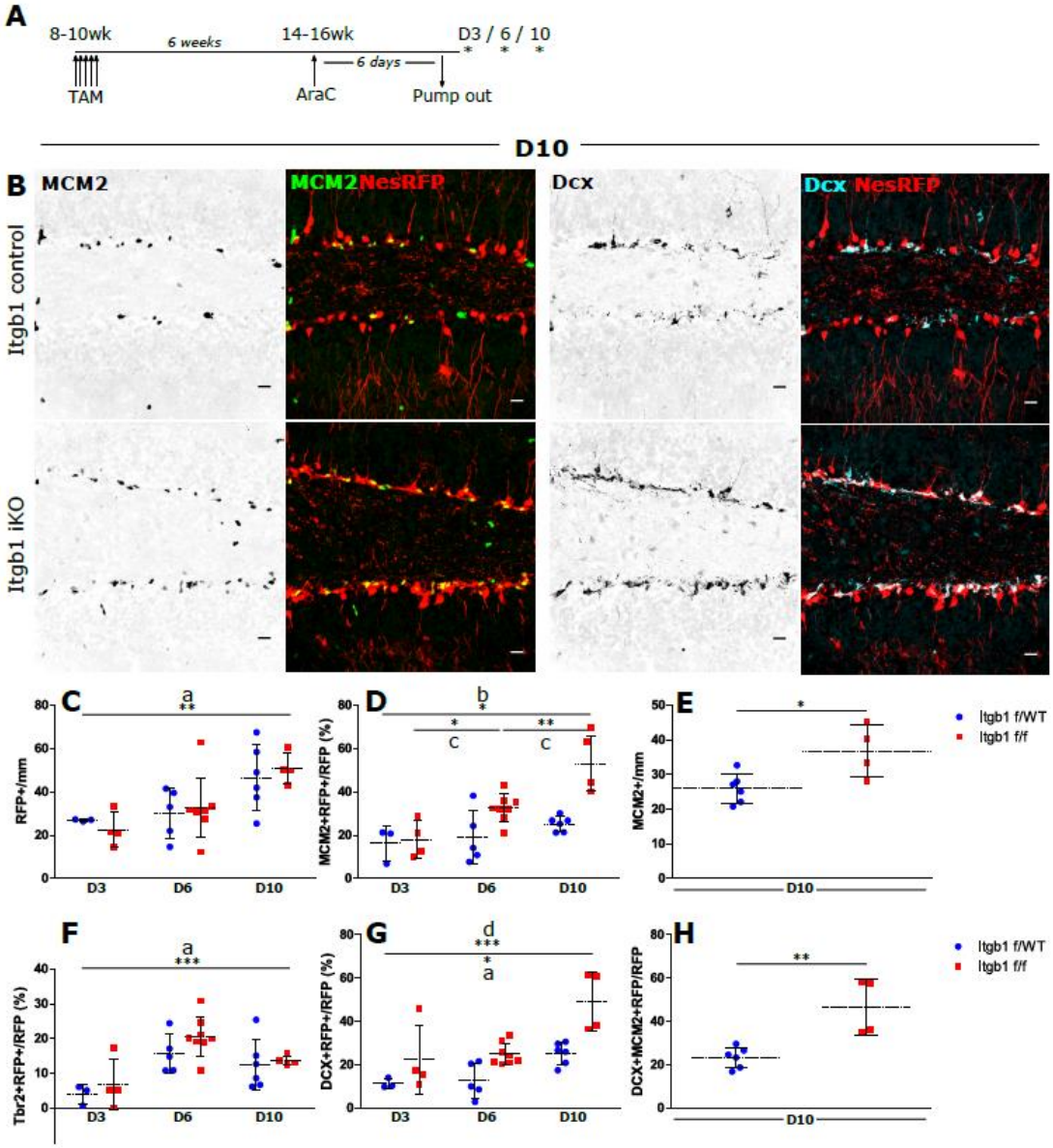

Figure 16. Itgb1 negatively regulates neurogenesis after injury.

A: Experimental schematic. **B:** Representative figures of control (upper panels) versus iKO animals (lower panels). SGZ proliferation (MCM2, left-hand side) and differentiation (Dcx, right-hand side) were both increased in iKO mice. Hoechst has been omitted from the merge images for clarity. **C:** Quantification of RFP+ cell density at D3, D6 and D10. **D:** Quantification of the proliferating RFP+ fraction at the time-points studied. **E:** Quantification of the overall density of all MCM2+ cells at D10. **F:** Quantification of RFP+ IPs over time. **G:** Quantification of the fraction of RFP+ neuroblasts over time. **H:** Quantification of the fraction of RFP+ neuroblasts that were proliferating at D10. * $p<0.05$; ** $p<0.01$; *** $p<0.001$; a= main effect of time; b= interaction between gene group and time; c= post-hoc pairwise comparisons between timepoints; d= main effect of gene; n=3-8 animals per group; scale bars= 20 microns.

At the D10 time-point there was no evidence of an expansion in astrocytic differentiation of iKO NSPCs within the SGZ (Ctr mean S100B+RFP+/RFP= 1.2% [SD=0.8], iKO=2.6 [1.3]; t[8]=2.149; p=0.383).

Summarising these results, AraC triggered a regenerative neurogenesis in both control and experimental animals. Itgb1 iKO animals however displayed an enhanced proliferative response that was first apparent at D6 and even stronger at D10. No significant differences were observed between experimental groups in the response of NesRFP+MCM2+ aNSCs (at D3), nor in Tbr2+ IPs (at D3, D6, and D10), nor in the astrocytic fate specification of regenerating NSPCs (at D10). The Itgb1-dependent, injury-induced proliferative expansion was driven in part by a comparative increase in the fraction of proliferating Dcx+ NBs in Itgb1 iKO animals. These results corroborate the homeostatic data and suggest that Itgb1 regulates SGZ regeneration following injury, in part by negatively regulating the density of proliferating DCX+ neuroblasts.

4.2.4 Itgb1 negatively regulates NSC activation after ECS.

Although AraC is of some biological relevance (it is used to treat some kinds of human cancers), I wished to understand whether Itgb1 regulates hippocampal neurogenesis in other biologically relevant paradigms. I first considered its role in regulating NSC activation following neuronal activity. AraC was a limited tool in this respect because it did not cause an obvious rebound expansion of the population of aNSC. I therefore turned to electroconvulsive shock (ECS, the analogue of human electroconvulsive therapy) to synchronise neuronal activity and induce SGZ NSC activation. [e.g., Ma et al. 2009]

My question was whether Itgb1 regulated NSC activation. Following earlier results my hypothesis was of negative regulation. As before, Itgb1 iKO and control animals were recombined at 8 weeks of age. Six weeks later I delivered a single electroconvulsive stimulus as reported in **Ch. 2.3**. Animals were returned to their cages, sacrificed two days later (D2 time-point, see **Figure 17A**). Brains were processed for immunofluorescence in floating sections as described in **Ch. 2.5** and **Ch. 2.6.** Between groups I compared the fraction of NesRFP+ cells that had a detectable radial process and which also expressed the proliferative marker MCM2 (signifying ‘aNSC’). To accurately identify radial processes I

analysed the z-stack without projection, scrolling up and down through the section to trace RFP+ radial processes precisely to an RFP+ cell body.

All data were normally distributed (all Shapiro-Wilk's test $p>0.05$) with homogeneity of variances (all Levene's test $p>0.05$). Inspection of box plots across each analysis identified three outliers (all in the control group). To examine whether these outliers might meaningfully affect results I ran a sensitivity analysis, first including them and then omitting them, and the results did not change. I therefore used unpaired t-tests to compare groups.

There were no statistically significant differences between groups in total RFP+ cell density, total MCM2+ proliferating cell density, and in MCM2+RFP-ve compartmental density. In control animals at D2 post-shock, as anticipated, ECS caused a greater proportion of NSC to be active (MCM2RFP/RFP Ctr=22.2% [SD=4.3]) compared to that expected under non-stimulated, physiological conditions (which would be approximately 5%). Remarkably however, Itgb1 iKO animals showed an even greater response (MCM2RFP/RFP iKO=31.7% [SD=2.3], $t(7)=3.924$, $p=0.006$) (**Figure 17 B-F**). These results suggested that Itgb1 negatively regulates NSC activation occurring in response to synchronous neuronal activity, in a cell-autonomous manner.

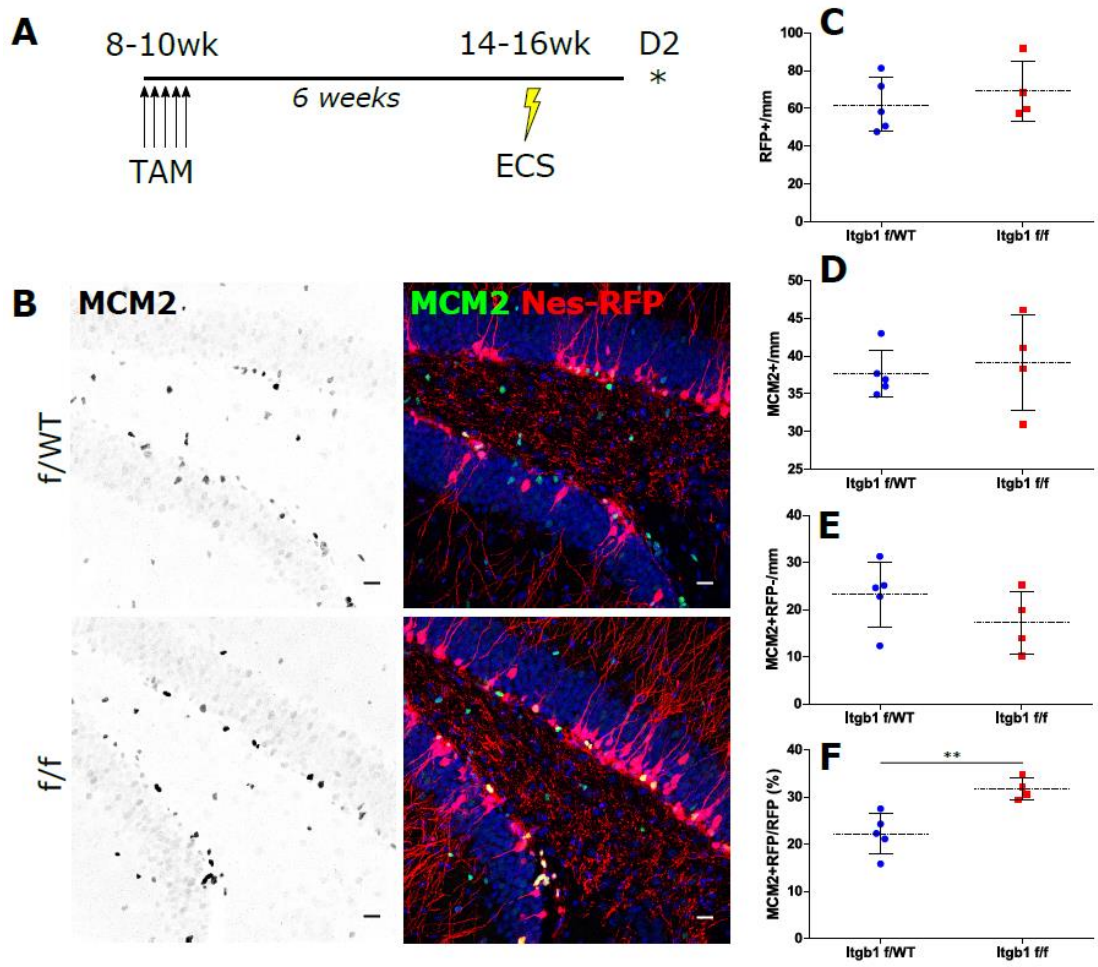

Figure 17. Itgb1 negatively regulates NSC activation after ECS.

A: Schematic for ECS following Itgb1 iKO. **B:** Representative images of activated NSCs at D2 post-ECS in control (upper panels) and iKO animals (lower panels). **C:** Quantification of RFP+ cell density at D2 post-ECS. **D:** Quantification of total MCM2+ cell density at D2 post-ECS. **E:** Quantification of MCM2+RFP- cell density at D2 post-ECS. **F:** Quantification of [B] showing increased Nestin+ stem cell (RGL) activation in Itgb1 iKO animals at D2 post-ECS. ** $p<0.01$; n=3-5 animals per group. ECS= Electroconvulsive shock group; SHAM= control (no shock) group. Scale bars= 20 microns.

4.2.5 Itgb1 regulates the dynamics of the ageing SGZ.

Given consistent data indicating a negative regulatory role, I next asked whether Itgb1 might regulate the normal age-related decline in neurogenesis observed in the SGZ of ageing mice. I hypothesised a negative regulatory role in line with earlier results.

To test this hypothesis, Itgb1 iKO and control animals were Tamoxifen- recombined at 8-10 weeks of age and maintained in their home cages without further intervention until they were one year old, then sacrificed (**Figure 18A**). Brains were processed for immunofluorescence on both slides and floating sections as described in **Ch. 2.5** and **Ch. 2.6**. I analysed total RFP+ cell density, total Ki67+ proliferating cell density, Ki67+RFP-ve proliferating cell density, the Ki67+RFP+/RFP fraction, and the Dcx+RFP+/RFP fraction. For all analyses except as stated below, data were normally distributed (Shapiro-Wilk's $p>0.05$), there was homogeneity of variances (Levene's test $p>0.05$), and there were no outliers as assessed by inspection of a boxplot. Data meeting these assumptions were analysed using an unpaired t-test. Data for the Ki67+RFP+/RFP fraction were normally distributed with homogenous variances, but there were two outliers in the control group. Sensitivity analysis including and then omitting these outliers (in unpaired t-tests) did alter the results, so I analysed these data using the Mann-Whitney U test. Frequency distributions were dissimilar as assessed by visual inspection, and therefore mean ranks are reported (not medians). Data for the Dcx+RFP+/RFP fraction were of unequal variance (Levene's test $p=0.025$), so this analysis was also conducted using the Mann-Whitney U test.

Compared to young adult mice (whose data are previously reported in **Figure 15**), both control and experimental aged mice showed a reduction in SGZ proliferation. There were no significant differences between experimental groups in total RFP+ cell density, total Ki67+ proliferating cell density, Ki67+RFP-ve proliferating cell density, or the Dcx+RFP+/RFP fraction (**Figure 18 C-D** and not shown). There was evidence of a statistically significant increase in cell-autonomous proliferation after Itgb1 iKO (control Ki67RFP/RFP mean rank=3.2; iKO mean rank=7.5, $U=19.000$, $z=2.205$, $p=0.032$) (**Figure 18F**). These results suggest that Itgb1 regulates the dynamics of the SGZ neurogenic niche in a cell-autonomous manner across the adult mammalian lifespan.

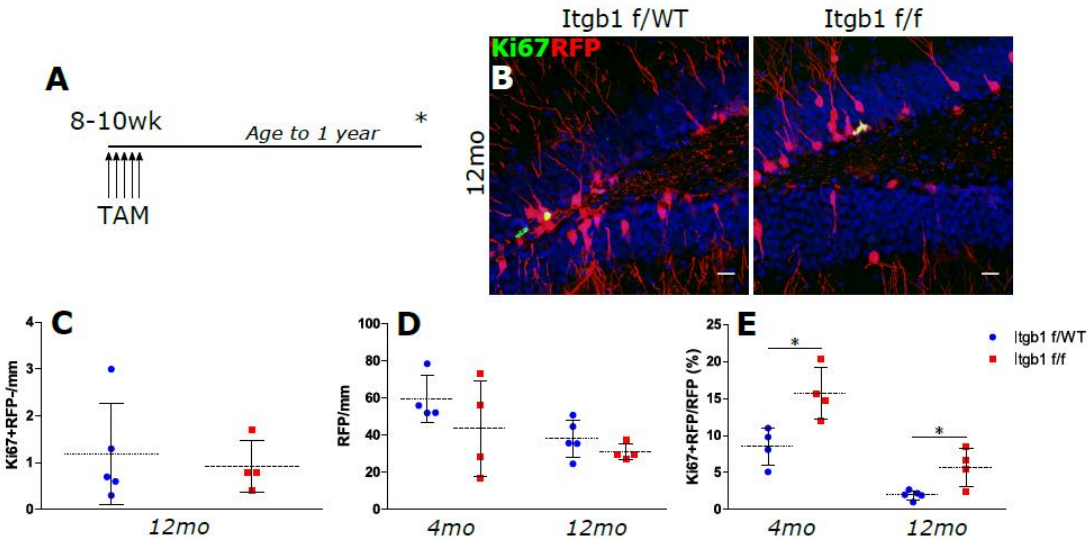

Figure 18. Itgb1 regulates the dynamics of the ageing SGZ.

A: Experimental schematic. **B:** Representative images of aged control (left panel) and Itgb1 iKO animals (right panel). Arrowheads indicate Ki67+RFP+ double-labelled cells. **C:** Quantification of Ki67+RFP- proliferating cell density in aged animals. **D:** Quantification of RFP+ cell density in aged animals. Data from homeostatic iKO animals sacrificed at 4 months of age (Fig 15G) is reproduced here for context. **E:** Quantification of cell-autonomous proliferation in aged animals, showing a persisting significant effect of Itgb1 iKO on SGZ proliferation. * $p<0.05$; n=4-5 animals per group. Mo= Months. Scale bars= 20 microns.

4.2.6 Proliferating NSPCs express Itgb3 after ECS and loss of Itgb1.

I wished to explore potential mechanisms for these surprising data. Because cancer cells - following lentiviral Itgb1 knockdown - may up-regulate integrin β3 (Itgb3) in association with trophic changes [Parvani et al. 2013], I explored the possibility that Itgb3 mediated the response to Itgb1 iKO.

First I asked whether Itgb3 was expressed in the wild-type SGZ. Adult wild-type animals (n=3) were sacrificed and processed for immunofluorescence on slides as described in **Ch. 2.5** and **Ch. 2.6**. Itgb3 was characterised in relation to its co-expression with Ascl1 (IPs) and Dcx (neuroblasts).

A total n=228 Itgb3+ cells in the SGZ were counted. The majority were DCX+ neuroblasts (mean=74.7% co-expressing Dcx [SD=7.7]). A small additional proportion were DCX-

negative Ascl1+ IPs (mean=2.1% co-expressing Ascl1 [SD=2.0]). Itgb3+ cells represented a subset of each NSPC type (mean=12.3% of DCX+ neuroblasts [SD=3.6] and 5.9% of DCX-negative Ascl1+ IPs [SD=6.9]). These data indicate that Itgb3 is expressed under homeostatic conditions, by a subset of NSPCs which are mainly neuroblasts.

Next I asked whether Itgb3 was up-regulated on NSPCs following Itgb1 iKO, under homeostatic conditions. Given that Itgb3 is expressed on Dcx+ neuroblasts and associated with proliferation, and that both these indices were increased following Itgb1 iKO, I hypothesised that Itgb3 would indeed be expressed preferentially on Itgb1 iKO NSPCs. To study this I re-analysed tissue from the experiment reported in **Ch. 4.2.2**. In that experiment 8-10 week-old $Itgb1^{f/WT}$ or $Itgb1^{f/f}$ animals had been recombined and subsequently sacrificed six weeks later ('homeostatic' iKO conditions). I conducted immunofluorescence on slides, comparing gene groups both on the density of RFP+ cells and the expression of Itgb3 on RFP+ NSPCs. These data were normally distributed (Shapiro-Wilk's $p>0.05$) with homogeneity of variances (Levene's test $p>0.05$), and there were no outliers as assessed by inspection of a box-plot. Data were therefore analysed using an unpaired t-test.

There was no significant difference between control and iKO animals in total RFP+ cell density. However Itgb1 iKO animals showed significantly higher proportional expression of Itgb3 on recombined cells (Control: mean Itgb3+RFP+/RFP=3.8% [SD=2.6]; iKO: mean Itgb3+RFP+/RFP=13.3% [SD=2.4], $t(6)=5.270$, $p=0.002$). This result suggested that Itgb3 is up-regulated on NSPCs lacking Itgb1 under homeostatic conditions. Qualitatively, but reflecting the wild-type state, many Itgb3+ cells in Itgb1 iKO animals were Dcx+ neuroblasts. Nearly all Itgb3+RFP cells, whether in control or iKO animals, expressed the proliferation marker MCM2 (**Fig 19A-D**).

To corroborate this I asked whether Itgb3 was up-regulated on NSPCs after Itgb1 iKO and following injury. To study this I analysed tissue remaining from the experiment reported in **Ch. 4.2.3**. In that experiment, 8-10 week-old $Itgb1^{f/WT}$ or $Itgb1^{f/f}$ animals had been recombined, followed for six weeks, and then underwent the AraC procedure. For the current analysis I examined solely the time-point of D10 post-AraC as the time-point of greatest differences in proliferation and neurogenesis between the groups. I conducted immunofluorescence on slides as described in **Ch. 2.5** and **Ch. 2.6**. I analysed the total density of RFP+ cells and their expression of Itgb3. For total density, data were normally distributed (Shapiro-Wilk's $p>0.05$) with homogeneity of variances (Levene's test $p>0.05$),

and there were no outliers as assessed by inspection of a box-plot. These data were analysed using an unpaired t-test. In iKO animals, data for the Itgb3+RFP+/RFP fraction were not normally distributed (Shapiro-Wilk's p=0.027) with inhomogeneity of variances (Levene's test p<0.001), so I analysed these data using the non-parametric Mann-Whitney U test. Visual inspection of the frequency distributions between groups showed a dissimilar shape, so mean ranks are reported rather than medians.

There was no significant difference in total RFP+ cell density between groups. However similar to the homeostatic state, the proportion of RFP+ NSPCs expressing Itgb3 was higher in iKO animals (Control: mean rank=3.5; iKO: mean rank=8.5, U=24.000, z=2.558, p=0.010). This result suggested that Itgb3 is up-regulated after injury on NSPCs lacking Itgb1.

To confirm that Itgb3 was up-regulated specifically on Itgb1-iKO cells, I analysed the same tissue with triple-channel immunofluorescence for RFP, Itgb1, and Itgb3. I reasoned that the critical analysis was of the proportion of RFP-positive, Itgb1-negative cells that expressed Itgb3. Data for this careful RFP+Itgb1-Itgb3+/RFP+Itgb1- analysis were not normally distributed in control animals (Shapiro-Wilk's p=0.015), with inhomogeneity of variances (Levene's test p<0.001), and therefore were analysed using the non-parametric Mann-Whitney U test. Visual inspection of the frequency distributions between groups showed a dissimilar shape, so mean ranks are reported.

The RFP+Itgb1-Itgb3+/RFP+Itgb1- proportion was significantly higher in iKO animals (Control: mean rank=3.5; iKO: mean rank=8.5, U=24.000, z=2.556, p=0.010), indicating that Itgb3 was indeed specifically up-regulated on Itgb1 iKO NSPCs (**Fig 19E**).

Finally, I asked whether SGZ Itgb3 expression could be dynamically regulated in animals with wild-type integrin alleles and under biologically relevant conditions. To study this I used tissue from 8-10 week-old $NesCre^{ERT2}$;$RFP^{f/f}$ animals who had been recombined and two weeks later had received a single ECS, or sham (as reported in **Ch. 2.3** and which provided the data for **Ch 3.2.4**). A further seven days later animals were sacrificed and processed for immunofluorescence on slides as described in **Ch. 2.5** and **Ch. 2.6**.

Itgb3 was characterised in relation to its co-expression with the proliferating marker MCM2. In analyses I compared Sham and ECS groups with regards to the total density of MCM2+

cells, the density of MCM2+Itgb3+ cells, and the MCM2+Itgb3+/MCM2+ proportion. I did not examine co-labelling with RFP. For each analysis, data were normally distributed (Shapiro-Wilk's test $p>0.05$) with homogeneity of variances (Levene's test $p>0.05$). There were three modest outliers across analyses as assessed by inspection of a boxplot. Sensitivity analysis (first including then omitting these outliers) showed no influence on results. They were therefore retained in the analysis with unpaired t-tests.

Technically replicating data reported previously in **Ch 3.2.4**, ECS caused a significant increase in the density of MCM2+ proliferating cells (Sham mean MCM2+ =15.2/mm [SD=2.4]; ECS mean MCM2+ =27.6/mm [SD=3.5], $t(8)=6.500$, $p<0.001$). Itgb3 co-localised with a subset of MCM2+ cells, and accordingly the density of Itgb3+MCM2+ cells was also significantly higher after ECS (Sham mean MCM2+Itgb3+ =4.5/mm [SD=1.4]; ECS mean MCM2+Itgb3+ =14.1/mm [SD=1.0], $t(8)=12.352$, $p<0.001$) (**Fig 19F**). To study whether this increase in Itgb3 expression was truly dynamic rather than a linear consequence of increased proliferation, I also analysed the proportion of proliferating cells expressing Itgb3 in each group. Importantly, ECS caused an increase in the relative proportion of proliferating cells expressing Itgb3 (Sham mean MCM2+Itgb3+/MCM2=29.1% [SD=7.2]; ECS mean MCM2+Itgb3+/MCM2=51.4% [SD=5.4], $t(8)=5.526$, $p=0.001$) (**Fig 19G**).

These data indicated that Itgb3 is expressed by almost 1/3 of proliferating SGZ cells in control animals, and that its expression within the proliferating SGZ population is dynamic, with an increase in proportional expression in association with increased proliferation and neurogenesis following ECS.

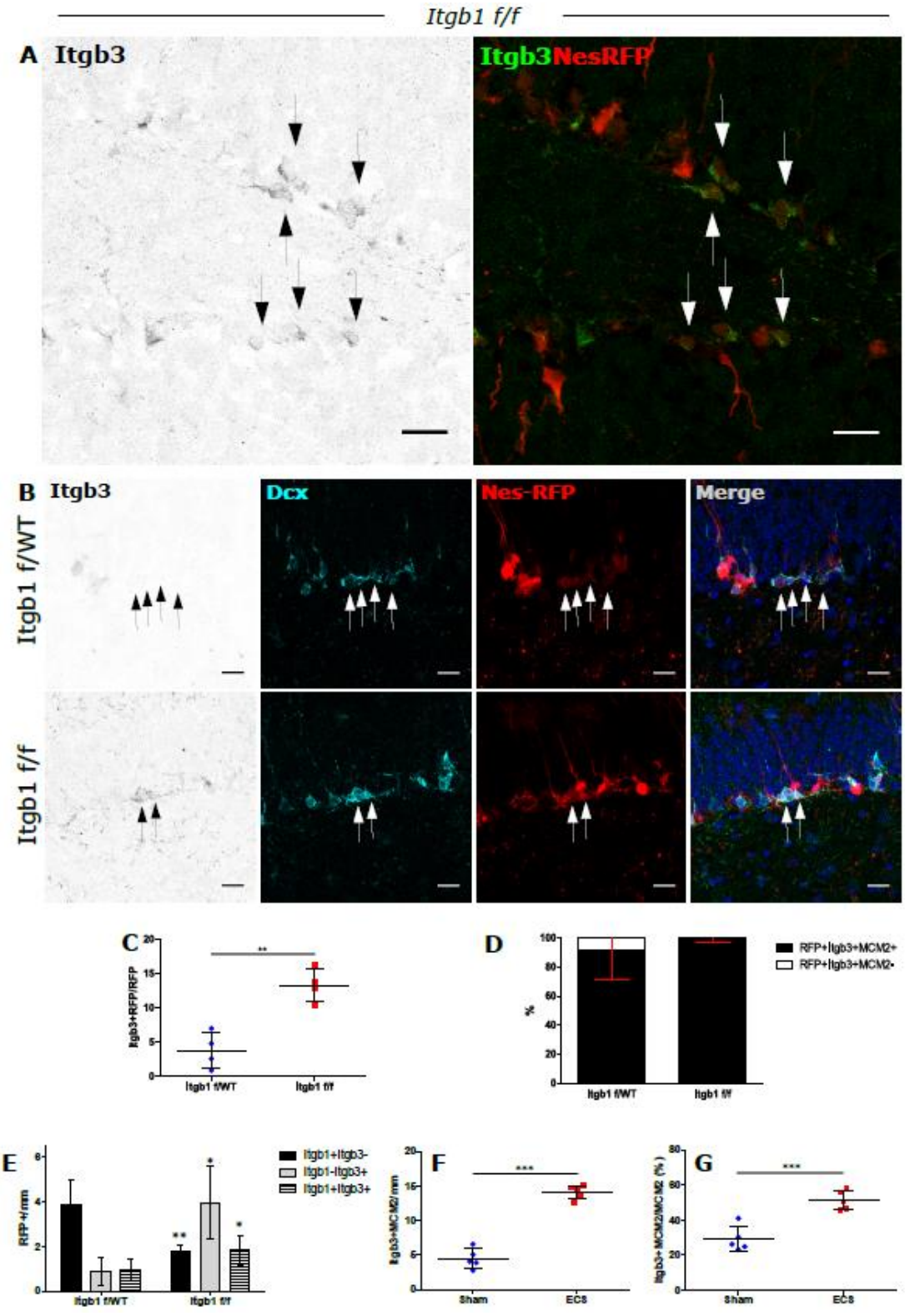
Itgb1 f/f
A Itgb3
Itgb3NesRFP
B Itgb3
Itgb1 f/WT
Itgb1 f/f
Dcx
Nes-RFP
Merge
C
Itgb3+RFP/RFP
Itgb1 f/WT
Itgb1 f/f
D
%
RFP+Itgb3+MCM2+
RFP+Itgb3+MCM2-
E
RFP+/mm
Itgb1+Itgb3-
Itgb1-Itgb3+
Itgb1+Itgb3+
F
Itgb3+MCM2/mm
Sham
ECS
G
Itgb3+MCM2/MCM2 (%)
Sham
ECS

Fig 19. Proliferating NSPCs dynamically express Itgb3. (from previous page)
A: Image of Itgb3 expression (arrows) on RFP+ NSPCs of Itgb1 iKO. **B:** Itgb3 expression is low in control SGZ (arrows, upper panels) but is increased on Dcx+ NBs in iKO mice (arrows, lower panels). **C:** Quantification of Itgb3 expression after homeostatic Itgb1 iKO. **D:** Itgb3 expression associates strongly with MCM2+ proliferation independently of genotype. **E:** Control and experimental density of RFP+ cells positive for Itgb1, Itgb3, or both. Note marked upregulation of Itgb3 on Itgb1-null cells in iKO mice. **F:** G: Quantification of Itgb3+ proliferating cell density after ECS. **G:** Quantification of proportional Itgb3 expression on proliferating cells after ECS. Note basal level of homeostatic Itgb3 expression in control mice with intact Itgb1 alleles. * $p<0.05$; ** $p<0.01$; *** $p<0.001$. n=4-6 animals per group. Scale bars: 20 microns.

Taken together these experiments suggest that Itgb3 is expressed in the homeostatic SGZ by a subset of proliferating neuroblasts. Following Itgb1 iKO, NSPCs lacking Itgb1 up-regulate Itgb3 in a cell-autonomous manner and in association with increased proliferation and neurogenesis. However in animals with intact Itgb1 alleles and following electroconvulsive shock, NSPCs nonetheless retain the ability to dynamically increase their proportional expression of Itgb3, again in association with increased proliferation and neurogenesis.

4.3 Discussion

In this Chapter I set out to study the role of a major ECM receptor, Integrin β1, in regulating hippocampal neurogenesis. I found that Itgb1 is expressed by subpopulations of NSPCs that are in cell cycle. Inducible knockout of the Itgb1 gene caused a cell-autonomous increase in the NSPC proliferative fraction and/or expansion of the neuroblast lineage. This effect was consistent across experimental conditions of homeostasis, injury, synchronous neuronal stimulation, and ageing. Seeking to explain this mechanistically, I uncovered a capacity for dynamic up-regulation of Integrin β3 in Itgb1 iKO NSPCs, and separately following electroconvulsive shock in animals with intact Itgb1 alleles, suggesting that adult NSPCs retain the capability to regulate integrin β sub-unit expression regardless of Itgb1 gene status. This capacity makes it difficult, at this stage, to draw direct conclusions about the function of Itgb1 in adult neurogenesis (see below). It raises the wider possibility that the ECM may interact differentially and dynamically with cell-surface integrin receptors to regulate adult neurogenesis.

4.3.1 Limitations

Before interpreting these results some limitations should be considered. First, although I was able to show loss of Itgb1 protein in recombined NSPCs (see **Figure 15B**), I did not sequence recombined cells to confirm that genetic excision was restricted to the Itgb1 locus. The mouse genome is thought to harbour 'pseudo-LoxP' sequences sufficiently similar to the LoxP allele to undergo Cre-mediated recombination. [Thyagarajan et al. 2000] These sequences remain largely cryptic and I cannot exclude the possibility that unknown 'off-target' genetic changes may have contributed to the phenotype.

Second, because the floxed Itgb1 locus and the floxed RFP locus were on separately-bred alleles rather than on a single allele, it is possible that some NSPCs expressed RFP without loss of Itgb1 and vice versa. The RFP reporter allele used in my experiments is thought to be relatively sensitive [Liu et al. 2013], so the former situation (RFP expression with retained Itgb1 gene function) may have been more likely in the current study. Such non-parallel recombination may explain why not all RFP+ cells showed loss of Itgb1 protein on immunofluorescence. The consequence for analysis would presumably be to dilute the effects of Itgb1 knockout, lowering power.

Third, expression of CreERT2 recombinase may have affected NSPCs in both control and experimental groups to behave in a non-physiological manner. I considered examining NSPC proliferation and differentiation in CreERT2 controls but the proportional mode of reporting results, which is a sensitive way to detect subtle cell-autonomous effects in NSPC subpopulations, cannot be conducted in CreERT2-negative mice that will not express Nes-RFP.

These three limitations seem inherent to mammalian Cre-loxP systems. I think in general they show the need for caution when appraising any study of this kind. Other limitations are potentially inherent to any study using immunofluorescence. These include: fourth, the question of specificity of primary antibodies. The best way of testing specificity is either to stain null tissue, or (if the primary is a monoclonal antibody) to incubate it beforehand with a blocking peptide. In either case, the staining that disappears can be considered specific. The antibody to Itgb1 showed reduced staining on Itgb1-iKO cells but - strikingly - not on directly adjacent blood vessels, suggesting that it did indeed label Itgb1 on NSPCs. However I have been unable yet to test the specificity of the polyclonal antibody to Itgb3. Standard

positive and negative immunofluorescent controls showed good staining in tissues known to highly express Itgb3 (spleen and bladder, data not shown), with a lack of non-specific staining of the secondary antibody in the same, but null tissue will be required to test the specificity of the signal to Itgb3 (see **Ch. 6**).

As well as these technical limitations there are two further scientific caveats. The first is that I used male and female transgenic mice in my experiments. This was necessary with a modest breeding rate, three transgenes, and multiple experimental time-points. However male and female mice are reported to differ in the half-life of Itgb1 protein in the dentate gyrus after recombination. [Brooker et al. 2016] Although I chose a baseline time- point six weeks after recombination, which should be long enough to ensure protein down-regulation in both sexes, it is possible that the functional role of Itgb1 also differs. With inconsistent and insufficient numbers of both sexes in both groups I was unable to examine this question statistically. Lastly, setting baseline at six weeks post-recombination is longer than previously used [Robel et al. 2009, Brooker et al. 2016]; a baseline perhaps at three weeks may in retrospect have made comparison with earlier studies easier.

4.3.2 Results in context

4.3.2.1 Comparison with similar studies

The expression pattern of Itgb1 in adult hippocampal NSPC subpopulations has not been deeply studied. Brooker et al. recently found it to be expressed by Sox2+ or MCM2+ NSPCs, and not by the (likely postmitotic) majority of DCX+ NBs. [Brooker et al. 2016] Their data are consistent with my more detailed breakdown of Itgb1 expression in proliferating aNSC, IPs and early NBs. Brooker et al. found Itgb1 to colocalise with Nes+GFAP+ radial processes of quiescent NSCs, whereas I omitted GFAP following technical concerns and found no Itgb1 staining on quiescent Nes+ NSCs. Nonetheless our studies concur on Itgb1 expression by NSPCs which are in cell cycle. This conclusion is supported by immunofluorescent [Kazanis et al. 2010] and single cell sequencing [Llorens-Bobadilla 2015] data which suggest that Itgb1 is up-regulated upon NSC activation in the adult mouse SEZ.

Brooker et al. also studied the function of Itgb1 in the adult dentate gyrus, using lentiviral Cre injection to Rosa-YFP mice homozygous for the floxed allele of Itgb1. They reported significant disruption of the structural integrity of the dentate gyrus, with striking loss of the

usual laminar division between hilus, GCL, and ML. These profound architectural distortions were associated with increased proliferation. The proliferating cells were mostly YFP negative, suggesting a non cell-autonomous effect of Itgb1 KO, which also markedly reduced the number of Dcx+ neuroblasts in the DG. Finally Brooker et al. reported an increased proportion of recombined cells expressing the astrocytic markers GFAP+, ALDH1L1, and S100B. They concluded that Itgb1 functioned to restrain astrocytic differentiation in a cell-autonomous manner. My results, by contrast, suggest a cell-autonomous effect of Itgb1 in regulating proliferation, an increase in Dcx+ neuroblasts, and no effect on astrocytic differentiation.

A partial explanation for the conflicting results may lie in technical differences between studies. The current study is the first to restrict Itgb1 iKO in the SGZ specifically to NSCs. Brooker et al. achieved Itgb1 iKO by lentiviral Cre injection, demonstrating convincingly that widespread Itgb1 loss significantly disrupts adult brain tissue. I am unsure as to what extent the rest of their findings could have been influenced by such unusual architectural disruption. Analyses for which interpretation depended on localising cells to the subgranular zone - such as attributing NSPC identity to proliferating cells - were potentially compromised. The cell populations in which Itgb1 might serve to constrain neighbouring proliferation in the hippocampus therefore remained unclear. Additionally many components of the niche may regulate neurogenesis [Ehret et al. 2015, Ottone et al. 2014, Ashton et al. 2012, Sierra 2010] and their functions in this respect may have been affected by profound alterations in the 3D microenvironment.

Their suggestion of a role for Itgb1 in regulating astrocytic cell fate decisions in the adult hippocampus was more convincing. However the specificity of this to NSPCs was questionable. Conditional Itgb1 deletion in non-neurogenic GFAP+ astrocytes has been found to cause reactive gliosis [Robel et al. 2009] so the possibility remains that Brooker et al. observed the same phenomenon localised to the hippocampus. The reduction in DCX+ neuroblast density could meanwhile be explained by loss of adhesion and niche disruption causing increased cell death. A critical cell-autonomous role for Itgb1 in mediating NSC fate may not be the only explanation for their results. Overall though, the study by Brooker et al. is difficult to compare directly to the present study, which used a precise RGL-specific manipulation and did not cause detectable architectural disruption.

Others investigated a role for Itgb1 in adult hippocampal neurogenesis indirectly. Integrin-

linked kinase (ILK) is a component of the canonical Itgb1 intracellular signalling pathway. [Hannigan 1996] Porcheri et al. studied the functional role of ILK in hippocampal neurogenesis. [Porcheri et al. 2014] Nestin-CreER^{T2};R26YFP;ILK iKO animals displayed more SGZ proliferation, and proportionally more YFP-labelled GFAP+Sox2+ cells and Ascl1+ IPs. The proportion of YFP+Dcx+ neuroblasts was significantly decreased. These results suggested that ILK, and possibly by extension the integrin family, regulates proliferation and NSPC dynamics in the adult hippocampus. The authors did not seek to determine which of the NSPC subpopulations contributed to the increase in proliferation.

I think that identifying the proliferating NSPC subpopulation could have been helpful for interpreting ILK function. For example, if GFAP+Sox2+ cells contributed significantly to the proliferating population, it could suggest that ILK regulates NSC maintenance, or possibly astrocytic fate specification. [Brooker et al. 2016, North et al. 2014, Robel et al. 2009] A highly proliferative Ascl1+ fraction could suggest either that ILK mediates proliferation of RGLs [Andersen 2014] or alternatively of IPs. Or the function of ILK could be to simultaneously regulate (negatively) the proliferation and (positively) the survival of NBs. Porcheri et al. therefore suggested that ILK negatively regulates proliferation in the SGZ, but at what stage of neurogenesis remained unclear.

Porcheri et al. asserted that their observed phenotype was “integrin-dependent”, but as an experimental strategy to understand the role of Itgb1 in adult neurogenesis, ILK deletion is limited. ILK does have a canonical role transducing Itgb1 signalling but can also be stimulated by, for instance, Itgb3 and Itgb5 [Hannigan et al. 1996], BDNF [Xu et al. 2015], sonic hedgehog [Barakat et al. 2013], and VEGF. [Kaneko et al. 2004] ILK is a promiscuous signal transducer of multiple upstream receptor pathways, some of which may be independent of Itgb1. Consequently while Porcheri et al. uncovered potential matrix-cell interactions in adult neurogenesis, the precise functional role of Itgb1 remained unclear.

Taken together the studies by Brooker et al. and Porcheri et al. began to unpick the functional role of ECM-derived signalling in the regulation of adult hippocampal neurogenesis. Directly comparing their results is difficult. Nonetheless despite significant methodological differences some general trends could be tentatively identified. These hints converged on the finding that Itgb1 and ILK may negatively regulate proliferation in the adult hippocampus. Whether in a cell autonomous or non-autonomous manner remained unclear, as did the identity of the proliferating cells. Both suggested too that intact ECM-

derived signalling normally contributes to maintain neuroblast density. Finally, both papers were to some extent compromised by a lack of specificity: Porcheri et al. in terms of proving specificity to Itgb1, Brooker et al. in terms of proving specificity of results to the undisrupted niche.

My results go some way towards addressing these gaps. A highly specific Itgb1 knockout strategy corroborated the suggestion of increased NSPC proliferation in the mutant SGZ, and suggested that this is a cell-autonomous effect, unexpectedly advancing Dcx+ NBs as a contributory NSPC subpopulation.

4.3.2.2 Proliferation and the question of Itgb3

The effect of Itgb1 iKO on NSPC proliferation deserves a little further thought. From previous in vitro studies of the role of Itgb1 in NSCs (and without the benefit of the papers by Porcheri et al. and Brooker et al., which were only published after I had started experiments) I had predicted that it would function biologically to promote NSPC turnover. An increase in proliferation after Itgb1 loss - the opposite result - was surprising.

In fact there was already a contrary signal in the adult CNS. Kazanis and colleagues, following Shen et al., had also reported increased NSPC proliferation in the adult SEZ after i.c.v. infusion of an Itgb1 blocking antibody. [Kazanis et al. 2010, Shen et al. 2008] Like Brooker et al, this manoeuvre disrupted niche architecture and made the result difficult to interpret. However adding the NSC-specific manipulations of Porcheri et al., and now my own experiments, I would tentatively identify a consensus. Indeed two further very recent reports propose a similar negative regulatory effect of Itgb1 on proliferation in regenerating planaria. [Seebeck et al. 2017, Bonar et al. 2017] We have, in other words, consistently observed in vivo the opposite effect on proliferation to that predicted from many experiments conducted in vitro. What is going on?

One explanation may be compensatory upregulation of different integrin β subunit(s) in vivo. In my experiments, NSPCs lacking Itgb1 showed a greater Itgb3 immunofluorescent signal than controls. A small number of prior studies have reported similar upregulation of one β subunit to compensate for loss of another [Parvani 2014, Li 2010], but in general this effect appears to have been scarcely studied. At present my data on this point are associative. However they raise the possibility that ECM might interact differentially and dynamically

with cell-surface integrin receptors to regulate adult neurogenesis (see **Ch. 6**). Importantly I was able to show Itgb3 protein expression on a subset of NSPCs under homeostatic conditions in WT mice, and its dynamic regulation in mice with intact Itgb1 alleles following electroconvulsive shock. These latter data suggest that dynamic Itgb3 upregulation is not a simple 'technical artefact' of Itgb1 iKO, but rather an inherent capability of adult SGZ NSPCs.

4.4 Chapter Summary

In summary, in this Chapter I asked whether integrin β1 regulates hippocampal neurogenesis. I undertook a highly specific knockout of Itgb1 in SGZ NSCs in various experimental conditions including homeostasis and injury. Results suggest that integrin signaling regulates multiple aspects of adult hippocampal neurogenesis, including proliferation and neural differentiation. The precise contributory role of Itgb1 remains unclear, with experiments ongoing to confirm whether Itgb3 is indeed up-regulated as preliminary data suggest.

In the next Chapter I turn from a candidate approach to studying matrix signalling and adult neurogenesis, to a candidate-free approach.

5 ENDOTHELIAL CELL-DERIVED MATRIX GLA PROTEIN IS A POTENTIAL NOVEL REGULATOR OF STEM CELL ACTIVATION

5.1 Introduction

In **Chapter 1** I reviewed the extent of published literature on the instructive role of extracellular matrix (ECM) in neural stem cell biology. Excepting laminin, fibronectin, and collagen - which are widely used as technical substrates for experiments in vitro - there was in general a marked lack of understanding of how the ECM contributes to the regulation of NSCs at any developmental stage. In my search of 274 "Core Matrisome" genes only around 10% had been the subject of more than one publication, and approximately 80% had not been studied at all. It follows that the potential role of extracellular matrix in regulating NSCs in the adult hippocampus remains poorly understood. Only a small group of ECM genes as discussed in **Ch. 1** have been the subject of manipulation in the adult brain.

These studies, my own included, have generally been hypothesis-led. A distinct but complementary framework, however, is to take a hypothesis-free approach. A study of this nature would seek to 'screen' the neurogenic niche in an unbiased way as possible, thereby identifying candidate ECM genes that may influence adult neurogenesis. Such a screen would ideally cover distinct biological stages of adult neurogenesis in order to provide a more fine-grained analysis of the possible role of ECM in regulating different NSPC subpopulations.

In **Chapter 3** I also reported the results of experiments to optimise the AraC procedure. My conclusion was that AraC infusion effectively 're-boots' neurogenesis, triggering a temporally predictable regenerative neurogenesis. I realised that the sequential recovery of NSPC subpopulations following ablation by AraC - aNSC by D3, IPs by D6 - provides a model to study ECM gene expression in sequential stages of hippocampal neurogenesis in a hypothesis-free manner.

In the current Chapter I set out to identify novel ECM genes that are differentially expressed during the stages of neural stem cell activation and IP proliferation. I used laser capture microdissection to isolate the adult SGZ niche at three time-points following AraC. I extracted high-quality RNA and had the transcriptome sequenced. Bioinformatic analysis generated a list of novel ECM candidate regulators, from which I selected Matrix Gla protein

(Mgp) for further study. I used fluorescent in situ hybridisation first to validate the bioinformatic analysis and then to localise Mgp expression to the cerebral microvasculature. These experiments led me to the hypothesis that Mgp is expressed by endothelial cells in the SGZ and speculatively - through its function as a Bone Morphogenetic Protein (BMP) inhibiter - may regulate the balance of adult neural stem cell quiescence and activation.

5.2 Results

5.2.1 Microdissection of the SGZ niche yields high quality RNA

In this group of experiments, I began by asking whether it was possible to extract sequencing-quality RNA from the adult subgranular zone at key time-points of regeneration following AraC. The experimental design is shown schematically in **Figure 20A**. In brief, 10-12 week-old male C57Bl/6 mice received the AraC procedure as outlined in **Ch. 2.2**. Following a six-day infusion and mini-pump removal, animals were then sacrificed by cervical dislocation at: D1 (AraC n=4, Saline n=4); D3 (AraC n=4); and D6 (AraC n=4). Their brains were bisected sagittally, with operated hemispheres processed for immunofluorescence as described in **Chs. 2.4 - 2.6**. I analysed SGZ proliferating MCM2+ cell density from the operated hemisphere to verify that the AraC procedure had worked. To this end I first compared AraC- versus Saline-treated animals at D1 to confirm a significant reduction in NSPC proliferation. Data from these animals were normally distributed (Shapiro-Wilk's $p > 0.05$), with no outliers as assessed by inspection of a box-plot, and homogeneity of variances (Levene's test $p > 0.05$). They were therefore analysed using an independent samples t-test. I then analysed AraC-treated animals across D1, D3, and D6 to confirm rebound proliferation in these animals. Their data were normally distributed (Shapiro-Wilk's $p > 0.05$), with no outliers as assessed by inspection of a box-plot, but with inhomogeneous variances (Levene's test $p = 0.034$). They were therefore analysed using Welch's ANOVA.

AraC caused a significant reduction in MCM2+ proliferating cell density of the operated hemispheres (mean Sal D1 MCM2=23.9/mm, Ara D1=9.1/mm; $t(6)=4.130$, $p=0.006$). There was then a significant rebound proliferation over time (mean Ara D1 MCM2=9.1/mm, Ara D3=34.1/mm, Ara D6=53.3/mm; Welch's $F[2,5.457]=26.519$, $p=0.002$). Therefore as anticipated, AraC effectively ablated proliferating NSPCs, followed by regeneration during the follow-up period (**Figure 20B-C**).

Meanwhile, non-operated hemispheres of the same animals were rapidly frozen on liquid nitrogen, and processed for laser capture microdissection / RNA extraction as described in detail in **Ch. 2.4.** To ensure the best balance of yield and quality I ran a preliminary comparative experiment of four different RNA extraction kits (FFPE [Quiagen 73504], Microkit [Quiagen 74004], miRNeasy FFPE [Quiagen 217504], and Masterpure [MCR85102]).

These steps established that the Quiagen FFPE kit gave the best balance of RNA yield and integrity (**Figure 20D-G**). I therefore used it to extract RNA of sufficient quality from laser-microdissected SGZ (n=16 animals, RIN=7.2-8.7, mean=8.2) for downstream sequencing (**Table 8**).

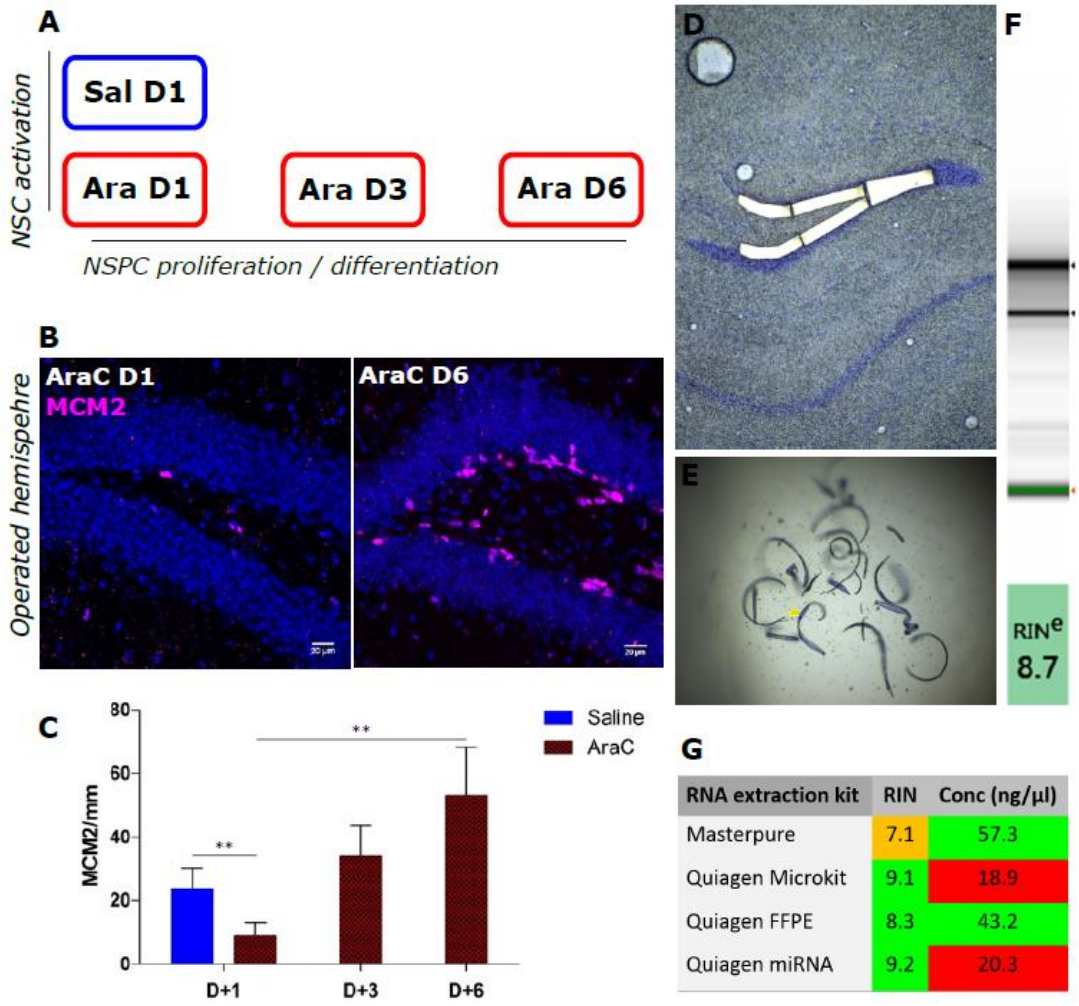

RNA extraction kit	RIN	Conc (ng/µl)
Masterpure	7.1	57.3
Quiagen Microkit	9.1	18.9
Quiagen FFPE	8.3	43.2
Quiagen miRNA	9.2	20.3

Figure 20. Laser capture microdissection of the SGZ niche yields high quality RNA.

A: Experimental schematic. **B:** Representative images of the ipsilateral (operated) hemisphere confirming the effectiveness of ablation of proliferating MCM2+ NPSCs at D1 after AraC (left panel) and the subsequent rebound proliferation at D6 (right panel). **C:** Quantification of (B). **D:** Representative image of contralateral (non-operated) hemisphere on the laser capture stage, illustrating the specificity of microdissection to the SGZ. **E:** Illustrative image of microdissected tissue in the collection cap. **F:** Sample RNA gel electrophoresis. Note distinct 18S and 28S ribosomal RNA peaks indicating a low level of RNA degradation. **G:** RIN and RNA yield obtained from four different RNA extraction kits. Note the best balance of integrity and yield from the FFPE kit. ** $p<0.01$; ** $p<0.001$; n=4 animals per group. Scale bars= 20 microns.

Label/Name	Microlitres	Concentration (ng)	Total RNA (ng/µl)	RIN
Ara_D1_1	10	0.95	9.5	7.4
Sal_D1_1	9	1.5	13.5	8.6
Ara_D3_1	9	1.1	9.9	8.6
Ara_D1_2	9	1.5	13.5	8.7
Ara_D6_1	5	2.4	12	8.4
Ara_D1_3	9	2.6	23.4	8.5
Ara_D6_2	9	1.6	14.4	8.5
Sal_D1_2	9	1.4	12.6	8.6
Ara_D6_3	9	1.2	10.8	7.3
Sal_D1_3	9	1.8	16.2	8.3
Ara_D1_4	8	2.8	22.4	8.5
Ara_D3_2	9	1.6	14.4	7.2
Sal_D1_4	9	1.9	17.1	8.4
Ara_D3_3	8	1.9	15.2	8.3
Ara_D3_4	9	1.9	17.1	8.0
Ara_D6_4	8	1.6	12.8	7.4

Table 8: RNA quantities and RIN.

5.2.2 AraC reveals molecular signatures of neurogenesis

Next, I asked whether there was any evidence of differentially-expressed SGZ genes in association with the ablation and regeneration of NSPCs. RNA sequencing and bioinformatic analysis were conducted as described in **Ch. 2.7** and **Ch. 2.8**, and as outlined in **Figure 21** and **Table 9**. Multiple testing corrections were made in EdgeR using the Benjamini-Hochberg method.

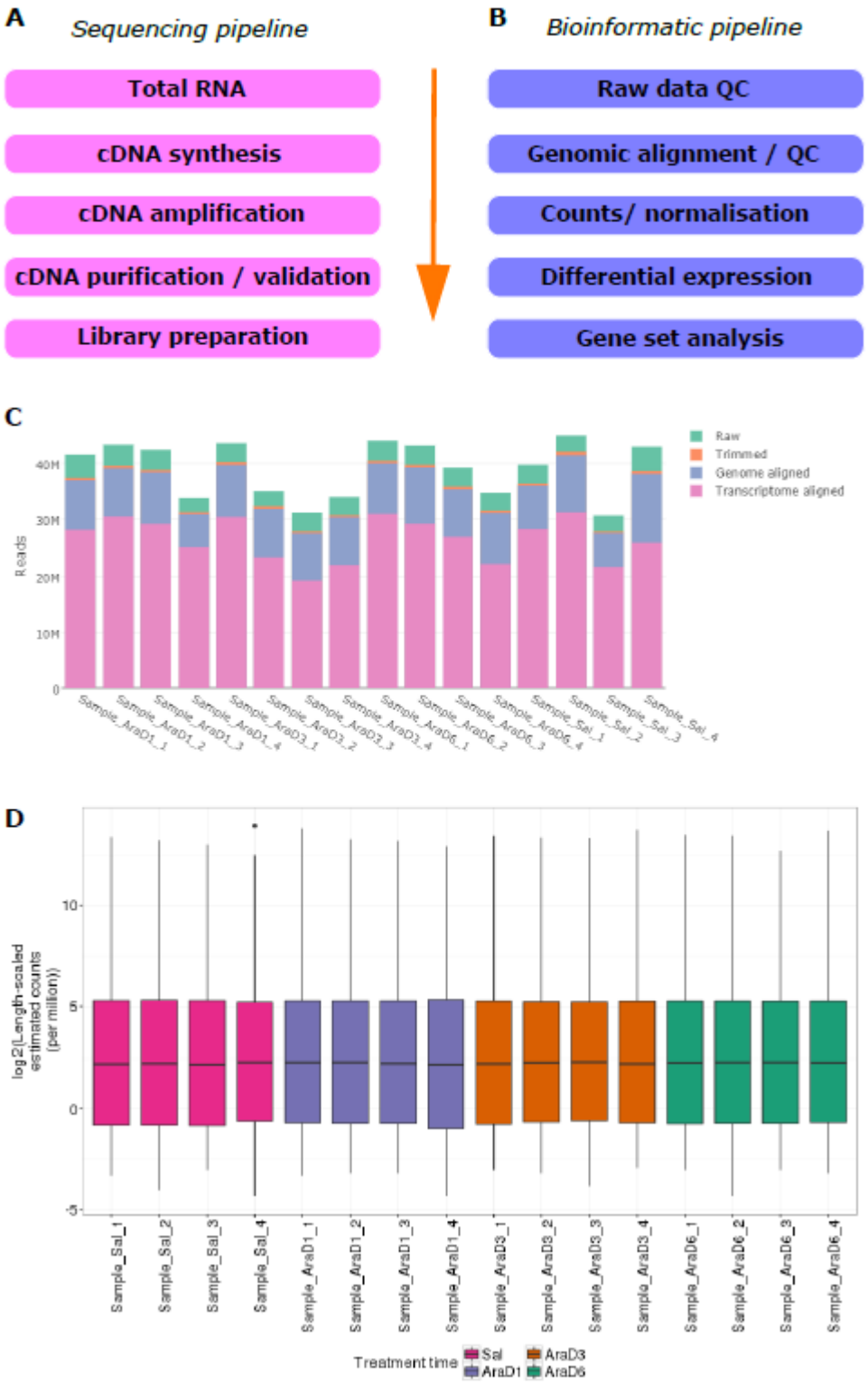

Figure 21. RNA sequencing / bioinformatic analysis pipelines and QC.

A: RNA sequencing pipeline. **B:** Bioinformatic pipeline. **C:** Read attrition plot for individual samples. D: Quartile plots of normalized read data.

Sample name	Treatment/time	Rep	Flowcell	Lane
Sample_Sal_1	SalD1	1	FC2015_101	7
Sample_Sal_2	SalD1	2	FC2015_103	7
Sample_Sal_3	SalD1	3	FC2015_103	8
Sample_Sal_4	SalD1	4	FC2015_103	7
Sample_AraD1_1	AraD1	1	FC2015_103	8
Sample_AraD1_2	AraD1	2	FC2015_101	7
Sample_AraD1_3	AraD1	3	FC2015_101	7
Sample_AraD1_4	AraD1	4	FC2015_103	7
Sample_AraD3_1	AraD3	1	FC2015_101	7
Sample_AraD3_2	AraD3	2	FC2015_103	8
Sample_AraD3_3	AraD3	3	FC2015_103	7
Sample_AraD3_4	AraD3	4	FC2015_103	8
Sample_AraD6_1	AraD6	1	FC2015_101	7
Sample_AraD6_2	AraD6	2	FC2015_103	7
Sample_AraD6_3	AraD6	3	FC2015_103	8
Sample_AraD6_4	AraD6	4	FC2015_103	8

Table 9. RNA sequencing experimental metadata.

A mean trimmed read depth of 35.6M (range 27.7M-42.1M) was achieved, with 98.7% aligned to the genome and 74.4% to the transcriptome (**Table 10**). Using Principal Components Analysis (PCA), PCA association matrices, and cluster dendrograms, I conducted three initial comparisons of the data: 1) the entire dataset; 2) Saline day 1 (SalD1) versus AraC day 1 (AraD1); and 3) AraD1 versus AraD3 versus AraD6.

Sample name	Raw	Trimmed	Genome aligned	Transcriptome aligned
Sample_Sal_1	39779589	36362014	35970827	28225828
Sample_Sal_2	45003898	42102398	41407651	31235111
Sample_Sal_3	30636258	27751041	27454802	21682121
Sample_Sal_4	43051391	38594686	38055026	26133543
Sample_AraD1_1	41541920	37450602	37009920	28091833
Sample_AraD1_2	43336807	39588587	39125332	30433618
Sample_AraD1_3	42459133	38795384	38363589	29202831
Sample_AraD1_4	33798734	31271994	30907155	25295760
Sample_AraD3_1	43548478	40281888	39744576	30354329
Sample_AraD3_2	35093761	32302146	31879094	23509433
Sample_AraD3_3	31180459	27777187	27419742	19269496
Sample_AraD3_4	33985772	30677115	30321491	22012181
Sample_AraD6_1	44024916	40531782	40062985	30942828
Sample_AraD6_2	43260728	39755723	39281583	29233713
Sample_AraD6_3	39231163	35795972	35296742	26916698
Sample_AraD6_4	34778354	31549289	31121908	22228654
MEAN VALUE	**39044460**	**35661738**	**35213901**	**26547999**

Table 10. RNA sequencing bioinformatic read report.

For the entire dataset (see **Figure 22 A'-A'''**) PCA revealed a modest treatment effect size of 12.3% and a trend to statistical significance (p=0.059). Consistent with this the PCA plot did not show a clear distinction between groups, and the cluster dendrogram suggested the presence of factors in the data that were independent of experimental group. For the comparison between SalD1 and AraD1 (see **Figure 22 B'-B'''**), the PCA plot showed a clear distinction between groups with a stronger treatment effect size of 20.4% (p=0.009). For the third comparison (see **Figure 22 C'-C'''**), the PCA plot showed a clear distinction between AraD1 and the later time-points. The association matrix showed that treatment phase (early vs late) was the strongest explanatory variable in the data (effect size 23.2%, p=0.059). The variables of replicate, flowcell, and/or flowcell lane also contributed consistently to variance in the data, but to a lower extent than the variables of interest.

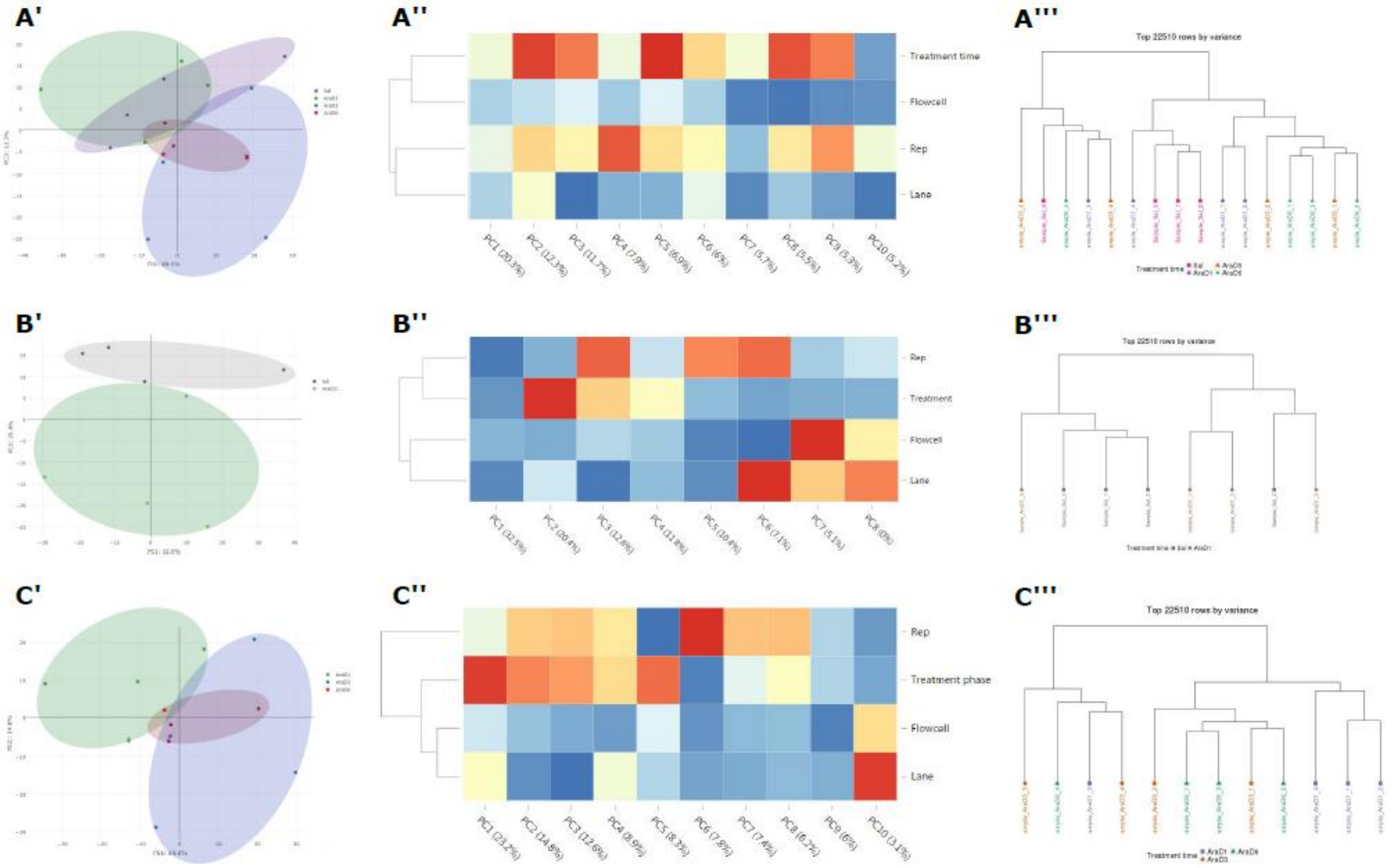
A'
A''
A'''
Treatment time
Flowcell
Rep
Lane
PC1 (20.3%)
PC2 (12.3%)
PC3 (11.7%)
PC4 (7.9%)
PC5 (6.9%)
PC6 (6%)
PC7 (5.7%)
PC8 (5.5%)
PC9 (5.3%)
PC10 (5.2%)
Top 22510 rows by variance
B'
B''
B'''
Rep
Treatment
Flowcell
Lane
PC1 (32.5%)
PC2 (20.4%)
PC3 (12.6%)
PC4 (11.8%)
PC5 (10.4%)
PC6 (7.1%)
PC7 (5.1%)
PC8 (0%)
Top 22510 rows by variance
C'
C''
C'''
Rep
Treatment phase
Flowcell
Lane
PC1 (23.2%)
PC2 (14.6%)
PC3 (12.6%)
PC4 (8.9%)
PC5 (8.3%)
PC6 (7.8%)
PC7 (7.4%)
PC8 (6.2%)
PC9 (6%)
PC10 (3.1%)
Top 22510 rows by variance

Figure 22. PCA, association matrices, and cluster dendrograms. (from previous page) For each row '= PCA plot; ''= PCA association matrix; '''= cluster dendrogram. **A'-A''':** The whole dataset. **B'-B''':** SalD1 vs AraD1. **C'-C''':** AraD1 vs AraD3 vs AraD6.

Before proceeding with further analysis I sought to confirm that transcriptional signals of regenerative neurogenesis were represented in the whole data. To do this I constructed a list of genes with a known function in hippocampal neurogenesis. A heatmap of these selected genes showed clear clustering of treatment group over time **(Figure 23)**. Three groups can be discerned in the data shown in this figure. Saline-treated controls expressed high levels of genes with known roles in NSC maintenance such as Hes5, Id1, FoxO3, and Pax6. At D1 post-AraC, these same genes were markedly down-regulated indicating transcriptional activation of NSCs. Meanwhile at D3 and D6 genes critical to neurogenesis such as Ascl1, Tbr2 and Neurog2 were up-regulated together with markers of cell cycle. This analysis established that AraC could be used to study molecular signatures of regenerative neurogenesis. The pattern suggested that transcriptional signals of NSC activation can be detected as soon as D1 following AraC, with no clear transcriptional distinction between D3 and D6 for the selected genes.

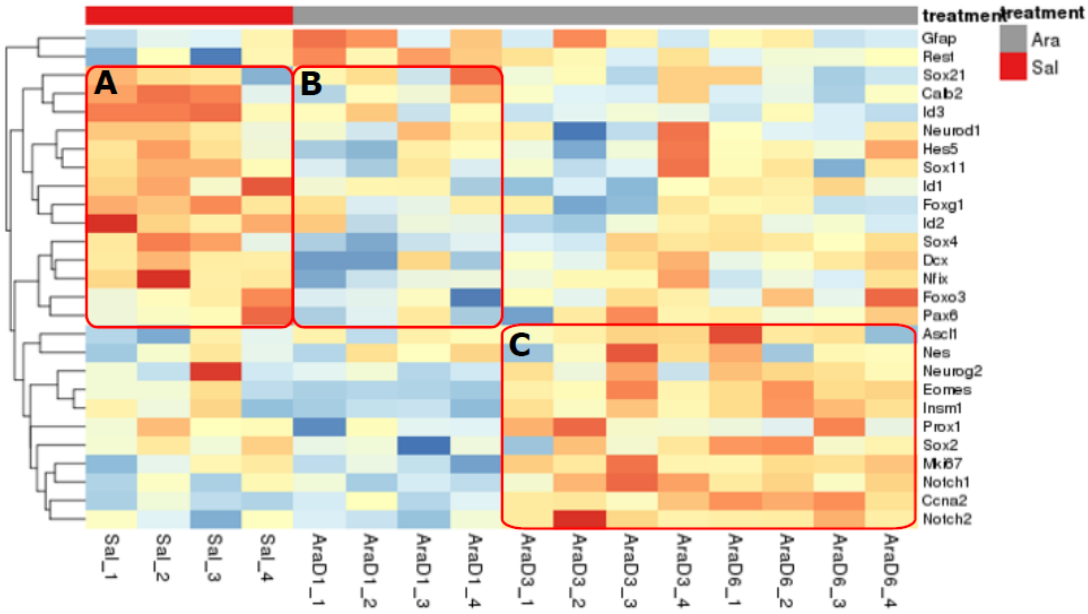

Figure 23. Expression heatmap of genes relevant to neurogenesis.

A. Saline-treated controls showed high levels of genes involved in NSC maintenance. **B.** At D1 following AraC, the NSC maintenance genes were downregulated. **C.** At D3 and D6 post-AraC, transcriptional signatures of increased hippocampal neurogenesis were seen.

5.2.3 RNA sequencing identifies candidate matrix-related genes for adult neurogenesis

Based on these findings I concentrated further analyses on two specific comparisons: SalD1 versus AraD1 (targeting NSC activation); and AraD1 versus AraD3 and D6 combined (targeting NSPC proliferation and early differentiation). To construct a list of differentially-expressed genes for each analysis, I first selected those with a q-value ("corrected p value" or False Discovery Rate [FDR]) of 0.20 or less. This FDR threshold has been employed by others in the study of murine adult neurogenesis [e.g., Dulken et al. 2017] and in human hippocampal biology [e.g. Zhou et al. 2011]. It is a more permissive threshold than used by some [Llorens-Bobadilla 2015], but was used here because my primary aim was to construct a list of candidates. I then selected the retained genes against a fold change >2. This fold change threshold has been widely used to study differential gene expression in adult neurogenesis [e.g., Pardo et al. 2017, Pohodich et al. 2018, Llorens-Bobadilla 2015]. To subsequently explore the genes surviving these expression change criteria, I then conducted a basic gene ontology analysis using the GO Ontology database (released 03/07/2018) available at http://www.geneontology.org/page/go-enrichment-analysis, analysed against the reference Mus musculus genome.

Using the criteria stated, n=67 genes were differentially expressed between SalD1 and AraD1 (**Tables 11a, 11b, and 11c)**, and n=55 genes between AraD1 and AraD3-6 **(Tables 12a, 12b, and 12c)**. Note that these groups of tables present the differentially-expressed genes first in alphabetical order ("a"), and the same genes ordered instead by q value ("b") and then by fold change ("c").

Ensembl gene ID	Gene name	Sal	AraD1	FC	p value	q value
ENSMUSG00000041707	1810011H11Rik	0.21	0.59	2.83	6.96E-06	0.021395
ENSMUSG00000032363	Adamts7	1.05	0.23	-4.6	0.0001081	0.0711
ENSMUSG00000039116	Adgrg6	0.53	2.52	4.73	4.56E-05	0.050983
ENSMUSG00000029762	Akr1b8	0.3	1.11	3.7	0.0004036	0.14759
ENSMUSG00000090256	Alms1-ps1	0.19	0.59	3.12	0.0005837	0.16973
ENSMUSG00000039529	Atp8b1	1.28	0.4	-3.2	0.0007954	0.19595
ENSMUSG00000028457	Atp8b5	0.44	1.16	2.66	0.0005437	0.16454
ENSMUSG00000000317	Bcl6b	1.14	0.36	-3.2	0.0001139	0.0711
ENSMUSG00000035352	Ccl12	0.32	2.88	9.13	0.0003314	0.1333
ENSMUSG00000028459	Cd72	0.82	2.67	3.27	0.0004807	0.16132
ENSMUSG00000062778	Chia1	0.55	1.54	2.79	0.0005168	0.16423
ENSMUSG00000016356	Col20a1	5.68	11.77	2.07	4.99E-06	0.021395
ENSMUSG00000032380	Dapk2	0.17	0.36	2.12	4.65E-05	0.050983
ENSMUSG00000026674	Ddr2	1.14	3.42	3.02	8.91E-05	0.069334
ENSMUSG00000062393	Dgkk	0.42	0.21	-2.1	0.0003042	0.12788
ENSMUSG00000031616	Ednra	3.83	9.74	2.54	0.0007378	0.19018
ENSMUSG00000032446	Eomes	1.57	0.38	-4.1	7.10E-05	0.066662
ENSMUSG00000021750	Fam107a	41.8	123.52	2.95	0.0001784	0.095679
ENSMUSG00000021186	Fbln5	3.07	10.63	3.47	0.0006468	0.17944
ENSMUSG00000028214	Gem	0.96	3.88	4.06	4.04E-06	0.021395
ENSMUSG00000020932	Gfap	81.5	372.84	4.58	0.000499	0.16275
ENSMUSG00000086256	Gm12052	0.46	0.2	-2.4	0.0004002	0.14759
ENSMUSG00000085828	Gm15612	2.9	1.36	-2.1	0.000389	0.14759
ENSMUSG00000097618	Gm26507	0.18	0.49	2.64	1.38E-05	0.027694
ENSMUSG00000094622	Gm3055	2.76	6.31	2.29	0.0002571	0.12165
ENSMUSG00000033255	Gm5134	0.62	2.31	3.72	7.18E-05	0.066662
ENSMUSG00000096775	Gm5796	0.89	0.32	-2.8	0.0008037	0.19595
ENSMUSG00000102493	Gm8010	0.76	0.34	-2.2	0.0004489	0.15707
ENSMUSG00000038811	Gngt2	0.5	1.34	2.65	0.0001047	0.0711
ENSMUSG00000052229	Gpr17	33.8	0.74	-45	0.0006302	0.17895
ENSMUSG00000082029	H3f3c	1.78	0.33	-5.4	0.0007252	0.19018
ENSMUSG00000052305	Hbb-bs	7.42	1.49	-5	0.0005308	0.16423
ENSMUSG00000004328	Hif3a	1.09	4.12	3.78	1.03E-05	0.025693
ENSMUSG00000064220	Hist2h2aa1	0.18	0.87	4.96	7.92E-05	0.069206
ENSMUSG00000064215	Ifi27	8.23	21.18	2.57	8.65E-05	0.069334
ENSMUSG00000026896	Ifih1	0.94	3.06	3.24	1.49E-06	0.012018
ENSMUSG00000074896	Ifit3	4.37	16.8	3.84	0.0004728	0.16132
ENSMUSG00000062488	Ifit3b	3.18	8.85	2.78	0.0004984	0.16275
ENSMUSG00000025492	Ifitm3	2	13.54	6.78	0.0002045	0.10293
ENSMUSG00000068154	Insm1	3.68	1.37	-2.7	0.0003859	0.14759
ENSMUSG00000002325	Irf9	11.7	28.91	2.47	0.0006583	0.18055
ENSMUSG00000030789	Itgax	0.16	0.44	2.72	1.82E-05	0.030367
ENSMUSG00000024903	Lao1	0.65	0.25	-2.6	0.0005281	0.16423

ENSMUSG00000021423	Ly86	3.37	8.93	2.65	0.000141	0.07917
ENSMUSG00000030218	Mgp	0.37	1.45	3.95	1.52E-05	0.028238
ENSMUSG00000071715	Ncf4	0.3	0.89	2.98	9.61E-05	0.070315
ENSMUSG00000029561	Oasl2	5.08	12.53	2.47	0.0002689	0.12236
ENSMUSG00000021390	Ogn	7.26	16.59	2.28	7.09E-06	0.021395
ENSMUSG00000066632	Pgk1-rs7	0.73	0.23	-3.1	0.0001411	0.07917
ENSMUSG00000033149	Phldb2	4.04	1.54	-2.6	0.000527	0.16423
ENSMUSG00000032369	Plscr1	0.74	1.68	2.28	0.0008015	0.19595
ENSMUSG00000009734	Pou6f2	3.05	0.84	-3.7	7.14E-08	0.001722
ENSMUSG00000028036	Ptgfr	0.66	0.27	-2.5	9.92E-05	0.070409
ENSMUSG00000009281	Rarres2	0.94	2.34	2.49	0.0003702	0.14649
ENSMUSG00000044921	Rassf9	0.56	0.19	-2.9	9.26E-05	0.069864
ENSMUSG00000033355	Rtp4	0.83	3.84	4.61	0.0002738	0.12236
ENSMUSG00000023945	Slc5a7	0.45	0.21	-2.1	0.0003073	0.12788
ENSMUSG00000072620	Slfn2	0.34	1.99	5.81	4.87E-05	0.051068
ENSMUSG00000043298	Smco3	0.3	1.07	3.54	0.0003145	0.12865
ENSMUSG00000027315	Spint1	0.56	1.6	2.86	0.0007139	0.18934
ENSMUSG00000026104	Stat1	23	51.18	2.22	0.0001181	0.071252
ENSMUSG00000027762	Sucnr1	0.2	0.45	2.28	0.0006781	0.18186
ENSMUSG00000034881	Tbxa2r	0.55	1.47	2.67	0.0005717	0.16827
ENSMUSG00000021702	Thbs4	1.25	5.41	4.32	3.62E-05	0.043665
ENSMUSG00000025519	Tktl2	0.88	0.26	-3.4	2.10E-07	0.002533
ENSMUSG00000026728	Vim	11.9	41.27	3.46	6.61E-06	0.021395
ENSMUSG00000039814	Xkr5	0.23	0.52	2.27	0.0008011	0.19595

Table 11a. Differentially expressed genes: Sal vs. AraD1, sorted by alphabetical order.
FC= fold change.

Ensembl gene ID	Gene name	Sal	AraD1	FC	p value	q value
ENSMUSG00000009734	Pou6f2	3.05	0.84	-3.7	7.14E-08	0.001722
ENSMUSG00000025519	Tktl2	0.88	0.26	-3.4	2.10E-07	0.002533
ENSMUSG00000026896	Ifih1	0.94	3.06	3.24	1.49E-06	0.012018
ENSMUSG00000041707	1810011H11Rik	0.21	0.59	2.83	6.96E-06	0.021395
ENSMUSG00000016356	Col20a1	5.68	11.77	2.07	4.99E-06	0.021395
ENSMUSG00000028214	Gem	0.96	3.88	4.06	4.04E-06	0.021395
ENSMUSG00000021390	Ogn	7.26	16.59	2.28	7.09E-06	0.021395
ENSMUSG00000026728	Vim	11.9	41.27	3.46	6.61E-06	0.021395
ENSMUSG00000004328	Hif3a	1.09	4.12	3.78	1.03E-05	0.025693
ENSMUSG00000097618	Gm26507	0.18	0.49	2.64	1.38E-05	0.027694
ENSMUSG00000030218	Mgp	0.37	1.45	3.95	1.52E-05	0.028238
ENSMUSG00000030789	Itgax	0.16	0.44	2.72	1.82E-05	0.030367
ENSMUSG00000021702	Thbs4	1.25	5.41	4.32	3.62E-05	0.043665
ENSMUSG00000039116	Adgrg6	0.53	2.52	4.73	4.56E-05	0.050983
ENSMUSG00000032380	Dapk2	0.17	0.36	2.12	4.65E-05	0.050983
ENSMUSG00000072620	Slfn2	0.34	1.99	5.81	4.87E-05	0.051068
ENSMUSG00000032446	Eomes	1.57	0.38	-4.1	7.10E-05	0.066662
ENSMUSG00000033255	Gm5134	0.62	2.31	3.72	7.18E-05	0.066662
ENSMUSG00000064220	Hist2h2aa1	0.18	0.87	4.96	7.92E-05	0.069206
ENSMUSG00000026674	Ddr2	1.14	3.42	3.02	8.91E-05	0.069334
ENSMUSG00000064215	Ifi27	8.23	21.18	2.57	8.65E-05	0.069334
ENSMUSG00000044921	Rassf9	0.56	0.19	-2.9	9.26E-05	0.069864
ENSMUSG00000071715	Ncf4	0.3	0.89	2.98	9.61E-05	0.070315
ENSMUSG00000028036	Ptgfr	0.66	0.27	-2.5	9.92E-05	0.070409
ENSMUSG00000032363	Adamts7	1.05	0.23	-4.6	0.0001081	0.0711
ENSMUSG00000000317	Bcl6b	1.14	0.36	-3.2	0.0001139	0.0711
ENSMUSG00000038811	Gngt2	0.5	1.34	2.65	0.0001047	0.0711
ENSMUSG00000026104	Stat1	23	51.18	2.22	0.0001181	0.071252
ENSMUSG00000021423	Ly86	3.37	8.93	2.65	0.000141	0.07917
ENSMUSG00000066632	Pgk1-rs7	0.73	0.23	-3.1	0.0001411	0.07917
ENSMUSG00000021750	Fam107a	41.8	123.52	2.95	0.0001784	0.095679
ENSMUSG00000025492	Ifitm3	2	13.54	6.78	0.0002045	0.10293
ENSMUSG00000094622	Gm3055	2.76	6.31	2.29	0.0002571	0.12165
ENSMUSG00000029561	Oasl2	5.08	12.53	2.47	0.0002689	0.12236
ENSMUSG00000033355	Rtp4	0.83	3.84	4.61	0.0002738	0.12236
ENSMUSG00000062393	Dgkk	0.42	0.21	-2.1	0.0003042	0.12788
ENSMUSG00000023945	Slc5a7	0.45	0.21	-2.1	0.0003073	0.12788
ENSMUSG00000043298	Smco3	0.3	1.07	3.54	0.0003145	0.12865
ENSMUSG00000035352	Ccl12	0.32	2.88	9.13	0.0003314	0.1333
ENSMUSG00000009281	Rarres2	0.94	2.34	2.49	0.0003702	0.14649
ENSMUSG00000029762	Akr1b8	0.3	1.11	3.7	0.0004036	0.14759
ENSMUSG00000086256	Gm12052	0.46	0.2	-2.4	0.0004002	0.14759
ENSMUSG00000085828	Gm15612	2.9	1.36	-2.1	0.000389	0.14759

ENSMUSG00000068154	Insm1	3.68	1.37	-2.7	0.0003859	0.14759
ENSMUSG00000102493	Gm8010	0.76	0.34	-2.2	0.0004489	0.15707
ENSMUSG00000028459	Cd72	0.82	2.67	3.27	0.0004807	0.16132
ENSMUSG00000074896	Ifit3	4.37	16.8	3.84	0.0004728	0.16132
ENSMUSG00000020932	Gfap	81.5	372.84	4.58	0.000499	0.16275
ENSMUSG00000062488	Ifit3b	3.18	8.85	2.78	0.0004984	0.16275
ENSMUSG00000062778	Chia1	0.55	1.54	2.79	0.0005168	0.16423
ENSMUSG00000052305	Hbb-bs	7.42	1.49	-5	0.0005308	0.16423
ENSMUSG00000024903	Lao1	0.65	0.25	-2.6	0.0005281	0.16423
ENSMUSG00000033149	Phldb2	4.04	1.54	-2.6	0.000527	0.16423
ENSMUSG00000028457	Atp8b5	0.44	1.16	2.66	0.0005437	0.16454
ENSMUSG00000034881	Tbxa2r	0.55	1.47	2.67	0.0005717	0.16827
ENSMUSG00000090256	Alms1-ps1	0.19	0.59	3.12	0.0005837	0.16973
ENSMUSG00000052229	Gpr17	33.8	0.74	-45	0.0006302	0.17895
ENSMUSG00000021186	Fbln5	3.07	10.63	3.47	0.0006468	0.17944
ENSMUSG00000002325	Irf9	11.7	28.91	2.47	0.0006583	0.18055
ENSMUSG00000027762	Sucnr1	0.2	0.45	2.28	0.0006781	0.18186
ENSMUSG00000027315	Spint1	0.56	1.6	2.86	0.0007139	0.18934
ENSMUSG00000031616	Ednra	3.83	9.74	2.54	0.0007378	0.19018
ENSMUSG00000082029	H3f3c	1.78	0.33	-5.4	0.0007252	0.19018
ENSMUSG00000039529	Atp8b1	1.28	0.4	-3.2	0.0007954	0.19595
ENSMUSG00000096775	Gm5796	0.89	0.32	-2.8	0.0008037	0.19595
ENSMUSG00000032369	Plscr1	0.74	1.68	2.28	0.0008015	0.19595
ENSMUSG00000039814	Xkr5	0.23	0.52	2.27	0.0008011	0.19595

Table 11b. Differentially expressed genes: Sal vs. AraD1, sorted by False Discovery Rate (q-value). FC= fold change.

Ensembl gene ID	Gene name	Sal	AraD1	FC	p value	q value
ENSMUSG00000035352	Ccl12	0.32	2.88	9.13	0.0003314	0.1333
ENSMUSG00000025492	Ifitm3	2	13.54	6.78	0.0002045	0.10293
ENSMUSG00000072620	Slfn2	0.34	1.99	5.81	4.87E-05	0.051068
ENSMUSG00000064220	Hist2h2aa1	0.18	0.87	4.96	7.92E-05	0.069206
ENSMUSG00000039116	Adgrg6	0.53	2.52	4.73	4.56E-05	0.050983
ENSMUSG00000033355	Rtp4	0.83	3.84	4.61	0.0002738	0.12236
ENSMUSG00000020932	Gfap	81.5	372.84	4.58	0.000499	0.16275
ENSMUSG00000021702	Thbs4	1.25	5.41	4.32	3.62E-05	0.043665
ENSMUSG00000028214	Gem	0.96	3.88	4.06	4.04E-06	0.021395
ENSMUSG00000030218	Mgp	0.37	1.45	3.95	1.52E-05	0.028238
ENSMUSG00000074896	Ifit3	4.37	16.8	3.84	0.0004728	0.16132
ENSMUSG00000004328	Hif3a	1.09	4.12	3.78	1.03E-05	0.025693
ENSMUSG00000033255	Gm5134	0.62	2.31	3.72	7.18E-05	0.066662
ENSMUSG00000029762	Akr1b8	0.3	1.11	3.7	0.0004036	0.14759
ENSMUSG00000043298	Smco3	0.3	1.07	3.54	0.0003145	0.12865
ENSMUSG00000021186	Fbln5	3.07	10.63	3.47	0.0006468	0.17944
ENSMUSG00000026728	Vim	11.9	41.27	3.46	6.61E-06	0.021395
ENSMUSG00000028459	Cd72	0.82	2.67	3.27	0.0004807	0.16132
ENSMUSG00000026896	Ifih1	0.94	3.06	3.24	1.49E-06	0.012018
ENSMUSG00000090256	Alms1-ps1	0.19	0.59	3.12	0.0005837	0.16973
ENSMUSG00000026674	Ddr2	1.14	3.42	3.02	8.91E-05	0.069334
ENSMUSG00000071715	Ncf4	0.3	0.89	2.98	9.61E-05	0.070315
ENSMUSG00000021750	Fam107a	41.8	123.52	2.95	0.0001784	0.095679
ENSMUSG00000027315	Spint1	0.56	1.6	2.86	0.0007139	0.18934
ENSMUSG00000041707	1810011H11Rik	0.21	0.59	2.83	6.96E-06	0.021395
ENSMUSG00000062778	Chia1	0.55	1.54	2.79	0.0005168	0.16423
ENSMUSG00000062488	Ifit3b	3.18	8.85	2.78	0.0004984	0.16275
ENSMUSG00000030789	Itgax	0.16	0.44	2.72	1.82E-05	0.030367
ENSMUSG00000034881	Tbxa2r	0.55	1.47	2.67	0.0005717	0.16827
ENSMUSG00000028457	Atp8b5	0.44	1.16	2.66	0.0005437	0.16454
ENSMUSG00000038811	Gngt2	0.5	1.34	2.65	0.0001047	0.0711
ENSMUSG00000021423	Ly86	3.37	8.93	2.65	0.000141	0.07917
ENSMUSG00000097618	Gm26507	0.18	0.49	2.64	1.38E-05	0.027694
ENSMUSG00000064215	Ifi27	8.23	21.18	2.57	8.65E-05	0.069334
ENSMUSG00000031616	Ednra	3.83	9.74	2.54	0.0007378	0.19018
ENSMUSG00000009281	Rarres2	0.94	2.34	2.49	0.0003702	0.14649
ENSMUSG00000002325	Irf9	11.7	28.91	2.47	0.0006583	0.18055
ENSMUSG00000029561	Oasl2	5.08	12.53	2.47	0.0002689	0.12236
ENSMUSG00000094622	Gm3055	2.76	6.31	2.29	0.0002571	0.12165
ENSMUSG00000021390	Ogn	7.26	16.59	2.28	7.09E-06	0.021395
ENSMUSG00000032369	Plscr1	0.74	1.68	2.28	0.0008015	0.19595
ENSMUSG00000027762	Sucnr1	0.2	0.45	2.28	0.0006781	0.18186
ENSMUSG00000039814	Xkr5	0.23	0.52	2.27	0.0008011	0.19595

ENSMUSG00000026104	Stat1	23	51.18	2.22	0.0001181	0.071252
ENSMUSG00000032380	Dapk2	0.17	0.36	2.12	4.65E-05	0.050983
ENSMUSG00000016356	Col20a1	5.68	11.77	2.07	4.99E-06	0.021395
ENSMUSG00000062393	Dgkk	0.42	0.21	-2.1	0.0003042	0.12788
ENSMUSG00000023945	Slc5a7	0.45	0.21	-2.1	0.0003073	0.12788
ENSMUSG00000085828	Gm15612	2.9	1.36	-2.1	0.000389	0.14759
ENSMUSG00000102493	Gm8010	0.76	0.34	-2.2	0.0004489	0.15707
ENSMUSG00000086256	Gm12052	0.46	0.2	-2.4	0.0004002	0.14759
ENSMUSG00000028036	Ptgfr	0.66	0.27	-2.5	9.92E-05	0.070409
ENSMUSG00000024903	Lao1	0.65	0.25	-2.6	0.0005281	0.16423
ENSMUSG00000033149	Phldb2	4.04	1.54	-2.6	0.000527	0.16423
ENSMUSG00000068154	Insm1	3.68	1.37	-2.7	0.0003859	0.14759
ENSMUSG00000096775	Gm5796	0.89	0.32	-2.8	0.0008037	0.19595
ENSMUSG00000044921	Rassf9	0.56	0.19	-2.9	9.26E-05	0.069864
ENSMUSG00000066632	Pgk1-rs7	0.73	0.23	-3.1	0.0001411	0.07917
ENSMUSG00000000317	Bcl6b	1.14	0.36	-3.2	0.0001139	0.0711
ENSMUSG00000039529	Atp8b1	1.28	0.4	-3.2	0.0007954	0.19595
ENSMUSG00000025519	Tktl2	0.88	0.26	-3.4	2.10E-07	0.002533
ENSMUSG00000009734	Pou6f2	3.05	0.84	-3.7	7.14E-08	0.001722
ENSMUSG00000032446	Eomes	1.57	0.38	-4.1	7.10E-05	0.066662
ENSMUSG00000032363	Adamts7	1.05	0.23	-4.6	0.0001081	0.0711
ENSMUSG00000052305	Hbb-bs	7.42	1.49	-5	0.0005308	0.16423
ENSMUSG00000082029	H3f3c	1.78	0.33	-5.4	0.0007252	0.19018
ENSMUSG00000052229	Gpr17	33.8	0.74	-45	0.0006302	0.17895

Table 11c. Differentially expressed genes: Sal vs. AraD1, sorted by fold-change. FC= fold change.

Ensembl gene ID	Gene name	AraD1	Late	FC	p value	q value
ENSMUSG00000090307	1700071M16Rik	1.13	2.6	2.3	0.0002178	0.095615
ENSMUSG00000087484	2900089D17Rik	1.04	2.61	2.5	0.0008192	0.19577
ENSMUSG00000044749	Abca6	2.45	0.67	-3.64	1.35E-06	0.0056129
ENSMUSG00000075023	Accsl	0.22	0.63	2.91	2.00E-05	0.024169
ENSMUSG00000028766	Alpl	2.2	0.82	-2.69	1.38E-05	0.020477
ENSMUSG00000022548	Apod	39.16	13.2	-2.97	0.0002072	0.095615
ENSMUSG00000057346	Apol9a	0.37	0.18	-2.01	0.0001027	0.064078
ENSMUSG00000029032	Arhgef16	0.48	0.22	-2.16	0.0004028	0.12793
ENSMUSG00000046718	Bst2	6.38	1.9	-3.36	0.0004916	0.13931
ENSMUSG00000049130	C5ar1	1.72	0.63	-2.72	0.0008471	0.19774
ENSMUSG00000073405	C920025E04Rik	0.43	0.19	-2.28	0.0001152	0.069568
ENSMUSG00000035352	Ccl12	2.88	0.5	-5.71	0.0001444	0.079961
ENSMUSG00000027715	Ccna2	3.02	6.66	2.2	5.79E-06	0.016899
ENSMUSG00000023067	Cdkn1a	11.14	4.98	-2.24	0.0007393	0.1821
ENSMUSG00000028813	CK137956	1.83	0.81	-2.27	0.0003629	0.12167
ENSMUSG00000074981	Dcdc5	0.38	1.01	2.64	0.0003385	0.11959
ENSMUSG00000062393	Dgkk	0.21	0.45	2.15	0.0005938	0.15579
ENSMUSG00000029005	Draxin	1.08	3.53	3.25	1.42E-05	0.020477
ENSMUSG00000072672	Duxbl3	0.2	0.45	2.21	4.59E-05	0.04234
ENSMUSG00000033788	Dysf	3.75	1.46	-2.57	0.0002493	0.10017
ENSMUSG00000032446	Eomes	0.38	3.49	9.07	1.24E-09	2.98E-05
ENSMUSG00000031196	F8	0.84	3.16	3.76	2.95E-05	0.028457
ENSMUSG00000059659	Gm10069	0.5	1.32	2.66	0.0002988	0.11097
ENSMUSG00000084774	Gm14110	0.34	0.78	2.27	0.0008869	0.19826
ENSMUSG00000084858	Gm1980	1.51	0.58	-2.6	9.75E-05	0.064078
ENSMUSG00000054589	Gm9949	0.47	0.19	-2.49	0.0001457	0.079961
ENSMUSG00000053164	Gpr21	0.57	3.21	5.58	7.37E-06	0.016899
ENSMUSG00000073421	H2-Ab1	0.2	0.56	2.75	4.91E-05	0.04234
ENSMUSG00000054717	Hmgb2	4.63	9.47	2.04	7.64E-05	0.057644
ENSMUSG00000036854	Hspb6	7.65	3.6	-2.12	0.0006540	0.16793
ENSMUSG00000074896	Ifit3	16.8	5.59	-3.01	0.0002174	0.095615
ENSMUSG00000062488	Ifit3b	8.85	3.82	-2.32	0.0003847	0.12548
ENSMUSG00000025492	Ifitm3	13.54	3.44	-3.93	0.0002455	0.10017
ENSMUSG00000068154	Insm1	1.37	5.8	4.24	7.33E-08	0.0008850
ENSMUSG00000024903	Lao1	0.25	0.81	3.25	2.13E-05	0.024436
ENSMUSG00000026822	Lcn2	0.8	0.22	-3.6	0.0008273	0.19577
ENSMUSG00000029561	Oasl2	12.53	6.06	-2.07	0.0002617	0.10017
ENSMUSG00000063230	Olfr535	0.23	0.67	2.92	0.0001667	0.085626
ENSMUSG00000066632	Pgk1-rs7	0.23	0.9	3.89	0.0004262	0.13191
ENSMUSG00000048827	Pkd1l3	4.9	10.21	2.08	1.54E-05	0.020667
ENSMUSG00000056529	Ptafr	0.91	0.45	-2.01	0.0008197	0.19577
ENSMUSG00000032648	Pygm	2.67	1.15	-2.33	8.70E-06	0.016899
ENSMUSG00000106877	Pygm	2.67	1.15	-2.33	8.70E-06	0.016899

ENSMUSG00000009281	Rarres2	2.34	1.13	-2.08	0.0002617	0.10017
ENSMUSG00000070327	Rnf213	8.42	3.58	-2.35	0.0004635	0.13419
ENSMUSG00000034177	Rnf43	0.3	1.49	5.03	8.74E-06	0.016899
ENSMUSG00000027547	Sall4	0.53	0.2	-2.65	0.0005308	0.14559
ENSMUSG00000020672	Sntg2	6.09	2.86	-2.13	1.40E-06	0.0056129
ENSMUSG00000069910	Spdl1	0.18	0.54	2.89	0.0003584	0.12167
ENSMUSG00000029797	Sspo	0.19	0.72	3.81	3.26E-06	0.011239
ENSMUSG00000027762	Sucnr1	0.45	0.2	-2.21	0.0005719	0.15511
ENSMUSG00000025519	Tktl2	0.26	0.72	2.77	6.06E-07	0.0036573
ENSMUSG00000023367	Tmem176a	7.81	3.66	-2.13	9.54E-05	0.064078
ENSMUSG00000036944	Tmem71	0.67	0.3	-2.27	6.37E-05	0.051243
ENSMUSG00000032554	Trf	175.64	83.8	-2.1	5.85E-05	0.048707

Table 12a. Differentially expressed genes: AraD1 vs. late (AraD3-6), sorted alphabetically. FC= fold change.

Ensembl gene ID	Gene name	AraD1	Late	FC	p value	q value
ENSMUSG00000032446	Eomes	0.38	3.49	9.07	0.0000000	0.0000298
ENSMUSG00000068154	Insm1	1.37	5.8	4.24	0.0000001	0.0008851
ENSMUSG00000025519	Tktl2	0.26	0.72	2.77	0.0000006	0.0036573
ENSMUSG00000044749	Abca6	2.45	0.67	-3.64	0.0000014	0.0056129
ENSMUSG00000020672	Sntg2	6.09	2.86	-2.13	0.0000014	0.0056129
ENSMUSG00000029797	Sspo	0.19	0.72	3.81	0.0000033	0.0112390
ENSMUSG00000027715	Ccna2	3.02	6.66	2.2	0.0000058	0.0168990
ENSMUSG00000053164	Gpr21	0.57	3.21	5.58	0.0000074	0.0168990
ENSMUSG00000032648	Pygm	2.67	1.15	-2.33	0.0000087	0.0168990
ENSMUSG00000106877	Pygm	2.67	1.15	-2.33	0.0000087	0.0168990
ENSMUSG00000034177	Rnf43	0.3	1.49	5.03	0.0000087	0.0168990
ENSMUSG00000028766	Alpl	2.2	0.82	-2.69	0.0000138	0.0204770
ENSMUSG00000029005	Draxin	1.08	3.53	3.25	0.0000142	0.0204770
ENSMUSG00000048827	Pkd1l3	4.9	10.21	2.08	0.0000154	0.0206670
ENSMUSG00000075023	Accsl	0.22	0.63	2.91	0.0000200	0.0241690
ENSMUSG00000024903	Lao1	0.25	0.81	3.25	0.0000213	0.0244360
ENSMUSG00000031196	F8	0.84	3.16	3.76	0.0000295	0.0284570
ENSMUSG00000072672	Duxbl3	0.2	0.45	2.21	0.0000459	0.0423400
ENSMUSG00000073421	H2-Ab1	0.2	0.56	2.75	0.0000491	0.0423400
ENSMUSG00000032554	Trf	175.64	83.8	-2.1	0.0000585	0.0487070
ENSMUSG00000036944	Tmem71	0.67	0.3	-2.27	0.0000637	0.0512430
ENSMUSG00000054717	Hmgb2	4.63	9.47	2.04	0.0000764	0.0576440
ENSMUSG00000057346	Apol9a	0.37	0.18	-2.01	0.0001027	0.0640780
ENSMUSG00000084858	Gm1980	1.51	0.58	-2.6	0.0000975	0.0640780
ENSMUSG00000023367	Tmem176a	7.81	3.66	-2.13	0.0000954	0.0640780
ENSMUSG00000073405	C920025E04Rik	0.43	0.19	-2.28	0.0001153	0.0695680
ENSMUSG00000035352	Ccl12	2.88	0.5	-5.71	0.0001445	0.0799610
ENSMUSG00000054589	Gm9949	0.47	0.19	-2.49	0.0001458	0.0799610
ENSMUSG00000063230	Olfr535	0.23	0.67	2.92	0.0001667	0.0856260
ENSMUSG00000090307	1700071M16Rik	1.13	2.6	2.3	0.0002179	0.0956150
ENSMUSG00000022548	Apod	39.16	13.2	-2.97	0.0002072	0.0956150
ENSMUSG00000074896	Ifit3	16.8	5.59	-3.01	0.0002174	0.0956150
ENSMUSG00000033788	Dysf	3.75	1.46	-2.57	0.0002493	0.1001700
ENSMUSG00000025492	Ifitm3	13.54	3.44	-3.93	0.0002456	0.1001700
ENSMUSG00000029561	Oasl2	12.53	6.06	-2.07	0.0002617	0.1001700
ENSMUSG00000009281	Rarres2	2.34	1.13	-2.08	0.0002617	0.1001700
ENSMUSG00000059659	Gm10069	0.5	1.32	2.66	0.0002989	0.1109700
ENSMUSG00000074981	Dcdc5	0.38	1.01	2.64	0.0003385	0.1195900
ENSMUSG00000028813	CK137956	1.83	0.81	-2.27	0.0003630	0.1216700
ENSMUSG00000069910	Spdl1	0.18	0.54	2.89	0.0003584	0.1216700
ENSMUSG00000062488	Ifit3b	8.85	3.82	-2.32	0.0003847	0.1254800
ENSMUSG00000029032	Arhgef16	0.48	0.22	-2.16	0.0004028	0.1279300
ENSMUSG00000066632	Pgk1-rs7	0.23	0.9	3.89	0.0004263	0.1319100

ENSMUSG00000070327	Rnf213	8.42	3.58	-2.35	0.0004636	0.1341900
ENSMUSG00000046718	Bst2	6.38	1.9	-3.36	0.0004917	0.1393100
ENSMUSG00000027547	Sall4	0.53	0.2	-2.65	0.0005308	0.1455900
ENSMUSG00000027762	Sucnr1	0.45	0.2	-2.21	0.0005720	0.1551100
ENSMUSG00000062393	Dgkk	0.21	0.45	2.15	0.0005939	0.1557900
ENSMUSG00000036854	Hspb6	7.65	3.6	-2.12	0.0006540	0.1679300
ENSMUSG00000023067	Cdkn1a	11.14	4.98	-2.24	0.0007394	0.1821000
ENSMUSG00000087484	2900089D17Rik	1.04	2.61	2.5	0.0008192	0.1957700
ENSMUSG00000026822	Lcn2	0.8	0.22	-3.6	0.0008274	0.1957700
ENSMUSG00000056529	Ptafr	0.91	0.45	-2.01	0.0008198	0.1957700
ENSMUSG00000049130	C5ar1	1.72	0.63	-2.72	0.0008472	0.1977400
ENSMUSG00000084774	Gm14110	0.34	0.78	2.27	0.0008870	0.1982600

Table 12b. Differentially expressed genes: AraD1 vs. late (AraD3-6), sorted by False Discovery Rate (q-value). FC= fold change.

Ensembl gene ID	Gene name	AraD1	Late	FC	p value	q value
ENSMUSG00000032446	Eomes	0.38	3.49	9.07	0.0000000	0.0000298
ENSMUSG00000053164	Gpr21	0.57	3.21	5.58	0.0000074	0.0168990
ENSMUSG00000034177	Rnf43	0.3	1.49	5.03	0.0000087	0.0168990
ENSMUSG00000068154	Insm1	1.37	5.8	4.24	0.0000001	0.0008851
ENSMUSG00000066632	Pgk1-rs7	0.23	0.9	3.89	0.0004263	0.1319100
ENSMUSG00000029797	Sspo	0.19	0.72	3.81	0.0000033	0.0112390
ENSMUSG00000031196	F8	0.84	3.16	3.76	0.0000295	0.0284570
ENSMUSG00000029005	Draxin	1.08	3.53	3.25	0.0000142	0.0204770
ENSMUSG00000024903	Lao1	0.25	0.81	3.25	0.0000213	0.0244360
ENSMUSG00000063230	Olfr535	0.23	0.67	2.92	0.0001667	0.0856260
ENSMUSG00000075023	Accsl	0.22	0.63	2.91	0.0000200	0.0241690
ENSMUSG00000069910	Spdl1	0.18	0.54	2.89	0.0003584	0.1216700
ENSMUSG00000025519	Tktl2	0.26	0.72	2.77	0.0000006	0.0036573
ENSMUSG00000073421	H2-Ab1	0.2	0.56	2.75	0.0000491	0.0423400
ENSMUSG00000059659	Gm10069	0.5	1.32	2.66	0.0002989	0.1109700
ENSMUSG00000074981	Dcdc5	0.38	1.01	2.64	0.0003385	0.1195900
ENSMUSG00000087484	2900089D17Rik	1.04	2.61	2.5	0.0008192	0.1957700
ENSMUSG00000090307	1700071M16Rik	1.13	2.6	2.3	0.0002179	0.0956150
ENSMUSG00000084774	Gm14110	0.34	0.78	2.27	0.0008870	0.1982600
ENSMUSG00000072672	Duxbl3	0.2	0.45	2.21	0.0000459	0.0423400
ENSMUSG00000027715	Ccna2	3.02	6.66	2.2	0.0000058	0.0168990
ENSMUSG00000062393	Dgkk	0.21	0.45	2.15	0.0005939	0.1557900
ENSMUSG00000048827	Pkd1l3	4.9	10.2	2.08	0.0000154	0.0206670
ENSMUSG00000054717	Hmgb2	4.63	9.47	2.04	0.0000764	0.0576440
ENSMUSG00000057346	Apol9a	0.37	0.18	-2.01	0.0001027	0.0640780
ENSMUSG00000056529	Ptafr	0.91	0.45	-2.01	0.0008198	0.1957700
ENSMUSG00000029561	Oasl2	12.53	6.06	-2.07	0.0002617	0.1001700
ENSMUSG00000009281	Rarres2	2.34	1.13	-2.08	0.0002617	0.1001700
ENSMUSG00000032554	Trf	175.64	83.8	-2.1	0.0000585	0.0487070
ENSMUSG00000036854	Hspb6	7.65	3.6	-2.12	0.0006540	0.1679300
ENSMUSG00000020672	Sntg2	6.09	2.86	-2.13	0.0000014	0.0056129
ENSMUSG00000023367	Tmem176a	7.81	3.66	-2.13	0.0000954	0.0640780
ENSMUSG00000029032	Arhgef16	0.48	0.22	-2.16	0.0004028	0.1279300
ENSMUSG00000027762	Sucnr1	0.45	0.2	-2.21	0.0005720	0.1551100
ENSMUSG00000023067	Cdkn1a	11.14	4.98	-2.24	0.0007394	0.1821000
ENSMUSG00000028813	CK137956	1.83	0.81	-2.27	0.0003630	0.1216700
ENSMUSG00000036944	Tmem71	0.67	0.3	-2.27	0.0000637	0.0512430
ENSMUSG00000073405	C920025E04Rik	0.43	0.19	-2.28	0.0001153	0.0695680
ENSMUSG00000062488	Ifit3b	8.85	3.82	-2.32	0.0003847	0.1254800
ENSMUSG00000032648	Pygm	2.67	1.15	-2.33	0.0000087	0.0168990
ENSMUSG00000106877	Pygm	2.67	1.15	-2.33	0.0000087	0.0168990
ENSMUSG00000070327	Rnf213	8.42	3.58	-2.35	0.0004636	0.1341900
ENSMUSG00000054589	Gm9949	0.47	0.19	-2.49	0.0001458	0.0799610

ENSMUSG00000033788	Dysf	3.75	1.46	-2.57	0.0002493	0.1001700
ENSMUSG00000084858	Gm1980	1.51	0.58	-2.6	0.0000975	0.0640780
ENSMUSG00000027547	Sall4	0.53	0.2	-2.65	0.0005308	0.1455900
ENSMUSG00000028766	Alpl	2.2	0.82	-2.69	0.0000138	0.0204770
ENSMUSG00000049130	C5ar1	1.72	0.63	-2.72	0.0008472	0.1977400
ENSMUSG00000022548	Apod	39.16	13.2	-2.97	0.0002072	0.0956150
ENSMUSG00000074896	Ifit3	16.8	5.59	-3.01	0.0002174	0.0956150
ENSMUSG00000046718	Bst2	6.38	1.9	-3.36	0.0004917	0.1393100
ENSMUSG00000026822	Lcn2	0.8	0.22	-3.6	0.0008274	0.1957700
ENSMUSG00000044749	Abca6	2.45	0.67	-3.64	0.0000014	0.0056129
ENSMUSG00000025492	Ifitm3	13.54	3.44	-3.93	0.0002456	0.1001700
ENSMUSG00000035352	Ccl12	2.88	0.5	-5.71	0.0001445	0.0799610

Table 12c. Differentially expressed genes: AraD1 vs. late (AraD3-6), sorted by fold-change. FC= fold change.

Gene ontology analysis of the list of differentially-expressed genes between SalD1 and AraD1 (n=67) showed significant enrichment of "inflammatory pathway" GO Biological Processes: *Positive regulation of neutrophil chemotaxis*; *Response to interferon alpha*; *Response to interferon beta*; *Defence response to virus*; *Response to lipopolysaccharide*; *Inflammatory response*; and *Innate immune response*. Analysis of genes differentially expressed between AraD1 and AraD3-6 (n=55) again showed significant enrichment of inflammatory pathway GO Biological Processes: *Response to interferon alpha*; *Defense response to virus*; *Regulation of leukocyte migration*; *Chemotaxis*; and *Innate immune response*. No significant enrichment was found in either dataset for GO Molecular Function or GO Cellular Component.

These inflammatory processes were generally enriched by genes which were *upregulated* in AraC-treated animals at D1, and *downregulated* in AraC-treated animals at later timepoints. (**Table 13**). Examples even of individual genes behaving in this way were Ifitm3, Ifit3, Ifit3b, Oasl2, Rarres2, and CCl12. The overall pattern was suggestive of inflammatory pathway upregulation following surgery, with attenuation of the inflammatory response over time. Although I could not exclude a role for inflammation in activating stem cells, marked inflammatory pathway activation tightly restricted to the peri-operative period was a possible artefact of the experimental design.

Comparison	GO Biological Process	Fold Enrichment	p-value	FDR	Genes
Sal vs AraD1	Positive regulation of neutrophil chemotaxis	47.6	4.83E-05	3.11E-02	Thbs4, Dapk2, Ednra
	Response to interferon alpha	45.6	5.42E-05	3.36E-02	Ifitm3, Plscr1, Ifit3
	Response to interferon beta	29.2	1.44E-05	1.49E-02	Stat1, Ifitm3, Plscr1, Ifit3
	Defense response to virus	19.4	1.29E-09	1.00E-05	Rtp4, Stat1, Ifitm3, Plscr1, Ifit3, Ifih1, Itgax, Oasl2, Ifit3b
	Response to lipopolysaccharide	8.2	1.00E-04	4.70E-02	Tbxa2r, Stat1, Ptgfr, CCl12, Ednra, Plscr1
	Inflammatory response	6.4	1.15E-04	4.83E-02	Tbxa2r, Ly86, Ptgfr, Rarres2, Ccl12, Plscr1, Chia1
	Innate immune response	5.2	2.05E-05	1.76E-02	Stat1, Ifitm3, Ifih1, Ly86, Rarres2, Ccl12, Oasl2, Vim, Col20a1, Ifit3
AraD1 vs AraD3-6	Response to interferon alpha	60.5	2.32E-05	3.26E-02	Ifitm3, Ifit3, Bst2
	Defence response to virus	14.3	2.88E-05	3.72E-02	Ifitm3, Ifit3, Bst2, Oasl2, Ifit3b
	Regulation of leukocyte migration	13.6	3.67E-05	4.37E-02	Ptafr, Rarres2, CCl12, Apod, C5ar1
	Chemotaxis	7.5	3.88E-05	4.29E-02	Hmgb2, Ptafr, Draxin, Arhgef16, Rarres2, Ccl12, C5ar1
	Innate immune response	6.2	1.19E-05	2.64E-02	Lcn2, Hmgb2, Ifitm3, Rarres2, Ccl12, Oasl2, Ifit3, H2-Ab1, Bst2

Table 13. Gene Ontology analysis of differentially-expressed SGZ genes after AraC. Upregulated individual genes are shown in green; downregulated genes in red. Note the pattern suggestive of inflammatory pathway activation (in AraD1) followed by attenuation (AraD3-6).

I then turned to my a priori interest and focus in this thesis: whether novel extracellular matrix genes have potential regulatory roles in hippocampal neurogenesis.

To approach this question first in an agnostic way, I ranked the 274 core matrisome genes by the mean level of their expression in the microdissected SGZ of wild-type saline-treated animals (n=4). This provided both a simple "census" of matrisome genes present in the SGZ and some indication of their relative abundance. As a partial step towards validating the in silico analysis I also cross-referenced this "census" with my earlier review of the expression levels of the same genes in the adult mouse SGZ via the Allan Brain Atlas (see previously **Table 3**). My hypothesis was that these two methods of quantifying matrisome gene expression would correlate well. I analysed their inter-relationship qualitatively rather than by using post-hoc statistics (such as a Spearman's correlation), as a formal statistical test seemed a little spurious in this context.

The in silico analysis of microdissected WT SGZ identified n=236 matrisome genes with detectable levels of expression (86.1% of the core matrisome, **Table 14**). Most of these genes (n=177) were expressed at relatively low levels (eCPM <10). Inspection of Table 14 revealed a qualitative correlation between the relative level of gene expression reported by the in silico analysis, and the intensity of in-situ signal displayed by the Allen Brain Atlas. This correlation was far from absolute: notable discrepancies included genes called highly in silico but not by the Allen Brain Atlas (such as Edil3, Crim1, Col4a2, and Nell1), and genes ranked highly by the Allen Brain Atlas, but not in silico (such as Fmod, Fga, Optc, and Otog). Overall however, genes expressed highly in one tended to be expressed highly in the other, whereas many genes expressed at lower levels in the RNA-seq dataset were either expressed at low levels or were undetectable in the Allen Brain Atlas. Where expression was present in both I concluded there was validation of the in silico analysis.

Ensembl gene ID	Gene name	WT expression (Sal)	Allen expression
ENSMUSG00000029309	Sparcl1	846.09	+++
ENSMUSG00000022454	Nell2	728.32	+++
ENSMUSG00000067242	Lgi1	427.96	+++
ENSMUSG00000025020	Slit1	214.82	+++
ENSMUSG00000058297	Spock2	182.85	+++
ENSMUSG00000026185	Igfbp5	172.72	+++
ENSMUSG00000002341	Ncan	157.56	+++
ENSMUSG00000054162	Spock3	143.73	+++

ENSMUSG00000041936	Agrn	141.61	+++
ENSMUSG00000015829	Tnr	131.38	+++
ENSMUSG00000040998	Npnt	118.36	++
ENSMUSG00000018593	Sparc	115.58	+++
ENSMUSG00000033595	Lgi3	111.48	+++
ENSMUSG00000030284	Creld1	108.14	+++
ENSMUSG00000038156	Spon1	105.81	+++
ENSMUSG00000035967	Ddx26b	102.03	+++
ENSMUSG00000034488	Edil3	98.7	0
ENSMUSG00000023886	Smoc2	97.72	+++
ENSMUSG00000020674	Pxdn	96.88	+++
ENSMUSG00000004892	Bcan	94.58	++
ENSMUSG00000020522	Mfap3	92.69	+++
ENSMUSG00000030605	Mfge8	88.52	+++
ENSMUSG00000048222	Mfap1b	80.79	NA
ENSMUSG00000059857	Ntng1	80.01	+++
ENSMUSG00000056427	Slit3	68.97	+++
ENSMUSG00000040488	Ltbp4	65.67	++
ENSMUSG00000031451	Gas6	61.69	+++
ENSMUSG00000056222	Spock1	60.14	+++
ENSMUSG00000022324	Matn2	53.09	++
ENSMUSG00000068479	Mfap1a	49.66	+++
ENSMUSG00000058897	Col25a1	49.13	+++
ENSMUSG00000050122	Vwa3b	41.99	+++
ENSMUSG00000024074	Crim1	41.01	0
ENSMUSG00000031503	Col4a2	35.48	+
ENSMUSG00000028047	Thbs3	32.54	+++
ENSMUSG00000026141	Col19a1	31.96	+++
ENSMUSG00000007594	Hapln4	31.45	++
ENSMUSG00000046613	Vwa5b2	30.11	++
ENSMUSG00000030889	Vwa3a	29.61	++
ENSMUSG00000017493	Igfbp4	28.8	+++
ENSMUSG00000026478	Lamc1	26.21	++
ENSMUSG00000023272	Creld2	25.33	++
ENSMUSG00000039252	Lgi2	23.69	+++
ENSMUSG00000031502	Col4a1	21.04	+++
ENSMUSG00000055409	Nell1	19.54	0
ENSMUSG00000063765	Chadl	18.43	NA
ENSMUSG00000033327	Tnxb	18.16	++
ENSMUSG00000001119	Col6a1	16.4	+++
ENSMUSG00000042453	Reln	16.24	+++
ENSMUSG00000024330	Col11a2	16.01	+
ENSMUSG00000024940	Ltbp3	15.97	+
ENSMUSG00000021613	Hapln1	15.95	++

ENSMUSG00000019880	Rspo3	14.72	++
ENSMUSG00000042436	Mfap4	11.85	++
ENSMUSG00000034687	Fras1	11.8	+
ENSMUSG00000006369	Fbln1	11.36	+
ENSMUSG00000031558	Slit2	10.34	0
ENSMUSG00000042116	Vwa1	10.32	0
ENSMUSG00000027570	Col9a3	10.01	++
ENSMUSG00000017344	Vtn	9.96	+++
ENSMUSG00000079022	Col22a1	9.92	0
ENSMUSG00000030607	Acan	9.69	0
ENSMUSG00000036560	Lgi4	9.56	+
ENSMUSG00000032289	Thsd4	9.34	0
ENSMUSG00000015647	Lama5	9.08	0
ENSMUSG00000023046	Igfbp6	9.01	0
ENSMUSG00000064080	Fbln2	8.86	++
ENSMUSG00000060572	Mfap2	8.57	0
ENSMUSG00000027204	Fbn1	8.32	+
ENSMUSG00000001870	Ltbp1	8.25	0
ENSMUSG00000036256	Igfbp7	7.46	+++
ENSMUSG00000034164	Emid1	7.36	+++
ENSMUSG00000021390	Ogn	7.26	++
ENSMUSG00000052911	Lamb2	7.11	0
ENSMUSG00000020427	Igfbp3	7.02	0
ENSMUSG00000047793	Sned1	6.89	+
ENSMUSG00000023186	Vwa5a	6.84	0
ENSMUSG00000004894	Hapln2	6.58	0
ENSMUSG00000026193	Fn1	6.3	++
ENSMUSG00000024909	Efemp2	6.25	+
ENSMUSG00000071984	Fndc1	6.16	++
ENSMUSG00000041577	Prelp	5.71	+
ENSMUSG00000016356	Col20a1	5.68	+
ENSMUSG00000043631	Ecm2	5.57	+
ENSMUSG00000031963	Bmper	5.5	+
ENSMUSG00000025650	Col7a1	5.41	+
ENSMUSG00000028364	Tnc	5.32	++
ENSMUSG00000015354	Pcolce2	5.23	0
ENSMUSG00000019899	Lama2	5.13	NA
ENSMUSG00000016995	Matn4	5.02	+
ENSMUSG00000021614	Vcan	4.78	+
ENSMUSG00000020019	Ntn4	4.6	+
ENSMUSG00000026639	Lamb3	4.58	+
ENSMUSG00000026837	Col5a1	4.37	0
ENSMUSG00000044006	Cilp2	4.32	NA
ENSMUSG00000046167	Gldn	4.3	0

ENSMUSG00000028108	Ecm1	4.19	+
ENSMUSG00000028753	Vwa5b1	4.11	0
ENSMUSG00000023885	Thbs2	4.06	+++
ENSMUSG00000028626	Col9a2	4.06	+
ENSMUSG00000031375	Bgn	4.03	+
ENSMUSG00000032572	Col6a4	4.01	0
ENSMUSG00000035551	Igfbpl1	3.96	+++
ENSMUSG00000053475	Tnfaip6	3.56	+++
ENSMUSG00000001930	Vwf	3.55	++
ENSMUSG00000018844	Fndc8	3.49	0
ENSMUSG00000035513	Ntng2	3.26	+++
ENSMUSG00000040690	Col16a1	3.26	+
ENSMUSG00000039323	Igfbp2	3.24	++
ENSMUSG00000024598	Fbn2	3.18	+
ENSMUSG00000021186	Fbln5	3.07	0
ENSMUSG00000021136	Smoc1	3.06	0
ENSMUSG00000029307	Dmp1	2.9	0
ENSMUSG00000026042	Col5a2	2.86	0
ENSMUSG00000051920	Rspo2	2.64	+
ENSMUSG00000036446	Lum	2.57	0
ENSMUSG00000020902	Ntn1	2.54	0
ENSMUSG00000025776	Crispld1	2.46	+++
ENSMUSG00000002020	Ltbp2	2.38	0
ENSMUSG00000054196	Cthrc1	2.36	+
ENSMUSG00000027966	Col11a1	2.33	+
ENSMUSG00000020473	Aebp1	2.25	0
ENSMUSG00000058806	Col13a1	2.25	+
ENSMUSG00000045672	Col27a1	2.21	+++
ENSMUSG00000051228	Nyx	2.19	+
ENSMUSG00000036334	Igsf10	2.13	0
ENSMUSG00000024053	Emilin2	2.08	0
ENSMUSG00000037362	Nov	2.03	++
ENSMUSG00000020467	Efemp1	2	0
ENSMUSG00000015314	Slamf6	1.97	0
ENSMUSG00000028871	Rspo1	1.94	0
ENSMUSG00000038112	AW551984	1.88	0
ENSMUSG00000042961	Egflam	1.88	0
ENSMUSG00000004098	Col5a3	1.82	+
ENSMUSG00000006014	Prg4	1.78	0
ENSMUSG00000064310	Zpld1	1.75	0
ENSMUSG00000026479	Lamc2	1.73	0
ENSMUSG00000029163	Emilin1	1.71	+
ENSMUSG00000021806	Nid2	1.7	0
ENSMUSG00000020241	Col6a2	1.65	+++

ENSMUSG00000022483	Col2a1	1.6	++
ENSMUSG00000066842	Hmcn1	1.58	0
ENSMUSG00000028369	Svep1	1.57	0
ENSMUSG00000035270	Impg2	1.53	+
ENSMUSG00000001435	Col18a1	1.49	0
ENSMUSG00000041445	Mmrn2	1.49	0
ENSMUSG00000024076	Vit	1.43	+
ENSMUSG00000020077	Srgn	1.4	0
ENSMUSG00000028776	Tinagl1	1.4	0
ENSMUSG00000048126	Col6a3	1.38	++
ENSMUSG00000024421	Lama3	1.36	+
ENSMUSG00000028195	Cyr61	1.36	0
ENSMUSG00000039899	Fgl2	1.33	0
ENSMUSG00000019846	Lama4	1.32	+
ENSMUSG00000005124	Wisp1	1.25	0
ENSMUSG00000021702	Thbs4	1.25	++
ENSMUSG00000031274	Col4a5	1.24	0
ENSMUSG00000030606	Hapln3	1.21	0
ENSMUSG00000020953	Coch	1.19	+
ENSMUSG00000028339	Col15a1	1.17	+
ENSMUSG00000029675	Eln	1.15	++
ENSMUSG00000029661	Col1a2	1.13	+
ENSMUSG00000009487	Otog	1.12	+++
ENSMUSG00000059022	Kcp	1.08	0
ENSMUSG00000031825	Crispld2	1.01	0
ENSMUSG00000091345	Col6a5	0.98	NA
ENSMUSG00000067158	Col4a4	0.97	0
ENSMUSG00000035258	Abi3bp	0.95	0
ENSMUSG00000063564	Col23a1	0.95	0
ENSMUSG00000001506	Col1a1	0.94	0
ENSMUSG00000019997	Ctgf	0.92	0
ENSMUSG00000029718	Pcolce	0.85	0
ENSMUSG00000031594	Fgl1	0.85	0
ENSMUSG00000037095	Lrg1	0.82	0
ENSMUSG00000035493	Tgfbi	0.79	0
ENSMUSG00000005397	Nid1	0.77	0
ENSMUSG00000024979	Tectb	0.77	NA
ENSMUSG00000021388	Aspn	0.74	0
ENSMUSG00000040152	Thbs1	0.74	++
ENSMUSG00000032332	Col12a1	0.7	+
ENSMUSG00000010311	Optc	0.69	+++
ENSMUSG00000033860	Fgg	0.65	0
ENSMUSG00000048368	Omd	0.65	0
ENSMUSG00000045326	Fndc7	0.64	++

ENSMUSG00000070564	Ntn5	0.64	NA
ENSMUSG00000032796	Lama1	0.63	0
ENSMUSG00000019929	Dcn	0.61	0
ENSMUSG00000079465	Col4a3	0.61	0
ENSMUSG00000012889	Podnl1	0.6	0
ENSMUSG00000009654	Oit3	0.59	0
ENSMUSG00000026840	Lamc3	0.58	0
ENSMUSG00000027386	Fbln7	0.56	0
ENSMUSG00000021223	Papln	0.55	0
ENSMUSG00000057606	Colq	0.54	0
ENSMUSG00000028600	Podn	0.52	+
ENSMUSG00000043789	Vwce	0.51	+
ENSMUSG00000068196	Col8a1	0.51	0
ENSMUSG00000028001	Fga	0.49	+++
ENSMUSG00000031273	Col4a6	0.48	0
ENSMUSG00000032343	Impg1	0.48	0
ENSMUSG00000055632	Hmcn2	0.48	NA
ENSMUSG00000026043	Col3a1	0.47	0
ENSMUSG00000029797	Sspo	0.42	0
ENSMUSG00000062074	Wisp3	0.42	NA
ENSMUSG00000026147	Col9a1	0.4	+
ENSMUSG00000037705	Tecta	0.4	0
ENSMUSG00000028763	Hspg2	0.38	0
ENSMUSG00000030218	Mgp	0.37	+
ENSMUSG00000020429	Igfbp1	0.36	0
ENSMUSG00000043719	Col6a6	0.36	0
ENSMUSG00000028197	Col24a1	0.35	0
ENSMUSG00000029304	Spp1	0.34	0
ENSMUSG00000053268	Dspp	0.34	0
ENSMUSG00000056174	Col8a2	0.32	0
ENSMUSG00000092200	Tnxa	0.32	NA
ENSMUSG00000027750	Postn	0.31	0
ENSMUSG00000022371	Col14a1	0.3	+
ENSMUSG00000041559	Fmod	0.3	+++
ENSMUSG00000049580	Tsku	0.3	0
ENSMUSG00000026574	Dpt	0.29	0
ENSMUSG00000031849	Comp	0.29	NA
ENSMUSG00000090084	Srpx	0.29	0
ENSMUSG00000109144	Ntn5	0.29	NA
ENSMUSG00000030116	Mfap5	0.28	0
ENSMUSG00000042379	Esm1	0.27	+
ENSMUSG00000031253	Srpx2	0.25	++
ENSMUSG00000039462	Col10a1	0.25	++
ENSMUSG00000004948	Zp3	0.24	0

ENSMUSG00000032852	Rspo4	0.24	0
ENSMUSG00000108715	Ltbp4	0.24	++
ENSMUSG00000108927	Ntn5	0.23	0
ENSMUSG00000030911	Zp2	0.22	0
ENSMUSG00000040533	Matn1	0.22	0
ENSMUSG00000019936	Epyc	0.21	0
ENSMUSG00000025064	Col17a1	0.2	0
ENSMUSG00000050700	Emilin3	0.2	0

Table 14: Intersection of RNA-seq and Allen Brain Atlas matrisome expression data. WT= wild-type. NA= not present in the Allen Brain Atlas. WT gene-level transcript expression in laser-dissected SGZ is presented as estimated counts per million (eCPM).

Having validated matrix gene expression in the SGZ of saline-treated animals, I asked whether any matrisome genes were differentially expressed following AraC. This question was aimed at identifying possible ECM regulators of neurogenesis seen following AraC. I hypothesised that a sub-set of ECM genes would be differentially expressed between the treatment groups. The gene ontology analysis presented earlier in **Table 13** had identified a few isolated ECM genes within enriched inflammatory pathways (specifically Thbs4 and Col20a1). It seemed possible that these genes were upregulated as experimental artefact from surgery-related inflammation. To look for any other signal of ECM-related genes I intersected my differentially expressed gene-set with the gene list of the core matrisome.

This analysis revealed significant upregulation of Thbs4, Col20a1, Fbln5, Mgp, and Ogn at D1 post-AraC, and of Sspo during the later period of NSPC proliferation (AraC D3-6) (**Table 15**).

Gene	Timepoint	Direction	Fold-change	p-value	FDR
Thbs4	AraD1	Up	4.3	3.62E-05	4.36E-02
Mgp	AraD1	Up	3.9	1.52E-05	2.82E-02
Sspo	AraD3-6	Up	3.8	3.26E-06	1.12E-02
Fbln5	AraD1	Up	3.5	6.46E-04	1.79E-01
Ogn	AraD1	Up	2.3	7.09E-06	2.13E-02
Col20a1	AraD1	Up	2.1	4.99E-06	2.13E-02

Table 15: Differentially-expressed matrisome genes following AraC. Genes are ranked in order of fold-change. FDR= False Discovery Rate.

As **Table 15** shows, the highest-expressed matrisome gene not to be implicated in a possible inflammatory reaction to surgery was matrix Gla protein (Mgp) (Sal= 0.37 eCPM [0.27-0.49]; AraD1= 1.45 eCPM [0.93-2.64], Fold change= 3.95, p=1.52e-05, q=0.028, and **Figure 24**). Indeed Mgp was in the top quintile of differentially expressed genes at AraD1 for both Fold-Change and FDR (see **Tables 11b and 11c**). Attractively, Mgp presented a biologically plausible mechanism of regulating neurogenesis: it is a calcium-binding ECM protein with a functional role in preventing arterial and cartilaginous calcification. [Luo et al. 1997] On binding calcium, Mgp is activated as a bone morphogenetic protein (BMP) antagonist. [Yao et al. 2006, Zebboudj et al. 2002] Because BMP signaling maintains NSC quiescence [Mira et al. 2010], Mgp presented as both a robustly expressed and biologically plausible, novel, potential matrix regulator of neural stem cell activation. I therefore selected matrix Gla protein as a target for further analysis.

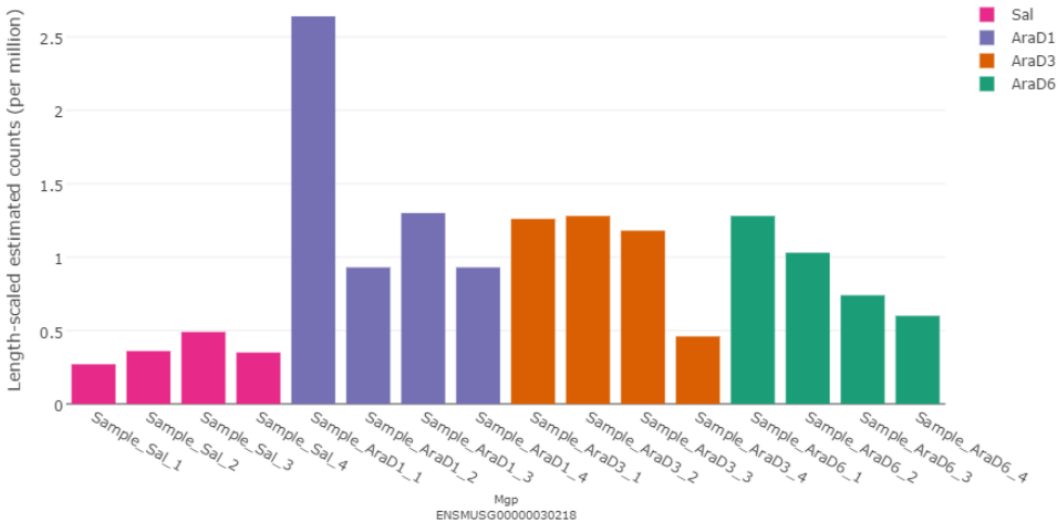

Figure 24. Matrix Gla protein is upregulated in the SGZ at the time of NSC activation. Gene expression bar plot of estimated counts per million per animal. Note Mgp upregulation at D1 following AraC, which is maintained at a lower level at later time-points. Bar plot generated on the Shiny platform (Dr. Jon Manning, University of Edinburgh).

5.2.4 Matrix Gla protein is up-regulated in association with NSC activation

I wished to validate the in silico analysis suggesting Mgp as a candidate ECM regulator of adult neurogenesis at D1 post-AraC. I infused AraC or Saline to an independent cohort of animals (n=4 per group) and processed tissue for analysis at D1 post-pump removal. Attempts to show upregulation of Mgp protein by immunofluorescence were unsuccessful. Interpretation of the negative staining was difficult owing to uncertainties over whether tissue preparation and staining conditions were suitable and whether the antibodies were effective.

I therefore switched to study Mgp expression at the transcriptional level using the 'RNAScope' in situ hybridisation technology. [Wang et al. 2012] Two RNAScope probe-sets were developed for the mouse Mgp transcript: one using a colorimetric detection assay and another using a more sensitive multiplex fluorescent detection assay. In situ hybridisation and analyses were conducted as previously described in **Ch 2.9.** For both the colorimetric and fluorescent assays, there were no outliers in the data as assessed by inspection of box-plots. Data from the colorimetric assay were normally distributed (Shapiro-Wilk's $p>0.05$) with equality of variances (Levene's test $p>0.05$), and were analysed using an independent-samples t-test. Data from Saline-treated animals for the multiplex fluorescent assay were non-normally distributed (Shapiro-Wilk's $p=0.021$). Accordingly the multiplex fluorescent assay was analysed using the Mann-Whitney U test, and since the between-group distribution of Mgp fluorescence was similar on visual inspection, medians are reported.

The colorimetric assay showed significant upregulation of Mgp mRNA in the SGZ and dentate gyrus at D1 post-AraC (mean Mgp+ signal area per field: Sal=647.6μm^2 [SD=234.8], AraD1=1641.9μm^2 [SD=665.1]; $t[6]=2.820$; $p=0.030$). In support, the multiplex fluorescent assay showed significantly higher median Mgp signal in AraC-treated animals (median Mgp+ signal area per field: Sal=5339μm^2, AraD1=7221μm^2; $U=16.000$; $z=2.309$; $p=0.029$) **(Figure 25)**. These analyses confirmed the in silico analysis in an independent group of animals and indicate that following AraC, Mgp mRNA is up-regulated in the DG and SGZ, in association with transcriptional signals of NSC activation highlighted previously.

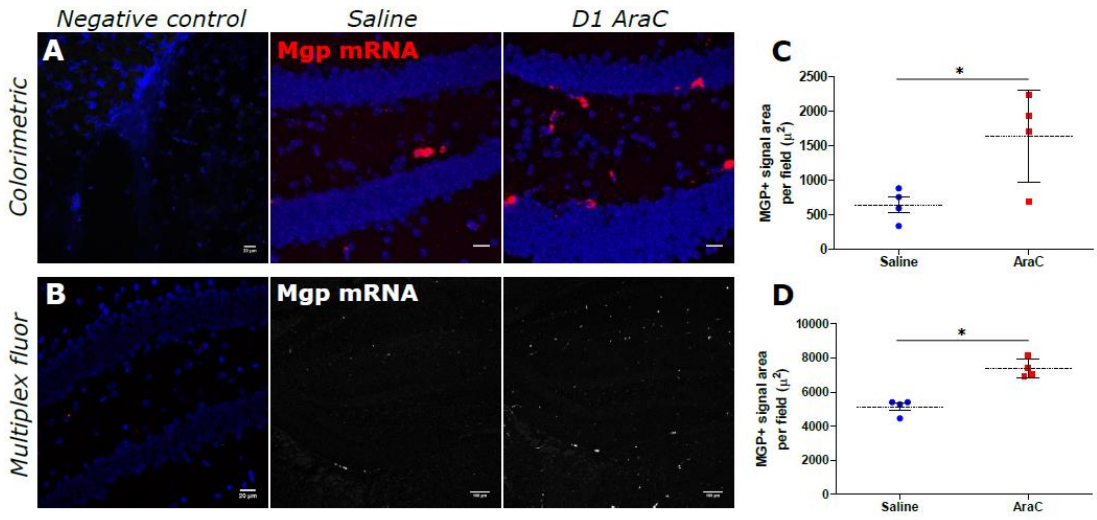

Figure 25. In-situ hybridisation confirms upregulation of Mgp mRNA following AraC.
A: Representative images from RNAScope Colorimetric/red fluorescent kit, (from left to right) negative control, Saline-treated mice, and AraC-treated mice at D1 post-infusion. **B:** RNAScope multiplex fluorescent kit, same. **C:** Quantification of (A). **D:** Quantification of (B). * $p<0.05$; n=4 animals per group; scale bars= 20 microns.

5.2.5 Axial sectioning effectively visualises the SGZ vascular niche

Matrix Gla protein has a known role in vascular biology, and the SGZ is known to be a vascular niche. [Palmer et al. 2000] However most studies examining blood vessels and NSPCs used coronal or saggital sections to illustrate these relationships. I reasoned that since the SGZ vasculature lies mainly in an axial (transverse) plane, it could be better illustrated by sectioning in the axial plane. I optimised tissue orientation and used this 'axial sectioning' approach to better show the close interrelationship of the SGZ vasculature with NSPCs. Using these views, the close relationship of NSPCs to blood vessels can be clearly visualised **(Figure 26)**. Interestingly and in passing, a subset of proliferating Dcx+ neuroblasts adhere very closely to blood vessels - a finding which was subsequently reported independently [Sun et al. 2015] and is not shown here.

5.2.6 Matrix Gla protein is expressed by endothelial cells in the adult DG

Since the SGZ is a vascular niche and Mgp has a known role in vascular biology, I next asked whether the increased expression of Mgp seen following AraC was localised to blood

vessels in the SGZ. The publicly-available Barres RNA sequencing database [Zhang et al. 2014] suggested that endothelial cells in the CNS do indeed express Mgp. To focus this suggestive finding on the adult SGZ post-AraC I used RNAScope fluorescent ISH with dual probes for Mgp and PECAM-1 (CD31), a protein expressed by endothelial cells. Results showed co-labelling of Mgp with PECAM-1, suggesting that the SGZ microvasculature is indeed the source of Mgp upregulation at D1 post-AraC **(Figure 27)**.

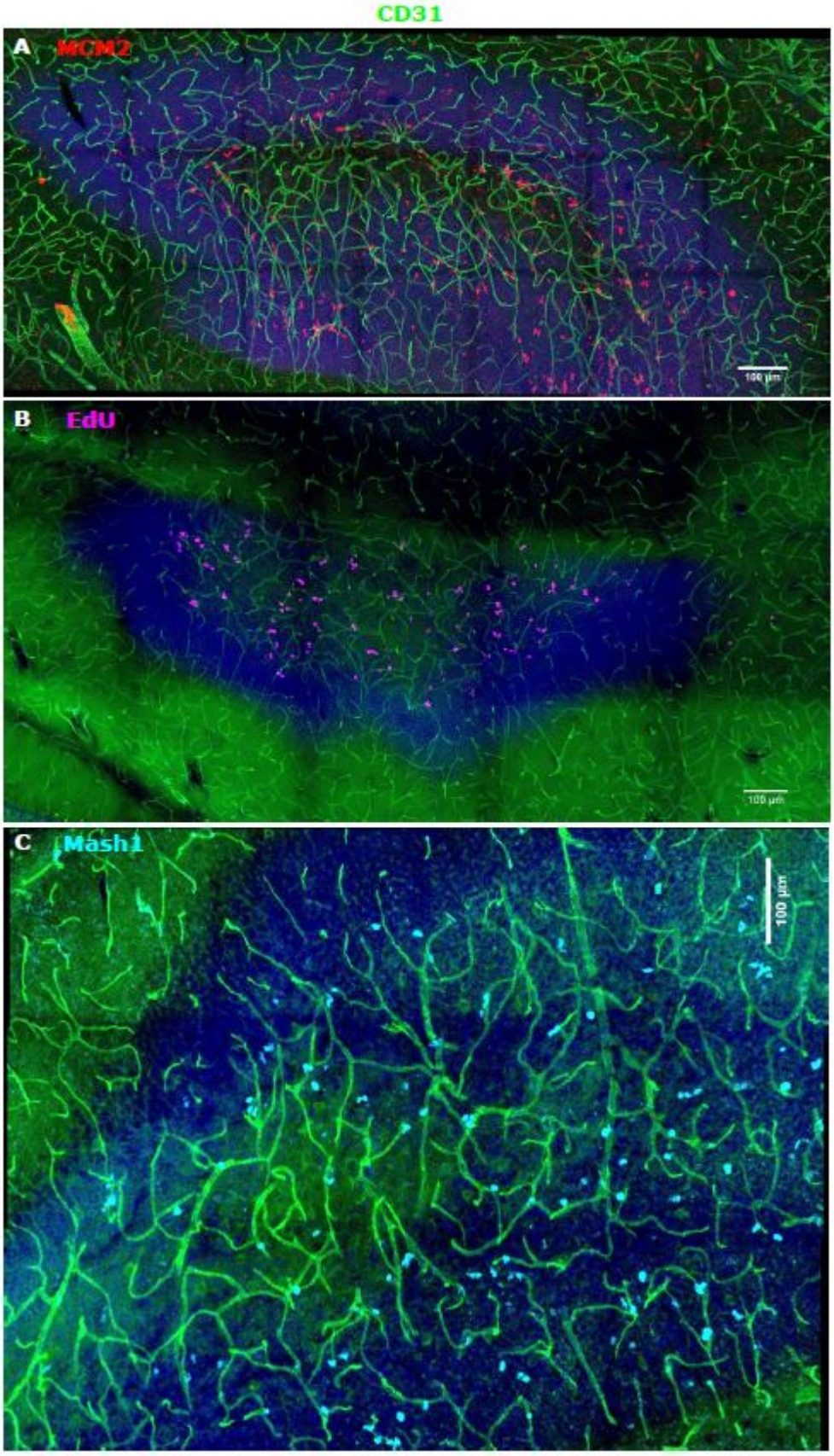
CD31
A
MCM2
100 µm
B
EdU
100 µm
C
Mash1
100 µm

Figure 26: Axial sectioning effectively visualises the SGZ vascular niche. (from previous page)

A: Axial plane view of the subgranular zone showing frequent clustering of MCM2+ proliferating NSPCs around CD31+ blood vessels. **B:** Axial view showing the relationship between mitotically active EdU+ cells and BVs. **C:** Mash1+ IPs. Scale bars = 100 microns.

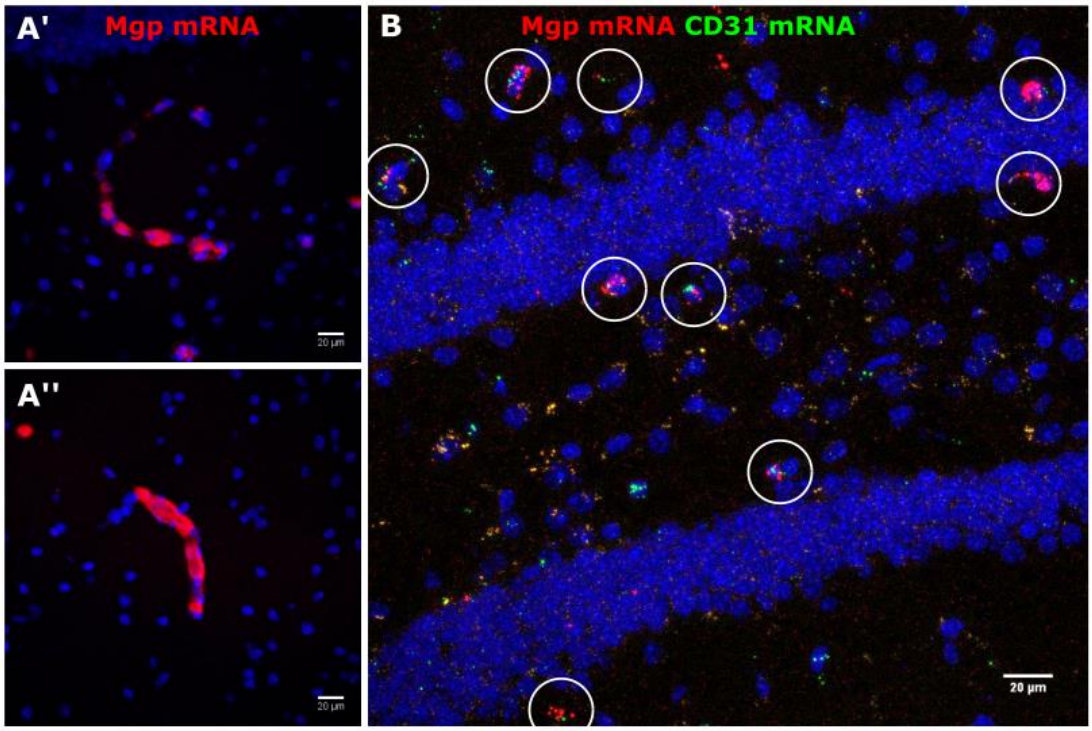

Figure 27. Matrix Gla protein is up-regulated by endothelial cells in the dentate gyrus following AraC.

A' and **A'':** RNAScope in situ hybridization (Colorimetric/red fluorescent kit) Mgp mRNA signal localising to structures that highly resemble blood vessels. **B:** RNAScope (Multiplex fluorescence kit) Mgp mRNA colabelled in close vicinity or colocalised to PECAM1/CD31 mRNA (examples circled). Scale bars= 20 microns.

5.3 Discussion

In this Chapter I sought to identify novel potential matrix regulators of hippocampal neurogenesis in a candidate-free way. I optimised the technique of laser capture microdissection of the subgranular zone, using knowledge gained in **Chapter 3** to target key time-points in the post-AraC regenerating niche. From the microdissected SGZ I extracted RNA of sufficient quality to allow RNA sequencing. I used Dr. Jonathan Manning's bioinformatic analysis of differential gene expression to uncover a transcriptional footprint of NSC activation and proliferation within the data, confirming that this ambitious experiment had worked. I then used the dataset to identify a group of previously unreported ECM genes at time-points of NSC activation, and differentiation. From this list of candidates I selected and validated matrix Gla protein (Mgp). I then used multi-channel in situ hybridisation to localise Mgp mRNA to cells co-expressing PECAM-1 (CD31) mRNA, suggesting that Mgp is expressed by the hippocampal microvasculature. Further studies will seek to establish mechanisms by which Mgp might regulate hippocampal neurogenesis.

5.3.1 Limitations

Before discussing these results in a wider context some limitations should again be acknowledged. First in terms of bias, although RNA sequencing has the advantage of avoiding the selection bias of microarrays, technical bias is still likely to exist. As an example within my data which can be seen at a glance above **(Fig. 22)**, Principal Components Analysis suggested a significant effect of 'replicate'. This suggested that I did not treat all samples identically at some point prior to sequencing. Additionally because only very small amounts of RNA could be extracted from the micro-dissected SGZ, PCR amplification was performed before sequencing. Amplification bias may lower power and/or increase the false discovery rate, and may not be fully corrected by computational methods. [Parekh et al. 2016]

Second and thinking about sources of error, false positives or false negatives in transcriptional-level analyses may occur when proteins are heavily post-translationally regulated. In this situation, levels of mRNA expression may not correlate with levels of protein expression. For example despite the clear signal of Itgb1 protein expression on proliferating NSPCs in **Chapter 4**, and a transcriptional signal of a regenerating,

proliferative SGZ in the current Chapter, Itgb1 mRNA was not differentially regulated between quiescent and activated states. This was consistent with the known high level of post-translational regulation of Itgb1. [Condic and Letourneau 1997] This is a relevant limitation here because Mgp is known to be post-translationally modified, indeed its functional ability to sequester BMPs is thought to depend on it. [Wallin et al. 2000]

These two examples of RNA sequencing limitations highlight the necessity of validating the bioinformatic analysis. Attempts to quantify Mgp using immunofluorescence were ultimately abandoned owing to concern about the sensitivity and specificity of the primary antibodies. I considered whether to conduct a proteomic analysis of the regenerating SGZ. Ultimately however even if the technical challenge of analysing the proteome of such a tiny amount of tissue could had been overcome, the current sensitivity of proteomics is far lower than it is for RNAseq. At present therefore Mgp upregulation has not been validated at the protein level (but see **Ch. 6** for further planned experiments).

Third and scientifically, data are derived from the septal pole and mid-section of the DG rather than the temporal pole. Although the septotemporal extent of microdissection was comparable between replicates, results may not necessarily apply to the temporal SGZ.

Fourth, although PECAM-1 and Mgp mRNA were often tightly colocalised within structures that looked like blood vessels, I did not exclude pericytes as a reported [Canfield et al. 2000] and alternative potential source.

5.3.2 Results in context

In the peripheral nervous system, Mgp is implicated in the regulation of BMP2-dependent neurite outgrowth of cultured postnatal rat sympathetic neurons. [Moon and Birren 2008] To the best of my knowledge however the candidate-driven experimental literature on Mgp in the CNS is sparse. Although much literature has focused on its expression by endothelial cells, its upregulation has also been reported in cultured P5 rat retinal ganglion cells exposed to glial-conditioned medium. Addition of recombinant Mgp to culture in an attempted 'gain-of-function' experiment did not alter the frequency and size of spontaneous excitatory postsynaptic currents, suggesting no effect on spontaneous synaptic activity. [Goritz et al. 2007] However as the authors also noted, Mgp is thought to require to be carboxylated in order to exert certain biological effects. It is not clear whether this was ensured for the recombinant protein, and its function was not established. Meanwhile in the cerebral

microvasculature, Mgp was found to induce notch signalling pathway via upregulation of activin receptor-like kinase 1 (Alk1), leading to disordered arteriovenous coupling. [Yao et al. 2013]

A potential role for Mgp in regulating hippocampal neurogenesis has not been previously reported. With a degree of healthy scepticism one might ask: if no-one has found it in the hippocampus yet, doesn't that rather suggest that it's not there?

One possible reason for the lack of prior focus on Mgp is that most RNA sequencing studies of adult hippocampal neurogenesis have been conducted on purified NSPCs. [e.g., Walker et al. 2016, Shin et al. 2015, Guo et al. 2011] Endothelial cell-derived transcripts may not appear highly in lists of differentially-expressed genes derived from NSPCs. Additionally although many microarray studies have characterised the hippocampus and DG, some may not have been sensitive enough to reliably detect the low quantities of Mgp mRNA which sequencing revealed. A third possibility is that Mgp may be up-regulated in response to injury or disease, making it dependent on the experimental paradigm.

Nonetheless upregulation of Mgp has, in fact, been reported incidentally within some CNS transcriptional datasets. To the best of my knowledge it has not been further validated or given a specific experimental focus in these studies. Perhaps the most intriguing example is that of Stankiewicz et al., who reported a gradual increase in Mgp mRNA expression over two weeks following the onset of social stress, with attenuation during subsequent recovery, in the hippocampus in mice. [Stankiewicz et al. 2015] The transcript was clustered with others annotated to be part of the 'injury response', and the authors accepted it as such. However this begs the question as to why two weeks of stress would trigger a hippocampal injury response. Chronic stress is however a robust negative regulator of hippocampal neurogenesis [Dranovsky and Hen 2006]; if one considers the 'injury response' as a homeostatic attempt to return balance to neurogenesis, is possible to see a potential consistency of signal in comparison with my data.

Mgp upregulation has been also reported acutely following MCA occlusion, in the peri-infarct region in rats. [Ramos-Cejudo et al. 2012] Interestingly in this study Mgp upregulation coincided with downregulation of genes associated with NSC quiescence (e.g. BMP4 and Hes5) and upregulation of cell cycle markers. Since ischaemic injury is well-known to trigger an attempted neurotrophic response in the adult CNS [Lindvall and Kokaia

2015], this study is also consistent with my hypothesis that it may function to mediate neurogenesis.

Others report significant upregulation of Mgp mRNA at time-points of D6-D10 following injury to the olfactory pathway in mice, followed by a negative rebound at D20-D30. [Roet et al. 2013] In vitro, the authors found that endothelial cells transfected with Mgp siRNA did not alter the outgrowth of embryonic dorsal root ganglia neurons, and went on to pursue other candidates. Mgp mRNA was also up-regulated chronically following peripheral airway allergy stimulus, in the frontal cortex in mice. [Sarlus et al. 2013]. Its functional role in the chronic response to allergy was not studied and remains obscure. Similarly Mgp is also reportedly expressed in human entorhinal cortex, a brain area implicated in the onset of Alzheimer's disease, although its function in this respect was not studied. [Santa-Maria et al. 2010] Lastly a discussion about Mgp in the adult brain requires acknowledgement of evidence for both pro-angiogenesis [Kuzontkoski et al. 2010] and pro-migratory effects in glioma. [Fu et al. 2017]

Along with my own, these studies do provide a consistent signal to suggest that the matrix molecule Mgp is expressed in the adult brain under certain experimental conditions. Whether injury or disease is a necessary condition, whether protein levels are altered, and its functional role remain unclear. These questions provide food for thought and suggest a clear forward experimental strategy (see **Ch. 6**).

5.3.3 Chapter summary

In summary, in this Chapter I asked whether it was possible to identify novel potential matrix regulators of hippocampal neurogenesis. I optimised and successfully executed laser capture microdissection of and RNA extraction from the regenerating SGZ niche. RNA sequencing, bioinformatic analysis, and transcriptional validation revealed endothelial cell-derived matrix Gla protein as a possible novel candidate regulator of NSC activation.

In the final chapter I will briefly summarise the main findings of this thesis, discuss the state of the science with respect to matrix regulation of hippocampal neurogenesis, and outline current hypotheses for future study.

6 DISCUSSION

6.1 Summary of main findings

In this thesis I asked the question: does extracellular matrix regulate hippocampal neurogenesis? In **Chapter 1** I searched for evidence linking ECM and the regulation of mouse neural stem cell biology at any developmental stage. Results from both targeted and agnostic search strategies suggested that most core matrisome genes remain unstudied with respect to NSCs, with existing literature highly skewed towards a small number of genes which act as model systems or for which productive transgenic models exist. I identified an even smaller list of ECM genes which have been implicated in the regulation of hippocampal neurogenesis specifically, despite the in situ expression of a high number of ECM genes in the adult SGZ.

I then searched for literature on a regulatory role for the archetypal cell surface receptor for ECM, Integrin β1. In vivo, conditional genetic knockout studies of Itgb1 function in the CNS included a wide range of neural cell types emerging at varying stages of development. Embryonic and early post-natal developmental stages were the best characterised. These studies suggested a critical role for Itgb1 in neurodevelopment, regulating the proliferation, survival, adhesion, and migration of developing neurons. In vitro, embryonic or early postnatal neurodevelopment were again the best-studied developmental stages. In general Itgb1 was again implicated in the positively regulation of adhesion, proliferation, differentiation, migration, and/or survival of NSCs at different developmental stages. These functions were found often to depend on interactions with specific molecules in the ECM such as laminin.

In **Chapter 3** I began my experiments by studying the reliability of two ways of manipulating hippocampal neurogenesis: AraC infusion, and a single electroconvulsive shock. Results confirmed that AraC ‘re-boots’ neurogenesis, with individual NSPC subpopulations recovering in a biologically sequential manner. A single electroconvulsive shock efficiently activated Nestin+ RGLs within one day, causing increased neurogenesis seven days later. Both models were therefore suitable to target specific subpopulations of NSPCs by varying the length of follow-up in future studies.

I then ran a series of experiments to test whether matrix signalling regulates adult neurogenesis. In **Chapter 4** I took a candidate approach to this question by hypothesising a regulatory role for Itgb1. Using an adult NSC-specific inducible knockout strategy, results suggested that integrin signaling regulates multiple aspects of adult hippocampal neurogenesis, including proliferation and neural differentiation. Preliminary data suggest a possible role for Itgb3 compensatory upregulation. At the time of writing the precise contributory role of Itgb1 therefore remains unclear. Although more studies are underway to confirm or refute Itgb3 status, the data support the general hypothesis that ECM signalling, via integrins, regulates hippocampal neurogenesis.

Meanwhile in **Chapter 5**, I asked whether it was possible to identify novel potential matrix regulators of hippocampal neurogenesis in a candidate-free way. The transcriptome of the regenerating SGZ was sequenced and analysed for differential gene expression. Results identified endothelial cell-derived matrix Gla protein as a validated, potential novel matrix regulator of adult neural stem cell activation. In addition the analysis identified a number of other novel candidate regulators that may be suitable for validation in future studies.

6.2 State of the science

6.2.1 Technical strategies to manipulate hippocampal neurogenesis

AraC infusion has rarely been studied with the specific intent of characterising the SGZ NSPC response (see **Ch. 1** and **Table 1**). Those authors that have done so reported initial ablation of proliferating cells, followed by recovery and subsequent rebound of NSPCs over a variable period of 4-15 days. My data corroborate these findings, adding that AraC - perhaps surprisingly - does not induce a clear rebound expansion of the aNSC population, which in post-hoc tests had merely recovered to baseline by D3 post-infusion. Instead the rebound appears to be mediated by proliferative expansion of the Tbr2+ and Ascl1+ IP subpopulations. In my experiments this proliferative rebound was apparent at D6-D8 post-infusion. By D10 a new population of Dcx+ NBs, lacking radial processes and still proliferative, was still recovering. I did not examine whether this population of new NBs continues to expand, but the study by Hodge et al. would suggest that it might. [Hodge et al. 2008]

These findings confirm that AraC triggers a biologically sequential, rebound regeneration of hippocampal neural progenitors. Because this sequential recovery was relatively predictable in time, my data suggest AraC as a tool to focus experimental questions of interest on large numbers of simultaneously-born, relatively homogeneous progenitor subpopulations. This manoeuvre may increase power to detect experimental effects. Whether mechanisms that regulate the NSPC response to AraC - being injury-mediated - are generalisable to homeostatic neurogenesis remains unclear (see below).

It was already established that a single electroconvulsive shock can activate adult hippocampal NSCs, most persuasively by Weber et al. [Weber et al. 2013] My data extend this finding to a different NSC lineage, namely that of nestin-expressing cells. I used lineage tracing to demonstrate for the first time that a single shock leads directly to increased neural fate specification in the daughter progenitor cells born from activated NSCs. I reported preliminary data suggesting that different NSC lineages may respond at differential rates to the stimulus. These signals lead naturally on to further questions about NSC heterogeneity in response to a single shock (see below).

6.2.2 The regulatory role of Itgb1 in hippocampal neurogenesis

When I started my experiments, the role of the matrix receptor Itgb1 in regulating hippocampal neurogenesis was unreported. Subsequently two papers were published exploring the role of Itgb1 or Itgb1-associated signalling in the process. [Brooker et al. 2016, Porcheri et al. 2014,] These studies suggested a negative regulatory function in respect to proliferation, and a positive regulatory role as regards neuronal fate commitment. However both were compromised by a lack of specificity with respect respectively to the NSPC lineage, and to Itgb1 itself. My experiments addressed this gap by inducibly deleting the Itgb1 gene in a highly specific manner from NSCs.

At the time of writing it remains difficult to reach a firm conclusion about the role of Itgb1 in regulating hippocampal neurogenesis. This is primarily due to recent preliminary data suggesting compensatory upregulation of a different β subunit, perhaps Itgb3. If true, it will be hard to attribute the observed phenotype of increased proliferation and increased neuronal fate commitment directly to Itgb1. Experiments are ongoing in this respect (see below) and any further interpretation will have to wait on the results. However also if true, my data may suggest a much wider issue. That would be the need potentially to challenge a large number

of previously-published knockout studies purporting to report the function of Itgb1 in vivo. Many may not have examined whether their results were confounded by compensatory expression of something else, and in fact reflect the positive characteristics of the up-regulated protein rather than simply the absence of the homeostatic functions of Itgb1. High-profile studies continue to report the "surprising" result that Itgb1 negatively regulates proliferation in vivo, without answering the question of what else might have taken its place. [e.g. Seebeck et al. 2017, Bonar et al. 2017] Yet results are just the tools - the correct interpretation is critical to biological understanding.

6.2.3 Matrix regulation of hippocampal neurogenesis

The role of extracellular matrix per se in regulating hippocampal neurogenesis has been only rarely studied. Reviews of matrix regulation of neurogenesis may have tended to skip over the hippocampus as a result, and focus mainly on embryonic neurodevelopment and perhaps the adult subependymal zone. Indeed the results of my search in **Chapter 1** suggest that this would be a very reasonable strategy, given that far more is known about embryonic and early postnatal systems than is the case in adult animals. However I did find a literature identifying or implicating a small number of ECM genes in hippocampal neurogenesis.

My subsequent hypothesis-free identification of matrix Gla protein as a potential regulator of adult neural stem cell activation is novel but remains work in progress (see below). In keeping with the rest of the ECM, Mgp has been studied only rarely in the adult CNS. Yet a small but consistent literature records its presence in conditions of injury or disease. This marks Mgp as a potentially intriguing candidate for study in the field of regenerative neurobiology.

6.3 Hypotheses and future studies

6.3.1 Technical strategies to manipulate neurogenesis

Based on the consistent observation of rebound SGZ proliferation following AraC-mediated injury, I am struck by the question as to whether and in what ways a 'regenerative' state in the neurogenic niche differs from that in non-neurogenic areas. The question is important because a better understanding of how the injured brain successfully regenerates (as it does

in the neurogenic niches) may generate clues to improve therapeutic strategies for brain repair following wider injury, such as stroke, trauma, or disease.

I would hypothesise that regenerating neurogenic niches express matrix genes which are unique both to the regenerating state and to the niche, and that these genes are critical in promoting a successful regenerative milieu. To force the niches to 'show their hand' I would administer AraC, then compare the transcriptome and proteome of microdissected tissue from neurogenic and non-neurogenic areas (e.g. cortex). Candidates would be those matrix transcripts or proteins that were elevated in the regenerating neurogenic niches, but not in non-neurogenic areas. Further studies could explore mechanisms of gain-of-function and loss-of-function using standard techniques. Injury-specific matrix products could additionally be identified by comparison with control animals.

Regarding ECS and with respect again to extracellular matrix regulation of neurogenesis, I would ask whether ECM regulates the proliferative response of NSPCs to a single shock. This would improve the understanding not only of how neuronal activity regulates neurogenesis in the otherwise healthy brain, but also how electroconvulsive therapy (ECT) might exert its antidepressant effects in humans. As outlined in **Chapter 1** and **Table 2**, profound molecular changes occur in the nuclei of NSCs very soon after the stimulus - an hour or less. However the upstream causes of these early molecular remain unknown. I could hypothesise that secretion of matrix or matrix-associated proteins is triggered immediately by the stimulus, and that matrix-associated signalling may lie upstream even of these early epigenetic and transcriptional changes. Testing this hypothesis would be tricky because the short timescales involved suggest that analyses would need to be at protein level. Proteomic analysis may be too insensitive to detect changes in the tiny volumes of tissue involved. However on-slide mass spectrometry, or perhaps use of a Single Molecule Array (SIMOA)[5] may be techniques to explore. I could also hypothesise a role for matrix in regulating or maintaining the later stages of neurogenesis after a single shock, such as the expansion of Dcx+ NBs at D7. Here, as shown in **Table 2**, there is more of a research base to build on and more scope to start with transcriptional analysis.

The hypotheses outlined above do not follow directly from my thesis. This is because the development of these techniques as reported in **Chapter 3** did not specifically focus on

[5] A digital ELISA that can detect zeptomolar concentrations of protein.

ECM. They are suggestions of ways in which AraC and ECS themselves could combine with matrix biology as it relates to neurogenesis.

6.3.2 The regulatory role of Itgb1

As to the role of Itgb1 in regulating hippocampal neurogenesis, and as outlined in **Chapter 4** and above, interpretation and hypotheses will be influenced by the outcome of current experiments. I wish to confirm whether or not Itgb3 is up-regulated after Itgb1 iKO, as others have shown it to be. [Parvani et al. 2013] As a first step I will immunostain the Itgb3-null SGZ for Itgb3. This will test the specificity of the primary antibody, which in control animals gave an immunofluorescent signal on around 5% of proliferating SGZ NSPCs in my earlier experiments.

If the staining disappears then I will conclude that the antibody is specific to Itgb3. My interpretation will be that Itgb1 and Itgb3 differentially regulate the dynamics of hippocampal neurogenesis. This will generate the scientific hypothesis that the two β subunits recognise different ECM ligands within the same niche, suggest that neurogenesis could be controlled by finding ways to manipulate β subunit expression, and lead to studies designed to identify their binding partners. As outlined above it may also put the cat of methodology amongst the pigeons of interpreting a large body of previous literature.

If staining persists in Itgb3-null tissue then I will conclude that it is non-specific. I will explore potential biological mechanisms for a negative regulatory function of Itgb1. Loss of Itgb1 might induce a loss of BMP signalling mediated through integrin-ligand complexes on the cell surface. Hippocampal NSCs express BMPr1a, a BMP receptor which functions to maintain stem cell quiescence. [Mira et al. 2010] Itgb1 can sequester BMPr1a into functional complexes and thereby enhance inhibitory signaling during development. [Ashe et al. 2016] Analogous loss of inhibition in iKO animals could have the effect of ‘releasing the brake’ on neurogenesis.

Alternatively loss of BMPr1b signalling, which is also enhanced in association with Itgb1, may be responsible. The BMPr1b receptor is gradually up-regulated by proliferating NSPCs, reportedly triggering mitotic arrest once its expression levels reach a critical point. [Panchison et al. 2000] The hypothesis would be that the population of proliferating NBs is expanded after Itgb1 iKO because the BMPr1b ‘stop switch’ is not activated.

Lastly in terms of experiments, I want to ask whether Itgb1 is indeed down-regulated on highly proliferating cells at D10 post-AraC. The possibility remains that the higher levels of proliferation are a rebound phenomenon caused by expansion of cells in which the Itgb1 gene was not excised.

Thinking for the future, I am interested as to whether the cell-surface integrin proteome on NSPCs is fixed from birth, with adhesion mediated solely by activation or inactivation of various permanently-dwelling integrin subpopulations, or whether it is dynamically regulated at a transcriptional level in response to the microenvironment. In vitro studies [Condic and Letourneau 1997] suggest the latter; the question is what happens in vivo. How do cells regulate their own integrin expression? Is it innate - biologically programmed to advance at key developmental stages, or adaptive - reactive to changes in the microenvironment - or a mixture of both? The knowledge and ability to trigger NSCs to alter their own integrin expression could be a potentially therapeutically useful characteristic, for example in the field of brain cancer treatment.

6.3.3 The regulatory role of matrix Gla protein

In some ways the next experiments on Mgp are the simplest to lay out. The hypothesis is also simple: that Mgp sequesters BMP signalling in the neurogenic niche, thereby altering the balance of NSC quiescence and activation.

Before pressing on with what are likely to be expensive experiments it may be worth validating Mgp expression at the protein level using Western Blot. Mgp is well-studied as a secreted molecule in the cardiovascular field and good antibodies are likely to exist. RNAScope data also suggested that Mgp was up-regulated at least in the entire DG, not just the SGZ, meaning a reasonable chance of getting enough tissue to run a successful experiment.

After that the question will be one of functional manipulation. Gain-of-function will be tested using recombinant Mgp in an adult hippocampal slice culture system, with and without additional BMP2/4 in order to test the interaction with BMPs. The prediction is that adding MGP will activate NSCs and/or increase NSPC proliferation. Loss of function will be tested using lentiviral MGP shRNA injection to the DG. The prediction is that the shRNA

will reduce NSPC activation and/or proliferation, and that this can be rescued by infusion of recombinant protein.

Looking a little wider and depending on the outcome of these experiments, I would also consider the potential role of the niche in Mgp regulation of NSPCs. Microenvironmental levels of BMP2/4 may themselves regulate Mgp expression from the vasculature, via the Alk1 receptor. [Yao et al. 2006] To me this suggests the existence of a possible feedback mechanism by which the SGZ microvasculature might regulate the pace of hippocampal neurogenesis.

6.4 Conclusions

I began with the question: Does extracellular matrix regulate hippocampal neurogenesis?

My data suggest a role for the matrix receptors integrin β1 or β3 in regulating NSC activation, proliferation, and differentiation. Data further suggest that matrix Gla protein may be a novel candidate regulator of hippocampal neurogenesis. These results are consistent with the hypothesis that extracellular matrix does regulate hippocampal neurogenesis, and suggest specific further studies to pursue mechanisms.

7 REFERENCES

Abaskharoun M, Bellemare M, Lau E, Margolis RU. Expression of hyaluronan and the hyaluronan-binding proteoglycans Neurocan, Aggrecan and Versican by neural stem cells and neural cells derived from embryonic stem cells. Brain Res 2010a; 1327:6-15.

Abaskharoun M, Bellemare M, Lau E, Margolis RU. Glypican-1, phosphocan/receptor protein-tyrosine phosphatase-ζ/β and its ligand, tenascin-C, are expressed by neural stem cells and neural cells derived from embryonic stem cells. ASN Neuro 2010b; 2(3):e00039.

Ahmed M, ffrench-Constant C. Extracellular matrix regulation of stem cell behavior. Curr Stem Cell Rep 2016; 2(3):197-206.

Aihara K, Kuroda S, Kanayama N, Matsuyama S, Tanizawa K, Horie M. A neuron-specific EGF family protein, NELL2, promotes survival of neurons through mitogen-activated protein kinases. Brain Res Mol Brain Res 2003; 116(1-2):86-93.

Aimone JB, Li Y, Lee SW, Clemonson GD, Deng W, Gage FH. Regulation and function of adult neurogenesis: from genes to cognition. Physiol Rev 2014; 94:991-1026.

Aimone JB, Wiles J, Gage FH. Computational influence of adult neurogenesis on memory encoding. Neuron 2009; 61(2):187-202.

Aimone JB, Wiles J, Gage FH. Potential role for adult neurogenesis in the encoding of time in new memories. Nat Neurosci 2006; 9(6):723-727.

Akers KG, Martinez-Canabal A, Restivo L, Yiu AP, De Cristofaro A, et al. Hippocampal neurogenesis regulates forgetting during adulthood and infancy. Science 2014; 344(6184):598-602.

Alcantara S, Ruiz M, D'Arcangelo G, Ezan F, de Lecea L, Curran T, et al. Regional and cellular patterns of reelin mRNA expression in the forebrain of the developing and adult mouse. J Neurosci 1998; 18(19):7779-7799.

Alcantara S, Ruiz M, De Castro F, Soriano E, Sotelo C. Netrin 1 acts as an attractive or as a repulsive cue for distinct migrating neurons during the development of the cerebellar system. Development 2000; 127(7):1359-1372.

Ali SA, Pappas IS, Parnavelas JG. Collagen type IV promotes the differentiation of neuronal progenitors and inhibits astroglial differentiation in cortical cultures. Brain Res Dev Brain Res 1998; 110(1):31-38.

Altar CA, Laeng P, Jurata LW, Brockman JA, Lemire A, Bullard J, et al. Electroconvulsive seizures regulate gene expression of distinct neurotrophic signaling pathways. J Neurosci 2004; 24(11):2667-2677.

Altman J, Brunner RL, Bayer SA. The hippocampus and behavioral maturation. Behav Biol 1973; 8(5):557-596.

Altman J, Das GD. Autoradiographic and histological evidence of postnatal hippocampal neurogenesis in rats. J Comp Neurol 1965; 124(3):319-335.

Amrein I. Adult hippocampal neurogenesis in natural populations of mammals. Cold Spring Harb Perspect Biol 2015; 7(5):a021295.

Amrein I, Lipp HP. Adult hippocampal neurogenesis of mammals: evolution and life history. Biol Lett 2009; 5(1):141-144.

Anacker C, Hen R. Adult hippocampal neurogenesis and cognitive flexibility – linking memory and mood. Nat Rev Neurosci 2017; 18(6):335-346.

Andres RH, Horie N, Slikker W, Keren-Gill H, Zhan K, Sun G, et al. Human neural stem cells enhance structural plasticity and axonal transport in the ischaemic brain. Brain 2011; 134(6):1777-1789.

Andressen C, Adrian S, Fassler R, Arnhold S, Addicks K. The contribution of beta1 integrins to neuronal migration and differentiation depends on extracellular matrix molecules. Eur J Cell Biol 2005; 84(12):973-982.

Andersen J, Urban N, Achimastou A, Ito A, Simic M, Ullom K, et al. A transcriptional mechanism integrating inputs from extracellular signals to activate hippocampal stem cells. Neuron 2014; 83(5):1085-1097.

Apkarian AV, Mutso AA, Centeno MV, Kan L, Wu M, Levinstein M, Banisadr G, et al. Role of adult hippocampal neurogenesis in persistent pain. Pain 2016; 157(2):418-428.

Ariza CA, McHugh KP, White SJ, Sakaguchi DS, Mallapragada SK. Extracellular matrix proteins and astrocyte-derived soluble factors influence the differentiation and proliferation of adult neural progenitor cells. J Biomed Mater Res A 2010; 94(3):816-824.

Arnold SJ, Huang GJ, Cheung AF, Era T, Nishikawa S, Bikoff EK, et al. The T-box transcription factor Eomes/Tbr2 regulates neurogenesis in the cortical subventricular zone. Genes Dev 2008; 22(18):2479-2484.

Arulmoli J, Pathak MM, McDonnell LP, Nourse JL, Tombola F, Earthman JC, et al. Static stretch affects neural stem cell differentiation in an extracellular matrix-dependent manner. Sci Rep 2015; 5:8499.

Arvanitis DN, Behar A, Tryoen-Toth P, Bush JO, Jungas T, Vitale N, Davy A. Ephrin B1 maintains apical adhesion of neural progenitors. Development 2013; 140(10):2082-92.

Ashe HL. Modulation of BMP signalling by integrins. Biochem Soc Trans 2016; 44(5):1465-73.

Ashton RS, Conway A, Pangarkar C, Bergen J, Lim KI, Shah P, et al. Astrocytes regulate adult hippocampal neurogenesis through ephrin-B signaling. Nat Neurosci 2012; 15(10):1399-406.

Aumailley M, Pesch M, Tunggal L, Gaill F, Fassler R. Altered synthesis of laminin 1 and absence of basement membrane component deposition in beta 1 integrin-deficient embryoid bodies. J Cell Sci 2000; 113 Pt 2:259-268.

Banerjee SB, Rajendran R, Dias BG, Ladiwala U, Tole S, Vaidya A. Recruitment of the Sonic hedgehog signalling cascade in electroconvulsive seizure-mediated regulation of adult rat hippocampal neurogenesis. Eur J Neurosci 2005; 22(7):1570-1580.

Barakat B, Yu L, Lo C, Vu D, De Luca E, Cain JE, et al. Interaction of smoothened with integrin-linked kinase in primary cilia mediates Hedgehog signalling. EMBO Rep 2013; 14(9):837-44.

Barczyk M, Carracedo S, Gullberg D. Integrins. Cell Tissue Res 2010; 339(1):269-280.

Barkho BZ, Song H, Aimone JB, Smrt RD, Kuwabara T, Nakashima K, et al. Identification of astrocyte-expressed factors that modulate neural stem/progenitor differentiation. Stem Cells Dev 2006; 15(3):407-421.

Barrallobre MJ, Del Rio JA, Alcantara S, Borrell V, Aquado F, Ruiz M, et al. Aberrant development of hippocampal circuits and altered neural activity in netrin 1-deficient mice. Development 2000; 127(22):4797-4810.

Barros CS, Nguyen T, Spencer KSR, Nishiyama A, Colognato H, Muller U. Beta1 integrins are required for normal CNS myelination and promote AKT-dependent myelin outgrowth. Development 2009; 136:2717-2724.

Becker S. A computational principle for hippocampal learning and neurogenesis. Hippocampus 2005; 15(6):722-738.

Beckervordesandforth R, Ebert B, Schaffner I, Moss J, Fiebig C, Shin J, et al. Role of mitochondrial metabolism in the control of early lineage progression and aging phenotypes in adult hippocampal neurogenesis. Neuron 2017; 93(3):560-573.

Beckervordesandforth R, Zhang CL, Lie DC. Transcription-factor-dependent control of adult hippocampal neurogenesis. Cold Spring Harb Perspect Biol 2015; 7:a018879.

Becq H, Jorquera I, Ben-Ari Y, Weiss S, Represa A. Differential properties of dentate gyrus and CA1 neural precursors. J Neurobiol 2005; 62(2):243-261.

Belvindrah R, Graus-Porta D, Goebbels S, Nave K-A, Muller U. Beta1 integrins in radial glia but not in migrating neurons are essential for the formation of cell layers in the cerebral cortex. Journal of Neuroscience 2007; 27(50):13854-13865.

Belvindrah R, Hankel S, Walker J, Patton BL, Muller U. Beta1 integrins control the formation of cell chains in the adult rostral migratory stream. Journal of Neuroscience 2007; 27(10):2704-2717.

Benner EJ, Luciano D, Jo R, Abdi K, Paez-Gonzalez P, Sheng H, et al. Protective astrogenesis from the SVZ niche after injury is controlled by Notch modulator Thbs4. Nature 2013; 497(7449):369-373.

Benninger Y, Colognato H, Thurnherr T, Franklin RJ, Leone DP, Atanasoski S, et al. Beta1 integrin signaling mediates premyelinating oligodendrocyte survival but is not required for CNS myelination and remyelination. Journal of Neuroscience 2006; 26(29):7665-7673.

Bergstrom T, Holmqvist K, Tararuk T, Johansson S, Forsberg-Nilsson K. Developmentally regulated collagen/integrin interactions confer adhesive properties to early postnatal neural stem cells. Biochim Biophys Acta 2014;1840(8):2526-2632.

Blaess S, Graus-Porta D, Belvindrah R, Radakovits R, Pons S, Littlewood-Evans A, et al. Beta1-integrins are critical for cerebellar granule cell precursor proliferation. Journal of Neuroscience 2004; 24(13):3402-3412.

Blake SM, Strasser V, Andrade N, Duit S, Hofbauer R, Schneider WJ, et al. Thrombospondin-1 binds to ApoER2 and VLDL receptor and functions in postnatal neuronal migration. EMBO J 2008; 27(22):3069-3080.

Bloch-Gallego E, Ezan F, Tessier-Lavigne M, Sotelo C. Floor plate and netrin-1 are involved in the migration and survival of inferior olivary neurons. J Neurosci 1999; 19(11):4407-4420.

Bonaguidi MA, Wheeler MA, Shapiro JS, Stadel RP, Sun GJ, Ming GL, et al. In vivo clonal analysis reveals self-renewing and multipotent adult neural stem cell characteristics. Cell 2011; 145(17):1142-1155.

Bonar NA, Petersen CP. Integrin suppresses neurogenesis and regulates brain tissue assembly in planarian regeneration. Development 2017; 144(5):784-794.

Bond AM, Ming GL, Song H. Adult mammalian neural stem cells and neurogenesis: five decades later. Cell Stem Cell 2015; 17:385-395.

Borrell V, Cardenas A, Ciceri G, Galceran J, Flames N, Pla R, et al. Slit/Robo signaling modulates the proliferation of central nervous system progenitors. Neuron 2012; 76(2):338-352.

Bosch C, Masachs N, Exposito-Alonso D, Martinez A, Teixeira CM, Fernaud I, et al. Reelin regulates the maturation of dendritic spines, synaptogenesis, and glial ensheathement of newborn granule cells. Cereb Cortex 2016; 26(11):4282-4298.

Braisted JE, Catalano SM, Stimac R, Kennedy TE, Tessier-Lavigne M, Shatz CJ, et al. Netrin-1 promotes thalamic axon growth and is required for proper development of the thalamocortical projection. J Neurosci 2000; 20(15):5792-5801.

Brakebusch C, Fassler R. Beta 1 integrin function in vivo: adhesion, migration and more. Cancer Metastasis Rev 2005; 24(3):403-411.

Bray N, Pimentel H, Mellsted P, Pachter L. Near-optimal RNA-Seq quantification. arXiv 2015; arXiv:1505.02710

Brooker SM, Bond AM, Peng CY, Kessler JA. β1-integrin restricts astrocytic differentiation of adult hippocampal neural stem cells. Glia 2016; 64(7):1235-1251.

Bruckner G, Grosche J, Hartlage-Rubsamen M, Schmidt S, Schachner M. Region and lamina-specific distribution of extracellular matrix proteoglycans, hyaluronan and tenascin-R in the mouse hippocampal formation. J Chem Neuroanat 2003; 26(1):37-50.

Bruggeman SWM, Hulsman D, van Lohuizen M. Bmi1 deficient neural stem cells have increased integrin dependent adhesion to self-secreted matrix. Biochim Biophys Acta 2009; 1790(5):351-360.

Brunne B, Franco S, Bouche E, Herz J, Howell BW, Pahle J, et al. Role of the postnatal radial glial scaffold for the development of the dentate gyrus as revealed by Reelin signaling mutant mice. Glia 2013; 61(8): 1347-1363.

Campologno M, Benedetti L, Podhajcer OL, Pitossi F, Depino AM. Hippocampal SPARC regulates depression-related behavior. Genes Brain Behav 2012; 11(8):966-976.

Campos LS, Decker L, Taylor V, Skarnes W. Notch, epidermal growth factor receptor, and b1-integrin pathways are co-ordinated in neural stem cells. J Biol Chem 2006; 281(8):5300-5309.

Campos LS, Leone DP, Relvas JB, Brakebusch C, Fassler R, Suter U, et al. B1 integrins activate a MAPK signalling pathway in neural stem cells that contributes to their maintenance. Development 2004; 131(14):3433-3444.

Canfield AE, Doherty MJ, Kelly V, Newman B, Farrington C, Grant ME, et al. Matrix gla protein is differentially expressed during the deposition of a calcified matrix by vascular pericytes. FEBS Lett 2000; 487(2):267-271.

Cao X, Li LP, Qin XH, Li SJ, Zhang M, Wang Q, et al. Astrocytic adenosine 5'-triphosphate release regulates the proliferation of neural stem cells in the adult hippocampus. Stem Cells 2013; 31(8):1633-1643.

Cao X, Pfaff SL, Gage FH. A functional study of miR-124 in the developing neural tube. Genes Dev 2007; 21(5):531-536.

Caprile T, Osorio G, Henriquez JP, Montecinos H. Polarized expression of integrin beta1 in diencephalic roof plate during chick development, a possible receptor for SCO-spondin. Dev Dyn 2009; 238(10):2494-2504.

Cayre M, Courtes S, Martineau F, Giordano M, Arnaud K, Zamaron A, et al. Netrin 1 contributes to vascular remodeling in the subventricular zone and promotes progenitor emigration after demyelination. Development 2013; 140(15):3107-3117.

Chan CS, Weeber EJ, Zong L, Fuchs E, Sweatt D, Davis RL. B1-integrins are required for hippocampal AMPA receptor-dependent synaptic transmission, synaptic plasticity, and working memory. Journal of Neuroscience 2006; 26(1):223-232.

Chou CH, Sinden JD, Couraud PO, Modo M. In vitro modeling of the neurovascular environment by coculturing adult human brain endothelial cells with human neural stem cells. PLoS One 2014; 9(9):e106346.

Christian KM, Song H, Ming GL. Functions and dysfunctions of adult hippocampal neurogenesis. Annu Rev Neurosci 2014; 37:243-262.

Christopherson KS, Ullian EM, Stokes CC, Mullowney CE, Hell JW, Agah A, et al. Thrombospondins are astrocyte-secreted proteins that promote CNS synaptogenesis. Cell 2005; 120(3):421-433.

Clelland CD, Choi M, Romberg C, Clemenson GD Jr, Fragniere A, Tyers P, et al. A functional role for adult hippocampal neurogenesis in spatial pattern separation. Science 2009; 325(5937):210-213.

Clemenson GD, Deng W, Gage FH. Environmental enrichment and neurogenesis: from mice to humans. Curr Op Behav Sci 2015; 4:56-62.

Colucci-D'Amato L, Bonavita V, di Porzio U. The end of the central dogma of neurobiology: stem cells and neurogenesis in adult CNS. Neurol Sci 2006; 27(4):266-270.

Colón-Cesario M, Wang J, Ramos X, García HG, Dávila JJ, Laguna J, et al. An inhibitor of DNA recombination blocks memory consolidation, but not reconsolidation, in context fear conditioning. J Neurosci 2006; 26(20):5524-5533.

Condic ML, Letourneau PC. Ligand-induced changes in integrin expression regulate neuronal adhesion and neurite outgrowth. Nature 1997; 389(6653):852-856.

Corbo JC, Deuel TA, Long JM, LaPorte P, Tsai E, Wynshaw-Boris A, et al. Doublecortin is required in mice for lamination of the hippocampus but not the neocortex. J Neurosci 2002; 22(17):7548-7557.

Courtes S, Vernerey J, Pujadas L, Magalon K, Cremer H, Soriano E, et al. Reelin controls progenitor cell migration in the healthy and pathological adult mouse brain. PLoS One 2011; 6(5):e20430.

D'Arcangelo G, Miao GG, Chen SC, Soares HD, Morgan JI, Curran T. A protein related to extracellular matrix proteins deleted in the mouse mutant reeler. Nature 1995; 374(6524):719-723.

D'Ercole AJ, Dai Z, Xing Y, Boney C, Wilkie MB, Lauder JMm et al. Brain growth retardation due to the expression of human insulin like growth factor binding protein-1 in transgenic mice: an in vivo model for the analysis of IGF function in the brain. Brain Res Dev Brain Res 1994; 82(1-2):213-22.

DeCarolis NA, Mechanic M, Petrik D, Carlton A, Ables JL, Malhotra S, et al. In vivo contribution of nestin- and GLAST-lineage cells to adult hippocampal neurogenesis. Hippocampus 2013; 23(8):708-719.

Delannet M, Martin F, Bossy B, Cheresh DA, Reichardt LF, Duband JL. Specific roles of the aVb1, aVb3, and aVb5 integrins in avian neural crest cell adhesion and migration on vitronectin. Development 1994; 120(9):2687-2702.

Dietrich J, Han R, Yang Y, Mayer-Proschel M, Noble M. CNS progenitor cells and oligodendrocytes are targets of chemotherapeutic agents in vitro and in vivo. J Biol 2006; 5(7):22.

Djogo T, Robins SC, Schneider S, Kryzskaya D, Liu X, Mingay A, et al. Adult NG2-glia are required for median eminence-mediated leptin sensing and body weight control. Cell Metab 2016; 23(5):797-810.

Dobrunz LE. Long-term potentiation and the computational synapse. Proc Natl Acad Sci USA 1998; 95(8):4086-4088.

Doetsch F, Garcia-Verdugo JM, Alvarez-Buylla A. Regeneration of a germinal layer in the adult mammalian brain. Proc Natl Acad Sci USA 1999; 96(20):11619-11624.

Domogatskaya A, Rodin S, Boutaud A, Tryggvason K. Laminin-511 but not -332, -111, or -411 enables mouse embryonic stem cell self-renewal in vitro. Stem Cells 2008; 26(11):2800-2809.

Dranovsky A, Hen R. Hippocampal neurogenesis: regulation by stress and antidepressants. Biol Psychiatry 2006; 59(12):1136-1143.

Dulken BW, Leeman DS, Boutet SC, Hebestreit K, Brunet A. Single-cell transcriptomic analysis defines heterogeneity and transcriptional dynamics in the adult neural stem cell lineage. Cell Rep 2017; 18:777-790.

Eagleson KL, Ferri RT, Levitt P. Complementary distribution of collagen type IV and the epidermal growth factor receptor in the rat embryonic telencephalon. Cereb Cortex 1996; 6(3):540-549.

Easterday MC, Dougherty JD, Jackson RL, Ou J, Nakano I, Paucar AA, et al. Neural progenitor genes: germinal zone expression and analysis of genetic overlap in stem cell populations. Dev Biol 2003; 264(2):309-322.

Egeland M, Zunszain PA, Pariante CM. Molecular mechanisms in the regulation of adult neurogenesis during stress. Nat Rev Neurosci 2015; 16:189-200.

Egger K, Janz P, Dobrossy MD, Bienert T, Reisert M, Obmann M, et al. Microstructural effects of a neuro-modulating drug evaluated by diffusion tensor imaging. Neuroimage 2016; 127:1-10.

Ehret F, Vogler S, Kempermann G. A co-culture model of the hippocampal neurogenic niche reveals differential effects of astrocytes, endothelial cells, and pericytes on proliferation and differentiation of adult murine precursor cells. Stem Cell Res 2015; 15(3):514-521.

Encinas JM, Michurina TV, Peunova N, Park JH, Tordo J, Peterson DA, et al. Division-coupled astrocytic differentiation and age-related depletion of neural stem cells in the adult hippocampus. Cell Stem Cell 2011; 8(5):566-579.

Englund C, Fink A, Lau C, Pham D, Daza RA, Bulfone A, et al. Pax6, Tbr2, and Tbr1 are expressed sequentially by radial glia, intermediate progenitor cells, and postmitotic neurons in developing neocortex. J Neurosci 2005; 25(1):247-251.

Epp JR, Silva Mera R, Kohler S, Josselyn SA, Frankland PW. Neurogenesis-mediated forgetting minimizes proactive interference. Nat Commun 2016; 7:10838.

Eriksson PS, Perfilieva E, Bjork-Eriksson T, Alborn AM, Nordborg C, Peterson DA, et al. Neurogenesis in the adult human hippocampus. Nat Med 1998; 4:1313-1317.

Fagan AM, Gage FH. Mechanisms of sprouting in the adult central nervous system: cellular responses in areas of terminal degeneration and reinnervation in the rat hippocampus. Neuroscience 1994; 58(4):705-725.

Fainstein N, Cohen ME, Ben-Hur T. Time associated decline in neurotrophic properties of neural stem cell grafts render them dependent on brain region-specific environmental support. Neurobiol Dis 2013; 49:41-8

Fan Y, Abrahamsen G, Mills R, Calderon CC, Tee JY, Leyton L, et al. Focal adhesion dynamics are altered in schizophrenia. Biol Psychiatry 2013; 74(6):418-426.

Farioli-Vecchioli S, Tirone F. Control of cell cycle in adult neurogenesis and its relation with physical exercise. Brain Plasticity 2015; 1:41-54.

Fassler R, Meyer M. Consequences of lack of beta 1 integrin gene expression in mice. Genes Dev 1995; 9(15):1896-1908.

Filippov V, Kronenberg G, Pivneva T, Reuter K, Steiner B, Wang LP. Subpopulation of nestin-expressing progenitor cells in the adult murine hippocampus shows electrophysiological and morphological characteristics of astrocytes. Mol Cell Neurosci 2003; 23(3):373-382.

Flanagan LA, Rebaza LM, Derzic S, Schwartz PH, Monuki ES. Regulation of human neural precursor cells by laminin and integrins. J Neurosci Res 2006; 83(5):845-856.

Friedlander DR, Milev P, Karthikeyan L, Margolis RK, Margolis RU, Grumet M. The neuronal chondroitin sulfate proteoglycan neurocan binds to the neural cell adhesion molecules Ng-CAM/L1/NILE and N-CAM, and inhibits neuronal adhesion and neurite outgrowth. J Cell Biol 1994; 125(3):669-680.

Forster E, Tielsch A, Saum B, Weiss KH, Johanssen C, Graus-Porta D, et al. Reelin, Disabled 1, and beta 1 integrins are required for the formation of the radial glial scaffold in the hippocampus. Proc Natl Acad Sci USA 2002; 99(20):13178-13183.

Frick A, Grammel D, Schmidt F, Poschl J, Priller M, Pagella P, et al. Proper cerebellar development requires expression of beta1 integrin in Bergmann glia, but not in granule neurons. Glia 2012; 60(5):820-832.

Frotscher M, Haas CA, Forster E. Reelin controls granule cell migration in the dentate gyrus by acting on the radial glial scaffold. Cereb Cortex 2003; 13(6):634-640.

Fu MH, Wang CY, Hsieh YT, Fang KM, Tzeng SF. Functional role of matrix gla protein in glioma cell migration. Mol Neurobiol 2017; doi: 10.1007/s12035-017-0677-1. [Epub ahead of print]

Garcion E, Faissner A, ffrench-Constant C. Knockout mice reveal a contribution of the extracellular matrix molecule tenascin-C to neural precursor proliferation and migration. Development 2001; 128(13):2485-2496.

Garcion E, Halilagic A, Faissner A, ffrench-Constant C. Generation of an environmental niche for neural stem cell development by the extracellular matrix molecule tenascin C. Development 2004; 131(14):3423-3432.

Gates MA, Thomas LB, Howard EM, Laywell ED, Sajin B, Faissner A, et al. Cell and molecular analysis of the developing and adult mouse subventricular zone of the cerebral hemispheres. J Comp Neurol 1995; 361(2):249-266.

Gebara E, Bonaguidi MA, Beckervordersandforth R, Sultan S, Udry F, Gijs PJ, et al. Heterogeneity of radial glia-like cells in the adult hippocampus. Stem Cells 2016; 34(4):997-1010.

Gely-Pernot A, Coronas V, Harnois T, Prestoz L, Mandairon N, Didier A, et al. An endogenous vitamin K-dependent mechanism regulates cell proliferation in the brain subventricular stem cell niche. Stem Cells 2012; 30(4):719-731.

Gilley JA, Yang CP, Kernie SG. Developmental profiling of postnatal dentate gyrus progenitors provides evidence for dynamic cell-autonomous regulation. Hippocampus 2011; 21(1):33-47.

Girard F, Eichenberger S, Celio MR. Thrombospondin 4 deficiency in mouse impairs neuronal migration in the early postnatal and adult brain. Mol Cell Neurosci 2014; 61:176-86.

Giros A, Morante J, Gil-Sanz C, Fairen A, Costell M. Perlecan controls neurogenesis in the developing telencephalon. BMC Dev Biol 2007; 7:29.

Glaviano A, O'Donovan SM, Ryan K, O'Mara S, Dunn MJ, McLoughlin DM. Acute phase plasma proteins are altered by electroconvulsive stimulation. J Psychopharmacol 2014; 28(12):1125-1134.

Gobeske KT, Das S, Bonaguidi MA, Weiss C, Radulovic J, Disterhoft JF, et al. BMP signaling mediates effects of exercise on hippocampal neurogenesis and cognition in mice. PLoS One 2009; 4(10):e7506.

Gomez-Nicola D, Suzzi S, Vargas-Caballero M, Fransen NL, Al-Malki H, Cebrian-Silla A, et al. Temporal dynamics of hippocampal neurogenesis in chronic neurodegeneration. Brain 2014; 137(Pt 8):2312-2328.

Goncalves JT, Schafer ST, Gage FH. Adult neurogenesis in the hippocampus: from stem cells to behavior. Cell 2016; 167(4):897-914.

Gongidi C, Ring C, Moody M, Brekken R, Sage EH, Rakic P, et al. SPARC-like 1 regulates the terminal phase of radial glia-guided migration in the cerebral cortex. Neuron 2004; 41(1):57-69.

Goritz C, Thiebaut R, Tessier LH, Nieweg K, Moehle C, Buard I, et al. Glia-induced neuronal differentiation by transcriptional regulation. Glia 2007; 55(11):1108-1122.

Gotz M, Huttner WB. The cell biology of neurogenesis. Nat Rev Mol Cell Biol 2005; 6(10):777-788.

Gouaze A, Brenachot X, Rigault C, Krezymon A, Rauch C, Nedelec E, et al. Cerebral cell renewal in mice controls the onset of obesity. PLoS One 2013; 8(8):e72029.

Graus-Porta D, Blaess S, Senften M, Littlewood-Evans A, Damsky C, Huang Z, et al. Beta1-class integrins regulate the development of laminae and folia in the cerebral and cerebellar cortex. Neuron 2001; 31(3):367-379.

Grove EA, Tole S. Patterning events and specification signals in the developing hippocampus. Cereb Cortex 1999; 9(6):551-561.

Guijarro P, Simo S, Pascual M, Abasolo I, Del Rio JA, Soriano E. Netrin1 exerts a chemorepulsive effect on migrating cerebellar interneurons in a Dcc-independent way. Mol Cell Neurosci 2006; 33(4):389-400.

Guinazu MF, Richter HG, Rodriguez EM. Bovine floor plate explants secrete SCO-spondin. Cell Tissue Res 2002; 308(2):177-191.

Gu WL, Fu SL, Wang, YX, Li Y, Wang XF, Xu XM, et al. Expression and regulation of versican in neural precursor cells and their lineages. Acta Pharmacol Sin 2007; 28(10):1519-1530.

Guo JU, Ma DK, Mo H, Ball MP, Jang MH, Bonaguidi MA, et al. Neuronal activity modifies the DNA methylation landscape in the adult brain. Nat Neurosci 2011; 14:1345-1351.

Ha CM, Hwang EM, Kim E, Lee DY, Chang S, Lee BJ, et al. The molecular mechanism of NELL2 movement and secretion in hippocampal progenitor HiB5 cells. Mol Cells 2013; 36(6):527-33.

Hack I, Bancilla M, Loulier K, Carroll P, Cremer H. Reelin is a detachment signal in tangential chain migration during postnatal neurogenesis. Nat Neurosci 2002; 5(10):939-945.

Hakanen J, Duprat S, Salminen M. Netrin1 is required for neural and glial precursor migrations into the olfactory bulb. Dev Biol 2011; 355(1):101-114.

Halfter W, Dong S, Yip YP, Willem M, Mayer U. A critical function of the pial basement membrane in cortical histogenesis. J Neurosci 2002; 22(14):6029-6040.

Hall PE, Lathia JD, Miller NG, Caldwell MA, ffrench-Constant C. Integrins are markers of human neural stem cells. Stem Cells 2006; 24(9):2078-2084.

Hall PE, Lathia JD, Caldwell MA, ffrench-Constant C. Laminin enhances the growth of human neural stem cells in defined culture media. BMC Neurosci 2008; 9:71.

Hamasaki T, Goto S, Nishikawa S, Ushio Y. A role of netrin-1 in the formation of the subcortical structure striatum: repulsive action on the migration of late-born striatal neurons. J Neurosci 2001; 21(12):4272-4280.

Han D, Choi MR, Jung KH, Kim N, Kim SK, Chai JC, et al. Global transcriptome profiling of genes that are differentially regulated during differentiation of mouse embryonic neural stem cells into astrocytes. J Mol Neurosci 2015; 55(1):109-125.

Hannigan GE, Leung-Hagesteijn C, Fitz-Gibbon L, Coppolino MG, Radeva G, Filmus J, et al. Regulation of cell adhesion and anchorage-dependent growth by a new beta1-integrin-linked protein kinase. Nature 1996; 379(6560):91-96.

Haubst N, Georges-Labouesse E, De Arcangelis A, Mayer U, Gotz M. Basement membrane attachment is dispensable for radial glial cell fate and for proliferation, but affects positioning of neuronal subtypes. Development 2006; 133(16):3245-3254.

He J, Crews FT. Neurogenesis decreases during brain maturation from adolescence to adulthood. Pharmacol Biochem Behav 2007; 86(2):327-333.

Hellsten J, Wennstrom M, Mohapel P, Ekdahl CT, Bengzon J, Tingstrom A. Electroconvulsive seizures increase hippocampal neurogenesis after chronic corticosterone treatment. Eur J Neurosci 2002; 16(2):283-290.

Hellsten J, Wennstrom M, Bengzon J, Mohapel P, Tingstrom A. Electroconvulsive seizures induce endothelial cell proliferation in adult rat hippocampus. Biol Psychiatry 2004; 55(4):420-427.

Hennen E, Safina D, Haussmann U, Worsdorfer P, Edenhofer F, Poetsch A, et al. A LewisX glycoprotein screen identifies the low density lipoprotein receptor-related protein 1 (LRP1) as a modulator of oligodendrogenesis in mice. J Biol Chem 2013; 288(23):16538-16545.

Hirota Y, Nakajima K. Control of neuronal migration and aggregation by reelin signaling in the developing cerebral cortex. Front Cell Dev Biol 2017; 5:40.

Hodge RD, Kowalczyk TD, Wolf SA, Encinas JM, Rippey C, Enikolopov G, et al. Intermediate progenitors in adult hippocampal neurogenesis: Tbr2 expression and coordinate regulation of neuronal output. J Neurosci 2008; 28(14):3707-3717.

Hodge RD, Nelson BR, Kahoud RJ, Yang R, Mussar KE, Reiner SL, et al. Tbr2 is essential for hippocampal lineage progression from neural stem cells to intermediate progenitors and neurons. J Neurosci 2012; 32(18):6275-6287.

Hodge RD, Garcia AJ 3rd, Elsen GE, Nelson BR, Mussar KE, Reiner SL, et al. Tbr2 expression in Cajal-Retzius cells and intermediate neuronal progenitors is required for morphogenesis of the dentate gyrus. J Neurosci 2013; 33(9):4165-4180.

Holmes MM. Social regulation of adult neurogenesis: a comparative approach. Front Neuroendocrinol 2016; 41:59-70.

Honda S, Shirotani-Ikejima H, Tadokoro S, Maeda Y, Kinoshita T, Tomiyama Y, et al. Integrin-linked kinase associated with integrin activation. Blood 2009; 113(21):5304-5313.

Huang W, Zhang L, Niu R, Liao H. Tenascin-R distinct domains modulate migration of neural stem/progenitor cells in vitro. In Vitro Cell Dev Biol Anim 2009; 45(1-2):10-14.

Huang Z, Shimazu K, Woo NH, Zang K, Muller U, Lu B, et al. Distinct roles of the beta 1-class integrins at the developing and the mature hippocampal excitatory synapse. Journal of Neuroscience 2006; 26(43):11208-11219.

Husain BF, Nanavaty IN, Marathe SV, Rajendran R, Vaidya VA. Hippocampal transcriptional and neurogenic changes evoked by combination yohimbine and imipramine treatment. Prog Neuropsychopharmacol Biol Psychiatry 2015; 61:1-9.

Hynes RO. Integrins: bidirectional, allosteric signaling machines. Cell 2002; 110(6):673-87.

Hynes RO, Zhao Q. The evolution of cell adhesion. J Cell Biol 2000; 150(2):F89-96.

Hynes RO. Alteration of cell-surface proteins by viral transformation and by proteolysis. Proc Natl Acad Sci USA 1973; 70(11):3170-3174.

Hynes RO. The emergence of integrins: a personal and historical perspective. Matrix Biol 2004; 23(6):333-340.

Imayoshi I, Isomura A, Harima Y, Kawaguchi K, Kori H, Miyachi H, et al. Oscillatory control of factors determining multipotency and fate in mouse neural progenitors. Science 2013; 342(6163):1203-1208.

Jacques TS, Relvas JB, Nishimura S, Pytela R, Edwards GM, Streuli CH, et al. Neural precursor cell chain migration and division are regulated through different beta1 integrins. Development 1998; 125:3167-3177.

Jeong JK, Kim HR, Hwang SM, Park JW, Lee BJ. Region- and neuronal phenotype-specific expression of NELL2 in the adult rat brain. Mol Cells 2008; 26(2):186-192.

Jinno S. Topographic differences in adult neurogenesis in the mouse hippocampus: a stereology-based study using endogenous markers. Hippocampus 2011; 21(5)467-480.

Joester A, Faissner A. Evidence for combinatorial variability of Tenascin-C isoforms and developmental regulation in the mouse central nervous system. J Biol Chem 1999; 274(24):17144-17151.

Joo S, Kim Y, Lee E, Hong N, Sun W, Nam Y. Effects of ECM protein micropatterns on the migration and differentiation of adult neural stem cells. Sci Rep 2015; 5:13043.

Jun H, Hussaini SMQ, Cho CH, Welby J, Jang MH. Gadd45b mediates electroconvulsive shock induced proliferation of hippocampal neural stem cells. Brain Stim 2015; 8(6):1021-1024.

Jung KH, Chu K, Kim M, Jeong SW, Song YM, Lee ST, et al. Continuous cytosine-b-D-arabinofuranoside infusion reduces ectopic granule cells in adult rat hippocampus with attenuation of spontaneous recurrent seizures following pilocarpine-induced status epilepticus. Eur J Neurosci 2004; 19(12):3219-3226.

Kalluri HS, Dempsey RJ. Osteopontin increases the proliferation of neural progenitor cells. Int J Dev Neurosci 2012; 30(5):359-362.

Kamata T, Katsube K, Michikawa M, Yamada M, Takeda S, Mizusawa H. R-spondin, a novel gene with thrombospondin type 1 domain, was expressed in the dorsal neural tube and affected in Wnts mutants. Biochim Biophys Acta 2004; 1676(1):51-62.

Kaneko Y, Kitazato K, Basaki Y. Integrin-linked kinase regulates vascular morphogenesis induced by vascular endothelial growth factor. J Cell Sci 2004; 117(3):407-415.

Karus M, Denecke B, ffrench-Constant C, Wiese S, Faissner A. The extracellular matrix molecule tenascin C modulates expression levels and territories of key patterning genes during spinal cord astrocyte specification. Development 2011; 138(24):5321-5331.

Kazanis I, Belhadi A, Faissner A, ffrench-Constant C. The adult mouse subependymal zone regenerates efficiently in the absence of Tenascin-C. J Neurosi 2007; 27(51):13991-13996.

Kazanis I, Lathia JD, Vadakkan TJ, Raborn E, Wan R, Mughal MR, et al. Quiescence and activation of stem and precursor cell populations in the subependymal zone of the mammalian brain are associated with distinct cellular and extracellular matrix signals. Journal of Neuroscience 2010; 30(29):9771-9781.

Kearns SM, Laywell ED, Kukekov VK, Steindler DA. Extracellular matrix effects on neurosphere cell motility. Exp Neurol 2003; 182(1):240-244.

Keilani S, Sugaya K. Reelin induces a radial glial phenotype in human neural progenitor cells by activation of Notch-1. BMC Dev Biol 2008; 8:69.

Keilani S, Healey D, Sugaya K. Reelin regulates differentiation of neural stem cells by activation of notch signaling through Disabled-1 tyrosine phosphorylation. Can J Physiol Pharmacol 2012; 90(3):361-369.

Kempermann G, Kuhn HG, Gage FH. Genetic influence on neurogenesis in the dentate gyrus of adult mice. Proc Natl Acad Sci USA 1997; 94(19):10409-10414.

Kerever A, Mercier F, Nonaka R, de Vega S, Oda Y, Zalc B, et al. Perlecan is required for FGF-2 signaling in the neural stem cell niche. Stem Cell Res 2014; 12(2):492-505.

Kerever A, Schnack J, Vellinga D, Ichikawa N, Moon C, Arikawa-Hirasawa E, et al. Novel extracellular matrix structures in the neural stem cell niche capture the neurogenic factor fibroblast growth factor 2 from the extracellular milieu. Stem Cells 2007; 25(9):2146-2157.

Kim HM, Qu T, Kriho V, Lacor P, Smalheiser N, Pappas GD, et al. Reelin function in neural stem cell biology. Proc Natl Acad Sci USA 2002; 99(6):4020-4025.

Kim C, Ye F, Ginsberg MH. Regulation of integrin activation. Annu Rev Cell Dev Biol 2011; 27:321-345.

Klar A, Baldassare M, Jessell TM. F-spondin: a gene expressed at high levels in the floor plate encodes a secreted protein that promotes neural cell adhesion and neurite extension. Cell 1992; 69(1):95-110.

Koizumi H, Higginbotham H, Poon T, Tanaka T, Brinkman BC, Gleeson JG. Doublecortin maintains bipolar shape and nuclear translocation during migration in the adult forebrain. Nat Neurosci 2006; 9(6):779-786.

Kriegstein A, Alvarez-Buylla A. The glial nature of embryonic and adult neural stem cells. Annu Rev Neurosci 2009; 32:149-184.

Kukekov VG, Laywell ED, Suslov O, Davies K, Scheffler B, Thomas LB, et al. Multipotent stem/progenitor cells with similar properties arise from two neurogenic regions of the adult human brain. Exp Neurol 1999; 156(2):333-344.

Kuzontkoski PM, Mulligan-Kehoe MJ, Harris BT, Israel MA. Inhibitor of DNA binding-4 promotes angiogenesis and growth of glioblastoma multiforme by elevating matrix GLA levels. Oncogene 2010; 29(26):3793-3802.

Kwon HJ, Ma S, Huang Z. Radial glia regulate Cajal-Retzius cell positioning in the early embryonic cerebral cortex. Developmental Biology 2011; 351(1)25-34.

Lagace DC, Whitman MC, Noonan MA, Ables JL, DeCarolis NA, Arguello AA, et al. Dynamic contribution of nestin-expressing stem cells to adult neurogenesis. J Neurosci 2007; 12623-12629.

Lakoma J, Garcia-Alonso L, Luque JM. Reelin sets the pace of neocortical neurogenesis. Development 2011; 138(23):5223-5234.

Lathia JD, Patton B, Eckley DM, Magnus T, Mughal MR, Sasaki T, et al. Patterns of laminins and integrins in the embryonic ventricular zone of the CNS. J Comp Neurol 2007; 505(6):630-43.

Laywell ED, Dorries U, Bartsch U, Faissner A, Schachner M, Steindler DA. Enhanced expression of the developmentally regulated extracellular matrix molecule tenascin following adult brain injury. Proc Natl Acad Sci 1992; 89(7):2634-2638.

Lau BW, Yau SY, Lee TM, Ching YP, Tang SW, So KF. Intracerebroventricular infusion of cytosine-arabinoside causes prepulse inhibition disruption. Neuroreport 2009; 20(4):371-377.

Le Dreau G, Nicot A, Benard M, Thibout H, Vaudry D, Martinerie C, et al. NOV/CCN3 promotes maturation of cerebellar granule neuron precursors. Mol Cell Neurosci 2010; 43(1):60-71.

Lei W-L, Xing S-G, Deng C-Y, Ju X-C, Jiang X-Y, Luo Z-G. Laminin/β1 integrin signal triggers axon formation by promoting microtubule assembly and stabilization. Cell Research 2012; 22:954-972.

Leone DP, Relvas JB, Campos LS, Hemmi S, Brakebusch C, Fassler R, et al. Regulation of neural progenitor proliferation and survival by beta1 integrins. J Cell Sci 2005; 118(Pt 12):2589-2599.

Li B, Piao CS, Liu XY, Guo P, Xue YQ, Duan WM, et al. Brain self-protection: the role of endogenous neural progenitor cells in adult rat brain after cerebral cortical ischemia. Brain Res 2010; 1327:91-102.

Li CQ, Liu D, Huang L, Wang H, Zhang JY, Luo XG. Cytosine arabinoside treatment impairs the remote spatial memory function and induces dendritic retraction in the anterior cingulate cortex of rats. Brain Res Bull 2008; 77(5):237-240.

Li H, Chang YW, Mohan K, Su HW, Ricupero CL, Baridi A, et al. Activated Notch1 maintains the phenotype of radial glial cells and promotes their adhesion to laminin by upregulating nidogen. Glia 2008; 56(6):646-658.

Li H, Leung TC, Hoffman S, Balsamo J, Lilien J. Coordinate regulation of cadherin and integrin function by the chondroitin sulfate proteoglycan neurocan. J Cell Biol 2000; 149(6):1275-1288.

Li L, Welser JV, Milner R. Absence of the alpha v beta 3 integrin dictates the time-course of angiogenesis in the hypoxic central nervous system: accelerated endothelial proliferation correlates with compensatory increases in alpha 5 beta 1 integrin expression. J Cereb Blood Flow Metab 2010; 30(5):1031-1043.

Liao H, Huang W, Schachner M, Guan Y, Guo J, Yan J. Beta 1 integrin-mediated effects of tenascin-R domains EGFL and FN6-8 on neural stem/progenitor cell proliferation and differentiation in vitro. J Biol Chem 2008a; 283(41):27927-27936.

Liao H, Huang W, Niu R, Sun L, Zhang L. Cross-talk between the epidermal growth factor-like repeats/fibronectin 6-8 repeats domains of Tenascin-R and microglia modulates neural stem/progenitor cell proliferation and differentiation. J Neurosci Res 2008b; 86(1):27-34.

Liberzon A, Subramanian A, Pinchback R, Thorvaldsdottir H, Tamayo P, Mesirov JP. Molecular signatures database (MSigDB) 3.0. Bioinformatics 2011; 27(12):1739-1740.

Licht T, Rothe G, Kreisel T, Wolf B, Benny O, Rooney AG, et al. VEGF preconditioning leads to stem cell remodeling and attenuates age-related decay of adult hippocampal neurogenesis. Proc Natl Acad Sci USA 2016; 113(48):E7828-E7836.

Licht T, Goshen I, Avital A, Kreisel S, Zubedat R, Eavri M, et al. Reversible modulations of neuronal plasticity by VEGF. Proc Natl Acad Sci USA 2011; 108(12):5081-5086.

Lindvall O, Kokaia Z. Neurogenesis following stroke affecting the adult brain. Cold Spring Harb Perspect Biol 2015; 7(11): pii:a019034.

Liu J, Willet SG, Bankaitis ED, Xu Y, Wright C, Gu G. Non-parallel recombination limits Cre-LoxP-based reporters as precise indicators of conditional genetic manipulation. Genesis. 2013 Jun; 51(6): 436–442.

Llambi F, Causeret F, Bloch-Gallego E, Mehlen P. Netrin-1 acts as a survival factor via its receptors UNC5H and DCC. Embo J 2001; 20(11):2715-2722.

Llorens-Bobadilla E, Zhao S, Baser A, Saiz-Castro G, Zwadlo K, Martin-Villalba A. Single-cell transcriptomics reveals a population of dormant neural stem cells that become activated upon brain injury. Cell Stem Cell 2015; 17(3):329-340.

Long K, Moss L, Laursen L, Boulter L, ffrench-Constant C. Integrin signalling regulates the expansion of neuroepithelial progenitors and neurogenesis via Wnt7a and Decorin. Nat Commun 2016; 7:10354.

Loulier K, Lathia JD, Marthiens V, Relucio J, Mughal MR, Tang SC, et al. Beta1 integrin maintains integrity of the embryonic neocortical stem cell niche. PLoS Biol 2009; 7(8):e1000176.

Lu H, Song X, Wang F, Wang G, Wu Y, Wang Q, et al. Hyperexpressed Netrin-1 promoted neural stem cells migration in mice after focal cerebral ischaemia. Front Cell Neurosci 2016; 10:223.

Lu Z, Kipnis J. Thrombospondin 1—a key astrocyte-derived neurogenic factor. FASEB J 2010; 24(6):1925-1934.

Lugert S, Basak O, Knuckles P, Haussler U, Fabel K, Gotz M, et al. Quiescent and active hippocampal neural stem cells with distinct morphologies respond selectively to physiological and pathological stimuli and aging. Cell Stem Cell 2010; 6(5):445-456.

Luo G, Ducy P, McKee MD, Pinero GJ, Loyer E, Behringer RR, et al. Spontaneous calcification of arteries and cartilage in mice lacking matrix GLA protein. Nature 1997; 386(6620):78-81.

Ma DK, Jang MH, Guo JU, Kitabatake Y, Chang ML, Pow-anpongkul N, et al. Neuronal activity-induced Gadd45b promotes epigenetic DNA demethylation and adult neurogenesis. Science 2009; 323:1074-1077.

Ma SM, Chen LX, Lin YF, Yan H, Lv JW, Xiong M, et al. Periostin promotes neural stem cell proliferation and differentiation following hypoxic-ischaemic injury. PLoS One 2015; 10(4):e0123585.

Ma W, Tavakoli T, Derby E, Serecryakova Y, Rao MS, Mattson MP. Cell-extracellular matrix interactions regulate neural differentiation of human embryonic stem cells. BMC Dev Biol 2008; 8:90.

Madsen TM, Treschow A, Bengzon J, Bolwig TG, Lindvall O, Tingstrom A. Increased neurogenesis in a model of electroconvulsive therapy. Biol Psychiatry 2000; 47(12):1043-1049.

Madisen L, Zwingman TA, Sunkin SM, Oh SW, Zariwala HA, Gu H, et al. A robust and high-throughput Cre reporting and characterization system for the whole mouse brain. Nat Neurosci 2010; 13(1):133-140.

Mahmoud R, Wainwright SR, Galea LAM. Sex hormones and adult hippocampal neurogenesis: regulation, implications, and potential mechanisms. Front Neuroendocrinol 2016; 41:129-152.

Mak GK, Enwere EK, Gregg C, Pakarainen T, Poutanen M, Huhtaniemi I, et al. Male pheromone-stimulated neurogenesis in the adult female brain: possible role in mating behavior. Nat Neurosci 2007; 10:1003-1011.

Martinez-Morales JR, Barbas JA, Marti E, Bovolenta P, Edgar D, Rodriguez-Tebar A. Vitronectin is expressed in the ventral region of the neural tube and promotes the differentiation of motor neurons. Development 1997; 124(24):5139-5147.

Mashayekhi F, Sadeghi M, Rajaei F. Induction of perlecan expression and neural cell proliferation in the developing cerebral cortex: an in vivo study. J Mol Neurosci 2011; 45(2):87-93.

Massalini S, Pellegatta S, Pisati F, Finocchiaro G, Farace MG, Ciafre SA. Reelin affects chain-migration and differentiation of neural precursor cells. Mol Cell Neurosci 2009; 42(4):341-349.

Mehta B, Bhat KM. Slit signalling promotes the terminal asymmetric division of neural precursor cells in the Drosophila CNS. Development 2001; 128(16):3161-3168.

Meier S, Brauer AU, Heimrich B, Nitsch R, Savaskan NE. Myelination in the hippocampus during development and following lesion. Cell Mol Life Sci 2004; 61(9):1082-1094.

Mendes FA, Coelho Aguiar JM, Khan SA, Reis AH, Dubois LG, Romao LF, et al. Connective-tissue growth factor (CTGF/CCN2) induces astrogenesis and fibronectin expression of embryonic neural cells in vitro. PLoS One 2015; 10(8):e0133689.

Michael J, Schonzart L, Israel I, Beutner R, Scharnweber D, Worch H, et al. Focal adhesion kinase modulates cell adhesion strengthening via integrin activation. Mol Biol Cell 2009; 20(9):2508-2519.

Milev P, Maurel P, Chiba A, Mevissen M, Popp S, Yamaguchi Y, et al. Differential regulation of expression of hyaluronan-binding proteoglycans in developing brain: aggrecan, versican, neurocan, and brevican. Biochem Biophys Res Commun 1998; 247(2):207-12.

Miller JA, Nathanson J, Franjic D, Shim S, Dalley RA, Shapouri S, et al. Conserved molecular signatures of neurogenesis in the hippocampal subgranular zone of rodents and primates. Development 2013; 140(22):4633-4644.

Milner R. A novel three-dimensional system to study interactions between endothelial cells and neural cells of the developing nervous system. BMC Neurosci 2007; 8:3.

Mira H, Andreu Z, Suh H, Lie DC, Jessberger S, Consiglio A, et al. Signaling through BMPR-1A regulates quiescence and long-term activity of neural stem cells in the adult hippocampus. Cell Stem Cell 2010; 7(1):78-89.

Miyasaka N, Matsuoka I. Identification of basic fibroblast growth factor-responsive genes by mRNA-differential display in an immortalized neural stem cell line. Biol Pharm Bull 2000; 23(3):349-351.

Moeton M, Kanski R, Stassen OM, Sluijs JA, Geerts D, van Tijn P, et al. Silencing GFAP isoforms in astrocytoma cells disturbs laminin-dependent motility and cell adhesion. FASEB J 2014; 28(7):2942-2954.

Mohammad H, Marchisella F, Ortega-Martinez S, Hollos P, Eerola K, Komulainen E, et al. JNK1 controls adult hippocampal neurogenesis and imposes cell-autonomous control of anxiety behaviour from the neurogenic niche. Mol Psychiatry 2016 Nov 15. doi: 10.1038/mp.2016.203. [Epub ahead of print] (accessed 27th July 2017)

Monteiro BM, Moreira FA, Massensini AR, Moraes MF, Pereira GS. Enriched environment increases neurogenesis and improves social memory persistence in socially isolated adult mice. Hippocampus 2014; 24(2):239-248.

Moon JI, Birren SJ. Target-dependent inhibition of sympathetic neuron growth via modulation of a BMP signaling pathway. Dev Biol 2008; 315(2):404-417.

Mori H, Takahasgi T, Horimoto A, Hara M. Migration of glial cells differentiated from neurosphere-forming neural stem/progenitor cells depends on the stiffness of the chemically cross-linked collagen gel substrate. Neurosci Lett 2013; 555:1-6.

Moritz S, Lehmann S, Faissner A, von Holst A. An induction gene trap screen in neural stem cells reveals an instructive function of the niche and identifies the splicing regulator sam68 as a tenascin-C-regulated target gene. Stem Cells 2008; 26(9):2321-2331.

Mortillo S, Elste A, Ge Y, Patil SB, Hsiao K, Huntley GW, et al. Compensatory redistribution of neuroligins and N-cadherin following deletion of synaptic beta1 integrin. Journal of Comparative Neurology 2012; 520(9):2041-2052.

Moss J, Gebara E, Bushong EA, Sanchez-Pascual I, O'Laoi R, M'Ghari IE, et al. Fine processes of Nestin-GFP-positive radial glia-like stem cells in the adult dentate gyrus ensheathe local synapses and vasculature. Proc Natl Acad Sci USA 2016; 113(18):E2536-E2545.

Mueller FJ, Serobyan N, Schraufstatter IU, DiScipio R, Wakeman D, Loring JF, et al. Adhesive interactions between human neural stem cells and inflamed human vascular endothelium are mediated by integrins. Stem Cells 2006; 24(11):2367-2372.

Murase S, Horwitz AF. Deleted in colorectal carcinoma and differentially expressed integrins mediate the directional migration of neural precursors in the rostral migratory stream. J Neurosci 2002; 22(9):3568-3579.

Naba A, Clauser KR, Hoersch S, Liu H, Carr SA, Hynes RO. The matrisome: in silico definition and in vivo characterization by proteomics of normal and tumor extracellular matrices. Mol Cell Proteomics 2012; 11(4):M111.014617.

Nadel L, O'Keefe J, Black A. Slam on the brakes: A critique of Altman, Brunner, and Bayer's response-inhibition model of hippocampal function. Behav Biol 1975; 14(2):151-162.

Nagato M, Heike T, Kato T, Yamanaka Y, Yoshimoto M, Shimazaki T, et al. Prospective characterization of neural stem cells by flow cytometry analysis using a combination of surface markers. J Neurosci Res 2005; 80(4):456-466.

Nakamura K, Ito M, Liu Y, Seki T, Suzuki T, Arai H. Effects of single and repeated electroconvulsive stimulation on hippocampal cell proliferation and spontaneous behaviors in the rat. Brain Res 2013; 1491:88-97.

Newton SS, Collier EF, Hunsberger J, Adams D, Terwilliger R, Selvanayagam E, et al. Gene profile of electroconvulsive seizures: induction of neurotrophic and angiogenic factors. J Neurosci 2003; 23(24):10841-10851.

Nibuya M, Morinobu S, Duman RS. Regulation of BDNF and trkB mRNA in rat brain by chronic electroconvulsive seizure and antidepressant drug treatments. J Neurosci 1995; 15(11):7539-7547.

Nicola Z, Fabel K, Kempermann G. Development of the adult neurogenic niche in the hippocampus of mice. Front Neuroanat 2015; 9:53.

Nishio T, Kawaguchi S, Yamamoto M, Iseda T, Kawasaki T, Hase T. Tenascin-C regulates proliferation and migration of cultured astrocytes in a scratch wound assay. Neuroscience 2005; 132(1):87-102.

North HA, Pan L, McGuire TL, Brooker S, Kessler JA. Beta1 integrin alters ependymal stem cell BMP receptor localization and attenuates astrogliosis after spinal cord injury. Journal of Neuroscience 2015; 35(9):3725-3733.

O'Donovan SM, O'Mara S, Dunn MJ, McLoughlin DM. The persisting effects of electroconvulsive stimulation on the hippocampal proteome. Brain Res 2014; 1593:106-116.

Ohsawa I, Takamura C, Kohsaka S. Fibulin-1 binds the amino-terminal head of beta-amyloid precursor protein and modulates its physiological function. J Neurochem 2001; 76(5):1411-1420.

Ohtomo T, Kanamatsu T, Fujita M, Takagi M, Yamada J. Sustained downregulation of YY1-associated protein-related protein gene expression in rat hippocampus induced by repeated electroconvulsive shock. Biol Pharm Bull 2011; 34(2):249-252.

Orban PC, Chui D, Marth JD. Tissue- and site-specific DNA recombination in transgenic mice. Proc Natl Acad Sci USA 1992; 89(15):6861-6865.

Otabe H, Nibuya M, Shimazaki K, Toda H, Suzuki G, Nomura S, et al. Electroconvulsive seizures enhance autophagy signaling in rat hippocampus. Prog Neuropsychopharmacol Biol Psychiatry 2014; 50:37-53.

Ottone C, Krusche B, Whitby A, Clements M, Quadrato G, Pitulescu ME, et al. Direct cell-cell contact with the vascular niche maintains quiescent neural stem cells. Nat Cell Biol 2014; 16(11):1045-1056.

Palmer TD, Willhoite AR, Gage FH. Vascular niche for adult hippocampal neurogenesis. J Comp Neurol 2000; 425(4):479-494.

Pan L, North HA, Sahni V, Jeong SJ, Mcguire TL, Berns EJ, et al. B1-integrin and integrin linked kinase regulate astrocytic differentiation of neural stem cells. PLoS One 2014; 9(8):e104335.

Panchison DM, Pickel JM, Studer L, Lee SH, Turner PA, Hazel TG. Sequential actions of BMP receptors control neural precursor cell production and fate. Genes Dev 2001; 15(16):2094-2110.

Pardo J, Abba MC, Lacunza E, Francelle L, Morel GR, Outeiro TF, et al. Identification of a conserved gene signature associated with an exacerbated inflammatory environment in the hippocampus of ageing rats. Hippocampus 2017; 27(4):435-449.

Parekh S, Ziegenhain C, Vieth B, Enard W, Hellmann I. The impact of amplification on differential expression analyses by RNA-seq. Sci Rep 2016; 6:25533.

Park Y, Rangel C, Reynolds MM, Caldwell MC, Johns M, Nayak M. Drosophila perlecan modulates FGF and hedgehog signals to activate neural stem cell division. Dev Biol 2003; 253(2):247-257.

Parkash J, Cimino I, Ferraris N, Casoni F, Wray S, Cappy H, et al. Suppression of beta1 integrin in gonadotropin-releasing hormone cells disrupts migration and axonal extension resulting in severe reproductive alterations. Journal of Neuroscience 2012; 32(47):16992-17002.

Parras CM, Galli R, Britz O, Soares S, Galichet C, Battiste J, et al. Mash1 specifies neurons and oligodendrocytes in the postnatal brain. EMBO J 2004; 23(22):4495-4505.

Parvani JG, Galliher-Beckley AJ, Schiemann BJ, Schiemann WP. Targeted inactivation of b1 integrin induces b3 integrin switching, which drives breast cancer metastasis by TGF-b. Mol Biol Cell 2013; 24(21):3449-3459.

Pereira-Caixeta AR, Guarnieri LO, Pena RR, Dias TL, Pereira GS. Neurogenesis inhibition prevents enriched environment to prolong and strengthen social recognition memory, but not to increase BDNF expression. Mol Neurobiol 2017; 54(5):3309-3316.

Pohodich AE, Yalamanchili H, Raman AT, Wan YW, Gundry M, Hao S, et al. Forniceal deep brain stimulation induces gene expression and splicing changes that promote neurogenesis and plasticity. eLife 2018; 7:e34031.

Plantman S, Patarroyo M, Fried K, Domogatskaya A, Tryggvason K, Hammarberg H, et al. Integrin-laminin interactions controlling neurite outgrowth from adult DRG neurons in vitro. Mol Cell Neurosci 2008; 39(1):50-62.

Plow EF, Haas TA, Zhang L, Loftus J, Smith JW. Ligand binding to integrins. J Biol Chem 2000; 275(21):21785-21788.

Pollen AA, Nowakowski TJ, Chen J, Retallack H, Sandoval-Espinosa C, Nicholas CR, et al. Molecular identity of human outer radial glia during cortical development. Cell 2015; 163(1):55-67.

Ponferrada VG, Fan J, Hu S, Mamedova A, Rankin SA, Kofron M, Zorn AM, et al. CRIM1 complexes with B-catenins and cadherins, stabilizes cell-cell junctions and is critical for neural morphogenesis. PLoS One 2012; 7(3):e32635.

Pons S, Marti E. Sonic hedgehog synergizes with the extracellular matrix protein vitronectin to induce spinal motor neuron differentiation. Development 2000; 127(2):333-342.

Popp S, Andersen JS, Maurel P, Margolis RU. Localization of aggrecan and versican in the developing rat central nervous system. Dev Dyn 2003; 227(1):143-149.

Porcheri C, Suter U, Jessberger S. Dissecting integrin-dependent regulation of neural stem cell proliferation in the adult brain. J Neurosci 2014; 34(15):5222-5232.

Potocnik AJ, Brakebusch C, Fassler R. Fetal and adult hematopoietic stem cells require beta1 integrin function for colonizing fetal liver, spleen, and bone marrow. Immunity 2000; 12(6):653-663.

Prestoz L, Relvas JB, Hopkins K, Patel S, Sowinski P, Price J, et al. Association between integrin-dependent migration capacity of neural stem cells in vitro and anatomical repair following transplantation. Mol Cell Neurosci 2001; 18(5):473-484.

Pruszak J, Ludwig W, Blak A, Alavian K, Isacson O. CD15, CD24, and CD29 define a surface biomarker code for neural lineage differentiation of stem cells. Stem Cells 2009; 27(12):2928-2940.

Pujadas L, Gruart A, Bosch C, Delgado L, Teixera CM, Rossi D, et al. Reelin regulates postnatal neurogenesis and enhances spine hypertrophy and long-term potentiation. J Neurosci 2010; 30(13):4636-4649.

Rabenstein M, Hucklenbroich J, Willuweit A, Ladwig A, Fink GR, Schroeter M, et al. Osteopontin mediates survival, proliferation and migration of neural stem cells through the chemokine receptor CXCR4. Stem Cell Res Ther 2015; 6:99.

Radakovits R, Barros CS, Belvindrah R, Patton B, Muller U. Regulation of radial glial survival by signals from the meninges. Journal of Neuroscience 2009; 29(24):7694-7705.

Radice PD, Mathieu P, Leal MC, Farias MI, Ferrari C, Puntel M, et al. Fibulin-2 is a key mediator of the pro-neurogenic effect of TGF-beta1 on adult neural stem cells. Mol Cell Neurosci 2015; 67:75-83.

Radmanesh F, Caglayan AO, Silhavy JL, Yilmaz C, Cantagrel V, Omar T, et al. Mutations in LAMB1 cause cobblestone brain malformation without muscular or ocular abnormalities. Am J Hum Genet 2013; 92(3):468-474.

Radner S, Banos C, Bachay G, Li YN, Hunter DD, Brunken WJ, et al. β2 and γ3 laminins are critical cortical basement membrane components: ablation of Lamb2 and Lamc3 genes disrupts cortical lamination and produces dysplasia. Dev Neurobiol 2012; 73(3):209-229.

Raghavan S, Bauer C, Mundschau G, Li Q, Fuchs E. Conditional ablation of beta1 integrin in skin. Severe defects in epidermal proliferation, basement membrane formation, and hair follicle invagination. J Cell Biol 2000; 150(5):1149-1160.

Ramon y Cajal S. Estudios sobre la degeneración y regeneración del sistema nervioso. 1914, Madrid, Moya.

Ramos-Cejudo J, Gutierrez-Fernandez M, Rodriguez-Frutos B, Exposito Alcaide M, Sanchez-Cabo F, Dopazo A, et al. Spatial and temporal gene expression differences in core and peri-infarct areas in experimental stroke: a microarray analysis. PLoS One 2012; 7(12):e52121.

Reichert S, Randall RA, Hill CS. A BMP regulatory network controls ectodermal cell fate decisions at the neural plate border. Development 2013; 140(21):4435-4444.

Riccomagno MM, Sun LO, Brady CM, Alexandropoulos K, Seo S, Kurokawa M, et al. Cas adaptor proteins organize the retinal ganglion cell layer downstream of integrin signaling. Neuron 2014; 81(4):779-786.

Rice DS, Curran T. Role of the reelin signaling pathway in central nervous system development. Annu Rev Neurosci 2001; 24:1005-1039.

Ritchie ME, Phipson B, Wu D, Hu Y, Law CW, Shi W, et al. limma powers differential expression analyses for RNA-sequencing and microarray studies. Nucleic Acids Res 2015; 43(7):e47.

Robel S, Buckingham SC, Boni JL, Campbell SL, Danbolt NC, Riedemann T, et al. Reactive astrogliosis causes the development of spontaneous seizures. Journal of Neuroscience 2015; 35(8):3330-3345.

Robel S, Mori T, Zoubaa S, Schlegel J, Sirko S, Faissner A, et al. Conditional deletion of beta1 integrin in astroglia causes partial reactive gliosis. Glia 2009; 57(15):1630-1647.

Roccio M, Gobaa S, Lutholf MP. High-throughput clonal analysis of neural stem cells in microarrayed artificial niches. Integr Biol (Camb) 2012; 4(4):391-400.

Roet KC, Franssen EH, de Bree FM, Essing AH, Zijlstra SJ, Fagoe ND, et al. A multilevel screening strategy defines a molecular fingerprint of proregenerative olfactory ensheathing cells and identifies SCARB2, a protein that improves regenerative sprouting of injured sensory spinal axons. J Neurosci 2013; 33(27):11116–11135.

Rosenblum S, Smith TN, Wang N, Chua JY, Westbroek E, Wang K, et al. BDNF pretreatment of human embryonic-derived neural stem cells improves cell survival and functional recovery after transplantation in hypoxic-ischaemic stroke. Cell Transplant 2015; 24(12):2449-2461.

Ryan KM, O'Donovan SM, McLoughlin DM. Electroconvulsive stimulation alters levels of BDNF-associated microRNAs. Neurosci Lett 2013; 549:125-129.

Ryan KM, Glaviano A, O'Donovan SM, Dunne R, Kavanagh A, Jelovac A, et al. Electroconvulsive therapy modulates plasma pigment epithelium-derived factor in depression: a proteomics study. Transl Psychiatry 2017; 7(3):e1073.

Saghatelyan A, de Chevigny A, Schachner M, Lledo PM. Tenascin-R mediates activity-dependent recruitment of neuroblasts in the adult mouse forebrain. Nat Neurosci 2004; 7(4):347-356.

Sahay A, Scobie KN, Hill AS, O'Carroll CM, Kheirbek MA, Burghardt NS, et al. Increasing adult hippocampal neurogenesis is sufficient to improve pattern separation. Nature 2011; 472(7344):466-470.

Sailor KA, Dhodda VK, Rao VL, Dempsey RJ. Osteopontin infusion in normal adult rat brain fails to increase cell proliferation in dentate gyrus and subventricular zone. Acta Neurochir Suppl 2003; 86:181-185.

Sakaguchi M, Imaizumi Y, Shingo T, Tada H, Hayama K, Yamada O, et al. Regulation of adult neural progenitor cells by Galectin-1/beta1 integrin interaction. J Neurochem 2010; 113(6):1516-1524.

Santa-Maria I, Avila J, Rabano A. Differential gene expression analysis of human entorhinal cortex support a possible role of some extracellular matrix proteins in the onset of Alzheimer disease. Neurosci Lett 2010; 468(3):225-228.

Sarlus H, Wang X, Cedazo-Minguez A, Schultzberg M, Oprica M. Chronic airway-induced allergy in mice modifies gene expression in the brain toward insulin resistance and inflammatory responses. J Neuroinflammation 2013; 10:99.

Schmalfeldt S, Bandtlow CE, Dours-Zimmermann MT, Winterhalter KH, Zimmermann DR. Brain derived versican V2 is a potent inhibitor of axonal growth. J Cell Sci 2000; 113 (Pt5):807-816.

Schnapp LM, Hatch N, Ramos DM, Klimanskaya IV, Sheppard D, Pytela R. The human integrin alpha 8 beta 1 functions as a receptor for tenascin, fibronectin, and vitronectin. J Biol Chem 1995; 270(39):23196-23202.

Schwander M, Shirasaki R, Pfaff SL, Muller U. Beta1 integrins in muscle, but not in motor neurons, are required for skeletal muscle innervation. Journal of Neuroscience 2004; 24(37):8181-8191.

Scoville WB, Milner B. Loss of recent memory after bilateral hippocampal lesions. J Neurol Neurosurg Psychiatry 1957; 20(1):11-21.

Seebeck F, Marz M, Meyer AW, Reuter H, Vogg MC, Stehling M, et al. Integrins are required for tissue organization and restriction of neurogenesis in regenerating planarians. Development 2017; 144(5):795-807.

Seib DRM, Martin-Villalba AM. Neurogenesis in the normal ageing hippocampus: a mini-review. Gerontoloy 2015; 61:327-335.

Serafini T, Colamarino SA, Leonardo ED, Wang H, Beddington R, Skarnes WC, et al. Netrin-1 is required for commissural axon guidance in the developing vertebrate nervous system. Cell 1996; 87(6):1001-1014.

Seri B, Garcia-Verdugo JM, McEwen BS, Alvarez-Buylla A. Astrocytes give rise to new neurons in the adult mammalian hippocampus. J Neurosci 2001; 21(18):7153-7160.

Shen Q, Wang Y, Kokovay E, Lin G, Chuang SM, Goderie SK, et al. Adult SVZ stem cells lie in a vascular niche: a quantitative analysis of niche cell-cell interactions. Cell Stem Cell 2008; 3(3):289-300.

Shin J, Berg DA, Zhu Y, Shin JY, Song J, Bonaguidi MA, et al. Single-cell RNA-seq with Waterfall reveals molecular cascades underlying adult neurogenesis. Cell Stem Cell 2015; 17(3):360-372.

Shoja-Taheri F, DeMarco A, Mastick GS. Netrin1-DCC-mediated attraction guides post-crossing commissural axons in the hindbrain. J Neurosci 2015; 35(33):11707-11718.

Sibbe M, Forster E, Basak O, Taylor V, Frotscher M. Reelin and Notch1 cooperate in the development of the dentate gyrus. J Neurosci 2009; 29(26):8578-8585.

Sibbe M, Kuner E, Althof D, Frotscher M. Stem- and progenitor cell proliferation in the dentate gyrus of the Reeler mouse. PLoS One 2015; 10(3):e0119643.

Sierra A, Encinas JM, Deudero JJ, Chancey JH, Enikolopov G, Overstreet-Wadiche LS, et al. Microglia shape adult hippocampal neurogenesis through apoptosis-coupled phagocytosis. Cell Stem Cell 2010; 7(4):483-495.

Sierra A, Martin-Suarez-S, Valcarcel-Martin R, Pascual-Brazo J, Aelvoet SA, Abiega O, et al. Neuronal hyperactivity accelerates depletion of neural stem cells and impairs hippocampal neurogenesis. Cell Stem Cell 2015; 16(5):488-503.

Song J, Sun J, Moss J, Wen Z, Sun GJ, Hsu D, et al. Parvalbumin interneurons mediate neuronal circuitry-neurogenesis coupling in the adult hippocampus. Nat Neurosci 2013; 16(12):1728-1730.

Soulintzi N, Zagris N. Spatial and temporal expression of perlecan in the early chick embryo. Cells Tissues Organs 2007; 186(4):243-256.

Spalding KL, Bergmann O, Alkass K, Bernard S, Salehpour M, Huttner HB, et al. Dynamics of hippocampal neurogenesis in adult humans. Cell 2013; 153:1219-1227.

Stanco A, Szekeres C, Patel N, Rao S, Campbell K, Kreidberg JA, et al. Netrin1-a3b1 integrin interactions regulate the migration of interneurons through the cortical marginal zone. Proc Natl Acad Sci USA 2009; 106(18):7595-7600.

Stankiewicz AM, Goscik J, Majewska A, Swiergiel AH, Juszczak GR. The effect of acute and chronic social stress on the hippocampal transcriptome in mice. PLoS One 2015; 10(11):e0142195.

Staquicini FI, Dias-Neto E, Li J, Snyder EY, Pasqualini R, Arap W. Discovery of a functional protein complex of netrin-4, laminin gamma1 chain, and integrin alpha6beta1 in mouse neural stem cells. Proc Natl Acad Sci USA 2009; 106(8):2903-2908.

Stephens LE, Sutherland AE, Klimanskaya IV, Andrieux A, Meneses J, Pedersen RA, et al. Deletion of beta 1 integrins in mice results in inner cell mass failure and peri-implantation lethality. Genes Dev 1995; 9(15):1883-1895.

Su Y, Shin J, Zhong C, Wang S, Roychowdhury P, Lim J, et al. Neuronal activity modifies the chromatin accessibility landscape in the adult brain. Nat Neurosci 2017; 20(3):476-483.

Suh H, Consiglio A, Ray J, Sawai T, D'Amour KA, Gage FH. In vivo fate analysis reveals the multipotent and self-renewal capacities of Sox2+ neural stem cells in the adult hippocampus. Cell Stem Cell 2007; 1(5):515-528.

Sultan S, Mandairon N, Kermen F, Garcia S, Sacquet J, Didier A. Learning-dependent neurogenesis in the olfactory bulb determines long-term olfactory memory. FASEB J 2010; 24(7):2355-2363.

Sun D, Daniels TE, Rolfe A, Waters M, Hamm R. Inhibition of injury-induced cell proliferation in the dentate gyrus of the hippocampus impairs spontaneous cognitive recovery after traumatic brain injury. J Neurotrauma 2015; 32(7):495-505.

Sun GJ, Zhou Y, Stadel RP, Moss J, Yong JHA, Ito S, et al. Tangential migration of neuronal precursors of glutamatergic neurons in the adult mammalian brain. Proc Natl Acad Sci USA 2015; 112(30):9484-9489.

Suzuki Y, Yanagisawa M, Yagi H, Nakatani Y, Yu RK. Involvement of B1-integrin up-regulation in basic fibroblast growth-factor- and epidermal growth factor-induced proliferation of mouse neuroepithelial cells. J Biol Chem 2010; 285(24):18443-18451.

Tadokoro S, Shattil SJ, Eto K, Tai V, Liddington RC, de Pereda JM, et al. Talin binding to integrin beta tails: a final common step in integrin activation. Science 2003; 302(5642):103-106.

Takada Y, Huang C, Hemler ME. Fibronectin receptor structures in the VLA family of heterodimers. Nature 1987; 326(6113):607-609.

Takada Y, Takada YK, Fujita M. Crosstalk between insulin-like growth factor (IGF) receptor and integrins through direct integrin binding to IGF1. Cytokine Growth Factor Rev 2017; 34:67-72.

Tamkun JW, DeSimone DW, Fonda D, Patel RS, Buck C, Horwitz AF, et al. Structure of integrin, a glycoprotein involved in the transmembrane linkage between fibronectin and actin. Cell 1986; 46(2):271-282.

Tan X, Liu WA, Zhang X-J, Shi W, Ren S-Q, Li Z, et al. Vascular influence on ventral telencephalon progenitors and neocortical interneuron production. Developmental Cell 2016; 36(6):624-638.

Tate MC, Garcia AJ, Keselowsky BG, Schumm MA, Archer DR, LaPlaca MC. Specific beta1 integrins mediate adhesion, migration, and differentiation of neural progenitors derived from the embryonic striatum. Mol Cell Neursci 2004; 27(1):22-31.

Teixeira CM, Kron MM, Masachs N, Zhang H, Lagace DL, Martinez A, et al. Cell-autonomous inactivation of the Reelin pathway impairs adult neurogenesis in the hippocampus. J Neurosci 2012; 32(35):12051-12065.

Thiel J, Winter Y. Hierarchical strategy for relocating food targets in flower bats: spatial memory versus cue-directed search. Animal Behav 2005; 69(2):315-327.

Thomas LB, Gates MA, Steindler DA. Young neurons from the adult subependymal zone proliferate and migrate along an astrocyte, extracellular matrix-rich pathway. Glia 1996; 17(1):1-14.

Thyagarajan B, Guimaraes MJ, Groth AC, Calos MP. Mammalian genomes contain active recombinase recognition sites. Gene 2000; 244(1-2):47-54.

To WS, Midwood KS. Plasma and cellular fibronectin: distinct and independent functions during tissue repair. Fibrogenesis Tissue Repair 2011; 4:21.

Toni N, Laplagne DA, Zhao C, Lombardi G, Ribak CE, Gage FH, et al. Neurons born in the adult dentate gyrus form functional synapses with target cells. Nat Neurosci 2008; 11(8):901-907.

Uda M, Ishido M, Kami K. Features and a possible role of Mash1-immunoreactive cells in the dentate gyrus of the hippocampus in the adult rat. Brain Res 2007; 1171:9-17

Urabe N, Naito I, Saito K, Yonezawa T, Sado Y, Yoshioka K, et al. Basement membrane type IV collagen molecules in the choroid plexus, pia mater and capillaries in the mouse brain. Arch Histol Cytol 2002; 65(2):133-143.

Valentinea G, Chakravarty S, Sarvey J, Bramham C, Herkenham M (2000) Fragile X (fmr1) mRNA expression is differentially regulated in two adult models of activity-dependent gene expression. Brain Res Mol Brain Res 75:337–341.

Venkatesan C, Birch D, Peng C-Y, Kesslar JA. Astrocytic beta1 integrin affects cellular composition of murine blood brain barrier in the cerebral cortex. International Journal of Developmental Neuroscience 2015; 44:48-54.

Vera A, Stanic K, Montecinos H, Torrejon M, Marcellini S, Caprile T. SCO-spondin from embryonic cerebrospinal fluid is required for neurogenesis during early brain development. Front Cell Neurosci 2013; 7:80.

Villeda SA, Luo J, Mosher KI, Zou B, Britschgi M, Bieri G, et al. The ageing systemic milieu negatively regulates neurogenesis and cognitive function. Nature 2011; 477(7362):90-94.

von Holst A, Egbers U, Prochiantz A, Faissner A. Neural stem/progenitor cells express 20 tenascin C isoforms that are differentially regulated by Pax6. J Biol Chem 2007; 282(12):9172-9181.

Vukovic J, Colditz MJ, Blackmore DG, Ruitenberg MJ, Bartlett PF. Microglia modulate hippocampal neural precursor activity in response to exercise and aging. J Neurosci 2012; 32(19):6435-6443.

Walker TL, Overall RW, Vogler S, Sykes AM, Ruhwald S, Lasse D, et al. Lysophosphatidic Acid Receptor is a functional marker of adult hippocampal precursor cells. Stem Cell Reports 2016; 6(4):552-565.

Wallin R, Cain D, Hutson SM, Sane DC, Loeser R. Modulation of the binding of matrix Gla protein (MGP) to bone morphogenetic protein-2 (BMP-2). Thromb Haemost 2000; 84(6):1039-1044.

Walton NM, Shin R, Tajinda K, Heusner CL, Kogan JH, Miyake S, et al. Adult neurogenesis transiently generates oxidative stress. PLoS One 2012; 7(4):e35264.

Wang F, Flanagan J, Su N, Wang LC, Bui S, Nielson A, et al. RNAScope: a novel in situ RNA analysis platform for formalin-fixed, paraffin-embedded tissues. J Mol Diagn 2012; 14(1):22-29.

Warren MS, Bradley WD, Gourlay SL, Lin YC, Simpson MA, Reichardt LF, et al. Integrin beta1 signals through Arg to regulate postnatal dendritic arborization, synapse density, and behavior. Journal of Neuroscience 2012; 32(8):2824-2834.

Weber T, Baier V, Lentz K, Herrmann E, Krumm B, Sartorius A, et al. Genetic fate mapping of type-1 stem cell-dependent increase in newborn hippocampal neurons after electroconvulsive seizures. Hippocampus 2013; 23(12):1321-1330.

Wennstrom M, Hellsten J, Ekdahl CT, Tingstrom A. Electroconvulsive seizures induce proliferation of NG2-expressing glial cells in adult rat hippocampus. Biol Psychiatry 2003; 54(10):1015-1024.

Won SJ, Kim SH, Xie L, Wang Y, Mao XO, Jin K, et al. Reelin-deficient mice show impaired neurogenesis and increased stroke size. Exp Neurol 2006; 198(1):250-259.

Wright LS, Li J, Caldwell MA, Wallace K, Johnson JA, Svendsen CN. Gene expression in human neural stem cells: effects of leukaemia inhibitory factor. J Neurochem 2003; 86(1):179-195.

Wu B, Chen Y, Huang J, Ning Y, Bian Q, Shan Y, et al. Icariin improves cognitive deficits and activates quiescent neural stem cells in aging rats. J Ethnopharmacol 2012; 142(3):746-753.

Wu Y, Sheng W, Chen L, Dong H, Lee V, Lu F, et al. Versican V1 isoform induces neuronal differentiation and promotes neurite outgrowth. Mol Biol Cell 2004; 15(5):2093-2104.

Xu XF, Li T, Wang DD, Chen B, Wang Y, Chen ZY. Integrin-linked kinase is essential for environmental enrichment enhanced hippocampal neurogenesis and memory. Sci Rep 2015; 5:11456.

Xu JC, Xiao MF, Jakovcevski I, Sivukhina E, Hargus G, Cui YF, et al. The extracellular matrix glycoprotein tenascin-R regulates neurogenesis during development and in the adult dentate gyrus of mice. J Cell Sci 2014; 127(Pt 3):641-652.

Yagi H, Yanagisawa M, Suzuki Y, Nakatani Y, Ariga T, Kato K. HNK-1 epitope-carrying tenascin-C spliced variant regulates the proliferation of mouse embryonic neural stem cells. J Biol Chem 2010; 285(48):37293-37301.

Yamada KM, Even-Ram S. Integrin regulation of growth factor receptors. Nat Cell Biol 2002; 4(4):E75-76.

Yamagata M, Sanes JR. Versican in the developing brain: lamina-specific expression in interneuronal subsets and role in presynaptic maturation. J Neurosci 2005; 25(37):8457-8467.

Yamagishi S, Yamada K, Sawada M, Nakano S, Mori N, Sawamoto K, et al. Netrin-5 is highly expressed in neurogenic regions of the adult brain. Front Cell Neurosci 2015; 9:146.

Yan YP, Lang BT, Vemuganti R, Dempsey RJ. Persistent migration of neuroblasts from the subventricular zone to the injured striatum mediated by osteopontin following intracerebral haemorrhage. J Neurochem 2009a; 109(6):1624-1635.

Yan YP, Lang BT, Vemuganti R, Dempsey RJ. Osteopontin is a mediator of the lateral migration of neuroblasts from the subventricular zone after focal cerebral ischaemia. Neurochem Int 2009b; 55(8):826-832.

Yanagisawa M, Nakamura K, Taga T. Roles of lipid rafts in integrin-dependent adhesion and gp130 signalling pathway in mouse embryonic neural precursor cells. Genes Cells 2004; 9(9):801-809.

Yanagisawa M, Taga T, Nakamura K, Ariga T, Yu RK. Characterisation of glycoconjugate antigens in mouse embryonic neural progenitor cells. J Neurochem 2005; 95(5):1311-1320.

Yang HJ, Ma SP, Ju F, Zhang YP, Li ZC, Zhang BB, et al. Thrombospondin-4 promotes neuronal differentiation of NG2 cells via the ERK/MAPK pathway. J Mol Neurosci 2016; 60(4):517-524.

Yanpallewar SU, Barrick CA, Palko ME, Fulgenzi G, Tessarollo L. Tamalin is a critical mediator of electroconvulsive shock-induced adult neuroplasticity. J Neurosci 2012; 32(7):2252-2262.

Yao Y, Yao J, Radparvar M, Blazquez-Medela AM, Guihard PJ, Jumabay M, et al. Reducing Jagged 1 and 2 levels prevents cerebral arteriovenous malformations in matrix Gla protein deficiency. Proc Natl Acad Sci USA 2013; 110(47):19071-19076.

Yao Y, Zebboudj AF, Shao E, Perez M, Bostrom K. Regulation of bone morphogenetic protein-4 by matrix GLA protein in vascular endothelial cells involves activin-like kinase receptor 1. J Biol Chem 2006; 281(45):33921-33930.

Yau SY, Lau BW, Tong JB, Wong R, Ching YP, Qiu G, et al. Hippocampal neurogenesis and dendritic plasticity support running-improved spatial learning and depression-like behaviour in stressed rats. PLoS One 2011; 6(9):e24263.

Yee KT, Simon HH, Tessier-Lavigne M, O'Leary DM. Extension of long leading processes and neuronal migration in the mammalian brain directed by the chemoattractant netrin-1. Neuron 1999; 24(3):607-622.

Yeh ML, Gonda Y, Mommersteeg MT, Barber M, Ypsilanti AR, Hanashima C, et al. Robo1 modulates proliferation and neurogenesis in the developing neocortex. J Neurosci 2014; 34(16):5717-5731.

Yoshida N, Hishiyama S, Yamaguchi M, Hashiguchi M, Miyamoto Y, Makinogawa S, et al. Decrease in expression of alpha 5 beta 1 integrin during neuronal differentiation of cortical progenitor cells. Exp Cell Res 2003; 287(2):262-271.

Yuasa S. Development of astrocytes in the mouse hippocampus as tracked by Tenascin-C gene expression. Arch Histol Cytol 2001; 64(2):149-158.

Zebboudj AF, Imura M, Bostrom K. Matrix GLA protein, a regulatory protein for bone morphogenetic protein-2. J Biol Chem 2002; 277(6):4388-4394.

Zetterstrom TS, Pei Q, Grahame-Smith DG. Repeated electroconvulsive shock extends the duration of enhanced gene expression for BDNF in rat brain compared with a single administration. Brain Res Mol Brain Res 1998; 57(1):106-110.

Zhao S, Chai X, Forster E, Frotscher M. Reelin is a positional signal for the lamination of dentate granule cells. Development 2004; 131(20):5117-5125.

Zhao S, Chai X, Frotscher M. Balance between neurogenesis and gliogenesis in the adult hippocampus: role for reelin. Dev Neurosci 2007; 29(1-2):84-90.

Zhang D, Guo M, Zhang W, Lu XY. Adiponectin stimulates proliferation of adult hippocampal neural stem/progenitor cells through activation of p38 mitogen-activated protein kinase (p38MAPK)/glycogen synthase kinase 3B (GSK-3B)/B-catenin signaling cascade. J Biol Chem 2011; 286(52):44913-44920.

Zhang K, Zhou Y, Zhao T, Wu L, Huang X, Wu K, et al. Reduced cerebral oxygen content in the DG and SVZ in situ promotes neurogenesis in the adult rat brain in vivo. PLoS One 2015; 10(10):e0140035.

Zhang Y, Chen K, Sloan SA, Bennett ML, Scholze AR, O'Keefe S, et al. An RNA-sequencing transcriptome and splicing database of glia, neurons, and vascular cells of the cerebral cortex. J Neurosci 2014; 34(36):11929-11947.

Zhang Y, Chopp M, Mahmood A, Meng Y, Qu C, Xiong Y. Impact of inhibition of erythropoietin treatment-mediated neurogenesis in the dentate gyrus of the hippocampus on restoration of spatial learning after traumatic brain injury. Exp Neurol 2012; 235(1):336-344.

Zhou Z, Yuan Q, Mash DC, Goldman D. Substance-specific and shared transcription and epigenetic changes in the human hippocampus chronically exposed to cocaine and alcohol. Proc Natl Acad Sci USA 2011; 108(16):6626-6631.

APPENDIX: List of Materials

Product (alphabetical order)	Company	Cat No.
10X PBS	Gibco	7001-036
Adhesivecaps	Zeiss	415190-9191-000
Arabinoside-b-D-cytarabine	Sigma	C6645
Brain infusion cannula	Charles River	BIK3
Carprofen	Zoetis	-
Cresyl violet	Acros Organics	229630050
Fluoromount G	SouthernBiotech	0100-01
High sensitivity screentape	Agilent	5067-5579
Hoechst 3342	Thermo Fisher Scientific	62249
Isoflurane	Merial	-
Ketamine	Zoetis	-
Masterpure	Epicentre	MCR85102
Medetomidate	Orion Pharma	-
miRNEasy FFPE kit	Quiagen	217504
Normal donkey serum	Millipore	S30
OCT	Cell Path	KMA-0100-00A
Osmotic minipumps	Charles River	1007D
PEN slides	Zeiss	415190-9041-000
PFA	Sigma	P6148
RNAScope 2.5 HD assay - Red	ACD	322360
RNAScope multiplex fluorescent kit	ACD	320850
RNAse-free ethanol	Sigma	E7023
RNAse-free water	Invitrogen	10977-035
RNEasy FFPE kit	Quiagen	73504
RNEasy Microkit	Quiagen	74004
SMARTer Ultra Low Input RNA kit v3	Clontech	634848
Sunflower seed oil	Sigma	S5007
Superfrost plus slides	Thermo Scientific	10149870
Tamoxifen	Sigma	T5648
Tissue glue	3M	1469sb
Triton X-100	Fisher Scientific	BP151-500